for the p_1 and p_2 networks of a cascade separable ladder network to be either lowpass, highpass, bandpass or bandstop type.

Generation of doubly-terminated cascade separable network functions is accomplished by two different methods, which are useful for the approximation of two-variable transfer functions. The conditions for cascade separability, which are obtained in the analog domain are extended to the case of 2-D digital transfer functions by formulating appropriate polynomials in the digital domain, which correspond to the even and odd polynomials in the analog variables. For the cascade separable network, the corresponding 2-D digital transfer function may have non-essential singularities of the second kind. It is shown that these cases can be detected and avoided.

A good approximation towards quadrantal symmetry and a linear phase response are shown to be obtainable for the 2-D cascade separable network even though the denominator of the transfer function is not variable separable. Two types of approximations are possible. In the first type, the required response is assumed along the ω_1 and ω_2 axes and the p_1 and p_2 doubly-terminated ladder networks, which produce these responses are synthesized. They are then cascaded to obtain the doubly-terminated cascade separable network. In the second case, the two single-variable transfer functions are synthesized as singly-terminated ladder networks and the

p_1 ladder is then inverted and cascaded with the p_2 ladder network. By suitable modifications, the resulting doubly-terminated cascade separable network function becomes nearly variable separable.

A new method for the approximation of single-variable analog as well as digital transfer functions having non-equiripple magnitude response in the passband for any specified ripple value is developed and this is used to optimize for the linearity in phase response in the passband. The resulting 1-D transfer funotions are used to obtain 2-D transfer functions by the methods discussed earlier.

The effects of product and coefficient quantizations are studied next. Firstly, it is shown that the different wave digital filter realizations available in the 1-D case can be extended to the 2-D case. With a fixed point arithmetic implementation of these filters in mind, a suitable method for scaling is utilized. The direct canonic and the wave digital filter realizations of the 2-D transfer function are compared for their noise performance with product quantization and for wordlength requirement with regard to the coefficient quantization. The performance of the wave ditigal filter is far superior to that of the direct canonic filter, for the case studied.

ACKNOWLEDGEMENTS

I wish to acknowledge the guidance and supervision of Dr. V. Ramachandran and Dr. M.N.S. Swamy throughout the period of my study. I also thank Dr. A. Antoniou and Dr. S. Morgera for their review and comments on my thesis. I am grateful to the Canadian Commonwealth Scholarship Committee, whose scholarship award enabled me to study at Concordia University.

I am also grateful to Marie Berryman for taking up the typing of this thesis and doing it at a very short notice.

TABLE OF CONTENTS

LIST OF TABLES

LIST OF FIGURES

LIST OF IMPORTANT ABBREVIATIONS AND SYMBOLS

BIBO	Bounded input bounded output
BP	Bandpass
BS	Bandstop
ERM	Equiripple magnitude
FIR	Finite impulse response
HP	Highpass
$H(z_1,z_2)$	Two-dimensional digital transfer function
IIR	Infinite inpulse response
LP	Lowpass
LSI	Linear shift invariant
MFM	Maximally flat magnitude
MHP	Multivariable Hurwitz polynomial
MPRF	Multivariable positive real function
Nu(Ev.Z)	Numerator of the even part of Z
$p_1,p_2,\ldots,p_m$	Complex frequency variables in the analog domain for m variables
PLSI	Planar least square inverse
PRF	Positive real function
PSD	Power spectral density
R_L	Load resistance
RPSD	Relative power spectral density
R_s	Source resistance
SBM	Stopband magnitude
$S_{c_i}^{H}(z_1,z_2)$	Sensitivity of $H(z_1,z_2)$ w.r.t. c_i

T_1, T_2	Sampling periods in two-dimensions
$T(p_1, p_2)$	Two-variable analog transfer function
TPRF	Two-variable positive real function
TRF	Two-variable reactance function
T_v	Voltage transfer function
y_{22}	Short circuit admittance parameter
z_1, z_2	Complex frequency variables in the digital domain for two variables
$z_{11}, z_{12}, z_{21}, z_{22}$	Open circuit impedance parameters
$Z(p_1, p_2)$	Driving point impedance function in two-variables
$\delta_i(Z)$	Degree of p_i in Z
ρ	Reflection coefficient
τ_1, τ_2	Group delays in two-variables
ω_1, ω_2	Analog domain frequencies in two-variables
Ω_1, Ω_2	Digital domain frequencies in two-dimensions
ω_p	Passband edge frequency
ω_s	Stopband edge frequency

CHAPTER 1

INTRODUCTION

1.1 General

Two-dimensional (2-D) digital filters find applications in areas such as image processing, X-ray tomography, seismic signal processing, data processing in 2-D pattern recognition systems, geophysical exploration, sonar, radar, radioastronomy, prefiltering for picture encoding etc. [1], where the data to be processed is essentially two-dimensional in nature. The processing is done off-line with the image or the 2-D data stored in the memory of a computer and processed by a causal or a non-causal digital filter. Although one-dimensional filters can be used for the above purposes it is preferable to use 2-D filters [1], because of the following important advantages:

(i) Simplicity in the filtering algorithm.

(ii) less computation time and storage capacity and

(iii) better performance and results.

The 2-D filters can be of two types, the finite impulse response [FIR] and the infinite impulse response [IIR] filter. The FIR filters are always stable and can be easily realized. Also they can be designed such that they have an exactly linear phase characteristic. On the other hand, for a sharp cut-off response, the order of the FIR filter has to be very large compared to that of an IIR filter having a similar response.

In the case of the IIR filters, an exact linear phase cannot be obtained and hence its design involves approximation of both the magnitude and phase response specifications. Another alternative is to include an allpass section in cascade to equalize the phase. This is important because the phase response has to be close to linear in order to preserve picture information in image processing applications [2]. Stability for the IIR filter is not guaranteed as in the case of the FIR filter and tests have to be carried out to ensure that the filter obtained by the approximation is stable. In this thesis, we shall discuss only the case of the IIR filters.

1.2 2-D Recursive IIR Filters

The design of 2-D recursive IIR filters has been difficult due to the non-existence of the Fundamental Thoerem of Algebra in the factorization of 2-D polynomials into lower order polynomials. Because of this problem, the testing for stability of the IIR filter is quite involved. A 2-D causal LSI (linear shift invariant) digital transfer function is represented by

$$H(z_1,z_2) = A(z_1,z_2)/B(z_1,z_2)$$

$$= \frac{\sum_{k_1=0}^{M_1}\sum_{k_2=0}^{M_2} a(k_1,k_2)\, z_1^{-k_1} z_2^{-k_2}}{\sum_{\ell_1=0}^{N_1}\sum_{\ell_2=0}^{N_2} b(\ell_1,\ell_2)\, z_1^{-\ell_1} z_2^{-\ell_2}} \qquad (1.2.1)$$

where $A(z_1,z_2)$ and $B(z_1,z_2)$ are the z-transforms of $\{a(k_1,k_2)\}$ and $\{b(l_1,l_2)\}$ respectively. The above filter is stable if $H(z_1,z_2)$ is analytic

$$\text{i.e. } B(z_1,z_2) \neq 0 \quad \text{for } |z_1| \geq 1 \text{ and } |z_2| \geq 1 \tag{1.2.2}$$

The converse of the above theorem is true except for cases where $H(z_1,z_2)$ has a non-essential singularity of the second kind [3] on the unit bicircle

$$\Gamma^2, \{(z_1,z_2)| \quad |z_1|=1, \quad |z_2|=1\},$$

$$\text{but} \sum_{n_1=0}^{\infty} \sum_{n_2=0}^{\infty} |h(n_1,n_2)| < \infty$$

Stabilization of unstable filters using Shanks' conjecture [4] does not hold in general and planar least square inverse (PLSI) polynomials of semicausal form have to be used for this purpose [5].

It is not always possible to realize the 2-D IIR filters as a cascade or parallel connection of lower order sections because of the problem of factorization. Thus an efficient method of realization is not possible for a general high-order IIR filter. A useful alternative to cascade or parallel realization is the wave digital filter realization, where we start with a passfve 2-D analog network transfer function which is guaranteed to be stable.

Because of the above difficulties, many design techniques have exploited 1-D techniques, either by employing separable filters or by using certain mapping techniques. The procedure of Shanks, Treital and Justice [4] starts with an analog transfer function and by rotation of the axes and applying the bilinear transformation obtains a two-dimensional recursive filter. Costa and Venetsanopoulos have suggested a design technique for circularly symmetric lowpass filters using Shanks' rotated filters [6]. A similar technique with rotation of axes in the digital domain is given by Chang and Aggarwal [7] which uses rational powers of z_1 and z_2 and the interpolation of input and output sequences. Unlike Shanks' filter, this is always stable if the prototype filter is stable and avoids the distortion due to the bilinear transformation. Another technique for transformation of a 1-D discrete filter into a 2-D discrete filter is discussed in [8]. Use of spectral transformation functions is described in [9], [10] and [11].

An approach utilizing separable planar filters is suggested by Treital and Shanks [12]. Computer aided design of separable 2-D recursive filters is discussed in [13]. A design technique for approximating nonseparable frequency characteristics by sums and products of separable transfer functions is described in [14] and [15].

Other computer aided design procedures use unconstrained minimization techniques [16-21]. In the case of Maria and Fahmy, the filter stability is checked at each iteration

of the procedure and if unstable, the step size is suitably reduced. In the other methods, the stability of the filter is ensured by a suitable change of variables. The above filters are chosen to be cascades of second order sections. In [16] and [17], the magnitude requirements are approximated by a 2-D filter, which is then cascaded with an all pass 2-D filter to equalize the resulting group delay. In [18] and [21], the approximation is done for both magnitude and group delay simultaneously. Realization of 2-D digital transfer functions is discussed in [22].

Recently, factorization of a magnitude-squared function has been explored using the 2-D complex cepstrum. Ekstrom and Woods [23] have used the 2-D spectral factorization for the design of 2-D all-pole filters, which are nonsymmetric half-plane (semicausal) filters having their impulse responses spread over more than a quarter plane but less than a half plane. Procedure for the design of half plane filters are discussed in [24-26].

Usually a certain type of symmetry such as circular symmetry or rectangular symmetry is desired in the magnitude response of 2-D filters [26], [27]. The constraints imposed on transfer functions by these symmetries are derived in [28] and [29]. Incorporation of these constraints reduces the complexity of the approximation problem, reduces the number of multipliers in the implementation and also assures the desired symmetry in the magnitude response. In this thesis, the approximation problem is studied with the above

constraints in mind.

Since testing for stability is a problem, the approximation is studied with respect to transfer functions in the analog domain which are realizable as doubly-terminated multivariable reactive networks. Upon double bilinear transformation, these transfer functions can be implemented as wave digital filters. Hence realization of the 2-D digital IIR filter in the direct form as well as the wave digital form is studied.

1.3 Wave digital filters

A technique for the design of stable 2-D digital filters by applying the bilinear transformation in two variables to the transfer function of a passive analog two-variable network was proposed by Dubois and Blostein [30]. This technique guarantees the stability of the digital filter except for non-essential singularities of the second kind [31], since the reference filter is passive and stable. Also it has been noted in the single-variable case that the good sensitivity properties of a doubly-terminated ladder network are carried over to the corresponding wave digital filter realization.

Using the techniques of 1-D wave digital filter design, extensions have been made to the design to 2-D and multidimensional wave digital filters [32-34]. 2-D wave digital rotated filters have been implemented on a minicomputer

system by Lennarz and Hofmann, using the design technique of Fettweis [35].

In the digital filter implementation, since the numbers are stored in finite length registers, the coefficients and signal values must be quantized either by rounding or by truncation. This gives rise to three kinds of errors:

(i) Product quantization errors arising due to quantization of the product obtained by the multiplication of a signal and a multiplier coefficient. Its effect is to inject a noise component into the output of each multiplier.

(ii) Coefficient quantization errors due to quantization of the transfer function coefficients in the implemented filter, thereby changing the frequency response of the filter. This can also cause instability in highly selective filters.

(iii) Input quantization errors due to quantization of the input signal in the analog-to-digital conversion process. This gives rise to output noise.

Detailed analysis of these effects are available in [36] for the case of 1-D digital filters. Comparison of the above types of 1-D digital filters on the basis of sensitivity and noise due to quantization and the computational efficiency have been carried out by various authors [37-46] for both fixed-point and floating-point arithmetic. Quantization can also lead to limit cycles when errors become correlated [47]. Another nonlinear effect is the overflow

oscillations which occur due to the circular nature of the 2's complement arithmetic system [48].

In the case of 2-D digital filters, the error analysis can be done in the same way as for the 1-D case. The analysis for the 2-D filters of the direct form has been carried out by Ni and Aggarwal [49]. Accumulation round-off error is analyzed for a particular type of filter in [50]. The effects of quantization errors on rotated filters is studied in [51]. Finite register length models for direct, cascade and parallel realizations and computation of error statistics for fixed point arithmetic are given in [52].

For realization of 2-D wave digital filters, it is necessary to start with a prototype two-variable analog filter network. A doubly-terminated lossless ladder type of network is considered for this purpose, since in single variable this type of network is known to possess good sensitivity properties [53]. Since a general procedure for the synthesis of a multivariable positive real function [MPRF] is not currently available [54], synthesis of classes of multivariable network functions have become important. The above doubly-terminated network realizes a class of such functions.

1.4 Scope of the thesis

The properties of singly-terminated and doubly-terminated multivariable lossless ladder networks are studied

in this thesis with the idea of using them for the realization of a class of multivariable transfer functions. Also it is necessary to start with this type of a prototype network in order to obtain a wave digital filter realization. In Chapter 2, we discuss the synthesis of singly-terminated multivariable lossless ladder networks using multivariable arrays. The properties of transfer functions which are realizable as doubly-terminated networks are studied in Chapter 3 and generation procedures to obtain such functions are discussed. The case of a cascade separable network which contains cascaded p_1 and p_2 lossless ladder sections is studied in detail because of its usefulness in the approximations. The properties and realizability conditions for the cascade separable functions in the digital domain are discussed in Chapter 4.

Analytical methods for the approximation of 2-D functions realizable as doubly-terminated networks are not currently available. It is important to take into account the requirements of symmetry in the magnitude response of the 2-D digital filter. This filter is also required to have a good linearity in the phase response. Chapter 5 discusses the methods of approximation of 2-D functions both in the analog and the digital domain. These transfer functions are realizable as doubly-terminated cascade separable networks in the analog domain. The double bilinear transformation which is used here to obtain the 2-D digital transfer function does

not preserve the phase properties of the analog function. The warping of the frequency response by the bilinear transformation can be taken into account only with regard to the magnitude response specifications by a prewarping technique. Hence our 2-D approximation has to take into account this warping effect on the phase response. It is to be noted that reactance transformations also do not preserve the phase response properties. In Chapter 6 methods are outlined which take into account these problems.

Since the transfer functions generated above are realizable as doubly-terminated ladder networks in the analog domain, they are always stable except for possible non-essential singularities of the second kind which lie on the unit bicircle. It is necessary to test for these singularities and avoid them if they lead to instability.

To date no error analysis has been carried out on 2-D wave digital filters. It is possible to evaluate the efficiency of a realization only by carrying out this analysis on different realizations. In Chapter 7, we analyze the quantization effects for the direct and the wave digital filter realizations.

CHAPTER 2

SYNTHESIS OF SINGLY-TERMINATED LADDER NETWORKS BY MULTIVARIABLE ARRAY USING HOMOGENEOUS POLYNOMIALS

2.1 Introduction

In the absence of a general method for synthesis of multivariable positive real functions (MPRFs), methods for synthesis of certain classes of MPRFs have been developed by several authors. In particular, resistively-terminated multivariable ladder realizations have received considerable attention and conditions for such realizations have been obtained in [55] and [56]. In [55], a multivariable array is proposed using the coefficients of the multivariable polynomials in the given function and this is applied for the synthesis of multivariable ladder networks. The multivariable polynomials considered here contain no missing terms. The ladder realization discussed in [56] is of a special type consisting of two-port lossless networks in each variable connected in cascade. The conditions for an MPRF, which is of the first degree in all variables except one, to be realizable as the input impedance of a resistively-terminated cascade of lossless two-ports separated by noncommensurate series and shunt stubs are published in [57] and the realizability of a function of the above type as a resistively-terminated ladder network with all its transmission zeros at zero or at infinity, is discussed

in [58]. Each of these above realizations can be regarded as a different class of ladder networks having some definite properties.

In this chapter, the necessary and sufficient conditions are obtained for the realization of a general MPRF as a resistively-terminated ladder network whose series arms consist of inductors in different variables connected in series and the shunt arms consist of capacitors in different variables connected in parallel. It is to be noted that in any given arm not all the variables need be present. Starting from this ladder network, it is shown that other structures can be obtained using reactance transformations. Based on the above conditions for the realizability of MPRFs, certain theorems on the realizability of multivariable transfer functions are proved.

A particular case of the above class of functions known as the cascade separable function [56] has been studied in detail where an MPRF in m-variables is realized as the driving point impedance of a resistively-terminated ladder network of m lossless two-ports connected in cascade. Each lossless two-port consists of elements of one variable and has all its zeros either at the origin or at infinty in that particular variable. In the present chapter, an extension of the above, where each of the lossless two-ports can be one of lowpass (LP), highpass (HP), bandpass (BP) or bandstop (BS) functions is carried out.

2.2 Multivariable array using homogeneous polynomials and its use in the realization of certain MPRFs

The numerator of the even part of a positive real function (PRF) plays an important role in single-variable network synthesis and methods are available for the generation of a PRF from the given even part. However, it has been proved in [59] that if the Nu(Ev.Z) is non-negative and (M_2+N_2) is a multivariable Hurwitz polynomial (MHP), then it may not be possible in general to generate an MPRF of the type $Z(p_1,\ldots,p_m) = (M_1+N_1)/(M_2+N_2)$. In fact, certain additional conditions need to be satisfied for the above generation. The two-variable reactance function (TRF) M_2/N_2 or N_2/M_2 must be realizable as a lossless ladder network. The above results have been obtained with a multivariable array built up using the coefficients of the multivariable polynomial with no missing terms. Here we define a new type of multivariable array which consists of homogeneous multivariable polynomials as its elements. The polynomials defined here can contain missing coefficients.

A given multivariable polynomial in the variables $p_1,\ldots,p_m$ is represented as

$$P(p_1,\ldots,p_m) = f_n+f_{n-1}+\ldots+f_1+f_0 \qquad (2.2.1)$$

where f_0 is a constant and f_i, $i=1,\ldots,n$ are homogeneous polynomials in the variables p_1 to p_m such that each of

the terms in f_i is of degree i.

i.e.,

$$f_i = \sum_{j_1+j_2+\ldots+j_m=i} a_{j_1 j_2 \ldots j_m} p_1^{j_1} p_2^{j_2} \ldots p_m^{j_m} \qquad (2.2.2)$$

Each f_i is a homogeneous polynomial of degree i and n is the total degree of the polynomial P. Before developing the array, we shall prove the following lemma.

Lemma 2.1

For an MPRF $F(p_1,\ldots,p_m) = (M_1+N_1)/(M_2+N_2)$ where M's and N's are even and odd polynomials, if $(M_1M_2-N_1N_2)$ equals a constant R, then the numerator and the denominator of F have a degree difference of unity.

Proof:

Let the given m-variable PRF be expressed as

$$F(p_1,\ldots,p_m) = \frac{M_1+N_1}{M_2+N_2} = \frac{f_n+f_{n-1}+\ldots+f_0}{g_n+g_{n-1}+\ldots+g_0} \qquad (2.2.3)$$

where f_i and g_i (i=1 to n) are homogeneous polynomials in the variables $p_1,\ldots,p_m$ such that the degree of each term is i and n is the total degree of the given function. By imposing the condition $M_1M_2-N_1N_2=R$ on F, we get the following set of equations.

$$f_n g_n = 0$$

$$f_n g_{n-2} + f_{n-2} g_n - f_{n-1} g_{n-1} = 0$$

$$f_n g_{n-4} + f_{n-2} g_{n-2} + f_{n-4} g_n - f_{n-1} g_{n-3} - f_{n-3} g_{n-1} = 0$$

$$\vdots \qquad (2.2.4)$$

$$f_2 g_0 + f_0 g_2 - f_1 g_1 = 0$$

$$f_0 g_0 = R$$

From the above, we get the following results.

(a) either $f_n \equiv 0$ or $g_n \equiv 0$ (2.2.5a)

(b) with $g_n \equiv 0$, $f_n/g_{n-1} = f_{n-1}/g_{n-2}$ (2.2.5b)

Hence the lemma follows.

It must be noted that in (2.2.5a) both f_n and g_n can never be simultaneously zero because in such a case the order of the given function F is reduced by one. Equation (2.2.5b) is used later as a condition in the development of the multivariable array of Table 2.1.

Given an MPRF $F = (f_n + f_{n-1} + \ldots + f_0)/(g_{n-1} + g_{n-2} + \ldots + g_0)$ we develop the multivariable array given in Table 2.1 comprising of homogeneous polynomials whose degree is indicated by the subscript. This array which we call as the multivariable array A continues until it reduces to a constant. With the conditions given in Table 2.1 satisfied for any MPRF F, there

TABLE 2.1

MULTIVARIABLE ARRAY A

MULTIVARIABLE ARRAY	RELATIONSHIPS	CONDITIONS
$f_n f_{n-1} f_{n-2} \cdots f_4 f_3 f_2 f_1 f_0$ $g_{n-1} g_{n-2} g_{n-3} g_{n-4} \cdots g_3 g_2 g_1 g_0$		$\frac{f_n}{g_{n-1}} = \frac{f_{n-1}}{g_{n-2}} = \alpha_{11}$ $= \sum_{i=1}^{m} a_{i1} p_i \leftarrow (1)$ $\alpha_{11} \neq 0 \quad a_{i1} \geq 0$
$h_{n-2} h_{n-3} h_{n-4} h_{n-5} \cdots h_2 h_1 h_0$	$h_{n-i} = f_{n-i}$ $-\alpha_{11} g_{n-i-1}$ for $i = 2, \ldots, n-1$ & $h_0 = f_0$	$\frac{g_{n-1}}{h_{n-2}} = \frac{g_{n-2}}{h_{n-3}} = \alpha_{21}$ $= \sum_{i=1}^{m} b_{i1} p_i \leftarrow (2)$ $\alpha_{21} \neq 0 \quad b_{i1} \geq 0$
$k_{n-3} k_{n-4} k_{n-5} k_{n-6} \cdots k_1 k_0$	$k_{n-i} = g_{n-i}$ $-\alpha_{21} h_{n-i-1}$ for $i = 3, \ldots, n-1$ & $k_0 = g_0$	$\frac{h_{n-2}}{k_{n-3}} = \frac{h_{n-3}}{k_{n-4}} = \alpha_{31}$ $= \sum_{i=1}^{m} c_{i1} p_i \leftarrow (3)$ $\alpha_{31} \neq 0 \quad c_{i1} \geq 0$
$\ell_{n-4} \ell_{n-5} \ell_{n-6} \ell_{n-7} \cdots \ell_0$	$\ell_{n-i} = h_{n-i}$ $-\alpha_{31} k_{n-i-1}$ for $i = 4, \ldots, n-1$ & $\ell_0 = h_0$	$\frac{k_{n-3}}{\ell_{n-4}} = \frac{k_{n-4}}{\ell_{n-5}} = \alpha_{41}$ $= \sum_{i=1}^{m} d_{i1} p_i \leftarrow (4)$ $\alpha_{41} \neq 0 \quad d_{i1} \geq 0$
...	...	...

exists a continued fraction expansion for F and hence F can be realized as a multivariable ladder network. Therefore, the following theorems can be proved. Without loss of generality, the theorems are enunciated and proved for impedance functions only; however, they can be suitably modified for admittance functions also.

Theorem 2.1

Any MPRF $Z(p_1,\ldots,p_m) = (f_n+f_{n-1}+\ldots+f_0)/(g_{n-1}+g_{n-2}+\ldots+g_0)$ can be realised as a resistively-terminated lossless ladder network shown in Fig. 2.1, iff the conditions for the multivariable array given in the Table 2.1 are satisfied.

Proof:

The necessity follows from the analysis of a multivariable lowpass ladder network of the type given in Fig. 2.1.

To prove the sufficiency, we proceed as follows. From condition (1) in Table 2.1, we have $f_n/g_{n-1} = f_{n-1}/g_{n-2} = \alpha_{11}$ where α_{11} is a multivariable polynomial of degree one. Hence $Z(p_1,\ldots,p_m)$ has a pole at $p_i=\infty$, $i=1,\ldots,m$. which can be extracted as $\alpha_{11} = a_{11}p_1+a_{21}p_2+\ldots+a_{m1}p_m$. This is realized as a series connection of inductors in the variables p_1 to p_m. After extraction of this section, the remaining function is given by

$$Z_1 = Z-\alpha_{11} = \frac{h_{n-2}+h_{n-3}+\ldots+h_0}{g_{n-1}+g_{n-2}+\ldots+g_0} = \frac{1}{Y_1} \qquad (2.2.6)$$

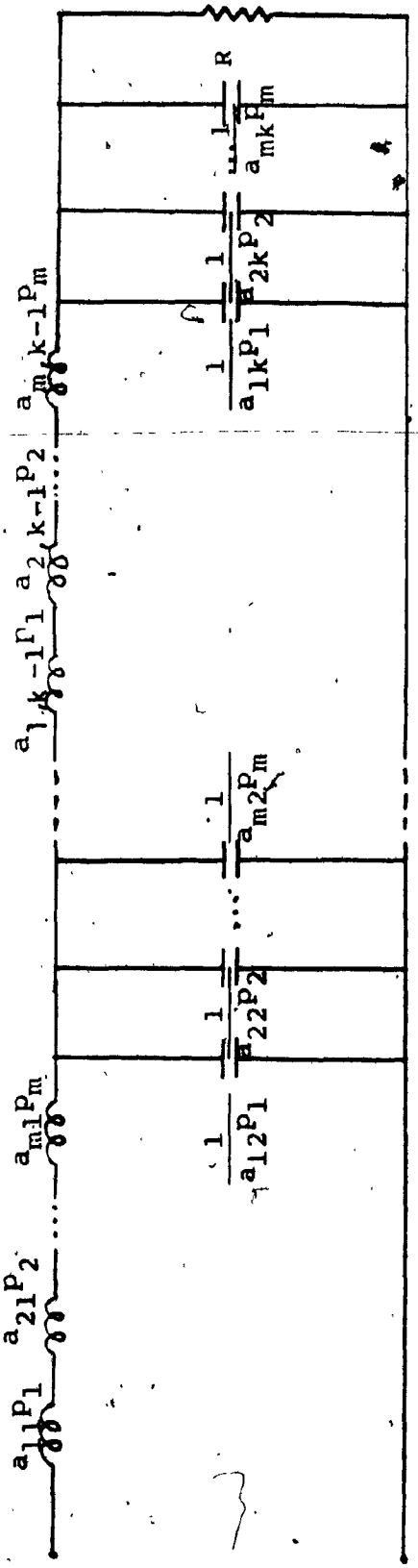

FIG. 2.1 LADDER REALIZATION OF THEOREM 2.1

By condition (2) on Y_1, we have $g_{n-1}/h_{n-2} = g_{n-2}/h_{n-3} = \alpha_{21}$ where α_{21} is a multivariable polynomial of degree one. The pole at $p_i=\infty$, $i=1,\ldots,m$ is extracted as

$$\alpha_{21} = \sum_{i=1}^{m} b_{i1}p_i,\ b_{i1} \geq 0$$

and this is realized as a shunt connection of capacitors in $p_1,\ldots,p_m$, all connected in parallel. This procedure of extraction is continued by virtue of the conditions imposed on each stage of the array until the finally remaining constant is realized as a resistance R.

The driving point impedance $Z(p_1,\ldots,p_m)=(M_1+N_1)/(M_2+N_2)$ of the network in Fig. 2.1 satisfies the condition

$$M_1M_2 - N_1N_2 = [redacted] \qquad (2.2.7)$$

It is noted that for admittance functions, the network of Fig. 2.1 begins with a shunt arm, with capacitances in parallel.*

Example 2.1

Consider the MPRF

---

* It should be noted that this theorem considers m-variable polynomials in the variables $p_1,\ldots,p_m$, whereas reference [22] considers such a continued fraction expansion in z_1 and z_2 domains for the realization of classes of 2-D.digital transfer functions.

$$Z(p_1,p_2,p_3) = \frac{M_1+N_1}{M_2+N_2} = \frac{f_4+f_3+f_2+f_1+f_0}{g_3+g_2+g_1+g_0}$$

$$(48p_1^2p_3^2+32p_1^2p_2p_3+60p_1p_2p_3^2+40p_1p_2^2p_3) +$$

$$(12p_1p_3^2+8p_1p_2p_3+15p_2p_3^2+10p_2^2p_3) +$$

$$(28p_1p_3+36p_1p_2+16p_1^2+30p_2p_3+20p_2^2) +$$

$$= \frac{(4p_1+5p_2+p_3) + 2}{(12p_1p_3^2+8p_1p_2p_3)+(3p_3^2+2p_2p_3)+(4p_1+4p_2+6p_3)+1}$$

$Z(p_1,p_2,p_3)$ can be expanded in the continued fraction form since it satisfies the conditions in Table 2.1.

$$Z(p_1,p_2,p_3) = 4p_1 + 5p_2 + \cfrac{1}{3p_3+2p_2 + \cfrac{1}{p_3 + \cfrac{1}{2p_1 + \frac{1}{2}}}}$$

This is realizable as a ladder network terminated in a resistance of 2 ohms.

Theorem 2.2

An MPRF $Z(p_1,\ldots,p_m)$ is realizable as the resistively-terminated highpass ladder network of Fig. 2.2a, iff after applying the transformation $p_i \rightarrow 1/p_i$, $i=1,\ldots,m$ to Z, the resulting function satisfies the conditions of thoerem 2.1.

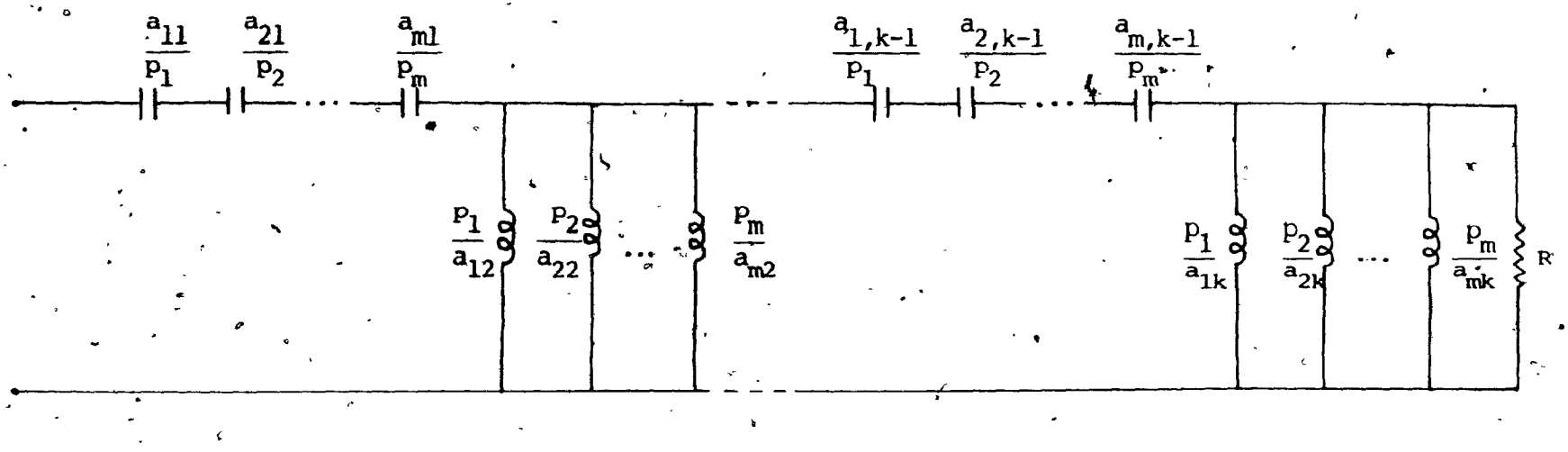

(a)

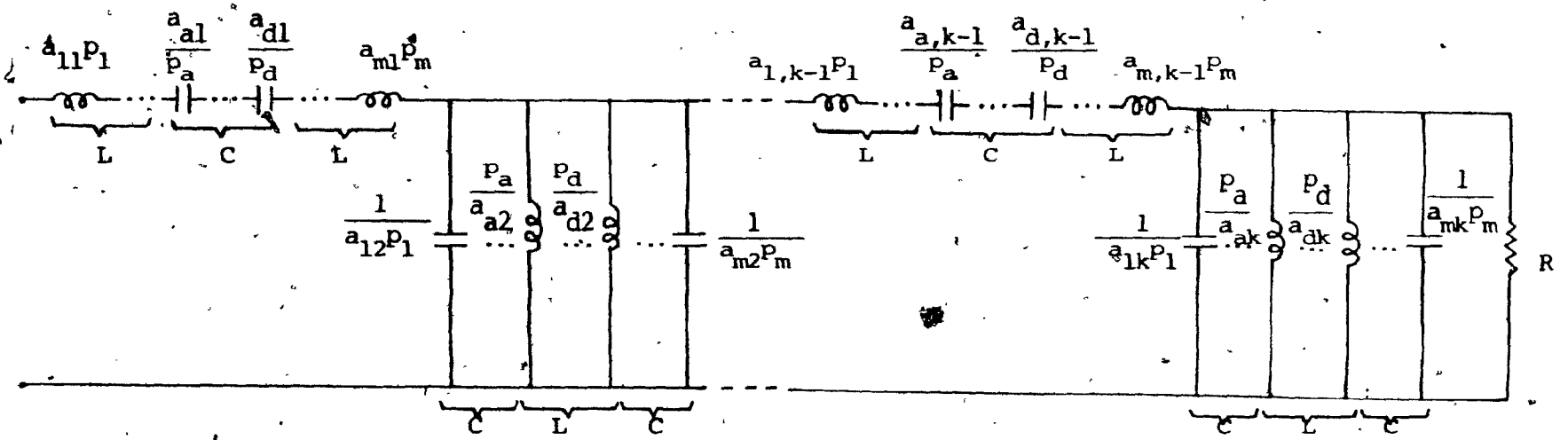

(b)

FIG.2.2 LADDER REALIZATIONS FOR THEOREMS 2.2 AND 2.3

The transformation $p_i \to 1/p_i$, being a lowpass to high-pass transformation, transforms inductances into capacitances and vice versa in the network. In this case, the driving point impedance $Z(p_1,\ldots,p_m) = (M_1+N_1)/(M_2+N_2)$ satisfies the condition

$$M_1M_2 - N_1N_2 = \pm R\, p_1^{2k_1} \ldots p_m^{2k_m} \qquad (2.2.8)$$

where $k_i = \delta_i(Z)$, the degree of p_i in Z for $i=1,\ldots,m$ and the sign is positive if $(k_1+k_2+\ldots+k_m)$ is even and negative if it is odd.

Theorem 2.3

An MPRF $Z(p_1,\ldots,p_m) = (M_1+N_1)/(M_2+N_2)$ is realizable as the resistively-terminated ladder network of Fig. 2.2b, iff after applying the transformation $p_i \to 1/p_i$, $i=a,b,c,d$ to Z, the resulting function satisfies the conditions of Theorem 2.1.

The proof is similar to that of Theorem 2.2 and hence is omitted. The driving point impedance $Z(p_1,\ldots,p_m)$ satisfies the condition

$$M_1M_2 - N_1N_2 = \pm R \prod_{i=a,b,c,d} p_i^{2k_i} \qquad (2.2.9)$$

where $k_i = \delta_i(Z)$ for $i=a,b,c,d$ and the sign is positive if $\sum_{i=a,b,c,d} k_i$ is even and negative if it is odd.

Theorem 2.4

An MPRF $Z(p_1,\ldots,p_m) = (M_1+N_1)/(M_2+N_2)$ is realizable as the resistively-terminated highpass ladder network of Fig. 2.3a, iff after applying to Z, the transformation

$$(a_{1j}p_1+a_{2j}p_2+\ldots+a_{mj}p_m) \rightarrow \frac{1}{(a_{1j}p_1+a_{2j}p_2+\ldots+a_{mj}p_m)}$$

for $j=1,\ldots,k$ where $2k$ is the degree of $M_1M_2-N_1N_2$, the resulting function satisfies the conditions of Theorem 2.1.

With the above transformation, the network of Fig. 2.3a is transformed into the lowpass network of Fig. 2.1.

$Z(p_1,\ldots,p_m)$ satisfies the condition

$$M_1M_2-N_1N_2 = \pm R \prod_{j=1}^{k} (a_{1j}p_1+a_{2j}p_2+\ldots+a_{mj}p_m)^2 \qquad (2.2.10)$$

where $a_{1j},\ldots,a_{mj}>0$ (with at least one of them $\neq 0$) and the sign is positive, if k is even and negative if k is odd.

Theorem 2.5

An MPRF $Z(p_1,\ldots,p_m)$ is realizable as the resistively-terminated lowpass ladder network of Fig. 2.3b, iff after applying the transformation $p_i \rightarrow 1/p_i$, $i=1,\ldots,m$ to Z, the resulting function satisfies the conditions of Theorem 2.4.

The proof is similar to that of Theorem 2.2 and hence is omitted.

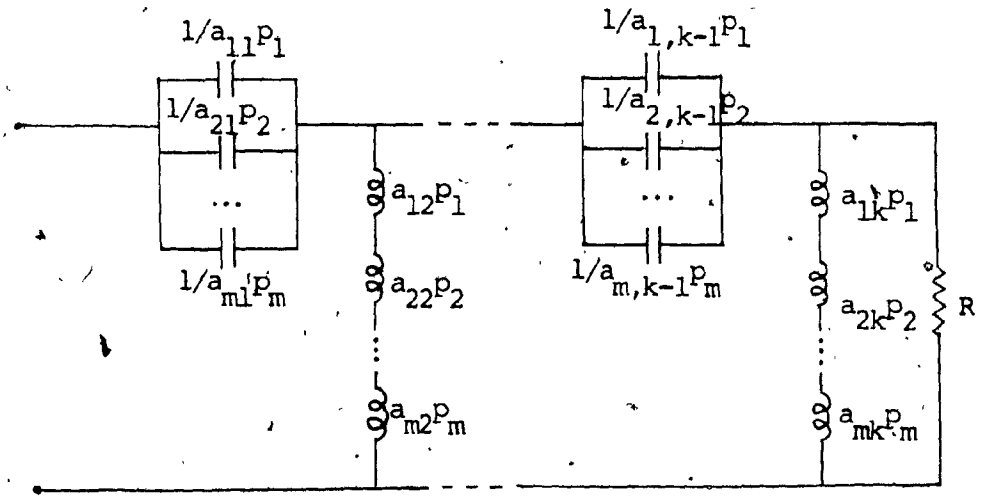

(a)

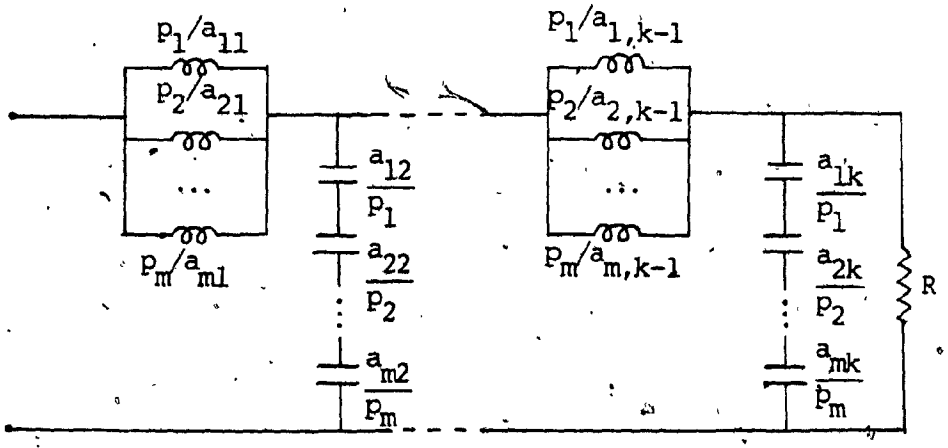

(b)

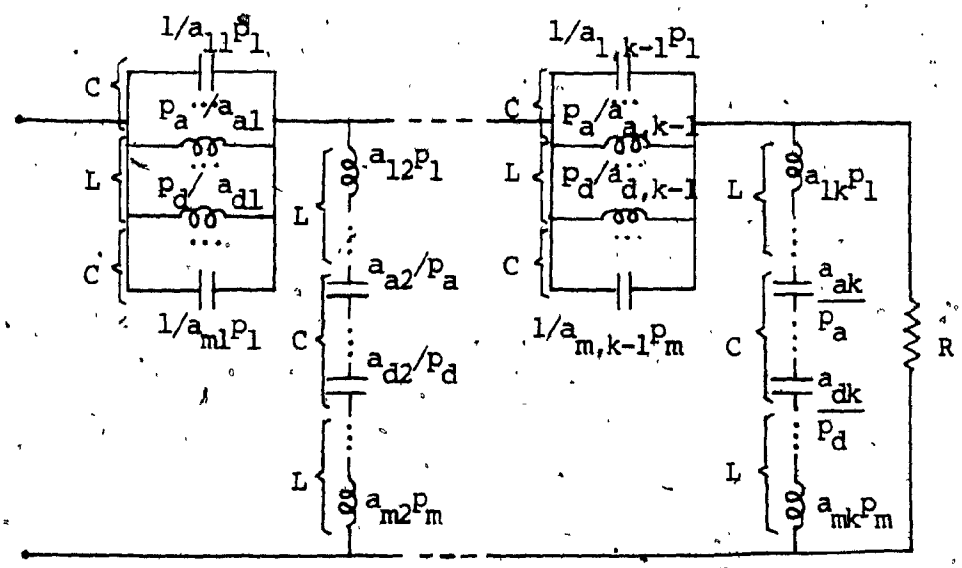

(c)

FIG. 2.3. LADDER REALIZATIONS FOR THEOREMS 2.4, 2.5 AND 2.6

Theorem 2.6

An MPRF $Z(p_1,\ldots,p_m)$ having a lowpass response in the variables p_i, $i=a,b,c,d \in m$ and a highpass response in the other variables p_i, $i=1,\ldots,m, i\neq a,b,c,d$ is realizable as the network of Fig. 2.3c, iff after applying the transformation $p_i \to 1/p_i$, $i=a,b,c,d$ to Z, the resulting function satisfies the conditions of Theorem 2.4.

The proof is similar to that of Theorem 2.2 and hence is omitted.

2.3 Realizability conditions for multivariable transfer functions

It is known that the generation of an MPRF Z from its real part is possible only when certain conditions are satisfied [59]. If for a given multivariable transfer function, a suitable driving point function can be constructed in such a way that it satisfies the conditions given in theorems of Section 2.2, then the realization of this driving point function as a resistively-terminated ladder network also realizes the given transfer function. The following theorems give conditions for the realizability of multivariable transfer functions as the ladder networks given in Figs. 2.1 to 2.3. We develop here a different multivariable array containing rows of multivariable homogeneous polynomials of even or odd degree. This array which we call as the multivariable array B is constructed from a given multivariable polynomial

$$F_1 = M_1+N_1 = \beta_n+\beta_{n-1}+\ldots+\beta_0 \qquad (2.3.1)$$

The array as given in Table 2.2 continues until it reduces to zero in the final step. As against the array A discussed earlier, the present array contains homogeneous polynomials of only the even degree or the odd degree in any particular row. If the multivariable polynomial $F_1 = M_1+N_1$ satisfies the conditions given in Table 2.2, then there exists a continued fraction expansion for M_1/N_1 and hence M_1/N_1 can be realized as a multivariable lossless ladder network. We use these conditions in the following theorems.

Theorem 2.7

Given a strictly Hurwitz m-variable polynomial M_1+N_1, where M_1 and N_1 are even and odd multivariable polynomials respectively, an MPRF $Z=(M_1+N_1)/(M_2+N_2)$ can be generated satisfying the condition $M_1M_2-N_1N_2 = R$, $R>0$, if and only if, M_1+N_1 satifies the conditions for the multivariable array given in Table 2.2.

Proof:

Necessity:- If the function $Z = (M_1+N_1)/(M_2+N_2)$ is realizable as the resistively-terminated lowpass ladder network of Theorem 2.1 satisfying the condition $M_1M_2-N_1N_2 = R$, then we can represent Z in the following manner.

$$Z = \frac{M_1+N_1}{M_2+N_2} = \frac{M_1}{N_2}\,\frac{\dfrac{N_1}{M_1}+1}{\dfrac{M_2}{N_2}+1} = z'_{11}\,\frac{\dfrac{1}{y_{22}}+1}{z_{22}+1} \qquad (2.3.2)$$

TABLE 2.2

MULTIVARIABLE ARRAY B

MULTIVARIABLE ARRAY	RELATIONSHIP	CONDITIONS
$\beta_n\beta_{n-2}\beta_{n-4}\cdots\beta_4\beta_2\beta_0$ $\beta_{n-1}\beta_{n-3}\beta_{n-5}\cdots\beta_3\beta_1$		$\frac{\beta_n}{\beta_{n-1}} = \alpha_{12} = \sum_{i=1}^{m} a_{i2}p_i$ ←(1) $a_{i2}\geq 0, \alpha_{12}\neq 0$
$\nu_{n-2}\nu_{n-4}\nu_{n-6}\cdots\nu_4\nu_2\nu_0$	$\nu_{n-i} = \beta_{n-i} - \alpha_{12}\beta_{n-i-1}$ for $i=2,4,\ldots,n-2$ & $\nu_0=\beta_0$	$\frac{\beta_{n-1}}{\nu_{n-2}} = \alpha_{22} = \sum_{i=1}^{m} b_{i2}p_i$ ←(2) $b_{i2}\geq 0, \alpha_{22}\neq 0$
$\delta_{n-3}\delta_{n-5}\delta_{n-7}\cdots\delta_3\delta_1$	$\delta_{n-i} = \beta_{n-i} - \alpha_{22}\nu_{n-i-1}$ for $i=3,5,\ldots,n-1$	$\frac{\nu_{n-2}}{\delta_{n-3}} = \alpha_{32} = \sum_{i=1}^{m} c_{i2}p_i$ ←(3) $c_{i2}\geq 0, \alpha_{32}\neq 0$
$\varepsilon_{n-4}\varepsilon_{n-6}\varepsilon_{n-8}\cdots\varepsilon_4\varepsilon_2\varepsilon_0$	$\varepsilon_{n-i} = \nu_{n-i} - \alpha_{32}\delta_{n-i-1}$ for $i=4,6,\ldots,n-2$ & $\varepsilon_0=\nu_0$	$\frac{\delta_{n-3}}{\varepsilon_{n-4}} = \alpha_{42} = \sum_{i=1}^{m} d_{i2}p_i$ ←(4) $d_{i2}\geq 0, \alpha_{42}\neq 0$
...	...	...

where z and y represent the open circuit impedance and short circuit admittance parameters respectively. M_1/N_1 can be interpreted from the above as the y_{22} of the lossless part of the above network.

Sufficiency: If M_1+N_1 satisfies the conditions given in Table 2.2, then M_1/N_1 or N_1/M_1 is realizable as a lossless lowpass ladder network with the series arms containing inductors in different variables connected in series and the shunt arms consisting of capacitors in different variables connected in parallel. The transmission zeros of such a network all lie at $p_i=\infty$, $i=1,\ldots,m$ independent of the other variables p_j, $j=1,\ldots,m$, $j\neq i$. If this ladder network is terminated in a resistance of 1 Ohm, then the input impedance of the resulting network is given by

$$z_1 = \frac{M_2+N_2}{M_1+N_1} = \frac{M_2}{N_1}\,\frac{\frac{N_2}{M_2}+1}{\frac{M_1}{N_1}+1} \qquad (2.3.3.)$$

$$= z'_{11}\,\frac{\frac{1}{y'_{22}}+1}{z'_{22}+1}$$

where M_1/N_1 is interpreted as the z_{22}' of the lossless network. The dual of this network realizes Z, satisfying (2.3.1). Both Z as well as Z_1, satisfy the condition $M_1M_2-N_1N_2 = R$. The procedure for the generation of a driving point function satisfying $M_1M_2-N_1N_2 = R$ is to synthesize M_1/N_1 as the z_{22}' of a lossless lowpass ladder network, terminate it with a resistance R and then find the dual of this network.

Theorem 2.8

The necessary and sufficient conditions for an m-variable rational function $T(p_1,\ldots,p_m)$ to be realizable as the voltage transfer function of the resistively-terminated lossless lowpass ladder network of Fig. 2.1, with all its transmission zeros at $p_i=\infty$, $i=1,\ldots,m$ are

(i) $T(p_1,\ldots,p_m)$ is expressible in the form
$T(p_1,\ldots,p_m) = K/(M_1+N_1)$ where $K>0$
is an arbitrary real constant.

(ii) M_1+N_1 satisfies the conditions of Theorem 2.7.

Proof:

Necessity: As all the transmission zeros of the network function are at $p_i=\infty$, $i=1,\ldots,m$, the transfer function $T(p_1,\ldots,p_m)$ is an all pole function of the form $K/(M_1+N_1)$ with $K>0$ and M_1+N_1 strictly Hurwitz. The driving point impedance of the network is of the form

$Z(p_1,\ldots,p_m) = (M_1+N_1)/(M_2+N_2)$ where $M_1M_2-N_1N_2=R$,

$R>0$

and M_1/N_1 is the y_{22} of the network.

Sufficiency:- If M_1/N_1 (or N_1/M_1) can be synthesized as the z_{22} of a lossless lowpass ladder network of the given type and if this network is terminated in a resistance of 1 Ohm at the output port, then the input impedance of the terminated network is given by

$$Z' = \frac{M_2+N_2}{M_1+N_1} = \frac{M_2}{N_1}\,\frac{\frac{N_2}{M_2}+1}{\frac{M_1}{N_1}+1} \quad \left(\text{or } \frac{N_2}{M_1}\,\frac{\frac{M_2}{N_2}+1}{\frac{N_1}{M_1}+1}\right) \qquad (2.3.4)$$

The dual of the above network realizes the driving point impedance $Z = (M_1+N_1)/(M_2+N_2)$ and its transfer function is of the form

$$T(p_1,\ldots,p_m) = K/(M_1+N_1) \qquad (2.3.5)$$

It must be noted that Z satisfies all the conditions of the array A in Table 2.1. Hence if M_1+N_1 satisfies the array B conditions in Table 2.2, an array A can always be generated by using M_1/N_1.

Example 2.2

$$T(p_1,p_2,p_3) = \frac{1}{M_1+N_1} = \frac{1}{(48p_1^2p_2^2+32p_1^2p_2p_3+40p_1p_2^2p_3+60p_1p_2p_3^2)}$$
$$+ (12p_1p_3^2+15p_2p_3^2+10p_2^2p_3+8p_1p_2p_3) +$$
$$(16p_1^2+20p_2^2+36p_1p_2+28p_1p_3+30p_2p_3)+$$
$$(4p_1+5p_2+p_3) + 2$$
$$= \frac{1}{\beta_4+\beta_3+\beta_2+\beta_1+\beta_0}$$

Since M_1+N_1 satisfies the multivariable array conditions of Table 2.2, M_1/N_1 can be expanded in the continued fraction form as

$$\frac{M_1}{N_1} = 4p_1 + \cfrac{1}{\frac{p_3}{2} + \cfrac{1}{6p_3+4p_2 + \cfrac{1}{2p_1 + \frac{5}{2}p_2}}}$$

The lossless ladder network is realized by considering M_1/N_1 as the z_{22} of the ladder and it is terminated in a resistance of 1 Ohm as shown in Fig. 2.4a. The dual of this network given in Fig. 2.4b realizes the transfer function $T(p_1,p_2,p_3)$. The transfer function is realized with a multiplying constant equal to 2.

Theorem 2.9

An m-variable transfer function $T(p_1,\ldots,p_m)$ is realizable as a resistively-terminated lossless ladder network

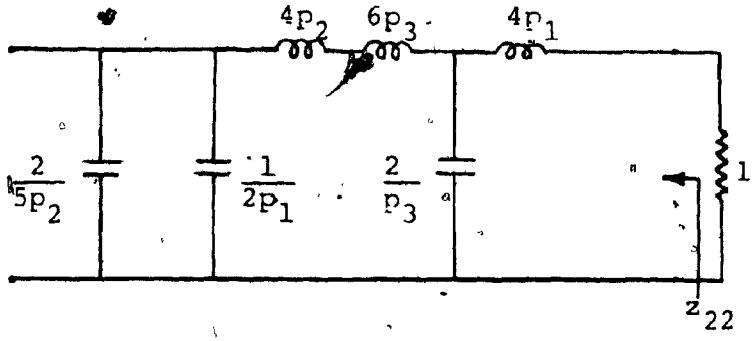

(a)

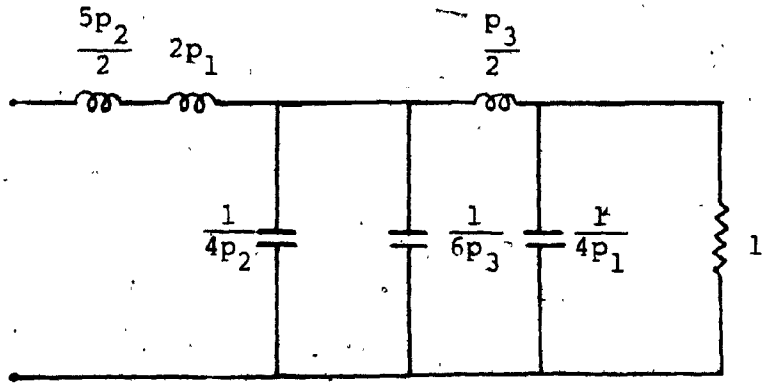

(b)

FIG. 2.4 REALIZATION OF THE TRANSFER FUNCTION GIVEN IN EXAMPLE 2.3

(A) NETWORK REALIZATION FOR M_1/N_1 AS z_{22}

(B) DUAL OF THE NETWORK IN (a)

of the type given in an one of the Figures 2.2a, 2.2b, 2.3a, 2.3b, or 2.3c, iff after performing the respective transformations as indicated in Table 2.3, the resulting transfer function satisfies the conditions of Theorem 2.8.

With the transformations indicated in Table 2.3, the given transfer functions are transformed into the lowpass all-pole transfer function realized by the network of Fig. 2.1.

We have discussed here only some types of reactance transformations. Ladder networks with bandpass or bandstop responses in any particular variable can be obtained by using suitable single-variable reactance transformations.

The realizability of the highpass ladder network of Fig. 2.2a can also be tested directly by the continued fraction of M_1/N_1 about the origin. Similarly the extraction of the ladder network of Fig. 2.2b can be carried out by continued fraction expansion around the origin for p_i, i=a,b,c,d and around infinity for the other variables. In general the realizability conditions for the networks given in Figs. 2.2 & 2.3 can be stated as follows.

(i) $T(p_1,\ldots,p_m)$ is of the form $\sqrt{M_1M_2-N_1N_2}/(M_1+N_1)$ where the numerator is as defined in Table 2.3 for each case.

(ii) M_1/N_1 (or N_1/M_1) is synthesizable as a lossless ladder network of the type which corresponds to the lossless portion of the particular network in Figs. 2.2 & 2.3.

TABLE 2.3

REACTANCE TRANSFORMATION USED TO OBTAIN NETWORKS IN FIGS. 2.2 & 2.3

Case	Fig.	$(M_1M_2-N_1N_2)$	Transformation
1	2.2a	$\pm R \prod_{i=1}^{m} p_i^{2k_i}$	$p_i \to \frac{1}{p_i}$, i=1,...,m
2	2.2b	$\pm R \prod_{i=a,b,c,d} p_i^{2k_i}$	$p_i \to \frac{1}{p_i}$, i=a,b,c,d
3	2.3a	$\pm R \prod_{j=1}^{k} (a_{1j}p_1+a_{2j}p_2+\ldots+a_{mj}p_m)^2$	$(a_{1j}p_1+a_{2j}p_2+\ldots+a_{mj}p_m) \to \frac{1}{(a_{1j}p_1+a_{2j}p_2+\ldots+a_{mj}p_m)}$ for i=1,...,k
4	2.3b	$\pm R \prod_{j=1}^{k} (\sum_{i=1}^{m} c_{ij} \prod_{\substack{\ell=1 \\ \ell\neq i}}^{m} p_\ell)^2$	$p_i \to \frac{1}{p_i}$, i=1,...,m and the transformation of case 3
5	2.3c	$\pm R \prod_{j=1}^{k} \{ p_a p_b p_c p_d (\sum_{\substack{i=1 \\ i\neq a,b,c,d}}^{m} a_{ij}p_i) + \sum_{q=a,b,c,d} c_{qj} \prod_{\substack{\ell=a,b,c,d \\ \ell\neq q}} p_\ell \}^2$	$p_i \to \frac{1}{p_i}$, i=a,b,c,d and the transformation of case 3

The realization of a multivariable transfer function is assured only after extraction of the ladder network from M_1/N_1 (or N_1/M_1); however, this becomes a part of the process in the realization of the transfer function. All the given ladder forms are related by the set of reactance transformations indicated in Table 2.3.

2.4 Synthesis of cascade separable two-variable ladder networks

We discuss here a particular case of the above ladder realization in which the elements in each variable are grouped together in the continued fraction expansion thereby resulting in a network which is a cascade connection of two-port lossless ladder networks in each variable, terminated in a load resistance. The properties of such a network have been studied in detail and the driving point impedance of this network has been classified as a 'cascade separable function'. For a two-variable case, this results in a network which is a cascade of p_1 and p_2-variable lossless ladder networks terminated in a load resistance, as shown in Fig. 2.5a [60]. Realization of such cascade separable network functions using the Darlington type of synthesis have been discussed in [61], [62] and [63]. The necessary and sufficient conditions for a two-variable positive real function (TPRF) to be realized in the above fashion include the condition of cascade separability for the given TPRF and the real part conditions in each variable [60].

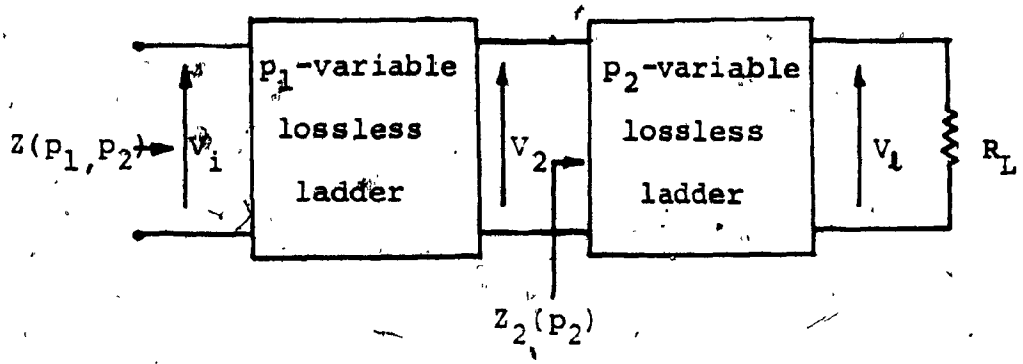

(a)

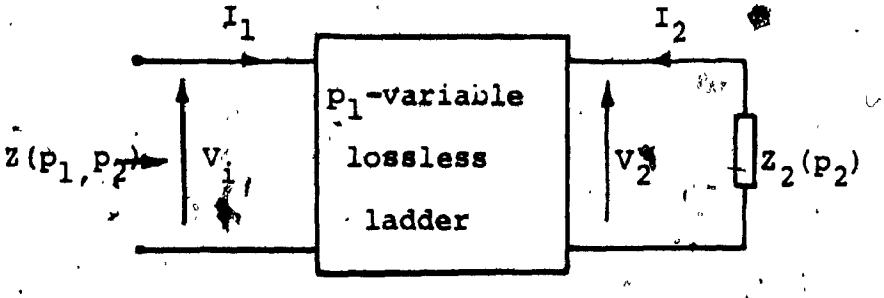

(b)

FIG. 2.5 (a) THE CASCADE SEPARABLE LADDER NETWORK AND (b) ITS EQUIVALENT

Here we find the conditions under which the p_1 and p_2 two-port networks can be either LP, HP, BP or BS type. These are useful in synthesis and in generation of two-variable cascade separable transfer functions of different types. It is shown later that the doubly-terminated cascade separable network is particularly useful since it exhibits good symmetry properties in its frequency response. In a subsequent Chapter, we describe how these conditions can be translated into the digital domain.

Theorem 2.10

The necessary and sufficient conditions for a TPRF $Z(p_1,p_2)$ to be expressible as the driving point impedance of a cascade of p_1 and p_2 ladder networks terminated in a resistance (where the p_2 network follows the p_1 network) are

(i) $Z(p_1,p_2)$ is cascade expressible, i.e., in the form

$$Z(p_1,p_2) = \frac{M_{11}(p_1)P(p_2) + N_{11}(p_1)Q(p_2)}{M_{21}(p_1)Q(p_2) + N_{21}(p_1)P(p_2)} \qquad (2.4.1)$$

where $M_{11}(p_1)$ and $M_{21}(p_1)$ are even polynomials in p_1, $N_{11}(p_1)$ and $N_{21}(p_1)$ are odd polynomials in p_1 and $P(p_2) = M_{12}(p_2)+N_{12}(p_2)$ and $Q(p_2) = M_{22}(p_2) + N_{22}(p_2)$ are polynomials in the variable p_2 with $M_{12}(p_2)$ and $M_{22}(p_2)$ as even and $N_{12}(p_2)$ and $N_{22}(p_2)$ as odd polynomials.

$$\text{(ii)} \quad M_{1i}(p_i)M_{2i}(p_i) - N_{1i}(p_i)N_{2i}(p_i) = R_i[S_i(p_i)]^2 \tag{2.4.2}$$

for $i=1,2$ where R_i is a non-zero constant and $S_i(p_i)$ is a polynomial in p_i of the form given in Table 2.4.

Proof:

The general proof of this heorem for a multivariable case, is available in [58]. Considering the equivalent of Fig. 2.5a, given in Fig. 2.5b, the driving point impedance is of the form

$$Z(p_1,p_2) = \frac{M_{11}(p_1)Z_2(p_2)+N_{11}(p_1)}{M_{21}(p_1)+N_{21}(p_1)Z_2(p_2)} \tag{2.4.3}$$

If $Z_2(p_2) = 1$, then

$$Z(p_1,p_2) = Z_1(p_1) = \frac{M_{11}(p_1)+N_{11}(p_1)}{M_{21}(p_1)+N_{21}(p_1)} \tag{2.4.4}$$

is the driving point impedance of the p_1 lossless network terminated in 1 Ohm. For Darlington type of synthesis, the open circuit parameter z_{12} for the p_1 network as well as the p_2 network must be a rational function, which imposes the condition (ii) that the real part in each case is a square of the polynomial in the particular variable. The specific cases under which the p_1 and p_2 networks can be LP, HP, BP or BS are listed below. The real part conditions are given below for each case.

Case 1. (LP + LP):

For the p_1 and p_2 networks to be LP ladders,

$$M_{1i}(p_i)M_{2i}(p_i) - N_{1i}(p_i)N_{2i}(p_i) = R_i \qquad (2.4.5)$$

for $i=1,2$ where $R_i>0$.

Here

$$z_{12}(i) = z_{21}(i) = \frac{\sqrt{R_i}}{N_{2i}(p_i)}$$

and (2.4.6)

$$z_{11}(i) = \frac{M_{1i}(p_i)}{N_{2i}(p_i)} \quad \text{for} \quad i=1,2$$

Since all the transmission zeros lie at $p_i=\infty$, the p_1 and p_2 networks are realized as lowpass ladders.

In this case, the array A in Table 2.1 is satisfied with extra conditions as follows.

(i) a_{11}, a_{21}, etc. are single degree terms only in a single variable (either p_1 alone or p_2 alone).

(ii) The terms in p_1 occur first followed by the terms in p_2.

Case 2. (HP + HP):

For the p_1 and p_2 networks to be HP ladders,

$$M_{1i}(p_i)M_{2i}(p_i) - N_{1i}(p_i)N_{2i}(p_i) = R_i p_i^{2n_i} \qquad (2.4.7)$$

for $i=1,2$ where R_i is a non-zero constant and n_i is the degree of p_i in $Z_i(p_i)$. R_i is positive for even n_i and negative for odd n_i. For this case,

$$z_{12}(i) = z_{21}(i) = \frac{\sqrt{R_i}\, p_i^{n_i}}{N_{2i}(p_i)} \quad \text{and}$$

$$z_{11}(i) = \frac{M_{1i}(p_i)}{N_{2i}(p_i)}, \quad i=1,2 \tag{2.4.8}$$

for positive R_i and

$$z_{12}(i) = z_{21}(i) = \frac{\sqrt{-R_i}\, p_i^{n_i}}{M_{2i}(p_i)} \quad \text{and}$$

$$z_{11}(i) = \frac{N_{1i}(p_i)}{M_{2i}(p_i)}, \quad i=1,2 \tag{2.4.9}$$

for negative R_i.

Since the transmission zeros lie at $p_i=0$ $(i=1,2)$, the p_1 and p_2 ladder networks can be synthesized as highpass ladder networks.

Case 3 (BP + BP):

For the p_1 and p_2 networks to be bandpass type ladders,

$$M_{1i}(p_i)M_{2i}(p_i) - N_{1i}(p_i)N_{2i}(p_i) = R_i p_i^{2k_i} \tag{2.4.10}$$

where $2k_i$ is the degree of p_i in $Z_i(p_i)$ and $R_i \neq 0$, is

positive if k_i is even and negative if k_i is odd. For positive R_i, the open circuit parameters are

$$z_{12}(i) = z_{21}(i) = \sqrt{R_i}\, p_i^{k_i}/N_{2i}(p_i)$$

and (2.4.11)

$$z_{11}(i) = M_{1i}(p_i)/N_{2i}(p_i)$$

and for negative R_i, they are

$$z_{12}(i) = z_{21}(i) = \sqrt{-R_i}\, p_i^{k_i}/M_{2i}(p_i)$$

and (2.4.12)

$$z_{11}(i) = N_{1i}(p_i)/M_{2i}(p_i)$$

for $i=1,2$.

Case 4. (BS + BS):

For the p_1 and p_2 networks to be bandstop type ladders,

$$M_{1i}(p_i)M_{2i}(p_i)-N_{1i}(p_i)N_{2i}(p_i) = R_i[S_i(p_i)]^2 \qquad (2.4.13)$$

where $R_i>0$ and $S_i(p_i)$ is a polynomial in p_i of the form

$$S_i(p_i) = (p_i^2+1)^{k_i}$$

where $2k_i$ is the degree of p_i in $Z_i(p_i)$, for $i=1,2$. The open circuit parameters are

$$z_{12}(i) = \sqrt{R_i}\, S_i(p_i)/N_{2i}(p_i) \quad \text{and}$$

$$z_{11}(i) = M_{1i}(p_i)/N_{2i}(p_i) \qquad (2.4.14)$$

for $i=1,2$.

The above conditions are listed in Table 2.4.

The transfer function V_ℓ/V_i for the network of Fig. 2.5 is given by

$$T(p_1,p_2) = \frac{V_\ell}{V_i} = \frac{R_L z_2(p_2) z_{21a} z_{21b}}{(\Delta z_a + z_{11a} z_2(p_2))(\Delta z_b + z_{11b} R_L)} \qquad (2.4.15)$$

where $\Delta z_a = z_{11a}z_{22a} - z_{12a}z_{21a}$,

$\Delta z_b = z_{11b}z_{22b} - z_{12b}z_{21b}$

and the subscripts a and b denote the p_1 and p_2 networks respectively. This is obtained from

$$\frac{V_2}{V_i} = \frac{z_2(p_2) z_{21a}}{\Delta z_a + z_{11a} z_2(p_2)} \quad \text{and} \quad \frac{V_\ell}{V_2} = \frac{R_L z_{21b}}{\Delta z_b + z_{11b} R_L} \qquad (2.4.16)$$

where V_2 is the voltage at the input port of the p_2 network and

$$z_2(p_2) = z_{11b} - \frac{z_{12b}z_{21b}}{R_L + z_{22b}} = \frac{z_{11b}R_L + \Delta z_b}{R_L + z_{22b}} \qquad (2.4.17)$$

TABLE 2.4

Real Part Conditions For Different Types of Ladder Networks

	Type of network function in p_1 and p_2	$M_{1i}(p_i)M_{2i}(p_i)-N_{1i}(p_i)N_{2i}(p_i)$ for i=1,2
(1)	LP + LP	R_i with $R_i>0$ for i=1,2
(2)	LP + HP	R_1 with $R_1>0$ for i=1 $(-1)^{n_2}R_2p_2^{2n_2}$, $R_2>0$ for i=2
(3)	LP + BP	R_1 with $R_1>0$ for i=1 $(-1)^{k_2}R_2p_2^{2k_2}$, $R_2>0$ for i=2
(4)	LP + BS	R_1 with $R_1>0$ for i=1 $R_2(p_2^2+1)^{2k_2}$, $R_2>0$ for i=2
(5)	HP + LP	$(-1)^{n_1}R_1p_1^{2n_1}$, $R_1>0$ for i=1 R_2 with $R_2>0$ for i=2
(6)	HP + HP	$(-1)^{n_i}R_ip_i^{2n_i}$, $R_i>0$ for i=1,2
(7)	HP + BP	$(-1)^{n_1}R_1p_1^{2n_1}$, $R_1>0$ for i=1 $(-1)^{k_2}R_2p_2^{2k_2}$, $R_2>0$ for i=2
(8)	HP + BS	$(-1)^{n_1}R_1p_1^{2n_1}$, $R_1>0$ for i=1 $R_2(p_2^2+1)^{2k_2}$, $R_2>0$ for i=2

TABLE 2.4

Real Part Conditions for Different Types of Ladder Networks

	Type of network function in p_1 and p_2	$M_{1i}(p_i)M_{2i}(p_i)-N_{1i}(p_i)N_{2i}(p_i)$ for i=1,2
(9)	BP + LP	$(-1)^{k_1} R_1 p_1^{2k_1}$, $R_1>0$ for i=1
		R_2 with $R_2>0$ for i=2
(10)	BP + HP	$(-1)^{k_1} R_1 p_1^{2k_1}$, $R_1>0$ for i=1
		$(-1)^{n_2} R_2 p_2^{2n_2}$, $R_2>0$ for i=2
(11)	BP + BP	$(-1)^{k_i} R_i p_i^{2k_i}$, $R_i>0$ for i=1,2
(12)	BP + BS	$(-1)^{k_1} R_1 p_1^{2k_1}$, $R_1>0$ for i=1
		$R_2(p_2^2+1)^{2k_2}$, $R_2>0$ for i=2
(13)	BS + LP	$R_1(p_1^2+1)^{2k_1}$, $R_1>0$ for i=1
		R_2 with $R_2>0$ for i=2
(14)	BS + HP	$R_1(p_1^2+1)^{2k_1}$, $R_1>0$ for i=1
		$(-1)^{n_2} R_2 p_2^{2n_2}$, $R_2>0$ for i=2
(15)	BS + BP	$R_1(p_1^2+1)^{2k_1}$, $R_1>0$ for i=1
		$(-1)^{k_2} R_2 p_2^{2k_2}$, $R_2>0$ for i=2
(16)	BS + BS	$R_i(p_i^2+1)^{2k_i}$, $R_i>0$ for i=1,2

By representing

$$z_{11a} = M_{11}/M_{21},\ z_{22a} = M_{21}/N_{21},\ y_{22a} = M_{11}/N_{11}$$

$$z_{11b} = M_{12}/N_{22},\ z_{22b} = M_{22}/N_{22},\ y_{22b} = M_{12}/N_{12} \qquad (2.4.18)$$

for p_1 and p_2 passive networks obeying reciprocity, we can also write $T(p_1,p_2)$ in the form

$$T(p_1,p_2) = \frac{R_L\sqrt{M_{11}M_{21}-N_{11}N_{21}}\ \sqrt{M_{12}M_{22}-N_{12}N_{22}}}{M_{11}(N_{12}+M_{12}R_L) + N_{11}(M_{22}+N_{22}R_L)} \qquad (2.4.19)$$

where M_{11}, M_{21}, N_{11} & N_{21} are polynomials in p_1 and M_{12}, M_{22}, N_{12} & N_{22} are polynomials in p_2.

Hence a cascade separable two-variable transfer function is of the form

$$T(p_1,p_2) = \frac{KS_1(p_1)S_2(p_2)}{M_{11}(p_1)P(p_2) + N_{11}(p_1)Q(p_2)} \qquad (2.4.20)$$

where K is a constant,

$$S_1(p_1) = \sqrt{M_{11}(p_1)M_{21}(p_1) - N_{11}(p_1)N_{21}(p_1)} \quad \text{and}$$

$$S_2(p_2) = \sqrt{M_{12}(p_2)M_{22}(p_2) - N_{12}(p_2)N_{22}(p_2)}$$

The conditions for $S_1(p_1)$ and $S_2(p_2)$ for different types of ladder networks, can be obtained from Table 2.4.

The HP, BP and BS transfer functions are related to the

LP transfer function by the following normalized reactance transformations [64].

$$\begin{aligned} &\text{LP to HP:} \quad p \rightarrow 1/p \\ &\text{LP to BP:} \quad p \rightarrow p + 1/p \\ &\text{LP to BS:} \quad p \rightarrow 1/(p+1/p) \end{aligned} \tag{2.4.21}$$

2.5 Summary and Conclusions

In this chapter, a new multivariable array has been proposed using which the conditions for a continued fraction expansion of an MPRF are obtained. This array is made up of homogeneous polynomials which may have missing terms in any of the variables. If these conditions are satisfied, then the given MPRF is realizable as the resistively-terminated multivariable lossless ladder network shown in Fig. 2.1. By the use of reactance transformtions other ladder networks are obtained. The realization discussed here can be considered to be a more general type of multivariable ladder realization compared to the existing ones because of the fact that in each arm of the ladder,

(i) the elements can be in any variable and

(ii) some of the variables can be missing.

Another multivariable array B containing homogeneous polynomials (in which some variables can be missing) of either odd or even degree in each row of the array, is constructed from a given MHP M_1+N_1 and conditions for the continued

fraction expansion of M_1/N_1 are obtained. It is shown that an all-pole transfer function $T=K/(M_1+N_1)$ is realizable as the LP ladder network of Fig. 2.1, iff M_1+N_1 satisfies the conditions of array B. This means that an MPRF Z satisfying the conditions in array A can be generated for the given transfer function iff the conditions of array B are satisfied. Testing for the above conditions actually forms part of the realization procedure.

The cascade separable ladder realization is shown to be a particular case of the above, in which the elements in any particular variable are grouped together, thus resulting in a cascade connection of lossless 2-ports in each variable. The conditions for the realization of a TPRF as a singly-terminated cascade separable ladder network in which the p_1 or the p_2 network can be either LP, HP, BP or BS are obtained. This is done with a view to extend these conditions to the digital domain and to facilitate generation of cascade separable transfer functions.

CHAPTER 3.

DOUBLY-TERMINATED MULTIVARIABLE NETWORKS

3.1 Introduction

Doubly terminated ladder networks in single variable have been found to be having good sensitivity properties if the termination resistances are equal. It is presumed here that these properties are carried over to the case of multivariable ladder networks also. In the previous chapter, the conditions for the synthesis of singly-terminated multivariable lossless ladder networks have been studied. A general procedure for synthesis of a doubly-terminated multivariable ladder network is presently not possible since no method is yet available for multivariable polynomial factorization and for the synthesis of MPRFs. Therefore it is of interest to study methods for the generation of doubly-terminated network transfer functions. We study here the generation of transfer functions for doubly-terminated multivariable ladder networks, using either or both of the arrays A and B described in Chapter 2. The special case of a doubly-terminated cascade separable network is studied in detail and two methods are outlined for the generation of a transfer function for this type of network. These two methods are used later for the approximation of two-variable transfer functions.

3.2 Generation of doubly-terminated network transfer functions

If a source resistance R_s is added as the input termination to a singly-terminated network, then the driving-point impedance of the resulting network is given by

$$Z = R_s + \frac{M_1+N_1}{M_2+N_2} = \frac{M_a+N_a}{M_b+N_b} \qquad (3.2.1)$$

where $(M_1+N_1)/(M_2+N_2)$ obeys the conditions of the multivariable array A. From (3.2.1) we have the following relationships.

$$M_a = M_1+R_sM_2 \qquad N_a = N_1+R_sN_2$$
$$M_b = M_2 \qquad N_b = N_2 \qquad (3.2.2)$$

Hence M_b+N_b satisfies the conditions of array B. Also from (3.2.2), the numerator of the even part of Z is given by

$$M_aM_b-N_aN_b = (M_1M_2-N_1N_2)+R_s(M_2^2-N_2^2)$$
$$= R+R_s(M_b^2-N_b^2) \qquad (3.2.3)$$

Given an MPRF $Z = (M_a+N_a)/(M_b+N_b)$, it is easy to compute $M_b^2 - N_b^2$ and compare it with the $Nu(Ev.Z)$ in (3.2.3) and find the value of R_s. If after the removal of R_s from Z, the remaining function satisfies the conditions of the multivariable array A, then Z is realized as the driving

point impedance of a doubly-terminated multivariable network.

The voltage transfer function for such a network is given by

$$T = \frac{K}{M_1+N_1+R_s(M_2+N_2)} = \frac{K}{M_a+N_a} \qquad (3.2.4)$$

where K is a non-zero constant. The following properties of T shall be noted:

(1) Unlike the case of singly-terminated networks, M_a+N_a does not satisfy the conditions of the multivariable array B. Hence M_a/N_a (or N_a/M_a) cannot be expanded in the continued fraction form.

(2) The denominator of T is decomposable in the form indicated in (3.2.4).

(3) $(M_1+N_1)/(M_2+N_2)$ satisfies the conditions of the multivariable array A and hence is realizable as a resistively-terminated lossless multivariable lowpass ladder network. The all-pole transfer function T represents a lowpass multivariable network with all its transmission zeros at $p_i=\infty$, $i=1,\ldots,m$.

In general, if any MPRF $F = (M_1+N_1)/(M_2+N_2)$ is realizable as a singly-terminated multivariable ladder network, then the transfer function for this network with an input termination R_s included, is given by

$$T = \sqrt{M_1M_2-N_1N_2}/[(M_1+N_1)+R_s(M_2+N_2)] \qquad (3.2.5)$$

This leads to a general procedure for the generation of multivariable doubly-terminated network transfer functions as follows.

(1) An MHP M_1+N_1 is chosen satisfying the conditions of the multivariable array B.

(2) The MPRF $F = (M_1+N_1)/(M_2+N_2)$ is generated from the above, satisfying the condition $M_1M_2 - N_1N_2 = R$, by using the procedure described in Chapter 2.

(3) Using the function F, the multivariable all-pole transfer function $T = K/[(M_1+N_1) + R_s(M_2+N_2)]$ is generated. This transfer function represents a doubly-terminated multivariable lowpass ladder network whose input termination is a resistance R_s.

The above procedure can be extended to other types of ladder networks as well, by the use of reactance transformations described in Chapter 2.

3.3 Doubly-terminated cascade separable ladder networks

In this section, we discuss two methods of transfer function generation for the case of the doubly-terminated cascade separable ladder networks.

3.3.1. Generation by method 1

In the case of the cascade separable network, the MHP M_1+N_1 we start with, is such that M_1/N_1 (or N_1/M_1)

is synthesizable as the cascade of lossless two-port ladder networks in each of the variables. We consider the case of a two-variable doubly-terminated cascade separable network shown in Fig. 3.1a.

This network can be considered as equivalent to a single-variable network with a source resistance R_s and a load of $Z_2(p_2)$ where $Z_2(p_2)$ is the driving point impedance of the resistively-terminated p_2 network, as shown in Fig. 3.1b. In terms of the open circuit impedance parameters of the p_1 network, the driving point impedance $Z(p_1,p_2)$ of the two-variable network is given by

$$Z(p_1,p_2) = R_s + z_{11a} - \frac{z_{12a}z_{21a}}{Z_2(p_2)+z_{22a}} \qquad (3.3.1.1)$$

where the subscript 'a' denotes the p_1 network and

$$\begin{aligned} z_{12a}z_{21a} &= z_{11a}z_{22a} - \Delta z_a \\ &= z_{11a}z_{22a} - (z_{11a}/y_{22a}) \end{aligned} \qquad (3.3.1.2)$$

With

$$z_{11a} = M_{11}(p_1)/N_{21}(p_1),\ z_{22a} = M_{21}(p_1)/N_{21}(p_1) \quad \text{and} \quad y_{22a} = M_{11}(p_1)/N_{11}(p_1) \qquad (3.3.1.3)$$

where the M's and N's are even and odd polynomials respectively in p_1, we have

$$Z(p_1,p_2) = \frac{Z_2(p_2)[M_{11}(p_1)+R_sN_{21}(p_1)]+[R_sM_{21}(p_1)+N_{11}(p_1)]}{M_{21}(p_1) + Z_2(p_2)N_{21}(p_1)} \qquad (3.3.1.4)$$

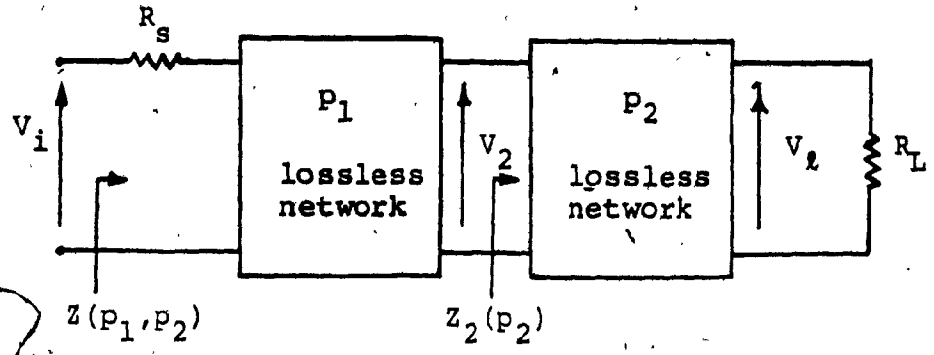

(a)

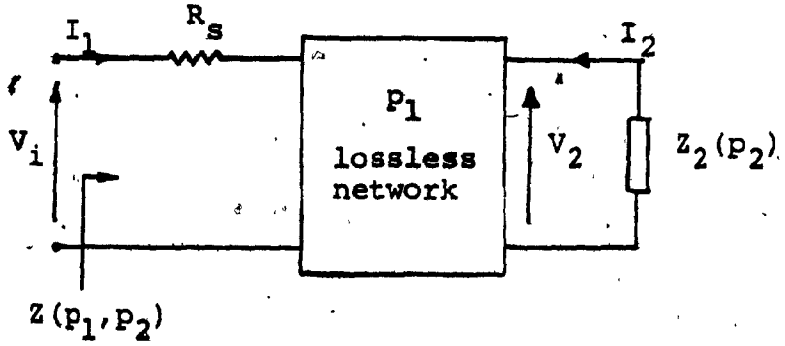

(b)

FIG. 3.1 (a) THE DOUBLY-TERMINATED CASCADE SEPARABLE NETWORK AND (b) ITS EQUIVALENT

If $Z_2(p_2) = P(p_2)/Q(p_2)$, then

$$Z(p_1,p_2) = \frac{[M_{11}(p_1)+R_s N_{21}(p_1)]P(p_2)+[R_s M_{21}(p_1)+N_{11}(p_1)]Q(p_2)}{M_{21}(p_1)Q(p_2) + N_{21}(p_1)P(p_2)} \tag{3.3.1.5}$$

This result can also be obtained by directly adding R_s to the driving point impedance of the singly-terminated network given in (2.4.3).

The voltage transfer function for the network of Fig. 3.1a is given by

$$T = \frac{V_\ell}{V_i} = \frac{R_L Z_2(p_2) z_{21a} z_{21b}}{[\Delta z_a + R_s z_{22a} + (z_{11a}+R_s)Z_2(p_2)](\Delta z_b + z_{11b} R_L)} \tag{3.3.1.6}$$

Since $Z_2(p_2) = (z_{11b}R_L + \Delta z_b)/(R_L + z_{22b})$ (3.3.1.7)

we have

$$T = \frac{R_L z_{21a} z_{21b}}{(\Delta z_a + R_s z_{22a})(R_L + z_{22b}) + (z_{11a}+R_s)(z_{11b}R_L + \Delta z_b)} \tag{3.3.1.8}$$

or

$$T = \frac{R_L \sqrt{M_{11}M_{21} - N_{11}N_{21}} \quad \sqrt{M_{12}M_{22} - N_{12}N_{22}}}{(M_{21}R_s + N_{11})(M_{22}+N_{22}R_L) + (M_{11}+N_{21}R_s)(M_{12}R_L + N_{12})} \tag{3.3.1.9}$$

where M_{11}, M_{21}, N_{11}, N_{21} are functions of p_1 and M_{12}, M_{22}, N_{12}, N_{22} are functions of p_2.

From the above expressions, we can state the properties of a lowpass doubly-terminated cascade separable betwork as follows:

A lowpass all-pole function $T(p_1,p_2)$ is realized as the transfer function of a doubly-terminated cascade of p_1 and p_2 lossless lowpass ladder networks if

(1) $T(p_1,p_2)$ is expressible in the form

$$T(p_1,p_2) = 1/D(p_1,p_2) = \frac{K}{[M_{11}(p_1)+N_{21}(p_1)][M_{12}(p_2)+N_{12}(p_2)] + [M_{21}(p_1)+N_{11}(p_1)][M_{22}(p_2)+N_{22}(p_2)]} \qquad (3.3.1.10)$$

where K is a constant, M's are even polynomials and N's are odd polynomials.

(2) $M_{1i}(p_i)\, M_{2i}(p_i) - N_{1i}(p_i)\, N_{2i}(p_i)$ (3.3.1.11)

$= R_i$, $R_i > 0$ for $i=1,2$.

If $T(p_1,p_2)$ is separable in the denominator as in (1) and also satisfies (2), then the p_1 network is obtained by choosing

$$Z_1(p_1) = \frac{M_{11}(p_1)+N_{11}(p_1)}{M_{21}(p_1)+N_{21}(p_1)} \quad \text{and} \quad Z_2(p_2) = \frac{P(p_2)}{Q(p_2)} = \frac{M_{12}(p_2)+N_{12}(p_2)}{M_{22}(p_2)+N_{22}(p_2)} \qquad (3.3.1.12)$$

The decomposition of the denominator polynomial in the above fashion is not always unique as shown below in the example 3.2. All such possible decompositions have to be tested for the property (2).

Example 3.1

$$T(p_1,p_2) = \frac{1}{30p_1^2p_2^2+30p_1^2p_2+15p_1p_2^2+17p_1p_2+10p_1^2 + 3p_2^2+7p_1+4p_2+2}$$

$$= 1/D(p_1,p_2)$$

The denominator polynomial is decomposed into the required form as follows.

$$D(p_1,p_2) = p_2^2(30p_1^2+15p_1+3)+p_2(30p_1^2+17p_1+4) +(10p_1^2+7p_1+2)$$

Separating the terms containing even powers and odd powers of p_1,

$$D(p_1,p_2) = p_2^2(30p_1^2+3)+p_2(30p_1^2+4)+(10p_1^2+2) + p_2^2(15p_1)+p_2(17p_1)+7p_1$$

$$= 10p_1^2(3p_2^2+3p_2+1)+(3p_2^2+3p_2+1)+(p_2+1)+5p_1(3p_2^2+p_2+1) + 2p_1(p_2+1)$$

$$= (3p_2^2+3p_2+1)(10p_1^2+1)+(p_2+1)+5p_1(3p_2^2+3p_2+1)+2p_1(p_2+1)$$

$$= (10p_1^2+5p_1+1)(3p_2^2+3p_2+1)+(2p_1+1)(p_2+1)$$

We choose

$$P(p_2) = M_{12}(p_2)+N_{12}(p_2) = 3p_2^2+3p_2+1$$

$$Q(p_2) = M_{22}(p_2)+N_{22}(p_2) = p_2+1$$

$$M_{11}(p_1) = 10p_1^2+1, \quad M_{21}(p_1) = 1$$

$$N_{21}(p_1) = 5p_1 \quad \text{and} \quad N_{11}(p_1) = 2p_1$$

The real part conditions are satisfied for both the p_1 and p_2 cases.

$$Z_1(p_1) = \frac{10p_1^2+2p_1+1}{5p_1+1} \quad \text{and} \quad Z_2(p_2) = \frac{3p_2^2+3p_2+1}{p_2+1}$$

can be synthesized as lowpass ladders.

Example 3.2

$$T(p_1,p_2) = 1/D(p_1,p_2)$$

$$= \frac{1}{p_1^2p_2^2+p_1^2p_2+p_1p_2^2+p_1^2+p_2^2+2p_1p_2+2p_1+2p_2+2}$$

$$\begin{aligned} D(p_1,p_2) &= p_1^2(p_2^2+p_2+1)+p_1(p_2^2+2p_2+2)+(p_2^2+2p_2+2) \\ &= p_1^2(p_2^2+1)+p_1(p_2^2+2)+(p_2^2+2)+p_1^2(p_2)+p_1(2p_2)+(2p_2) \\ &= p_2^2(p_1^2+p_1+1)+(p_1^2+p_1+1)+(p_1+1)+p_2(p_1^2+p_1+1) \\ &\quad + p_2(p_1+1) \\ &= (p_1^2+p_1+1)(p_2^2+p_2+1)+(p_1+1)(1+p_2) \end{aligned}$$

By choosing $P(p_2) = p_2^2+p_2+1$, $Q(p_2) = p_2+1$, $M_{11}(p_1) = p_1^2+1$, $M_{21}(p_1) = 1$ and $N_{21}(p_1) = N_{11}(p_1) = p_1$, we see that the real part conditions are satisfied.

However, the above decomposition is not unique since $D(p_1,p_2)$ can also be decomposed as $(p_1^2+p_1+1)\,p_2^2+(p_2+1)(p_1^2+2p_1+2)$ or as $(p_1^2)(p_2^2+p_2+1)+(p_1+1)(p_2^2+2p_2+2)$.

In these two cases, no suitable choice can be made which would satisfy the real part conditions. These two decompositions have to be rejected since they do not satisfy the real part conditions. The properties of the real part of an MPRF and its applications are discussed in [59].

The properties of a doubly-terminated cascade separable lowpass ladder network transfer function can also be stated in an alternate way as follows.

A lowpass all-pole transfer function $T(p_1,p_2)$ is realized as the transfer function of a doubly-terminated cascade of p_1 and p_2 lossless lowpass ladder networks if

(1) $T(p_1,0)$ and $T(0,p_2)$ are realizable as doubly-terminated lowpass ladder networks in their respective variables with identical termination resistances in both realizations using any synthesis method available in single variable [65].

(2) The transfer function of the network obtained by cascading the lossless p_1 and p_2 networks with the above terminations is identical to $T(p_1,p_2)$.

Let us consider the following example which illustrates the above properties.

Example 3.3

To find a realization for the all-pole lowpass transfer function $T(p_1,p_2) = 1/D(p_1,p_2)$

$$= \frac{K}{360p_1^2p_2^2+30p_1^2p_2+72p_1p_2^2+66p_1p_2+45p_1^2+24p_2^2+14p_1 +14p_2+4}$$

given that the source and load resistances are R_s=1 Ohm and R_L = 3 Ohms respectively.

Since $T(0,0)$ has to be 3/4 for the given terminating resistances, we must have $K=3$.

$$T(0,p_2) = \frac{3}{24p_2^2+14p_2+4}$$

p_2 network synthesis

$$|T(0,j\omega_2)|^2 = \frac{9}{(4-24\omega_2^2)^2+(14\omega_2)^2} = \frac{9}{576\omega_2^4+4\omega_2^2+16}$$

$$|\rho_2(j\omega_2)|^2 = 1 - 4\frac{R_s}{R_L}|T(0,j\omega_2)|^2$$

$$= \frac{576\omega_2^4+4\omega_2^2+4}{576\omega_2^4+4\omega_2^2+16}$$

where ρ_2 is the reflection coefficient of the p_2 network. Hence,

$$\rho_2(p_2')\rho_2(-p_2) = \frac{576p_2^4-4p_2^2+4}{576p_2^4-4p_2^2+16}$$

If the right half plane zeros are selected for the numerator of $\rho_2(p_2)$, we have

$$\rho_2(p_2) = \frac{24p_2^2-10p_2+2}{24p_2^2+14p_2+4}$$

$$\frac{Z_2(p_2)}{R_s} = \frac{1\mp\rho_2(p_2)}{1\pm\rho_2(p_2)}$$

$$Z_2(p_2) = \frac{48p_2^2+4p_2+6}{24p_2 + 2} \quad \text{or} \quad \frac{24p_2 + 2}{48p_2^2+4p_2+6}$$

If we select the left half plane zeros as the numerator of $\rho_2(p_2)$, we get

$$\rho_2(p_2) = \frac{24p_2^2+10p_2+2}{24p_2^2+14p_2+4}$$

In this case, we obtain

$$Z_2(p_2) = \frac{48p_2^2+24p_2+6}{4p_2 + 2} \quad \text{or} \quad \frac{4p_2 + 2}{48p_2^2+24p_2+6}$$

Thus we have four realizations for $Z_2(p_2)$, which are shown in Fig. 3.2.a. Now it can be checked whether the denominator is expressible as $P_1Q_2+Q_1P_2$ where P_1 and Q_1 are polynomials in p_1, and P_2 and Q_2 are given by either $P_2 = (24p_2^2+2p_2+3)$ and $Q_2 = (12p_2+1)$ or $P_2 = (24p_2^2+12p_2+3)$ and $Q_2 = (2p_2+1)$

It seen that

$$D(p_1,p_2)=(15p_1^2+3p_1+1)(24p_2^2+2p_2+1)+(5p_1+1)(12p_2+1)$$

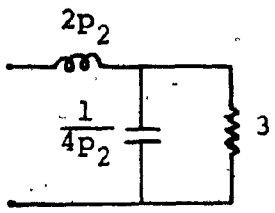

$$Z_2(p_2) = \frac{24p_2^2 + 2p_2 + 3}{12p_2 + 1}$$

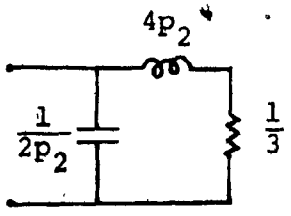

$$Z_2(p_2) = \frac{12p_2 + 1}{24p_2^2 + 2p_2 + 3}$$

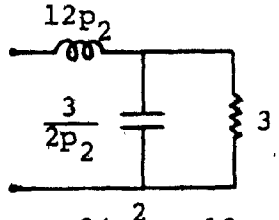

$$Z_2(p_2) = \frac{24p_2^2 + 12p_2 + 3}{2p_2 + 1}$$

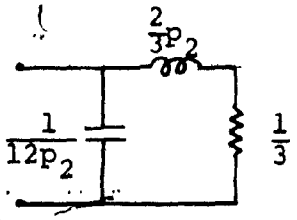

$$Z_2(p_2) = \frac{2p_2 + 1}{24p_2^2 + 12p_2 + 3}$$

(a)

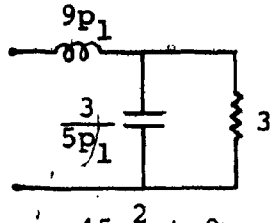

$$Z_1(p_1) = \frac{45p_1^2 + 9p_1 + 3}{5p_1 + 1}$$

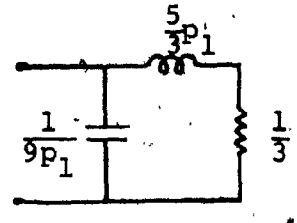

$$Z_1(p_1) = \frac{5p_1 + 1}{45p_1^2 + 9p_1 + 3}$$

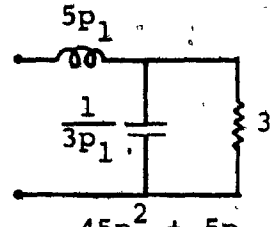

$$Z_1(p_1) = \frac{45p_1^2 + 5p_1 + 3}{9p_1 + 1}$$

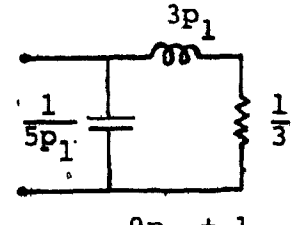

$$Z_1(p_1) = \frac{9p_1 + 1}{45p_1^2 + 5p_1 + 3}$$

(b)

FIG. 3.2 (a) p_2 NETWORK REALIZATIONS AND (b) p_1 NETWORK REALIZATIONS FOR EXAMPLE 3.3

The synthesis of $T(p_1,0)$ as a doubly-terminated network gives us the required p_1 network, as shown below.

$$|T(j\omega_1,0)|^2 = \frac{9}{(4-45\omega_1^2)^2+(14\omega_1)^2}$$

$$= \frac{9}{2025\omega_1^4-164\omega_1^2+16}$$

$$|\rho_1(j\omega_1)|^2 = 1 - \frac{4}{3}\,\frac{9}{(2025\omega_1^4-164\omega_1^2+16)}$$

$$= \frac{2025\omega_1^4-164\omega_1^2+4}{2025\omega_1^4-164\omega_1^2+16}$$

where ρ_1 represents the reflection coefficient of the p_1 network.

$$\rho_1(p_1) = \frac{45p_1^2\pm 4p_1+2}{45p_1^2+14p_1+4}$$

and $$\frac{Z_1(p_1)}{R_s} = \frac{1\mp\rho_1(p_1)}{1\pm\rho_1(p_1)}$$

The four realizations corresponding to the above, are shown in Fig. 3.2b.

Combining the above realizations for the p_1 network and those for the p_2 network, we get the realizations for $T(p_1,p_2)$. Four networks arise out of these combinations as shown in Fig. 3.3a to 3.3d, each of which realizes $T(p_1,p_2)$. In Fig. 3.3a and 3.3c, the p_1 network is

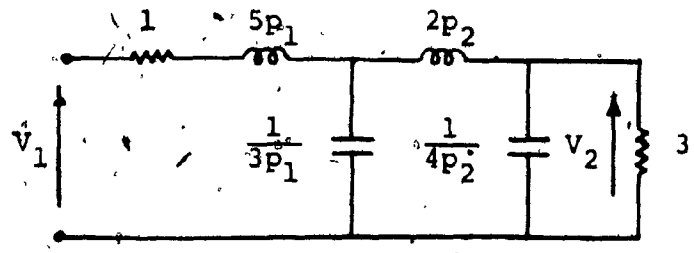

(a)

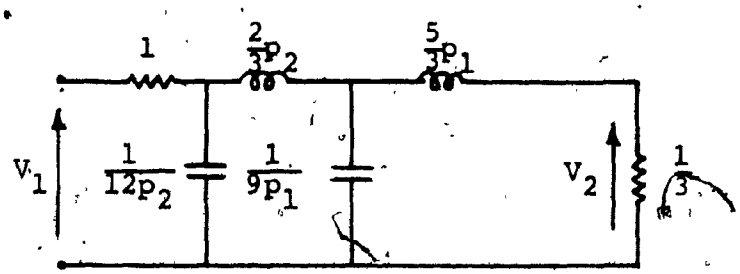

(b)

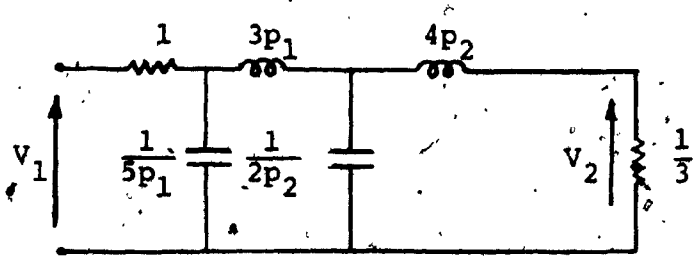

(c)

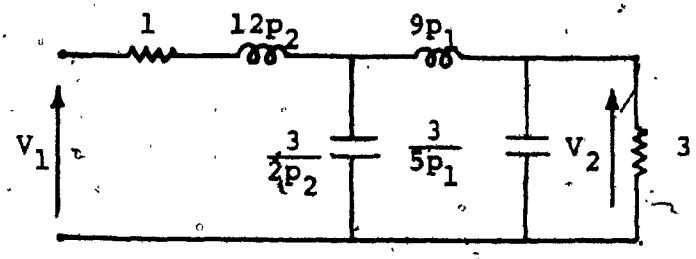

(d)

FIG. 3.3 REALIZATIONS FOR THE TRANSFER FUNCTION $T(p_1, p_2)$ OF EXAMPLE 3.3

followed by the p_2 network, whereas in 3.3b and 3.3d, it is the reverse. The ratio R_s/R_L is equal to 3 for Fig. 3.3a and 3.3d, whereas it is equal to 1/3 for the other two. The impedance level of each of these circuits can be changed without affecting the transfer function.

The networks in Fig. 3.3c and 3.3d are duals of those in 3.3a and 3.3b respectively. The network in Fig. 3.3b is the transpose of the network in Fig. 3.3a. It is obtained by short-circuiting the input port, open circuiting the output port at the load resistance and then reversing the ports. It is to be noted that the dual network, the transpose network and the dual of the transpose network all realize the same transfer function as that of the original network [66].

Using the above properties of doubly-terminated cascade separable networks we can generate two-variable transfer functions by the following method. $T(p_1,0)$ and $T(0,p_2)$ are synthesized as doubly-terminated ladder networks in p_1 and p_2 variables respectively, having identical termination resistances. These networks realize the specified frequency response along the ω_1 and ω_2 axes respectively where ω_1 and ω_2 are the frequency variables corresponding to p_1 and p_2. Then $T(p_1,p_2)$ is obtained as the transfer function of the network generated by combining the p_1 and p_2 lossless two-ports and adding the source and load terminations, as obtained by the above synthesis. The transfer function thus generated realizes the specified

response along the ω_1 and ω_2 axes. We have studied here only the case of the all-pole transfer function. Other types of ladder networks can be generated using the reactance transformations of Chapter 2. This generation by method 1 is used later for two-variable transfer function approximation.

3.3.2 Generation by method 2

Let us consider the doubly-terminated cascade separable network given in Fig. 3.4a. If we draw a partition P as indicated in the figure, we can represent the network to the left of the partition by its Thevenin's equivalent which consists of a voltage generator V_T and a series impedance z_{11a} which is a function of p_1. z_{11a} is the impedance looking into the output port of the p_1 network which is terminated in a resistance R_s at its input port. Similarly the network to the right side of the partition P is represented by z_{11b}, which is the driving point impedance of the p_2 network terminated in a load resistance R_L. The Thevenin's equivalent network is shown in Fig. 3.4b. We can derive the following equations for V_T, z_{11a} and z_{11b}.

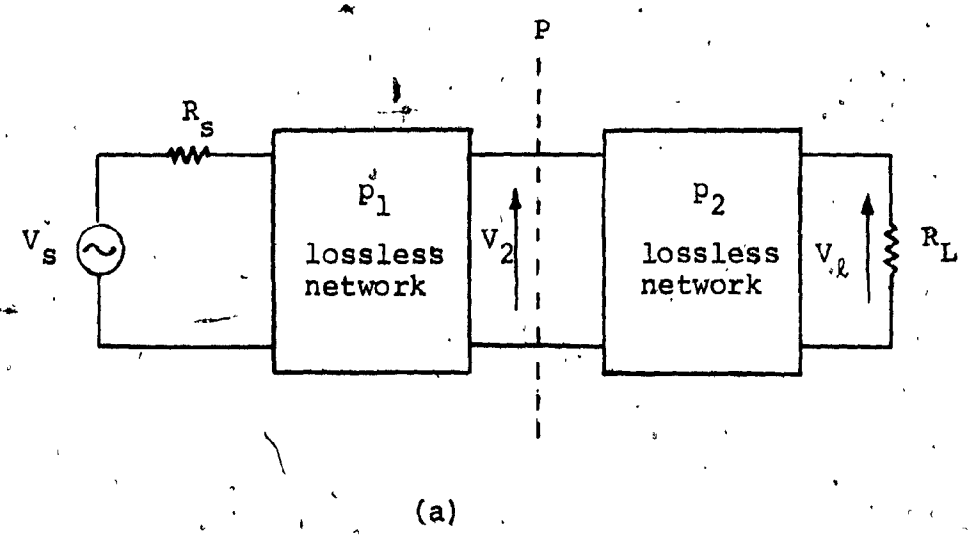

(a)

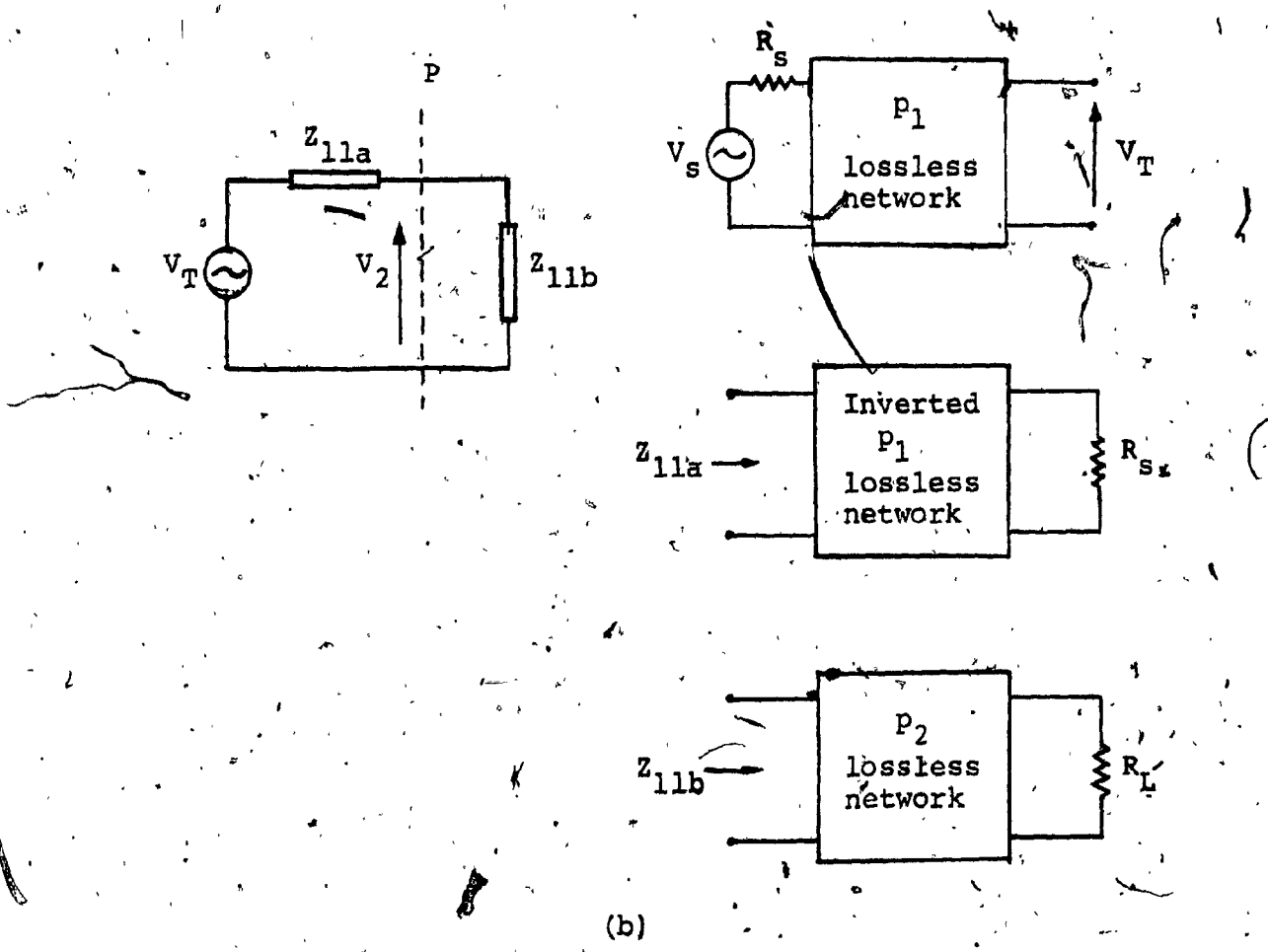

(b)

FIG. 3.4 (a) A DOUBLY-TERMINATED CASCADE SEPARABLE NETWORK AND (b) ITS THEVENIN'S EQUIVALENT

$$V_T = V_s \frac{\sqrt{M_{11}M_{21}-N_{11}N_{21}}}{M_{11}+N_{21}R_s}$$

$$z_{11a} = \frac{M_{21}R_s+N_{11}}{M_{11}+N_{21}R_s} \quad \text{and} \qquad (3.3.2.1)$$

$$z_{11b} = \frac{M_{12}R_L+N_{12}}{M_{22}+N_{22}R_L}$$

where M_{11}/N_{21}, M_{21}/N_{21} and M_{11}/N_{11} give the open and short circuit parameters z_{11a}, z_{22a} and y_{22a} respectively for the lossless p_1 network and M_{12}/N_{22}, M_{22}/N_{22} and M_{12}/N_{12} represent the corresponding parameters z_{11b}, z_{22b} and y_{22b} respectively for the lossless p_2 network.

From $\frac{V_2}{V_T} = \frac{z_{11b}}{z_{11a}+z_{11b}}$ and $\frac{V_\ell}{V_2} = \frac{R_L\sqrt{M_{12}M_{22}-N_{12}N_{22}}}{M_{12}R_L+N_{12}}$

we get

$$T(p_1,p_2) = \frac{\dfrac{R_L\sqrt{M_{12}M_{22}-N_{12}N_{22}}}{M_{22}+N_{22}R_L}\dfrac{\sqrt{M_{11}M_{21}-N_{11}N_{21}}}{M_{11}+N_{21}R_s}}{z_{11a}+z_{11b}}$$

$$= \frac{1}{R_s}\frac{z_{21a}z_{21b}}{z_{11a}+z_{11b}} \qquad (3.3.2.2)$$

where z_{21a} is the transfer impedance of the inverted p_1 network terminated in R_s and z_{21b} is the transfer impedance of the p_2 network terminated in R_L. Comparing (3.3.2.2) with (3.3.1.9) we can see that both are equivalent. With the above discussion, the following properties

of $T(p_1,p_2)$ can be observed. A two-variable all pole lowpass transfer function $T(p_1,p_2)$ can be realized by a doubly-terminated cascade of p_1 and p_2 lossless lowpass ladder networks if

(1) $T(p_1,p_2)$ is expressible in the form

$$T(p_1,p_2) = K/[Q_1P_2+P_1Q_2] \qquad (3.3.2.3)$$

where P_1 and Q_1 are polynomials in p_1, and P_2 and Q_2 are polynomials in p_2.

(2) P_1/Q_1 is realizable as a resistively terminated lossless lowpass ladder network in the p_1 variable and

(3) P_2/Q_2 is realizable as a resistively terminated lossless lowpass ladder network in the p_2 variable.

If $T(p_1,p_2)$ is expressible as $K/[Q_1P_2+P_1Q_2]$ with its denominator in the sum of products form, then from (3.3.1.9), the following can be identified.

Q_1(or P_1) = $M_{11}+R_sN_{21}$, P_2(or Q_2) = $M_{12}R_L+N_{12}$

P_1(or Q_1) = $M_{21}R_s+N_{11}$, Q_2(or P_2) = $M_{22}+R_LN_{22}$. If P_2/Q_2(or Q_2/P_2) is realizable as a resistively terminated lossless lowpass ladder network, then it realizes the p_2 network terminated in a load resistance R_L. If P_1/Q_1 is realizable as a resistively terminated lossless lowpass ladder network, then it realizes the inverted p_1 network terminated in R_s. The two-variable network is constructed by inverting the lossless p_1 network, cascading it with the lossless p_2 network and adding the termination resistances

R_s and R_L. The same $T(p_1,p_2)$ is also realized by the dual of the above network, the transpose network and the transpose of the dual network. The following example illustrates the above properties with the transfer function of example 3.3.

Example 3.4

$$T(p_1,p_2) = \frac{K}{360p_1^2p_2^2+30p_1^2p_2+72p_1p_2^2+66p_1p_2+45p_1^2 + 24p_2^2+14p_1+14p_2+4}$$

$$= \frac{K}{(15p_1^2+3p_1+1)(24p_2^2+2p_2+3)+(5p_1+1)(12p_2+1)}$$

We assume

$$\frac{P_1}{Q_1} = \frac{5p_1+1}{15p_1^2+3p_1+1} \quad \text{and} \quad \frac{P_2}{Q_2} = \frac{24p_2^2+2p_2+3}{12p_2+1}$$

P_1/Q_1 and P_2/Q_2 are realized as singly-terminated lowpass lossless ladder networks in the variables p_1 and p_2 respectively. The p_1 lossless network is inverted, cascaded with the p_2 network and the resistive termination of the p_1 network is added as the source resistance R_s. The resulting network is the same as that indicated in Fig. 3.3a.

The above method with certain modifications incorporated is used for the approximation of two-variable transfer functions in Chapter 5. P_1/Q_1 and P_2/Q_2 are generated

for the required type of response in each variable using the existing one variable approximations. $T(p_1,p_2)$ is then obtained by synthesizing P_1/Q_1 and P_2/Q_2 as singly terminated lossless ladder networks in the respective variables, inverting the p_1 network and cascading it with the p_2 network. It is to be noted that the transfer functions generated in this way can be the same as or entirely different from the ones generated by method 1. This is discussed in greater detail in Chapter 5, which deals with approximations of such functions.

3.4 Summary and Conclusions

Based on the results obtained in Chapter 2, a method for generation of doubly-terminated network transfer functions was developed. The properties of such transfer functions in relation to the multivariable arrays developed earlier has been studied. It has been shown that the denominator polynomial in these functions no longer satisfies the conditions of the multivariable array B.

In the case of the cascade separable doubly-terminated network, two methods are possible for the above generation. Though method 1 is discussed only with regard to two-variables, it can be generalized for the case of m-variables. However method 2 is applicable only for two-variable networks. The two methods discussed here are useful for generation of two-variable transfer functions of doubly-

terminated cascade-separable networks. Only the case of all-pole transfer functions has been considered since generation methods for the other cases such as HP, BP or BS can be obtained using the techniques described in Chapter 2.

The two methods described here are not much useful for the synthesis of doubly-terminated cascade separable networks as they are quite involved. A general procedure for the synthesis of a multivariable transfer function in a manner similar to the existing single-variable doubly-terminated network synthesis is not possible because there is no method in multivariables analogous to that of factorization of a single-variable polynomial and choosing the left half-plane poles for the transfer function.

CHAPTER 4.

CASCADE SEPARABLE TRANSFER FUNCTIONS IN THE DIGITAL DOMAIN

4.1 Introduction

In this chapter, conditions are obtained in the digital domain analogous to those derived earlier for the singly-terminated cascade separable two-variable network transfer function and this is made use of in the generation of doubly-terminated cascade separable digital transfer functions.

The properties of the polynomials in the digital domain which correspond to the even and odd polynomials in the analog domain are studied and it is shown how the cascade separability of a two-variable polynomial in z_1 and z_2 can be tested. Since the conditions obtained are in the digital domain, the testing or generation of a transfer function can be carried out directly in the digital domain. If the conditions are satisfied, the corresponding analog transfer function can be synthesized as a cascade separable ladder network and realized as a wave digital filter. We study the digital transfer functions derived from both the singly-terminated as well as the doubly-terminated cascade separable networks. In the case of the singly-terminated networks, the conditions for realization are translated into equivalent z-domain conditions. Since only generation is

possible in the case of the doubly-terminated networks, we discuss a generation procedure directly in the z-domain for the doubly-terminated cascade separable transfer function, based on the generation procedure given in Chapter 3.

The problems associated with the double bilinear transformation of cascade separable transfer functions are also discussed.

4.2 Cascade expressible polynomials in the digital domain

When a two-variable analog network is realized with the conditions given in the previous section, there are techniques for realization of the corresponding two-dimensional digital transfer function (obtained by the double bilinear transformation) as a wave digital filter [33]. The transformation from the analog to the digital domain is given by $p_i \rightarrow (z_i-1)/(z_i+1)$, i=1,2. We now derive the required conditions in the (z_1,z_2) domain for "cascade separability" of digital transfer functions [67]. The term "cascade separability" means that the given 2-D digital transfer function $H(z_1,z_2)$ when transformed, produces an analog function

$$T(p_1,p_2) = H(z_1,z_2)\Big|_{z_i = \frac{1+p_i}{1-p_i},\ i=1,2} \qquad (4.2.1)$$

which is realizable as the transfer function of a cascade of p_1 and p_2 two-port networks terminated in a

resistance. Thus cascade separable digital transfer functions are realizable as 2-D wave digital filters.

Before we derive the conditions for "cascade separability", let us see the properties of functions in the digital domain which are obtained by bilinear transformations applied to the even and odd polynomials in the single-variable analog domain. Polynomials similar to the ones obtained in these functions have been studied before and classified as mirror image and anti-mirror image polynomials [68]. Here we formulate the polynomials in a particular form, suitable for the derivations discussed here.

We can express any even polynomial $M(p_1)$ with roots on the $j\omega$ axis in the p_1 plane, in the form

$$M(p_1) = \prod_{i=1}^{k} (p_1^2+\alpha_i) \qquad (4.2.2)$$

where $2k$ is the degree of the polynomial and $\alpha_i > 0$. Similarly an odd polynomial $N(p_1)$ of degree $(2k-1)$ can be expressed as

$$N(p_1) = p_1 \prod_{i=1}^{k-1} (p_1^2+\beta_i) \qquad (4.2.3)$$

where $\beta_i > 0$. When $M(p_1)$ and $N(p_1)$ are transformed by the bilinear transformation, we get

$$M(p_1)\Big|_{p_1=\frac{z_1-1}{z_1+1}} = \prod_{i=1}^{k} \frac{z_1^2(1+\alpha_i)+2z_1(\alpha_i-1)+(1+\alpha_i)}{(z_1+1)^2}$$

and

$$N(p_1)\Big|_{p_1=\frac{z_1-1}{z_1+1}} = \frac{z_1-1}{z_1+1} \prod_{i=1}^{k-1} \frac{z_1^2(1+\beta_i)+2z_1(\beta_i-1)+(1+\beta_i)}{(z_1+1)^2} \qquad (4.2.4)$$

If we represent

$$m(z_1) = \prod_{i=1}^{k} \{z_1^2(1+\alpha_i)+2z_1(\alpha_i-1)+(1+\alpha_i)\} \qquad (4.2.5)$$

and $$n(z_1) = (z_1^2-1) \prod_{i=1}^{k-1} z_1^2(1+\beta_i)+2z_1(\beta_i-1)+(1+\beta_i)$$

then the polynomials $M(p_1)$ and $N(p_1)$ are given by

$$M(p_1) = \frac{m(z_1)}{(z_1+1)^{2k}}\Bigg|_{z_1=\frac{1+p_1}{1-p_1}}$$

$$\text{and} \quad N(p_1) = \frac{n(z_1)}{(z_1+1)^{2k}}\Bigg|_{z_1=\frac{1+p_1}{1-p_1}} \qquad (4.2.6)$$

In each factor of $m(z_1)$ and $n(z_1)$, the coefficients corresponding to the z_1^2 term and the constant term are identical. Hence $m(z_1)$ can be written as

conditions for a 2-D digital transfer function which has a lowpass response in both the frequency variables, are stated in the following theorem.

Theorem 4.1

A digital transfer function $H(z_1,z_2)$ has a corresponding analog transfer function $T(p_1,p_2)$ which can be realized as the transfer function of a resistively-terminated cascade of p_1 and p_2 lowpass lossless ladder networks if and only if the following conditions are satisfied.

(1) $H(z_1,z_2)$ is expressible in the form

$$\frac{K(z_1+1)^{n_1}(z_2+1)^{n_2}}{m_{11}(z_1)p(z_2) + n_{11}(z_1)q(z_2)} \qquad (4.3.1)$$

where n_1 and n_2 are the highest degrees of z_1 and z_2 in the denominator polynomial and K is a constant.

(2) $F_1(z_1) = \frac{m_{11}(z_1)+n_{11}(z_1)}{m_{21}(z_1)+n_{21}(z_1)}$ and $F_2(z_2) = \frac{p(z_2)}{q(z_2)}$ (4.3.2)

can be generated such that their poles lie inside or on the unit circles in their respective domains. The pole on the unit circle is single and occurs at $z_i=-1$, $i=1,2$ and

(3) $m_{1i}(z_i)m_{2i}(z_i)-n_{1i}(z_i)n_{2i}(z_i) = R_i(z_i+1)^{2n_i}$ (4.3.3)

where $R_i>0$ for $i=1,2$.

Proof:

The necessity is directly seen as a consequence of Theorem 2.10. Only the sufficiency part is proved here. From

$$H(z_1,z_2) = \frac{K(z_1+1)^{n_1}(z_2+1)^{n_2}}{m_{11}(z_1)p(z_2)+n_{11}(z_1)q(z_2)} ,$$

We can isolate $p(z_2)$, $q(z_2)$, $m_{11}(z_1)$ and $n_{11}(z_1)$. $F_2(z_2)$ is obtained as $p(z_2)/q(z_2)$. $F_1(z_1)$ is generated by using $m_{11}(z_1)$, $n_{11}(z_1)$, and the condition (3). It is always possible to generate the above, by assuming $m_{21}(z_1)$ and $n_{21}(z_1)$ as polynomials of appropriate order and then finding their coefficients which would satisfy condition (3).

$F_1(z_1)$ is given by $F_1(z_1) = \dfrac{m_{11}(z_1)+n_{11}(z_1)}{m_{21}(z_1)+n_{21}(z_1)}$.

If $F_1(z_1)$ and $F_2(z_2)$ have all poles inside the unit circles in their respective domains, then the corresponding analog functions

$$Z_1(p_1) = F_1(z_1)\Big|_{z_1 = \frac{1+p_1}{1-p_1}} \quad \text{and} \quad Z_2(p_2) = F_2(z_2)\Big|_{z_2=\frac{1+p_2}{1-p_2}} \tag{4.3.4}$$

have all their poles in the left half of the p_1 and p_2 planes respectively and hence the denominators of $Z_1(p_1)$

and $Z_2(p_2)$ are Hurwitz polynomials. Since $Z_1(p_1)$ and $Z_2(p_2)$ are impedance functions, they can have a numerator degree, one higher than the denominator degree. In such a case $F_1(z_1)$ and $F_2(z_2)$ can have single poles at $z_i=-1$, $i=1,2$. Also the zeros of $F_1(z_1)$ and $F_2(z_2)$ lie inside or on the unit circles in their respective domains.

The third condition makes it possible to realize the functions $Z_1(p_1)$ and $Z_2(p_2)$ as driving point impedance functions of resistively-terminated lowpass ladder networks in the variables p_1 and p_2 respectively.

Since

$$Z_1(p_1) = \frac{M_{11}(p_1)+N_{11}(p_1)}{M_{21}(p_1)+N_{21}(p_1)} \quad \text{and} \quad Z_2(p_2) = \frac{P(p_2)}{Q(p_2)} \tag{4.3.5}$$

are PRFs in p_1 and p_2, respectively, we can generate the TPRF

$$Z(p_1,p_2) = \frac{M_{11}(p_1)P(p_2)+N_{11}(p_1)Q(p_2)}{M_{21}(p_1)Q(p_2)+N_{21}(p_1)P(p_2)} \tag{4.3.6}$$

$Z(p_1,p_2)$ can be realized as the driving point function of a resistively terminated cascade of p_1 and p_2 lowpass ladder networks, because by condition (3), we see that

$$M_{1i}(p_i)M_{2i}(p_i)-N_{1i}(p_i)N_{2i}(p_i) = R_i, \; R_i>0. \tag{4.3.7}$$

for $i=1,2$ which is the same as (2.4.5). The above network realizes the transfer function $T(p_1,p_2)$ which is the

inverse double bilinear transform of $H(z_1,z_2)$.

Example 4:3

$$H(z_1,z_2) = \frac{(z_1+1)^2(z_2+1)^2}{8z_1^2z_2^2+2z_1^2z_2+2z_1^2+4z_2^2-2z_2+2}$$

is the given 2-D digital transfer function.

The denominator is expressible as

$$z_1^2(8z_2^2+2z_2+2) + (4z_2^2-2z_2+2)$$

$$= 2(z_1^2+1)(3z_2^2+1) + 2(z_1^2-1)(z_2^2+z_2)$$

We see that $p(z_2) = m_{12}(z_2) + n_{12}(z_2) = 3z_2^2+1$

and $q(z_2) = m_{22}(z_2) + n_{22}(z_2) = 2(z_2^2+z_2)$

satisfies the condition

$$m_{12}(z_2)m_{22}(z_2) - n_{12}(z_2)n_{22}(z_2) = (z_2+1)^4.$$

Hence

$$F_2(z_2) = \frac{3z_2^2+1}{2z_2^2+2z_2}$$

$m_{11}(z_1) = 2z_1^2+2$ and $n_{11}(z_1) = z_1^2-1$.

We find that $m_{21}(z_1) = z_1^2+2z_1+1$

and $n_{21}(z_1) = z_1^2-1$

in order to satisfy the condition

$$m_{11}(z_1)m_{21}(z_1) - n_{11}(z_1)n_{21}(z_1) = (z_1+1)^4.$$

$$F_1(z_1) = \frac{m_{11}(z_1)+n_{11}(z_1)}{m_{21}(z_1)+n_{21}(z_1)} = \frac{3z_1^2+1}{2z_1^2+2z_1}$$

The analog functions $Z_1(p_1) = F_1(z_1)\Big|_{z_1 = \frac{1+p_1}{1-p_1}}$

and $Z_2(p_2) = F_2(z_2)\Big|_{z_2 = \frac{1+p_2}{1-p_2}}$ are seen to be

$$Z_1(p_1) = \frac{p_1^2+p_1+1}{p_1+1} \quad \text{and} \quad Z_2(p_2) = \frac{p_2^2+p_2+1}{p_2+1}$$

which can be realized as resistively-terminated lowpass ladder networks in p_1 and p_2 respectively.

The conditions for realization of the p_1 and p_2 networks as highpass, bandpass or bandstop ladders are given in Theorems 4.2 to 4.4.

Theorem 4.2

A digital transfer function $H(z_1,z_2)$ has a corresponding analog transfer function $T(p_1,p_2)$ which can be realized as the transfer function of a resistively-terminated cascade of p_1 and p_2 highpass ladder networks, if and only if

(1) $H(z_1,z_2)$ is expressible in the form

$$H(z_1,z_2) = \frac{K(z_1-1)^{n_1}(z_2-1)^{n_2}}{m_{11}(z_1)p(z_2) + n_{11}(z_1)q(z_2)} \qquad (4.3.8)$$

where n_1 and n_2 are the highest powers of z_1 and z_2 respectively and K is a constant.

(2) Same as condition (2) of Theorem 4.1.

(3) $$m_{1i}(z_i)m_{2i}(z_i)-n_{1i}(z_i)n_{2i}(z_i) = R_i(z_i-1)^{2n_i} \qquad (4.3.9)$$

where R_i is a constant, for $i=1,2$.

The proof follows along the same lines as in Theorem 4.1. The condition (3) corresponds to condition (2.4.7) in the analog domain. When the above conditions are satisfied, both the p_1 and p_2 networks can be realized as resistively-terminated highpass ladders.

Theorem 4.3

A digital transfer function $H(z_1,z_2)$ has a corresponding analog transfer function $T(p_1,p_2)$ which can be realized as the resistively-terminated cascade of p_1 and p_2 bandpass ladder networks, if and only if

(1) $H(z_1,z_2)$ is expressible in the form

$$H(z_1,z_2) = \frac{K(z_1^2-1)^{k_1}(z_2^2-1)^{k_2}}{m_{11}(z_1)p(z_2) + n_{11}(z_1)q(z_2)} \qquad (4.3.10)$$

where $2k_1$ and $2k_2$ are the highest powers of z_1 and z_2 and K is a constant.

(2) Same as condition (2) of Theorem 4.1.

(3) $$m_{1i}(z_i)m_{2i}(z_i)-n_{1i}(z_i)n_{2i}(z_i) = R_i(z_i^2-1)^{2k_i} \qquad (4.3.11)$$

where R_i is a constant, for $i=1,2$.

The proof is similar to that of Theorem 4.1. In the analog

case, the condition (3) corresponds to (2.4.10).

Theorem 4.4

A digital transfer function $H(z_1,z_2)$ has a corresponding analog transfer function $T(p_1,p_2)$ which can be realized as the resistively-terminated cascade of p_1 and p_2 band-stop ladder networks if and only if

(1) $H(z_1,z_2)$ is expressible in the form

$$H(z_1,z_2) = \frac{KB_1(z_1)B_2(z_2)}{m_{11}(z_1)p(z_2)+n_{11}(z_1)q(z_2)} \qquad (4.3.12)$$

where K is a constant, $B_i(z_i)$ are polynomials in z_i of degree $2k_i$, having their roots located at $z_i=\pm j$ and $2k_i$ is the degree of z_i in the denominator polynomial, for $i=1,2$.

(2) Same as condition (2) of Theorem 4.1.

(3) $$m_{1i}(z_i)m_{2i}(z_i)-n_{1i}(z_i)n_{2i}(z_i) = R_i[B_i(z_i)]^2 \qquad (4.3.13)$$

where $R_i>0$ for $i=1,2$.

The corresponding real part condition in the analog case is given by (2.4.13).

The conditions to be satisfied by $m_{1i}(z_i)m_{2i}(z_i)-n_{1i}(z_i)n_{2i}(z_i)$ for all possible cases are tabulated in Table 4.2. From the above Theorems, it is seen that $H(z_1,z_2)$ can be represented as

TABLE 4.2

CONDITIONS IN THE DIGITAL DOMAIN CORRESPONDING TO THE REAL PART CONDITIONS IN TABLE 2.4

TYPE OF TRANSFER FUNCTION	$m_{1i}(z_i)m_{2i}(z_i) - n_{1i}(z_i)n_{2i}(z_i)$ for i=1,2		
(1) LP + LP	$R_i(z_i+1)^{2n_i}$	$R_i > 0$	for i=1,2
(2) LP + HP	$R_1(z_1+1)^{2n_1}$	$R_1 > 0$	for i=1
	$R_2(z_2-1)^{2n_2}$	$R_2 \neq 0$	for i=2
(3) LP + BP	$R_1(z_1+1)^{2n_1}$	$R_1 > 0$	for i=1
	$R_2(z_2^2-1)^{2k_2}$	$R_2 \neq 0$	for i=2
(4) LP + BS	$R_1(z_1+1)^{2n_1}$	$R_1 > 0$	for i=1
	$R_2(z_2^2+1)^{2k_2}$	$R_2 > 0$	for i=2
(5) HP + LP	$R_1(z_1-1)^{2n_1}$	$R_1 \neq 0$	for i=1
	$R_2(z_2+1)^{2n_2}$	$R_2 > 0$	for i=2
(6) HP + HP	$R_i(z_i-1)^{2n_i}$	$R_i \neq 0$	for i=1,2
(7) HP + BP	$R_1(z_1-1)^{2n_1}$	$R_1 \neq 0$	for i=1
	$R_2(z_2^2-1)^{2k_2}$	$R_2 \neq 0$	for i=2
(8) HP + BS	$R_1(z_1-1)^{2n_1}$	$R_1 \neq 0$	for i=1
	$R_2(z_2^2+1)^{2k_2}$	$R_2 > 0$	for i=2
(9) BP + LP	$R_1(z_1^2-1)^{2k_1}$	$R_1 \neq 0$	for i=1
	$R_2(z_2+1)^{2n_2}$	$R_2 > 0$	for i=2
(10) BP + HP	$R_1(z_1^2-1)^{2k_1}$	$R_1 \neq 0$	for i=1
	$R_2(z_2-1)^{2n_2}$	$R_2 \neq 0$	for i=2
(11) BP + BP	$R_i(z_i^2-1)^{2k_i}$	$R_i \neq 0$	for i=1,2

TABLE 4.2

CONDITIONS IN THE DIGITAL DOMAIN CORRESPONDING TO THE REAL PART CONDITIONS IN TABLE 2.4

TYPE OF TRANSFER FUNCTION	$m_{1i}(z_i)m_{2i}(z_i) - n_{1i}(z_i)n_{2i}(z_i)$ for $i=1,2$		
(12) BP + BS	$R_1(z_1^2-1)^{2k_1}$	$R_1 \neq 0$	for $i=1$
	$R_2(z_2^2+1)^{2k_2}$	$R_2 > 0$	for $i=2$
(13) BS + LP	$R_1(z_1^2+1)^{2k_1}$	$R_1 > 0$	for $i=1$
	$R_2(z_2+1)^{2n_2}$	$R_2 > 0$	for $i=2$
(14) BS + HP	$R_1(z_1^2+1)^{2k_1}$	$R_1 > 0$	for $i=1$
	$R_2(z_2-1)^{2n_2}$	$R_2 \neq 0$	for $i=2$
(15) BS + BP	$R_1(z_1^2+1)^{2k_1}$	$R_1 > 0$	for $i=1$
	$R_2(z_2^2-1)^{2k_2}$	$R_2 \neq 0$	for $i=2$
(16) BS + BS	$R_i(z_i^2+1)^{2k_i}$	$R_i > 0$	for $i=1,2$

NOTE: n_i and $2k_i$ denote the degree of z_i in $H(z_1,z_2)$ for $i=1,2$.

$$H(z_1,z_2) = \frac{K\sqrt{m_{11}m_{21}-n_{11}n_{21}}\sqrt{m_{12}m_{22}-n_{12}n_{22}}}{m_{11}p(z_2) + n_{11}q(z_2)} \qquad (4.3.14)$$

where K is a constant, m_{11}, n_{11}, m_{21} & n_{21} are polynomials in z_1, m_{12}, n_{12}, m_{22} & n_{22} are polynomials in z_2, $p(z_2) = m_{12}+n_{12}$ and $q(z_2) = m_{22}+n_{22}$. The similarity of (4.3.14) and (2.4.20) can be noted. The denominator of $H(z_1,z_2)$ is cascade expressible in the form given by (4.2.10) and the numerator gives rise to transmission zeros at the required frequencies as seen along the unit circles in the z_1 and z_2 domains. For all the above digital transfer functions, the numerator and denominator are of the same degree, in each variable.

The normalized HP, BP and BS transfer functions of Theorems 4.2 to 4.4 are related to the LP transfer function of Theorem 4.1 by the allpass transformations [69], [70] listed below, which correspond to the reactance transformations of (2.4.21).

$$\begin{aligned} &\text{LP to HP} && z \rightarrow -z \\ &\text{LP to BP} && z \rightarrow -\left(\frac{3z^2+1}{z^2+3}\right) \\ &\text{LP to BS} && z \rightarrow \frac{3z^2+1}{z^2+3} \end{aligned} \qquad (4.3.15)$$

4.4 Digital transfer functions derived from the doubly-terminated network

Just as in the case of the analog doubly-terminated network transfer function, we can obtain a generation method

directly in the digital domain for the corresponding digital transfer function.

If the analog lowpass transfer function of the type given in (3.3.2.3) is transformed using the double bilinear transformation $p_i = (z_i-1)/(z_i+1)$, $i=1,2$, where we have assumed $T_1=T_2=2$, then the resulting digital transfer function is of the form

$$H(z_1,z_2) = \frac{K(z_1+1)^{n_1}(z_2+1)^{n_2}}{q_1(z_1)p_2(z_2) + p_1(z_1)q_2(z_2)} \qquad (4.4.1)$$

where n_1 and n_2 are the highest degrees of the denominator polynomial in z_1 and z_2 respectively. This is directly obtained using the theory developed in the previous section for the singly-terminated cascade separable network transfer functions in the digital domain.

For the generation of 2-D digital lowpass transfer functions, we use the following procedure.

(i) $$\left.\begin{aligned} p_1(z_1) &= m_{11}(z_1) + n_{11}(z_1) \\ \text{and} \quad q_1(z_1) &= m_{21}(z_1) + n_{21}(z_1) \end{aligned}\right\} \qquad (4.4.2)$$

are found such that they satisfy the conditions (2) and (3) of Theorem 4.1 for the z_1 variable. Similarly

$$\left.\begin{aligned} p_2(z_2) &= m_{12}(z_2) + n_{12}(z_2) \\ \text{and} \quad q_2(z_2) &= m_{22}(z_2) + n_{22}(z_2) \end{aligned}\right\} \qquad (4.4.3)$$

are generated such that they satisfy the same conditions for

the z_2 variable. Once this is done, the functions

$$F_1(z_1) = p_1(z_1)/q_1(z_1) \text{ and } F_2(z_2) = p_2(z_2)/q_2(z_2) \tag{4.4.4}$$

correspond to $Z_1(p_1)$ and $Z_2(p_2)$ in the analog domain.

(ii) The transfer function is then generated using (4.4.1).

The generation of transfer functions of other types such as the HP, BP or BS is also directly possible since for a general case, we have

$$H(z_1,z_2) = \frac{K\sqrt{m_{11}m_{21}-n_{11}n_{21}}\ \sqrt{m_{12}m_{22}-n_{12}n_{22}}}{q_1(z_1)p_2(z_2) + p_1(z_1)q_2(z_2)} \tag{4.4.5}$$

where K is a non-zero constant, m_{11}, n_{11}, m_{21} & n_{21} are polynomials in z_1 and m_{12}, n_{12}, m_{22} & n_{22} are polynomials in z_2. To generate a digital transfer function of any required type in the z_1 or z_2 variable, we use the conditions of Table 4.2 in place of the condition (3) used above.

The generation methods 1 and 2 discussed in Chapter 3 for the doubly-terminated cascade separable analog transfer functions can now be directly applied also for the generation of 2-D digital transfer functions. In place of the single-variable analog transfer function or the impedance function used for the generation, we use the corresponding single-variable digital functions.

4.5 Problems with the double bilinear transformation

In this section we discuss the problems associated with the 2-D digital transfer functions obtained by the double bilinear transformation of the analog transfer functions discussed earlier.

4.5.1 Transfer functions derived from singly-terminated networks

A 2-D digital transfer function obtained by the double bilinear transformation can have non-essential singularities of the second kind as pointed out by Goodman [31]. It is better to avoid such cases even though the resulting digital transfer function may be BIBO stable [71]. The conditions to test for this problem, are given by Goodman. Recently a testing procedure in the analog domain and formulation of very strict Hurwitz polynomials have been forwarded [72]. Here we test the digital transfer function to see if it satisfies Goodman's conditions.

Condition 1

In the analog transfer function, the numerator powers of p_1 and p_2 must not exceed the denominator powers of the corresponding variables. If this condition is not satisfied, the transformed digital function will contain the factors $(z_1+1)^{\alpha}\ (z_2+1)^{\beta}$ in the denominator, where α and β are positive integers. In the case of cascade separable analog transfer functions, this problem does not occur,

because the numerator degree is always less or at the most equal to the denominator degree in p_1 and p_2.

Condition 2

(a) The denominator polynomial evaluated at $(-1, z_2)$ must not be zero for $|z_2| \geq 1$ and

(b) the denominator evaluated at $(z_1, -1)$ must not be zero for $|z_1| \geq 1$.

The denominator of $H(z_1,z_2)$ is of the form given in (4.2.11)

i.e.,

$$D(z_1,z_2) = m_{11}(z_1)p(z_2) + n_{11}(z_1)q(z_2)$$

where

$$m_{11}(z_1) = \prod_{i=1}^{k} (a_{0i}z_1^2+a_{1i}z_1+a_{0i}) \qquad (4.5.1.1)$$

and

$$n_{11}(z_1) = (z_1^2-1) \prod_{i=1}^{k-1} (b_{0i}z_1^2+b_{1i}z_1+b_{0i})$$

Substituting $z_1 = -1$ gives $m_{11}(z_1) = k_1$ a constant and $n_{11}(z_1) = 0$. Hence $D(-1,z_2) = k_1p(z_2)$. We know that $p(z_2)/q(z_2)$ corresponds to an impedance function $Z_2(p_2) = P(p_2)/Q(p_2)$ in the analog domain, which can have the numerator degree one greater than the denominator degree and vice versa. Because of this, either $p(z_2)$ or $q(z_2)$ contains (z_2+1) as a factor. If $p(z_2)$ contains the factor (z_2+1), then the condition 2(a) is violated and there is a root at $z_1=z_2=-1$.

Evaluating $D(z_1,z_2)$ at $z_2=-1$ gives

$D(z_1,-1) = m_{11}(z_1)\, p(-1) + n_{11}(z_1)q(-1)$. If $q(z_2)$ contains the factor (z_2+1), we have $D(z_1,-1) = m_{11}(z_1)p(-1)$. It is noted that the roots of the $m_{11}(z_1)$ polynomial always lie on the unit circle in the z_1 plane, since the roots of $M_{11}(p_1)$ lie on the $j\omega$ axis in the p_1 plane. Similarly if $p(z_2)$ contains the factor (z_2+1), then $D(z_1,-1) = n_{11}(z_1)q(-1)$, which again contains roots on the z_1 unit circle. This problem occurs also when $p(z_2)$ or $q(z_2)$ contains a factor (z_2-1). In example 4.3, it is seen that the denominator goes to zero at $z_2 = -1$, $z_1=\pm j$.

From the above arguments we see that with the cascade separable ladder type networks, the resulting digital transfer function always contains certain poles lying on the unit bicircle. These poles can be easily isolated. To ensure stability, coefficient perturbation has to be done such that these roots are located inside the bicircle. In any implementation, this has to be ensured, after the quantization is done. The above problem of second kind singularities is also discussed in [73].

The problem of second kind singularities does not occur if $Z_2(p_2)$ is of the form

$$Z_2(p_2) = \frac{a_n p_2^n + a_{n-1} p_2^{n-1} + \ldots + a_0}{b_n p_2^n + b_{n-1} p_2^{n-1} + \ldots + b_0} \qquad (4.5.1.2)$$

where a_n, b_n, a_0, $b_0 \neq 0$, as in the case of a minimum reactive, minimum susceptive function.

4.5.2. Transfer functions derived from doubly terminated networks

Let us consider the equation (3.3.2.3). We know that P_1 and Q_1 have a degree difference of unity in the variable p_1 and similarly P_2 and Q_2 have a degree difference of unity in the variable p_2, because the ratios $Z_{11a} = P_1/Q_1$ and $Z_{11b} = P_2/Q_2$ are impedances of ladder type networks. Let us consider the following conditions regarding the degrees of P_1, Q_1, P_2 and Q_2.

(a) degree of Q_1 > degree of P_1 and
degree of Q_2 > degree of P_2

(b) degree of Q_1 < degree of P_1 and
degree of Q_2 < degree of P_2

In case (a), $p_1(z_1)q_2(z_2)$ would contain a factor (z_1+1) and $q_1(z_1)p_2(z_2)$ would contain a factor (z_2+1). Hence we have a non-essential singularity of the second kind at the point $z_1 = z_2 = -1$. The same problem occurs in case (b), since $q_1(z_1)p_2(z_2)$ contains the factor (z_1+1) and $p_1(z_1)q_2(z_2)$ contains the factor (z_2+1). The second kind singularities can be avoided by assuming the degrees of both Q_1 and P_2 to be greater than (or less than) those of P_1 and Q_2 respectively.

4.6 Summary and Conclusions

Using the properties of polynomials in the z variable which correspond to the even and odd polynomials in the analog domain, cascade separable polynomials were formulated in the digital domain. The realizability conditions were translated into the digital domain so that any given digital transfer function can be checked directly for realizability. This also helps in the generation of transfer functions in the digital domain. The 2-D transfer function derived from the singly-terminated network always possesses a non-essential singularity of the second kind on the unit bidisc in the z_1-z_2 hyperplane. Additional tests have to be conducted to ensure BIBO stability of the resulting 2-D filter. If the filter is unstable, then the isolated singularity can be brought inside the unit bidisc by slightly perturbing the coefficients of the 2-D digital transfer function. This problem of second-kind singularities also occurs in the 2-D transfer functions derived from the doubly-terminated networks, in certain cases. Here the isolated singularity occurs at the point $z_1 = z_2 = -1$. It is shown later that these cases can be easily identified and avoided.

CHAPTER 5.

APPROXIMATION OF 2-D ANALOG AND DIGITAL TRANSFER FUNCTIONS USING DOUBLY-TERMINATED CASCADE SEPARABLE NETWORK PROPERTIES

5.1 Introduction

Techniques for magnitude or phase approximation in the case of realizable analog two-variable transfer functions are not extensively discussed in the literature. A general theory of approximation of two-variable filter specifications in the analog domain is discussed in [11] and its extension to the digital domain by the use of spectral transformations is dealt with in [74]. As we had seen earlier, synthesis procedures exist only for certain classes of two-variable analog transfer functions. For a stable analog transfer function, a synthesis may not always be possible. Therefore it is preferable to start with a realizable transfer function and use it for approximation purposes. Considering that the doubly-terminated networks can easily be transformed into 2-D wave digital filters, it is useful to find approximation techniques using these networks.

In the case of two-dimensional filters, the symmetry in all the four quadrants of the magnitude response, called the quadrantal symmetry, may be an important requirement. It has been found [30] that a good quadrantal symmetry in the magnitude response of a doubly-terminated two-variable analog network is obtained only when the analog network consists of

p_1 and p_2 lossless two-port sections connected in cascade as shown in Fig. 3.1a.

Conditions for quadrantal symmetry as well as circular symmetry have been derived and approximations have been made incorporating these conditions [75]. It is known that if quadrantal symmetry is required, then the transfer function $T(p_1,p_2)$ must be variable separable; i.e., $T(p_1,p_2)$ must be expressible as a product $T_1(p_1)T_2(p_2)$. We show here that for a cascade separable network, the transfer function is not variable separable. Since exact quadrantal symmetry is thus not achievable, only an approximation towards it is possible. In such an approximation the transfer function becomes almost variable separable in the passband. Two approximation methods are developed in this chapter which produce near quadrantal symmetry. Both these methods can be used for approximations which give maximally flat magnitude (MFM) response, equiripple magnitude (ERM) response or a linear phase response in two variables.

The MFM and ERM approximations can be extended to the digital domain, by using the double bilinear transformation since it preserves the magnitude characteristics. However, this transformation does not preserve the linear phase property and hence cannot be used to obtain linear phase digital filters. A method of circumventing this problem is discussed in Chapter 6.

5.2 Symmetry requirements

In many practical requirements such as digital image processing, a certain type of symmetry such as a rectangular symmetry or circular symmetry is needed in the magnitude response plotted in the (ω_1,ω_2) plane [26],[27]. Usually a quadrantal symmetry is desired, which requires that the magnitude response plotted in all the four quadrants of the (ω_1,ω_2) plane has a reflection symmetry about the ω_1,ω_2 axes. The constraints to be satisfied by a transfer function in order to possess different types of symmetries are given in [28]. Here we apply these constraints to the transfer function of a doubly-terminated network and find out the conditions imposed on the network transfer function.

A transfer function $T(j\omega_1,j\omega_2)$ possesses a 2-fold rotation symmetry (also known as reflection or centrosymmetry) if

$$|T(j\omega_1,j\omega_2)| = |T(-j\omega_1,-j\omega_2)| \quad \forall \ (\omega_1,\omega_2) \qquad (5.2.1)$$

This condition is satisfied by any rational function $T(p_1,p_2)$ with real coefficients. Because of this, the magnitude response is symmetric in the opposite quadrants.

If the magnitude function is symmetric about the two diagonals (lines bisecting the first and third quadrants and the second and fourth quadrants) of the (ω_1,ω_2) plane, it is said to possess a reflection symmetry about the diagonals. The constraint in this case is

$$|T(j\omega_1,j\omega_2)| = |T(j\omega_2,j\omega_1)| = |T(-j\omega_1,-j\omega_2)| = |T(-j\omega_2,-j\omega_1)| \quad \forall(\omega_1,\omega_2) \tag{5.2.2}$$

By analytic continuation of two-variable rational functions, the constraint becomes

$$T(p_1,p_2)T(-p_1,-p_2) \equiv T(p_2,p_1)T(-p_2,-p_1) \tag{5.2.3}$$

In the case of transfer functions of the type given in (3.3.1.10) this condition is satisfied if we have

$$D(p_1,p_2)D(-p_1,-p_2) \equiv D(p_2,p_1)D(-p_2,-p_1) \tag{5.2.4}$$

where

$$D(p_1,p_2) = (M_{11}+N_{21})(M_{12}+N_{12})+(M_{21}+N_{11})(M_{22}+N_{22})$$
$$D(-p_1,-p_2) = (M_{11}-N_{21})(M_{12}-N_{12})+(M_{21}-N_{11})(M_{22}-N_{22}) \tag{5.2.5}$$

$D(p_2,p_1)$ and $D(-p_2,-p_1)$ are obtained by interchanging p_1 and p_2 in the above two equations. M_{11}, M_{21}, N_{11} & N_{21} are polynomials in the p_1 variable and M_{12}, M_{22}, N_{12} & N_{22} are polynomials in the p_2 variable.

Since the symmetry requires the response to be identical along the ω_1 and ω_2 axes, we must have

$$D(0,p)D(0,-p) \equiv D(p,0)D(-p,0) \tag{5.2.6}$$

This can be satisfied if we have either

$$M_{11}(p) = k_1 M_{12}(p), \quad N_{11}(p) = k_2 N_{22}(p)$$
$$N_{21}(p) = k_1 N_{12}(p), \quad M_{21}(p) = k_2 M_{22}(p) \tag{5.2.7}$$

or

$$M_{11}(p) = k_1 M_{22}(p), \quad M_{21}(p) = k_2 M_{12}(p)$$
$$N_{11}(p) = k_2 N_{12}(p), \quad N_{21}(p) = k_1 N_{22}(p) \tag{5.2.8}$$

where k_1 and k_2 are constants. With these conditions, $D(p_1,p_2) = D(p_2,p_1)$ and $D(-p_1,-p_2) = D(-p_2,-p_1)$.

Quadrantal symmetry or reflection symmetry about the ω_1 and ω_2 axes is obtained if

$$|T(j\omega_1,j\omega_2)| = |T(-j\omega_1,j\omega_2)| = |T(j\omega_1,-j\omega_2)| = |T(-j\omega_1,-j\omega_2)| \quad \forall (\omega_1,\omega_2) \tag{5.2.9}$$

which gives

$$T(p_1,p_2)T(-p_1,-p_2) = T(-p_1,p_2)T(p_1,-p_2) \tag{5.2.10}$$

It has been shown [28] that for a transfer function possessing quadrantal symmetry to be stable, the denominator has to be product separable i.e., expressible as a product of two single-variable Hurwitz polynomials. This property has also been noted in certain numerical optimizations carried out for circular symmetry [30], [33]. To find the conditions for the transfer function to be product separable, let us assume the denominator to be a product of two polynomials $F_1(p_1)$ in the variable p_1 and $F_2(p_2)$ in the variable p_2.

i.e.,

$$D(p_1,p_2) = [M_{11}(p_1)+N_{21}(p_1)]P(p_2)+[M_{21}(p_1)+N_{11}(p_1)]Q(p_2)$$
$$= F_1(p_1)F_2(p_2) \qquad (5.2.11)$$

This is clearly possible only if we have either

$$\text{(a)} \quad M_{11}(p_1) = k_1 M_{21}(p_1) \text{ and } N_{21}(p_1) = k_1 N_{11}(p_1)$$

or (5.2.12)

$$\text{(b)} \quad P(p_2) = k_2 Q(p_2)$$

where k_1 and k_2 are constants.

This means that either the p_1 network or the p_2 network has to be a constant resistance type of network.

A similar condition can also be derived using (5.2.10). We must satisfy the condition

$$D(p_1,p_2)D(-p_1,-p_2) \equiv D(-p_1,p_2)D(p_1,-p_2) \qquad (5.2.13)$$

where $D(p_1,p_2)$ & $D(-p_1,-p_2)$ are as in (5.2.5) and

$$D(-p_1,p_2) = (M_{11}-N_{21})(M_{12}+N_{12})+(M_{21}-N_{11})(M_{22}+N_{22})$$
$$D(p_1,-p_2) = (M_{11}+N_{21})(M_{12}-N_{12})+(M_{21}+N_{11})(M_{22}-N_{22}) \qquad (5.2.14)$$

By substituting for $D(p_1,p_2)$, $D(-p_1,-p_2)$, $D(-p_1,p_2)$ & $D(p_1,-p_2)$ and simplifying the identity, we obtain the following conditions.

$$M_{11}(p_1)N_{11}(p_1) = M_{21}(p_1)N_{21}(p_1)$$

or (5.2.15)

$$M_{12}(p_2)N_{22}(p_2) = N_{12}(p_2)M_{22}(p_2)$$

These conditions show that we cannot obtain quadrantal symmetry in the magnitude response, unless we have either the p_1 network or the p_2 network as a constant resistance network. Hence with the p_1 and p_2 networks as lossless lowpass ladders, exact quadrantal symmetry cannot be achieved. However, quadrantal symmetry can be approximated to a good degree, over the passband as shown later in this chapter.

For octagonal symmetry, which is a reflection symmetry about four lines mutually separated by $\pi/4$ radians, passing through the origin, both the conditions for quadrantal symmetry as well as those for rotational symmetry about the diagonals, have to be satisfied.

5.3 Conditions for maximally flat magnitude (MFM) response

In this section, we derive the conditions for an nth order transfer function $T(p_1,p_2)$ of the form given in (3.3.1.10) to be maximally flat at the origin along ω_1 and ω_2 axes. We represent $T(p_1,p_2)$ as follows.

$$T(p_1,p_2) = \frac{1}{D(p_1,p_2)} = \frac{1}{M_A'+N_A'} \qquad (5.3.1)$$

where M_A' and N_A' are even and odd polynomials in p_1 and p_2 and are given by

$$M_A' = M_{11}(p_1)M_{12}(p_2)+M_{21}(p_1)M_{22}(p_2)+N_{21}(p_1)N_{12}(p_2)+N_{11}(p_1)N_{22}(p_2)$$

and (5.3.2)

$$N_A' = M_{11}(p_1)N_{12}(p_2)+M_{21}(p_1)N_{22}(p_2)+N_{21}(p_1)M_{12}(p_2)+N_{11}(p_1)M_{22}(p_2)$$

If we make the substitution $p_1 = j\omega_1$ and $p_2 = j\omega_2$, we see that $M'_A\Big|_{p_1=j\omega_1, p_2=j\omega_2} = M_A$ is an expression containing only real terms and $N'_A\Big|_{p_1=j\omega_1, p_2=j\omega_2} = N_A$ is an expression containing purely imaginary terms.

The magnitude-squared function is

$$|T(j\omega_1, j\omega_2)|^2 = \frac{1}{M_A^2 - N_A^2} \qquad (5.3.3)$$

If we take the partial derivative of (5.3.3) w.r.t. ω_1, we get

$$|T| \frac{\partial |T|}{\partial \omega_1} = -|T|^4 \left[M_A \frac{\partial M_A}{\partial \omega_1} - N_A \frac{\partial N_A}{\partial \omega_1}\right] \qquad (5.3.4)$$

where $|T|$ represents $|T(j\omega_1, j\omega_2)|$.

For $\partial|T|/\partial\omega_1 = 0$, we get the condition

$$M_A \frac{\partial M_A}{\partial \omega_1} = N_A \frac{\partial N_A}{\partial \omega_1} \qquad (5.3.5)$$

Similarly partial differentiation of (5.3.3) w.r.t. ω_2 gives

$$M_A \frac{\partial M_A}{\partial \omega_2} = N_A \frac{\partial N_A}{\partial \omega_2} \qquad (5.3.6)$$

Equating the second order partial derivatives to zero gives us the following conditions.

$$M_A \frac{\partial^2 M_A}{\partial \omega_1^2} + \left(\frac{\partial M_A}{\partial \omega_1}\right)^2 = N_A \frac{\partial^2 N_A}{\partial \omega_1^2} + \left(\frac{\partial N_A}{\partial \omega_1}\right)^2$$

$$M_A \frac{\partial^2 M_A}{\partial \omega_1 \partial \omega_2} + \frac{\partial M_A}{\partial \omega_1}\frac{\partial M_A}{\partial \omega_2} = N_A \frac{\partial^2 N_A}{\partial \omega_1 \partial \omega_2} + \frac{\partial N_A}{\partial \omega_1}\frac{\partial N_A}{\partial \omega_2} \qquad (5.3.7)$$

$$M_A \frac{\partial^2 M_A}{\partial \omega_2^2} + \left(\frac{\partial M_A}{\partial \omega_2}\right)^2 = N_A \frac{\partial^2 N_A}{\partial \omega_2^2} + \left(\frac{\partial N_A}{\partial \omega_2}\right)^2$$

Proceeding in the same fashion as above, we can see that the conditions obtained for higher order derivatives are just the expressions obtained by partially differentiating the set of conditions (5.3.5) and (5.3.6).

For a general nth order $D(p_1,p_2)$ given by

$$D(p_1,p_2) = A_{11}p_1^n p_2^n + A_{12}p_1^{n}p_2^{n-1} + \ldots + A_{n+1,n+1} \qquad (5.3.8)$$

where n is the order of the p_1 and p_2 networks, we can represent $D(p_1,p_2)$ as

$$D(p_1,p_2) = [p_1^n p_1^{n-1} \ldots 1]\ [A] \begin{bmatrix} p_2^n \\ p_2^{n-1} \\ \vdots \\ 1 \end{bmatrix} \qquad (5.3.9)$$

where the matrix

$$[A] = \begin{bmatrix} A_{11} & A_{12} & \cdots & A_{1,n+1} \\ A_{21} & A_{22} & \cdots & A_{2,n+1} \\ \vdots & \vdots & & \vdots \\ A_{n+1,1} & A_{n+1,2} & \cdots & A_{n+1,n+1} \end{bmatrix}$$

is the coefficient matrix.

If we make the substitution $p_1 = j\omega_1$, and $p_2 = j\omega_2$ in (5.3.9), we get

$$D(j\omega_1, j\omega_2) = [(j\omega_1)^n (j\omega_1)^{n-1} \ldots 1][A] \begin{bmatrix} (j\omega_2)^n \\ (j\omega_2)^{n-1} \\ \vdots \\ 1 \end{bmatrix} \tag{5.3.10}$$

$$= [\omega_1^n \omega_1^{n-1} \ldots 1] \begin{bmatrix} j^n & & 0 \\ & j^{n-1} & \\ & & \ddots \\ 0 & & 1 \end{bmatrix} [A] \begin{bmatrix} j^n & & 0 \\ & j^{n-1} & \\ & & \ddots \\ 0 & & 1 \end{bmatrix} \begin{bmatrix} \omega_2^n \\ \omega_2^{n-1} \\ \vdots \\ 1 \end{bmatrix}$$

$$= [\omega_1^n \omega_1^{n-1} \ldots 1] (-1)^n \begin{bmatrix} A_{11} & -jA_{12} & -A_{13} & jA_{14} & \\ -jA_{21} & -A_{22} & jA_{23} & & \\ -A_{31} & jA_{32} & & & \\ jA_{41} & & & (-1)^n jA_{n,n+1} & \\ & & (-1)^n jA_{n+1,n} & (-1)^n A_{n+1,n+1} & \end{bmatrix} \begin{bmatrix} \omega_2^n \\ \omega_2^{n-1} \\ \vdots \\ 1 \end{bmatrix}$$

Hence

$$D(j\omega_1, j\omega_2) = M_A + N_A \qquad (5.3.11)$$

where

$$M_A = [\omega_1^{n'}\omega_1^{n-1} \ldots 1](-1)^n \begin{bmatrix} A_{11} & 0 & -A_{13} & \\ 0 & -A_{22} & \ddots & \\ -A_{31} & \ddots & 0 & \\ & 0 & (-1)^n A_{n+1,n+1} & \end{bmatrix} \begin{bmatrix} \omega_2^n \\ \omega_2^{n-1} \\ \\ \vdots \\ 1 \end{bmatrix}$$

and

$$N_A = [\omega_1^n\omega_1^{n-1} \ldots 1](j)(-1)^n \begin{bmatrix} 0 & -A_{12} & 0 & A_{14} & \\ -A_{21} & 0 & A_{23} & \ddots & \\ 0 & A_{32} & \ddots & (-1)A_{n,n+1} & \\ A_{41} & \ddots & & & \\ & & (-1)^n A_{n+1,n} & 0 & \end{bmatrix} \begin{bmatrix} \omega_2^n \\ \omega_2^{n-1} \\ \vdots \\ 1 \end{bmatrix}$$

---

* The dotted lines are used to illustrate the structure of the elements and do not indicate partitioning of the matrix.

If an nth order two-variable polynomial is represented as

$$P = [\omega_1^n \omega_1^{n-1} \ldots 1] \left[P \begin{matrix}\text{coefficient} \\ \text{matrix}\end{matrix}\right] \begin{bmatrix} \omega_2^n \\ \omega_2^{n-1} \\ \vdots \\ 1 \end{bmatrix} \qquad (5.3.12)$$

then $\partial P/\partial \omega_1$ is given by

$$\frac{\partial P}{\partial \omega_1} = [\omega_1^n \ \omega_1^{n-1} \ldots 1] \begin{bmatrix} 0 & & & & & 0 \\ & 0 & & & & \\ n & & \ddots & & & \\ & n-1 & & \ddots & & \\ & & \ddots & & 0 & \\ & & & 2 & & 0 \\ 0 & & & & 1 & \\ & & & & & 0 \end{bmatrix} [P_c] \begin{bmatrix} \omega_2^n \\ \omega_2^{n-1} \\ \vdots \\ 1 \end{bmatrix}$$

(5.3.13)

where $[P_c]$ represents the P coefficient matrix.

The elements of the $\partial P/\partial \omega_1$ coefficient matrix are obtained by shifting the P coefficient matrix down by one row, thereby eliminating the bottom row and multiplying the rows by $1,2,3,\ldots,n$ from the bottom to the top and assuming the top most row as a zero row.

Similarly $\partial P/\partial \omega_2$ is given by

$$\frac{\partial P}{\partial \omega_2} = [\omega_1^n \ \omega_1^{n-1} \ldots 1] \ [P \text{ coefficient matrix}] \begin{bmatrix} 0 & n & & 0 \\ 0 & n-1 & & \\ & \ddots & \ddots & \\ & 0 & 2 & \\ & & 1 & \\ 0 & & 0 & 0 \end{bmatrix} \begin{bmatrix} \omega_2^n \\ \omega_2^{n-1} \\ \vdots \\ 1 \end{bmatrix} \qquad (5.3.14)$$

The elements of the $\partial P/\partial \omega_2$ coefficient matrix are obtained by shifting the P coefficient matrix to the right by one column and multiplying the columns by $1,2,3,\ldots,n$ from right to left, with the left most column assumed as a zero column. The second order derivatives are obtained by repeating the above operation on the $\partial P/\partial \omega_1$ and $\partial P/\partial \omega_2$ coefficient matrices.

Let us consider the P coefficient matrix for an nth order case.

$$[P_c] = \begin{bmatrix} P_{11} & P_{12} & \cdots & P_{1,n+1} \\ P_{21} & & & \vdots \\ \vdots & & & \vdots \\ \vdots & & & P_{n,n+1} \\ P_{n+1,1} & \cdots & P_{n+1,n} & P_{n+1,n+1} \end{bmatrix} \qquad (5.3.15)$$

Then the coefficient matrices for the first partial derivatives are given by

$$\left[\left(\frac{\partial P}{\partial \omega_1}\right)_C\right] = \begin{bmatrix} 0 & 0 & \cdots & 0 \\ nP_{11} & nP_{12} & \cdots & nP_{1,n+1} \\ \vdots & \vdots & & \\ 2P_{n-1,1} & 2P_{n-1,2} & \cdots & 2P_{n-1,n+1} \\ P_{n1} & P_{n2} & & P_{n,n+1} \end{bmatrix}$$

(5.3.16a)

$$\left[\left(\frac{\partial P}{\partial \omega_2}\right)_C\right] = \begin{bmatrix} 0 & nP_{11} & \cdots & 2P_{1,n-1} & P_{1n} \\ 0 & nP_{21} & \cdots & 2P_{2,n-1} & P_{2n} \\ \vdots & \vdots & & \vdots & \vdots \\ 0 & nP_{n+1,1} & \cdots & 2P_{n+1,n-1} & P_{n+1,n} \end{bmatrix}$$

(5.3.16b)

The coefficient matrices for the second partial dervatives are similarly obtained as

$$\left[\left(\frac{\partial^2 P}{\partial \omega_1^2}\right)_C\right] = \begin{bmatrix} 0 & 0 & \cdots & 0 \\ 0 & 0 & \cdots & 0 \\ n(n-1)P_{11} & n(n-1)P_{12} & \cdots & n(n-1)P_{1,n+1} \\ \vdots & \vdots & & \vdots \\ 6P_{n-2,1} & 6P_{n-2,2} & \cdots & 6P_{n-2,n+1} \\ 2P_{n-1,1} & 2P_{n-1,2} & \cdots & 2P_{n-1,n+1} \end{bmatrix}$$

(5.3.17a)

$$\left[\left(\frac{\partial^2 P}{\partial \omega_2^2}\right)_C\right] = \begin{bmatrix} 0 & 0 & n(n-1)P_{11} & 6P_{1,n-2} & 2P_{1,n-1} \\ 0 & 0 & n(n-1)P_{21} & 6P_{2,n-2} & 2P_{2,n-1} \\ \vdots & \vdots & \vdots & \vdots & \vdots \\ 0 & 0 & n(n-1)P_{n+1,1} & \cdots 6P_{n+1,n-2} & 2P_{n+1,n-1} \end{bmatrix} \qquad (5.3.17b)$$

and

$$\left[\left(\frac{\partial^2 P}{\partial \omega_1 \partial \omega_2}\right)_C\right] = \left[\left(\frac{\partial^2 P}{\partial \omega_2 \partial \omega_1}\right)_C\right]$$

$$= \begin{bmatrix} 0 & & \cdots & 0 \\ 0 & n^2 P_{11} & \cdots & nP_{1n} \\ \vdots & & & \\ 0 & 2nP_{n-1,1} & \cdots & 2P_{n-1,n} \\ 0 & nP_{n1} & \cdots & P_{nn} \end{bmatrix} \qquad (5.3.17c)$$

If the first order derivatives are equated to zero at $\omega_1=\omega_2=0$, then we have $P_{n,n+1} = P_{n+1,n} = 0$. By equating the second order derivatives to zero at $\omega_1=\omega_2=0$, we get the condition $P_{n-1,n+1} = P_{n+1,n-1} = P_{nn} = 0$. It is seen that making the higher order derivatives zero at the origin is equivalent to progressively equating the diagonals indicated in (5.3.15) to zero, starting from the diagonal

adjacent to the constant term $P_{n+1,n+1}$.

In our case, the requirement is to make the derivatives of $(M_A^2-N_A^2)$ equal to zero at the origin $\omega_1 = \omega_2 = 0$. The method of obtaining M_A^2 coefficient matrix is shown below. If the M_A coefficient matrix is given by

$$[(M_A)_C] = \begin{bmatrix} M_{11} & M_{12} & \cdots & M_{1,n+1} \\ M_{21} & M_{22} & \cdots & M_{2,n+1} \\ \vdots & \vdots & & \vdots \\ M_{n+1,1} & M_{n+1,2} & \cdots & M_{n+1,n+1} \end{bmatrix} \qquad (5.3.18)$$

then M_A^2 is obtained by multiplying the matrix

$$\left[\begin{array}{c|c|c} (M_A)_C & \begin{matrix} 0 & \cdots & 0 \end{matrix} & \\ \hline & (M_A)_C & 0 \\ \hline \begin{matrix} 0 & \cdots & 0 \end{matrix} & \begin{matrix} 0 & \cdots & 0 \end{matrix} & \\ \hline & & \begin{matrix} 0 & \cdots & 0 \end{matrix} \\ \hline & & (M_A)_C \\ \hline 0 & 0 & \end{array}\right] \qquad (5.3.19)$$

where the $(M_A)_C$ matrix repeats $n+1$ times as $n+1$ blocks, with the matrix

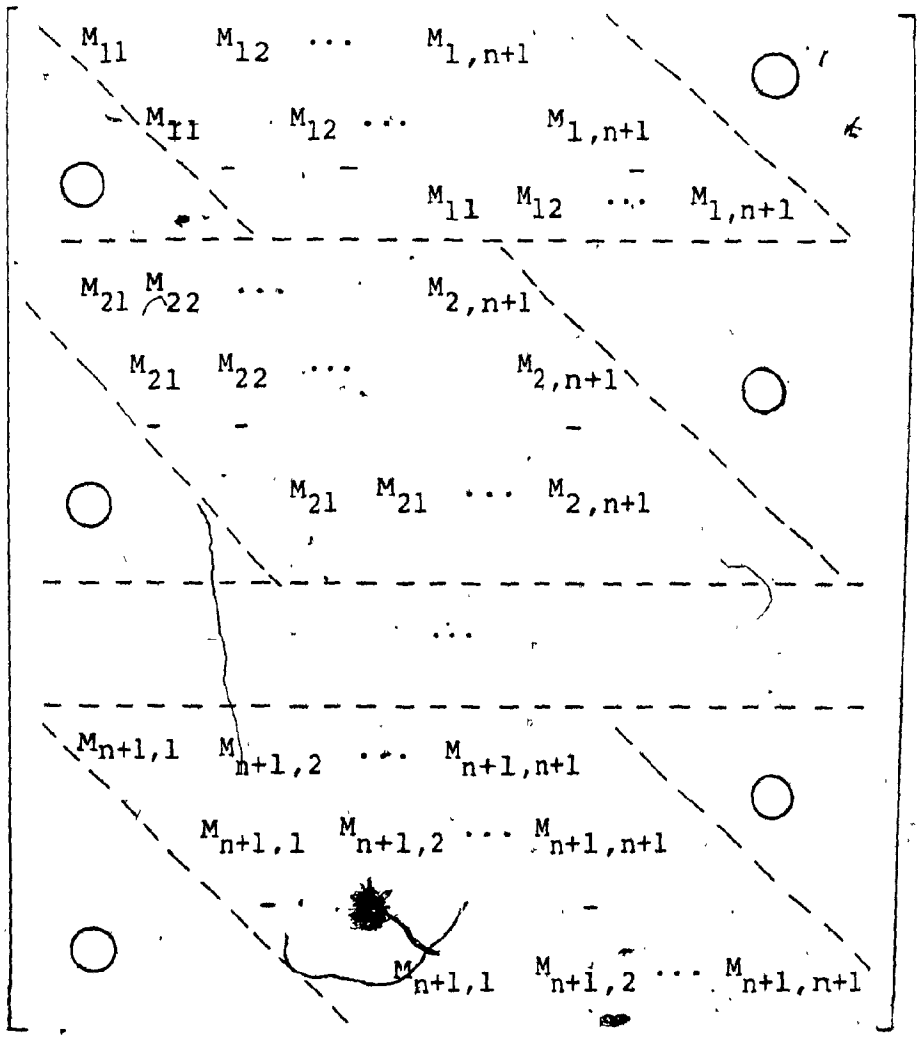

(5.3.20)

where each block indicated contains $n+1$ lines. The resuling M_A^2 coefficient matrix contains $2n+1$ rows and columns. Considering (5.3.11) which gives the M_A and N_A coefficient matrices, we can find the $(M_A^2-N_A^2)$ coefficient matrix using the above procedure. We can see that the M_A^2 and N_A^2 coefficient matrices are of the general form

$$
\begin{bmatrix}
A_{11}^2 & 0 & -2A_{11}A_{13} & 0 & 0\ldots0 & (-1)^{n+1}A_{1,n-1}A_{1,n+1} & 0 & (-1)^{n}A_{1,n+1}^2 \\
0 & -2A_{11}A_{22} & 0 & & \cdots & 0 & (-1)^{n}2A_{1,n+1}A_{2n} & 0 \\
-2A_{11}A_{31} & 0 & & & \cdots & & 0 & (-1)^{n+1}A_{3,n+1}A_{1,n+1} \\
0 & & & & \cdots & & & 0 \\
- & & & & \cdots & & & - \\
0 & & & & \cdots & & & 0 \\
(-1)^{n+1}A_{n-1,1}A_{n+1,1} & 0 & & & \cdots & & 0 & -2A_{n-1,n+1}A_{n+1,n+1} \\
0 & (-1)^{n+1}2A_{n+1,1}A_{n2} & & 0 & \cdots & 0 & -2A_{nn}A_{n+1,n+1} & 0 \\
(-1)^{n}A_{n+1,1}^2 & 0 & (-1)^{n+1}2A_{n+1,1}A_{n+1,3} & & 0\ldots0 & -2A_{n+1,n-1}A_{n+1,n+1} & 0 & A_{n+1,n+1}^2
\end{bmatrix}
\tag{5.3.21}
$$

and

$$\begin{bmatrix} 0 & 0 & -A_{12}^2 & 0\ldots0 & (-1)^{n+1}A_{1n}^2 & 0 & 0 \\ 0 & -2A_{12}A_{21} & 0 & \cdots & 0 & (-1)^{n}2A_{2,n+1}A_{1n} & 0 \\ -A_{21}^2 & 0 & & \cdots & & 0 & (-1)^{n+1}A_{2,n+1}^2 \\ 0 & & & \cdots & & & 0 \\ - & & & \cdots & & & - \\ 0 & & & \cdots & & & 0 \\ (-1)^{n+1}A_{n1}^2 & 0 & & \cdots & & 0 & -A_{n,n+1}^2 \\ 0 & (-1)^{n}2A_{n+1,2}A_{n1} & 0 & \cdots & 0 & -2A_{n+1,n}A_{n,n+1} & 0 \\ 0 & 0 & (-1)^{n+1}A_{n+1,2}^2 & 0\ldots0 & -A_{n+1,n}^2 & 0 & 0 \end{bmatrix} \qquad (5.3.22)$$

respectively. Substracting the matrix in (5.3.22) from that in (5.3.21) we get the $(M_A^2-N_A^2)$ coefficient matrix. By progressively making the diagonals to zero in this matrix, as explained earlier, we make the partial derivatives equal to zero at $\omega_1=\omega_2=0$. It is seen that all the odd ordered derivatives are zero by themselves, since the alternate diagonals are zero in both the M_A^2 and N_A^2 coefficient matrices. A maximally flat function is obtained if all the diagonals are made zero except for the highest degree term and the constant term. Thus a normalized maximally flat two-variable function is of the form

$$|T(j\omega_1, j\omega_2)|^2 = \frac{1}{1+\omega_1^{2n}\omega_2^{2n}} \qquad (5.3.23)$$

where n is the order of the function in each of the variables. It is to be noted that the response of this function however exhibits a constant value of unity along the ω_1 and ω_2 axes. Also this type of a maximally flat approximation is not realizable using a doubly-terminated cascade separable ladder network. Hence we apply the above conditions with an additional constraints to ensure the realizability of the function in the above fashion.

The approximation technique can be discussed starting from the doubly-terminated network of Fig. 5.1 with second order p_1 and p_2 lowpass ladder sections. The $[M_A^2-N_A^2]$ coefficient matrix is given by

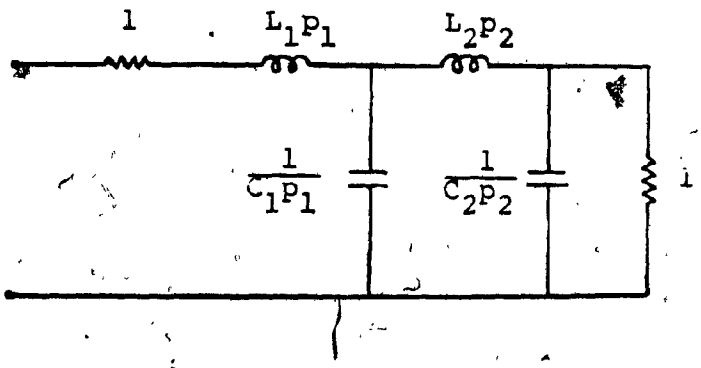

FIG. 5.1 DOUBLY-TERMINATED LADDER NETWORK WITH SECOND-ORDER p_1 AND p_2 SECTIONS

$$\begin{bmatrix} L_1^2L_2^2C_1^2C_2^2 & 0 & L_1^2C_1^2L_2(L_2-2C_2) & 0 & L_1^2C_1^2 \\ 0 & -2L_1^2L_2C_1C_2^2 & 0 & -2L_1^2C_1(L_2-C_2) & 0 \\ L_2^2C_2^2C_1(C_1-2L_1) & 0 & (L_1C_2+L_2C_1)^2+ & 0 & (L_1-C_1)^2 \\ 0 & 2L_2C_2^2(L_1-C_1) & 2L_2C_1(L_1C_2-L_1L_2-C_1C_2) & 2(L_1-C_1)(L_2-C_2) & 0 \\ L_2^2C_2^2 & 0 & (L_2-C_2)^2 & 0 & 4 \end{bmatrix}$$

(5.3.24)

where L_1 and C_1 are the elements of the p_1 network and L_2 and C_2 are the elements of the p_2 network. In order to make all the second order derivatives zero, we must have $L_1=C_1$ and $L_2=C_2$. This gives us the best possible approximation for an MFM response around $\omega_1 = \omega_2 = 0$ in the passband region, for the given network configuration. If we assume $L_1 = C_1 = \sqrt{2}$ and $L_2 = C_2 = \sqrt{2}$, then the cut off frequencies along the ω_1 and ω_2 axes are normalized to unity. The above choice results in a Butterworth response along the ω_1 and ω_2 axes as can be seen from the bottom most row and the right most column of the matrix in (5.3.24). The magnitude response for the network of Fig. 5.1 with $L_1 = C_1 = L_2 = C_2 = \sqrt{2}$, is

plotted in Fig. 5.2 as a contour plot.* It is seen that the p_1 and p_2 netowrks are none other than single-variable Butterworth ladders. The same results are observable for higher order networks. Hence the best MFM approximation for a cascade separable lowpass ladder network configuration is obtained by assuming the p_1 and p_2 ladder sections as Butterworth ladders.

The response of the network is vastly improved with higher order p_1 and p_2 sections as seen from Fig. 5.3, where the p_1 and p_2 sections contain the elements of a sixth order Butterworth network. The response is nearly quadrantal symmetric, approximating a rectangular symmetric response. Since there is a diagonal reflection symmetry, we can say that the response for the MFM approximation is nearly octagonal symmetric. Though it is sufficient to plot the response for two adjacent quadrants, the response in all four quadrants is shown for the sake of completeness.

---

* In this figure and the subsequent figures on the magnitude response, the following notation is used.

A: 0 to -0.45 db C:-3.74 to -5.19 db

1:-.45 to 1.41 db 3:-5.19 to -6.94 db

B:-1.41 to -2.5 db D:-6.94 to -9.12 db

2:-2.5 to -3.74 db 4:-9.12 to -12.04 db

E:-12.04 to -16.48 db

5:-16.48 to -26.02 db

The first three elements (inductors and capacitors) belong to the p_1, network and the rest, to the p_2 network.

COMPONENTS

INDUCTORS	1.4142	0.0000	0.0000	1.4142	0.0000	0.0000
CAPACITORS	1.4142	0.0000	0.0000	1.4142	0.0000	0.0000

RESISTORS RS= 1.0000 RL= 1.0000

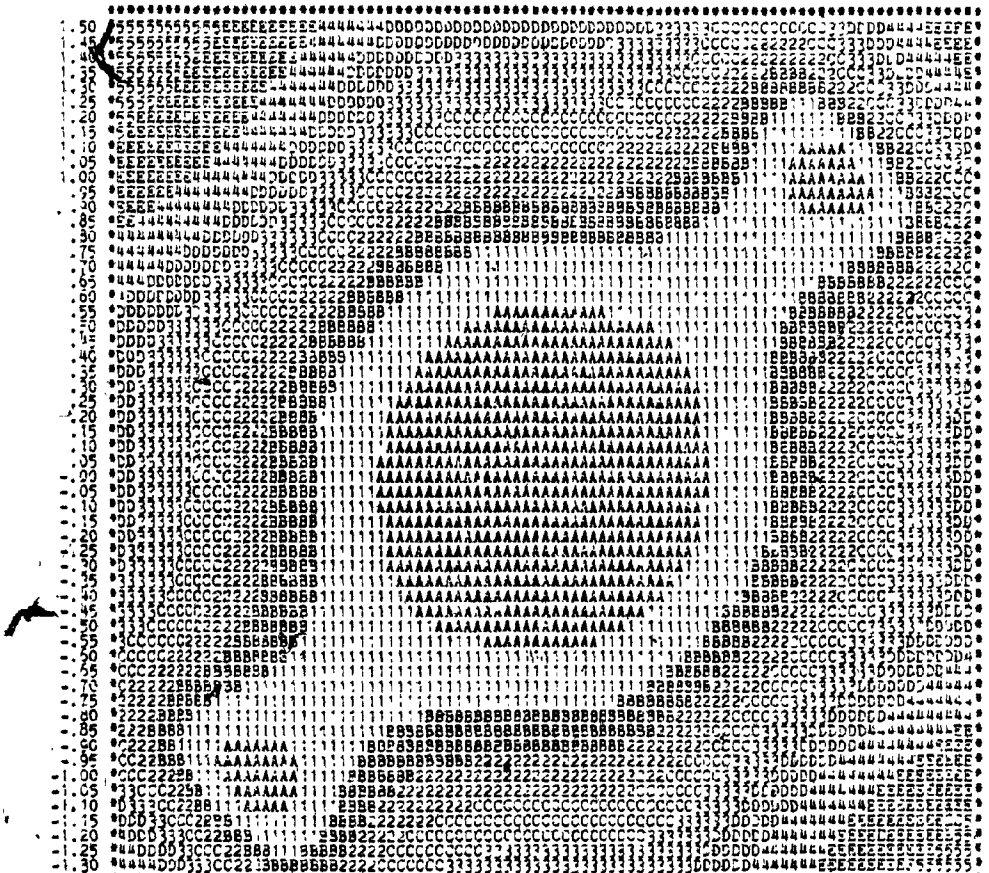

FIG. 5.2 MAGNITUDE RESPONSE OF THE NETWORK IN FIGURE 5.1 WITH BUTTERWORTH ELEMENTS

COMPONENTS

INDUCTORS	.5176	1.9319	1.4142	.5176	1.9319	1.4142
CAPACITORS	1.4142	1.9319	.5176	1.4142	1.3319	.5176

RESISTORS RS= 1.0000 RL= 1.0000

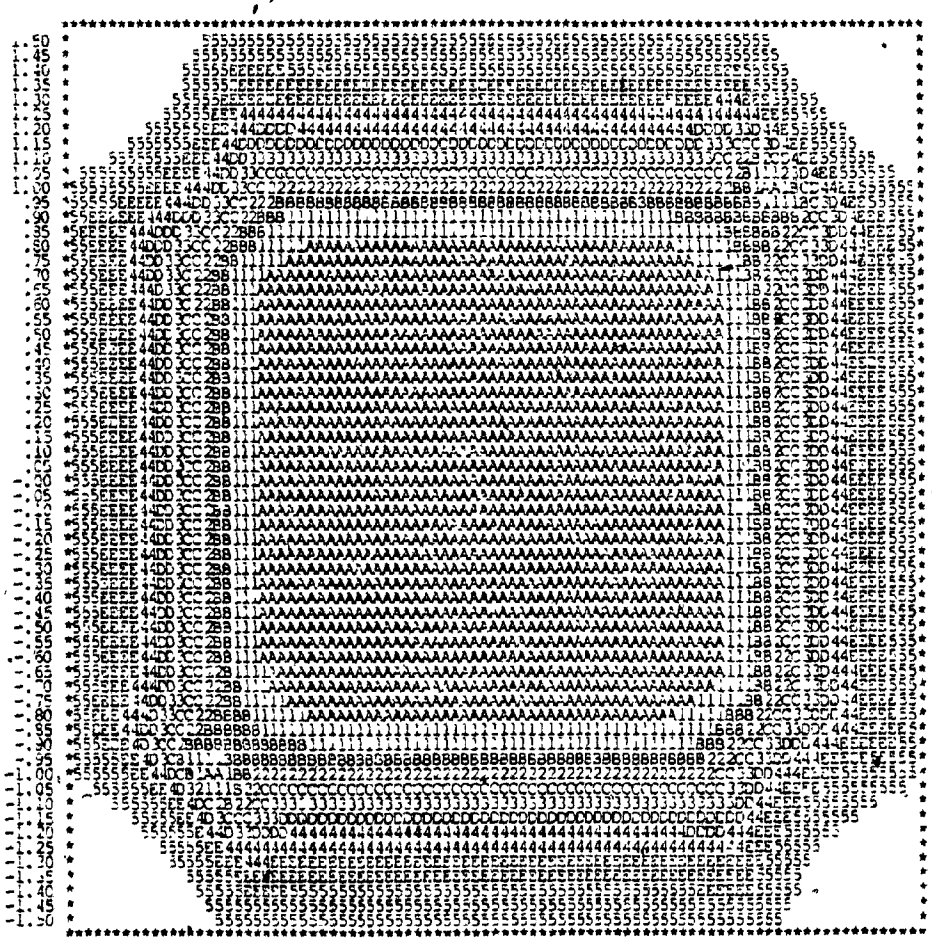

FIG. 5.3 RESPONSE OF A DOUBLY-TERMINATED CASCADE SEPARABLE NETWORK WITH P_1 AND P_2 NETWORKS AS SIXTH-ORDER BUTTERWORTH LADDERS

The symmetry properties can also be studied from the conditions obtained in the previous section for reflection symmetry about the diagonals and quadrantal symmetry. If in (5.2.7) or (5.2.8), we make

$$M_{11}(p) = M_{12}(p), \quad N_{11}(p) = N_{12}(p)$$
$$M_{21}(p) = M_{22}(p) \quad \text{and} \quad N_{21}(p) = N_{22}(p) \tag{5.3.25}$$

which is equivalent to having identical elements for the p_1 and p_2 networks, then the condition for reflection symmetry about the diagonals would be either

$$N_{11}(p) = k\, N_{21}(p)$$
or
$$M_{11}(p) = k\, M_{21}(p) \tag{5.3.26}$$

where k is a constant.

In the case of the Butterworth filter, we have $N_{11}(p) = kN_{21}(p)$ for even order and $M_{11}(p) = kM_{21}(p)$ for odd order, because the network is antisymmetrical for the even order case and symmetrical for the odd order case. Hence if the p_1 and p_2 networks are identical and contain the Butterworth filter elements, the resulting two-variable network possesses a reflection symmetry about the diagonals.

For quadrantal symmetry in the magnitude response, the conditions in (5.2.12) have to be satisfied. With Butterworth

filter elements, the network has the following properties. For even order, $N_{11}(p) = kN_{21}(p)$ and $M_{11}(p)$ is equal to $kM_{21}(p)$ except for the highest degree term. For odd order, $M_{11}(p) = kM_{21}(p)$ and $N_{11}(p)$ is equal to $kN_{21}(p)$ except for the highest degree term. This shows that in the passband, especially for low frequencies, the response is perfectly quadrantal symmetric. The two-variable approximations which are based on specified magnitude responses along the ω_1 and ω_2 axes as discussed above, are termed as type 1 approximations.

If equation (3.3.1.10) is written as

$$T(p_1,p_2) = \frac{K}{D(p_1,p_2)} = \frac{K}{P_1P_2+Q_1Q_2} = \frac{K/Q_1Q_2}{Z_1Z_2+1} \qquad (5.3.27)$$

where

$$P_1 = (M_{11}+N_{21}), \qquad Q_1 = (M_{21}+N_{11})$$

$$P_2 = (M_{12}+N_{12}), \qquad Q_2 = (M_{22}+N_{22})$$

$$Z_1 = P_1/Q_1 \quad \text{and} \quad Z_2 = P_2/Q_2$$

we can see that Z_2 is the driving point impedance of the resistively-terminated p_2 network and Z_1 is the driving point impedance of the inverted p_1 network terminated in a resistance. If the p_1 and p_2 networks have identical network elements, the response of Z_1 w.r.t. ω_1 is identical to that of Z_2 w.r.t. ω_2. For a general case, if the low-pass p_2 network and the inverted p_1 network begin with a capacitor, then Z_1 and Z_2 remain almost constant

over the low frequencies and approach a zero value for large frequncies. Hence from (5.3.27), $T(p_1,p_2)$ behaves almost like a variable separable function. A block diagram representation for the transfer function of (5.3.27) is given in Fig. 5.4a. If the above network sections start with an inductor, then Z_1 and Z_2 approach infinity for large frequencies and

$$T(p_1,p_2) = \frac{K}{P_1P_2+Q_1Q_2} = \frac{K/P_1P_2}{1+\frac{1}{Z_1Z_2}} \qquad (5.3.28)$$

behaves almost like a variable separable function. Fig. 5.4b gives a block diagram representation of the transfer function given by (5.3.28). Similar arguments can be put forth for other ladder sections where one of the networks has a capacitor as the leading element whereas the other begins with an inductor. Though exact quadrantal symmetry is not achieved by this method, a good approximation to quadrantal symmetry is obtained.

Since the magnitude approximation is carried out only along the ω_1 and ω_2 axes, $T(p_1,0)$ and $T(0,p_2)$ is realizable not only by the p_1 and p_2 networks mentioned above but also by their duals and transposes. If the single-variable transfer function $T_A(p)$ is realized by a network with a driving point impedance $Z_1 = (M_1+N_1)/(M_2+N_2)$, then the dual of the network realizing a driving point impedance $Z_2 = (M_2+N_2)/(M_1+N_1)$ and their transposes having driving point impedances $Z_3 = (M_2+N_1)/(M_1+N_2)$ and $Z_4 = (M_1+N_2)/(M_2+N_1)$

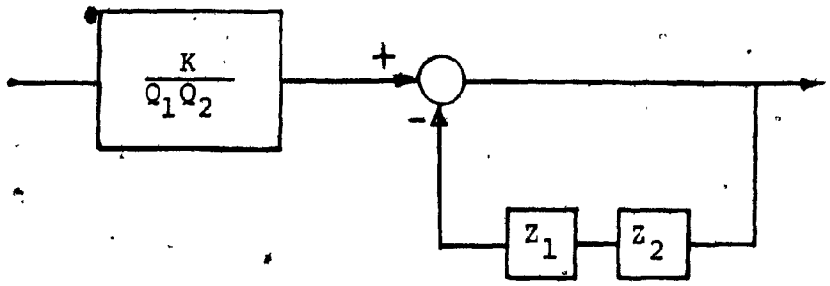

(a)

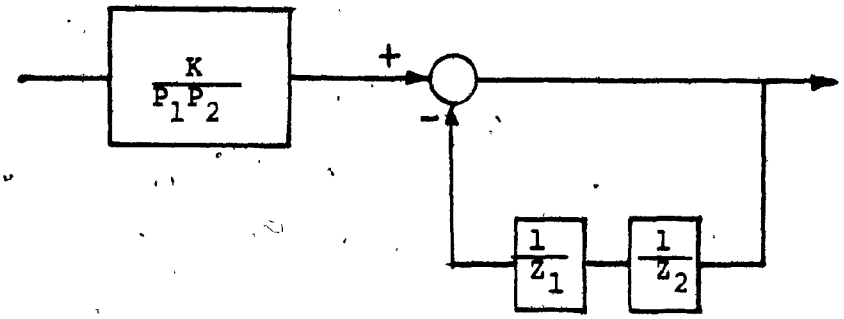

(b)

FIG. 5.4 BLOCK DIAGRAM REPRESENTATIONS FOR THE TRANSFER FUNCTIONS IN (5.3.27) and (5.3.28)

respectively also realize the transfer function $T_A(p)$. Hence the p_1 network as well as the p_2 network can each have 4 possible configurations, giving rise to a total of 16 combinations for $T(p_1,p_2)$. However, this gives only four distinct two-variable transfer functions, which are obtained by cascading a p_1 network with the four possible combinations for the p_2 network. All other combinations result in transfer functions which are identical to any one of the above two-variable transfer functions. The four transfer functions are as follows.

$$T_1(p_1,p_2) = k/[(M_{11}+N_{21})(M_{12}+N_{12})+(M_{21}+N_{11})(M_{22}+N_{22})] \quad (5.3.29a)$$

$$T_2(p_1,p_2) = k/[(M_{11}+N_{21})(M_{22}+N_{22})+(M_{21}+N_{11})(M_{12}+N_{12})] \quad (5.3.29b)$$

$$T_3(p_1,p_2) = k/[(M_{11}+N_{21})(M_{22}+N_{12})+(M_{21}+N_{11})(M_{12}+N_{22})] \quad (5.3.29c)$$

$$T_4(p_1,p_2) = k/[(M_{11}+N_{21})(M_{12}+N_{22})+(M_{21}+N_{11})(M_{22}+N_{12})] \quad (5.3.29d)$$

where the conditions of (5.3.25) are satisfied. If the p_1 and p_2 networks are symmetrical, then (5.3.29a) and (5.3.29c) are idential. Similarly (5.3.29b) and (5.3.29d) also become identical transfer functions. For antisymmetrical p_1 and p_2 networks, we have (5.3.29a) identical to (5.3.29d) and (5.3.29b) identical to (5.3.29c). If the p_2 network elements are identical to those of the inverted p_1 network, it

is seen that the response along the diagonal $\omega_1 = -\omega_2$ is equal to a constant. This is because at these frequencies the reactance of each of the elements of the p_1 network cancels exactly with the reactance of the corresponding element of the inverted p_2 network, starting from the middle of the network and looking in either direction and the network becomes purely resistive. A plot of the magnitude response of a network containing normalized 5th order Butterworth p_1 and p_2 sections with one ohm terminations, is shown in Fig. 5.5, which displays a constant magnitude of unity along the diagonal $\omega_1 = -\omega_2$. This happens because the p_2 and inverted p_1 networks have both identical element values. It is to be noted that the network of Fig. 5.3 which is made up of a different combination of Butterworth p_1 and p_2 networks, does not possess this problem. Thus we have only certain useful transfer functions which must be judiciously selected out of all the combinations.

In the above 5th order case, where the problem of unity magnitude along the diagonal is encountered (shown in Fig. 5.5), we see that the inverted p_1 network starts with a capacitor and the p_2 network also starts with a capacitor. From the discussions in section (4.5.2), it is easy to see that if the p_2 network and the inverted p_1 network both start with the same type of element (both either as capacitors or as inductors), then we encounter the problem of second kind singularities. Hence for symmetrical (odd order) or

COMPONENTS

INDUCTORS	0.0000	1.6180	1.6190	0.0000	1.6180	1.6180
CAPACITORS	.6180	2.0000	.6180	.6180	2.0000	.6190

RESISTORS RS= 1.0000 RL= 1.0000

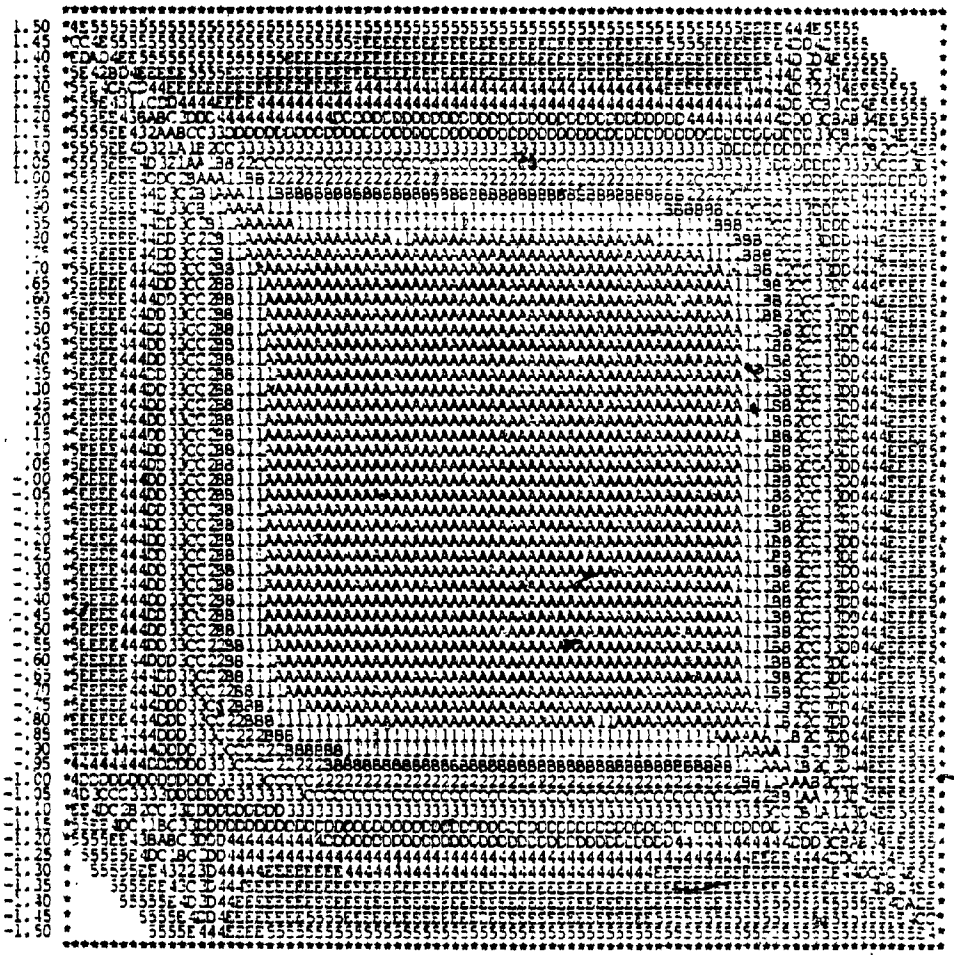

FIG. 5.5 TYPE 1 APPROXIMATION : MAGNITUDE RESPONSE FOR FIFTH-ORDER BUTTERWORTH p_1 AND p_2 SECTIONS DISPLAYING UNITY MAGNITUDE ALONG $\omega_1 = -\omega_2$

antisymmetrical (even order) p_1 and p_2 networks, in all the cases where the allpass diagonal response occurs, we also encounter the problem of second kind singularities. These cases can be avoided by proper choice of p_1 and p_2 networks so that the networks of the types used in Fig. 5.3 are only selected.

5.4 Other approximations of type 1

The type 1 approximations can be extended to other cases such as a Chebyshev, Gaussian or Bessel filter. If Chebyshev type of responses are desired along the ω_1 and ω_2 axes, then the p_1 and p_2 networks can be assumed as Chebyshev ladders. Since for the odd order case, the Chebyshev ladder is symmetrical, the condition for reflection symmetry about the diagonals is satisfied. The even order Chebyshev filter is physically realizable only for unequal termination resistances and here the reflection symmetry about the diagonals is not obeyed. However the magnitude response displays a good rectangular symmetry as can be observed in Fig. 5.6, which shows the magnitude response for a normalized Chebyshev filter having 6th order p_1 and p_2 sections. The elements correspond to those for a Chebyshev filter for 1/10 dB ripple, with a termination resistance ratio $r = R_s/R_L = 1/2$. In the case of the odd order Chebyshev filter, the termination resistances can be equal as shown for a network with 5th order p_1 and p_2 sections in Fig. 5.7.

COMPONENTS						
INDUCTORS	.3785	.8761	.8962	.3785	.8761	.8962
CAPACITORS	2.8071	3.3962	2.3561	2.8071	3.3962	2.3561

RESISTORS RS= .5000 RL= 1.0000

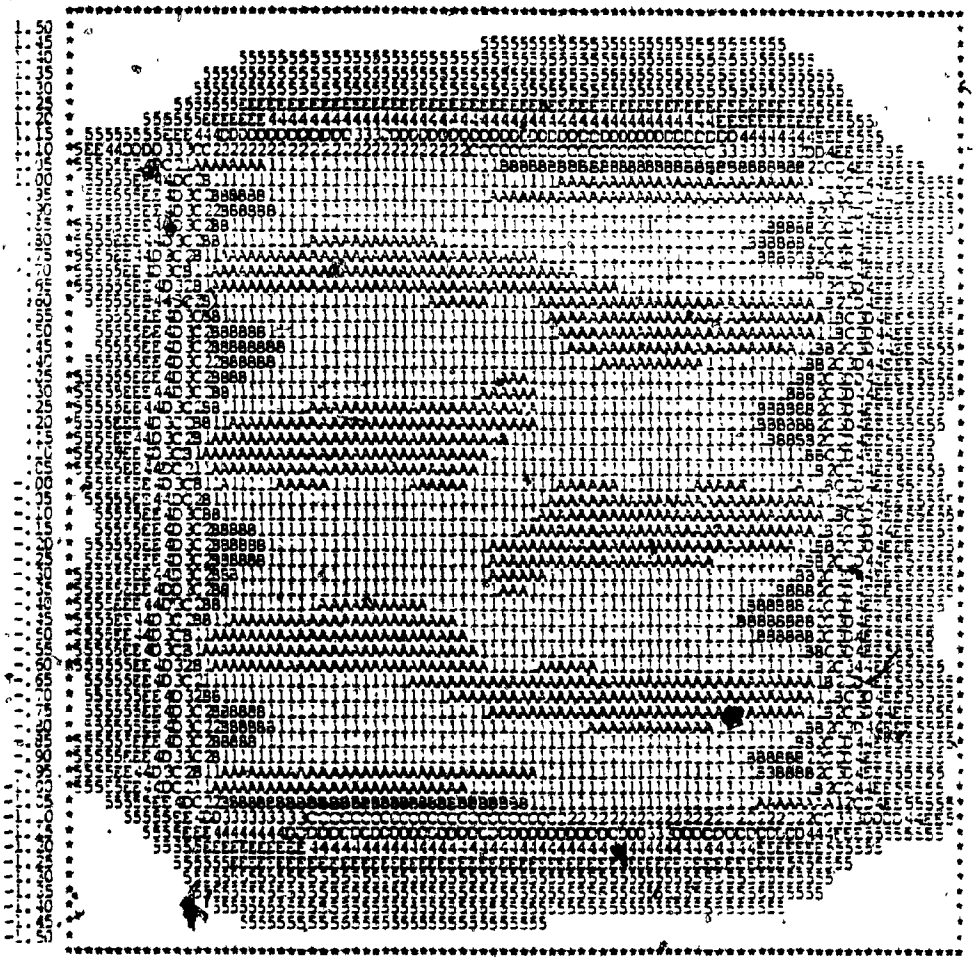

FIG. 5.6 TYPE 1 APPROXIMATION : MAGNITUDE RESPONSE FOR NETWORK USING SIXTH-ORDER CHEBYSHEV P_1 AND P_2 SECTIONS (RIPPLE 1/10 dB AND r = 1/2)

COMPONENTS						
INDUCTORS	0.0000	.7619	.7619	3.4813	4.5375	3.4813
CAPACITORS	3.4813	4.5375	3.4813	.7619	.7619	0.0000

RESISTORS RS= 1.0000 RL= 1.0000

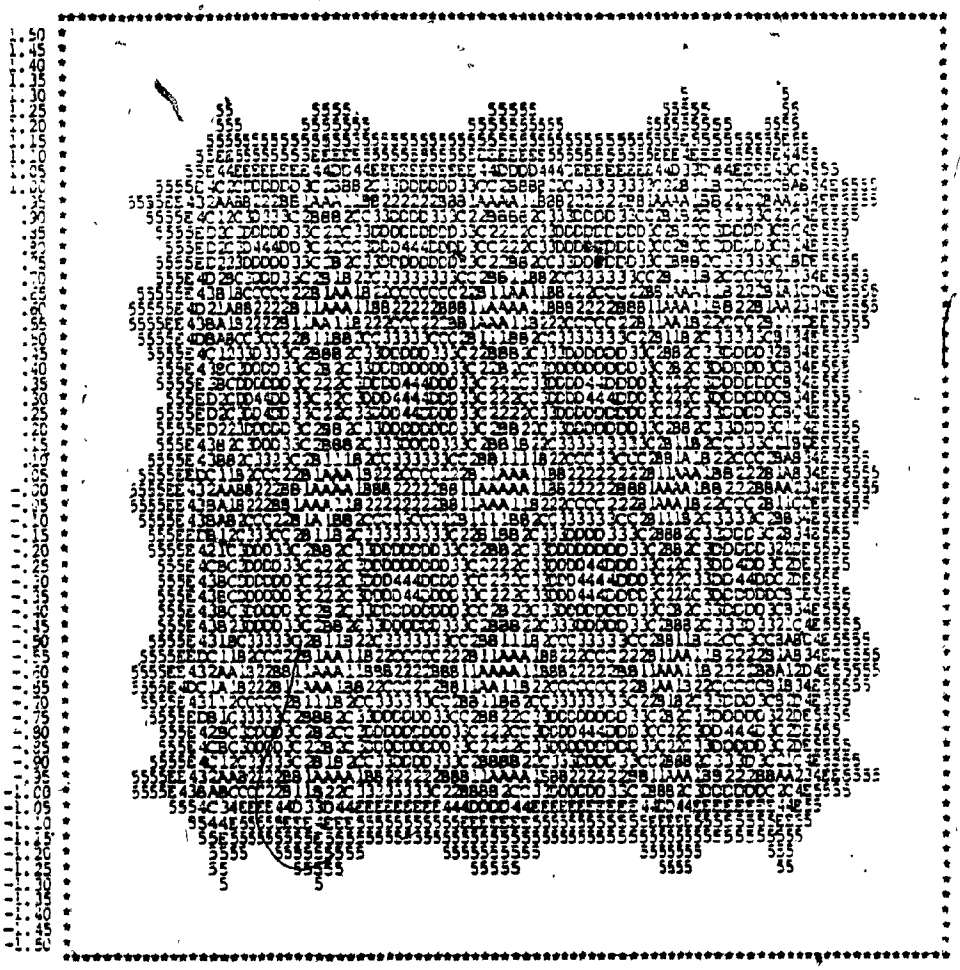

FIG. 5.7 TYPE 1 APPROXIMATION : MAGNITUDE RESPONSE FOR NETWORK USING FIFTH-ORDER CHEBYSHEV p_1 AND p_2 - SECTIONS (RIPPLE 3 dB AND r = 1)

The problems of both the allpass diagonal and the second kind singularity can be avoided by a suitable choice of the networks as follows. The allpass diagonal is avoided by taking care that the inverted p_1 network and the p_2 network elements are not identical. The second kind singularity is avoided by choosing the p_1 and p_2 networks such that their starting elements are not of the same type.

The nature of response for a Gaussian filter in single-variable and its synthesis are discussed in [76]. Since the square of the magnitude response of the Gaussian filter approximates $\exp(-\omega^2)$, it has been employed in variable separable filters to obtain a good circular symmetry [28]. The magnitude response of a network containing normalized 5th order Gaussian filter elements for the p_1 and p_2 sections, with one ohm source and load terminations, is shown in Fig. 5.8. Since the network is neither symmetrical nor antisymmetrical, there is no reflection symmetry about the diagonals. There is an accentuation of the response along the diagonal $\omega_1 = \omega_2$ and the contours are slightly elliptic.

Since linearity in phase is an important requirement in 2-D filters used for image processing applications, 2-D approximations have to take into account the phase specifications. Here we consider linear phase approximation in the analog domain for the doubly-terminated cascade separable ladder network. Let us represent the two-variable transfer function $T(p_1,p_2)$ given in (3.3.1.10) as

COMPONENTS						
INDUCTORS	0.0000	.3896	.9782	2.2533	.6485	.1312
CAPACITORS	.1312	.6485	2.2533	.9782	.3896	0.0000

RESISTORS RS= 1.0000 RL= 1.0000

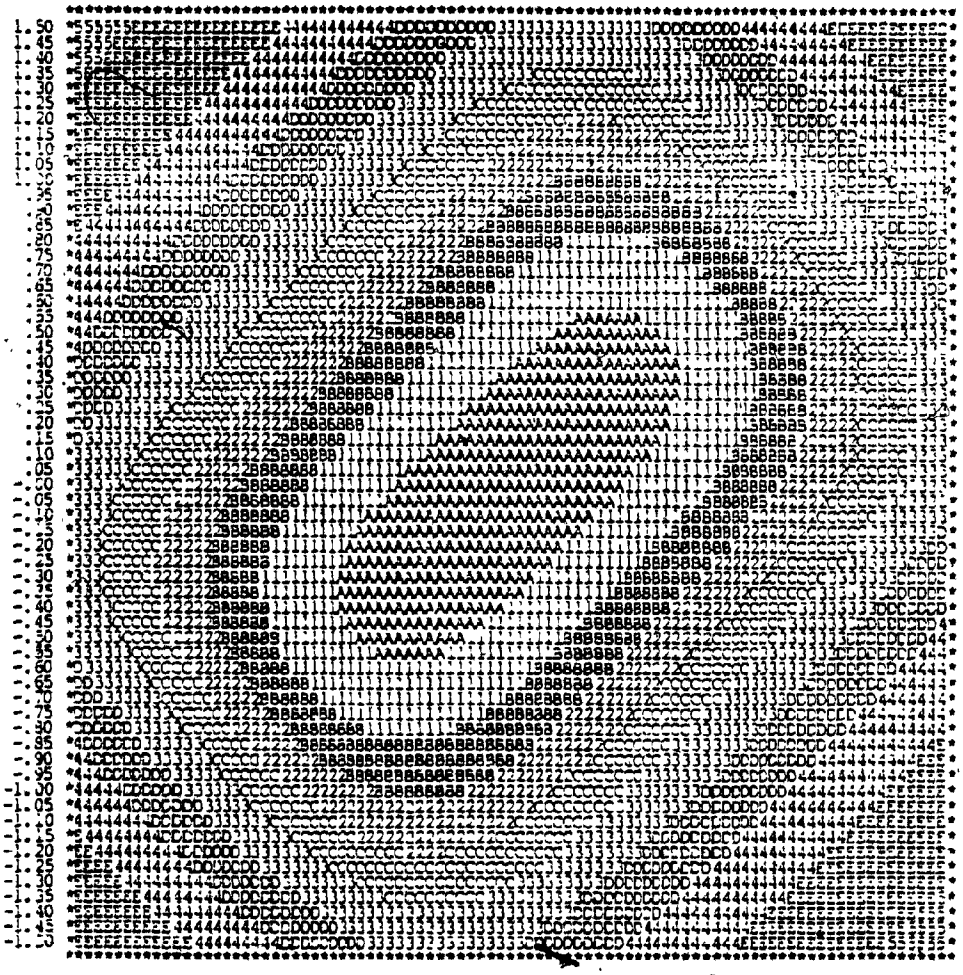

FIG. 5.8 TYPE 1 APPROXIMATION : MAGNITUDE RESPONSE FOR NETWORK USING FIFTH-ORDER GAUSSIAN FILTER AS p_1 AND p_2 SECTIONS

$$T(p_1,p_2) = \frac{1}{M+N} \tag{5.4.1}$$

where $M = M_{11}M_{12}+N_{21}N_{12}+M_{21}M_{22}+N_{11}N_{22}$ is the even part and $N = M_{11}N_{12}+N_{21}M_{12}+M_{21}N_{22}+N_{11}M_{22}$ is the odd part. The two-variable phase function for the given $T(p_1,p_2)$ is given by

$$\theta(\omega_1,\omega_2) = -\tan^{-1}\left(\frac{N}{jM}\right)\Bigg|_{\substack{p_1 = j\omega_1 \\ p_2 = j\omega_2}} \tag{5.4.2}$$

The group delay along the ω_1 direction is

$$\tau_1 = \frac{\partial\theta}{\partial\omega_1} = \frac{N\frac{\partial M}{\partial p_1} - M\frac{\partial N}{\partial p_1}}{M^2 - N^2}\Bigg|_{\substack{p_1 = j\omega_1 \\ p_2 = j\omega_2}} \tag{5.4.3}$$

Similarly the group delay along the ω_2 direction is given by

$$\tau_2 = \frac{\partial\theta}{\partial\omega_2} = \frac{N\frac{\partial M}{\partial p_2} - M\frac{\partial N}{\partial p_2}}{M^2 - N^2}\Bigg|_{\substack{p_1 = j\omega_1 \\ p_2 = j\omega_2}} \tag{5.4.4}$$

To have a constant group delay in both directions, τ_1 as well as τ_2 must be constants. To achieve this, we must satisfy the following conditions.

$$N\frac{\partial M}{\partial p_1} - M\frac{\partial N}{\partial p_1} = K_1(M^2-N^2) \tag{5.4.5a}$$

and

$$N\frac{\partial M}{\partial p_2} - M\frac{\partial N}{\partial p_2} = K_2(M^2-N^2) \qquad (5.4.5b)$$

where K_1 and K_2 are constants.

If we consider just the ω_1 axis, in order to have a constant group delay τ_1 along the ω_1 axis, we must satisfy (5.4.5a) with $p_2 = 0$. If $M_{12}(0) = M_{22}(0)$, then with $p_2 = 0$, we obtain the condition

$$\begin{aligned}(N_{21}+N_{11})(M'_{11}+M'_{21}) - (M_{11}+M_{21})(N'_{21}+N'_{11}) \\ = K_1[(M_{11}+M_{21})^2 - (N_{21}+N_{11})^2]\end{aligned} \qquad (5.4.6)$$

Similarly for a constant group delay τ_2 along the ω_2 axis, the equation (5.4.5b) must hold good for $p_1=0$. If $M_{11}(0) = M_{21}(0)$, then we have

$$\begin{aligned}(N_{12}+N_{22})(M'_{12}+M'_{22}) - (M_{12}+M_{22})(N'_{12}+N'_{22}) \\ = K_2[(M_{12}+M_{22})^2 - (N_{12}+N_{22})^2]\end{aligned} \qquad (5.4.7)$$

Conditions (5.4.6) and (5.4.7) show that the p_1 and p_2 networks must be networks with constant group delay, in their respective variables.

If we consider the phase of a two-variable transfer function, it can be represented as the sum of linear components in ω_1 and ω_2 and a two-variable component.

i.e.,

$$\theta(\omega_1,\omega_2) = K_1\omega_1 + K_2\omega_2 + \phi(\omega_1,\omega_2) \qquad (5.4.8)$$

In order to satisfy the conditions that $\partial\theta(\omega_1,\omega_2)/\partial\omega_1$ and $\partial\theta(\omega_1,\omega_2)/\partial\omega_2$ are constants, we must have $\phi(\omega_1,\omega_2) = 0$. In the case of a variable separable function

$$T(p_1,p_2) = T_1(p_1)T_2(p_2) \qquad (5.4.9)$$

the phase function is given by

$$\theta(\omega_1,\omega_2) = \theta_1(\omega_1) + \theta_2(\omega_2) \qquad (5.4.10)$$

where $\theta_1(\omega_1)$ and $\theta_2(\omega_2)$ are the phase responses of $T_1(p_1)$ and $T_2(p_2)$ respectively. Thus if $\theta_1 = K_1\omega_1$ and $\theta_2 = K_2\omega_2$, then the variable separable transfer function possesses constant group delays τ_1 and τ_2 along the ω_1 and ω_2 axes directions respectively. In image processing, it is known that with τ_1 and τ_2 as constants, the output image is spatially shifted w.r.t. the input image, without undergoing any distortion [77].

With p_1 and p_2 networks as ladders having elements identical to those of a normalized maximally flat time delay network, the resulting phase response is seen to have a good linearity in the ω_1 and ω_2 directions and the linearity improves as the order of the network is increased. The phase response of a network with identical 6th order p_1 and p_2 sections, containing the elements of a Bessel filter, is shown in Fig. 5.9. In Figure 5.9a, the region corresponding

COMPONENTS

INDUCTORS	.0505	.2364	.4116	.0505	.2364	.4116
CAPACITORS	.1480	.3158	.8377	.1480	.3158	.8377

RESISTORS RS= 1.0000 RL= 1.0000

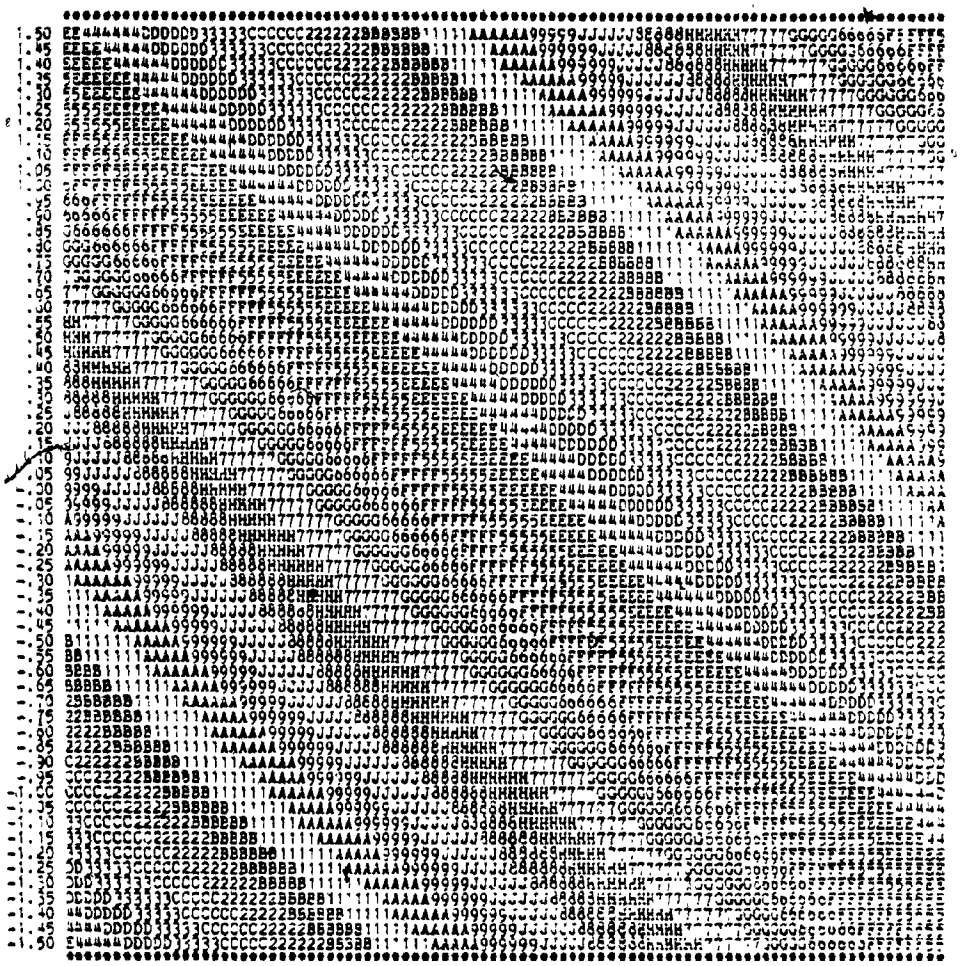

FIG. 5.9 TYPE 1 APPROXIMATION : PHASE RESPONSE OF A NETWORK WITH SIXTH-ORDER BESSEL FILTER P_1 AND P_2 SECTIONS

COMPONENTS						
INDUCTORS	.0505	.2364	.4116	.0505	.2364	.4116
CAPACITORS	.1480	.3158	.8377	.1480	.3158	.8377

RESISTORS RS= 1.0000 RL= 1.0000

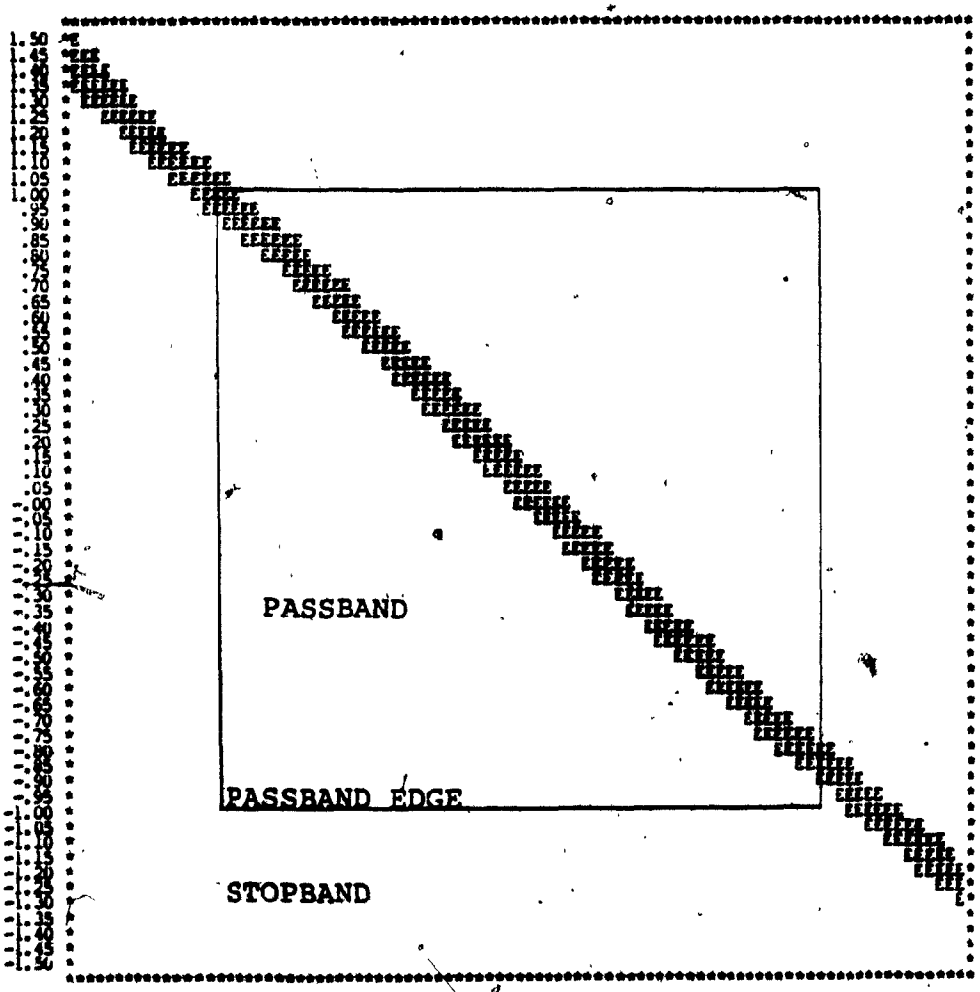

FIG. 5.9a PHASE RESPONSE PLOTTED FOR A SINGLE VALUE OF THE RESPONSE OF FIG. 5.9

to the phase variation of 0 to -10° is alone indicated to show the variation within and outside the passband. The magnitude response of this filter does not exhibit any quadrantal symmetry properties, because the transfer function is not variable separable. It is of interest to note that in the approximation for a two-dimensional IIR filter having a maximally flat group delay discussed in [78], the transfer function turns out to be variable separable; in our case, we have a maximally flat group delay approximation in the analog domain, with a non-separable transfer function. A good phase linearity is also obtained if the p_1 and p_2 networks are chosen as Gaussian filters. A phase response plot of such a network with normalized 5th order Gaussian p_1 and p_2 filter sections is shown in Fig. 5.10. *

---

* The notation used in the phase response plots is as follows.

5→0 to 10°	G →30 to 40°	8→ 60 to 70°
F→10 to 20°	7 →40 to 50°	J→ 70 to 80°
6→20 to 30°	H →50 to 60°	9→ 80 to 90°

The notation for the corresponding negative values are E,4, D,3,C,2,B,1 and A in the given order.

COMPONENTS

INDUCTORS	0.0000	.3696	.9782	2.2533	.6485	.1312
CAPACITORS	.1312	.6485	2.2533	.9782	.3896	0.0000

RESISTORS RS= 1.0000 RL= 1.0000

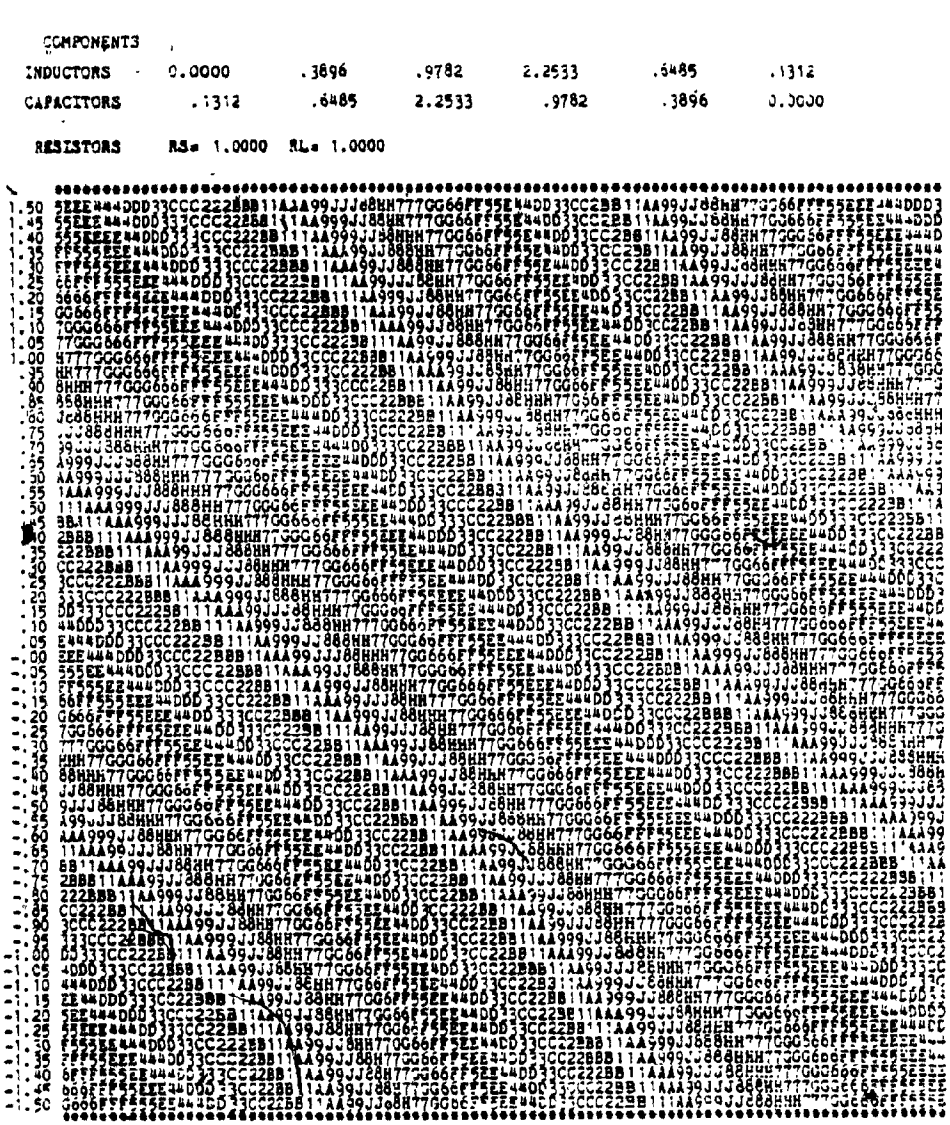

FIG. 5.10 TYPE 1 APPROXIMATION : PHASE RESPONSE OF A NETWORK WITH FIFTH-ORDER GAUSSIAN FILTER p_1 AND p_2 SECTIONS

6.5 2-D digital transfer functions derived from type 1 approximations

The doubly terminated network transfer functions obtained in the previous sections can be transformed into 2-D digital transfer functions by the double bilinear transformation. The digital transfer function is given by

$$H(z_1,z_2) = T(p_1,p_2)\Big|_{p_i = \frac{2}{T_i}\,\frac{z_i-1}{z_i+1}}, \quad (i=1,2) \qquad (5.5.1)$$

where T_1 and T_2 are the sampling periods along the two axes of the 2-D input signal. Let ω_1 and ω_2 represent the frequency variables in the two-variable analog filter and Ω_1 and Ω_2 be the corresponding frequency variables for the derived 2-D digital filter. The magnitude response of the digital filter is obtained by evaluating the digital transfer function on the unit bidisc in the z_1, z_2 hyperplane and is given by

$$H(z_1,z_2)\Big|_{\substack{z_1 = e^{j\Omega_1 T_1} \\ z_2 = e^{j\Omega_2 T_2}}} = H(e^{j\Omega_1 T_1}, e^{j\Omega_2 T_2}) \qquad (5.5.2)$$

The magnitude and phase responses of the derived digital filter are related to those of the analog filter with the warping of the frequency axes given by the relationship

$$\omega_i = \frac{2}{T_i}\tan\frac{\Omega_i T_i}{2} \qquad \forall\ (i=1,2) \qquad (5.5.3)$$

For low frequencies where $\Omega_i < 0.3/T_i$, it is seen that $\omega_i \simeq \Omega_i$ $(i=1,2)$ and the responses of both the filters are almost identical. But for higher frequencies, it is seen from (5.5.3) that there is a warping effect because of the highly nonlinear relationship between ω_i and Ω_i $(i=1,2)$. The magnitude response requirements can be satisfied by using a prewarping technique for both the frequency variables. The prewarped frequencies are first obtained from (5.5.3) and the two-variable analog filter is designed for these specifications. It is seen from (5.5.3) that the polarities of ω_1 and ω_2 are the same as those of Ω_1 and Ω_2 respectively. Hence the quadrantal symmetry property of the analog filter is carried over to the digital filter. This is also seen from the response of a 2-D digital filter in Fig. 5.11 obtained from the analog network of Fig. 5.2. In the case of specific symmetries such as circular symmetry, the symmetry is preserved only for low frequencies. Fig. 5.12 to 5.14 show the magnitude response of 2-D digital filters derived from analog networks which have the Butterworth, Chebyshev and Gaussian type of response as given in Fig. 5.3, 5.4 and 5.8 respectively.

It is to be noted that the double bilinear transformation does not preserve the phase linearity of a two-variable linear phase analog transfer function. Hence it is not possible to obtain an approximation for the 2-D linear phase digital filter from the linear phase analog approximation obtained earlier. In Chapter 6, we discuss a method of optimization

COMPONENTS

INDUCTORS	1.4142,	0.0000	0.0000	1.4142	0.0000,	0.0000
CAPACITORS	1.4142	0.0000	0.0000	1.4142	0.0000	0.0000

RESISTORS RS= 1.0000 RL= 1.0000

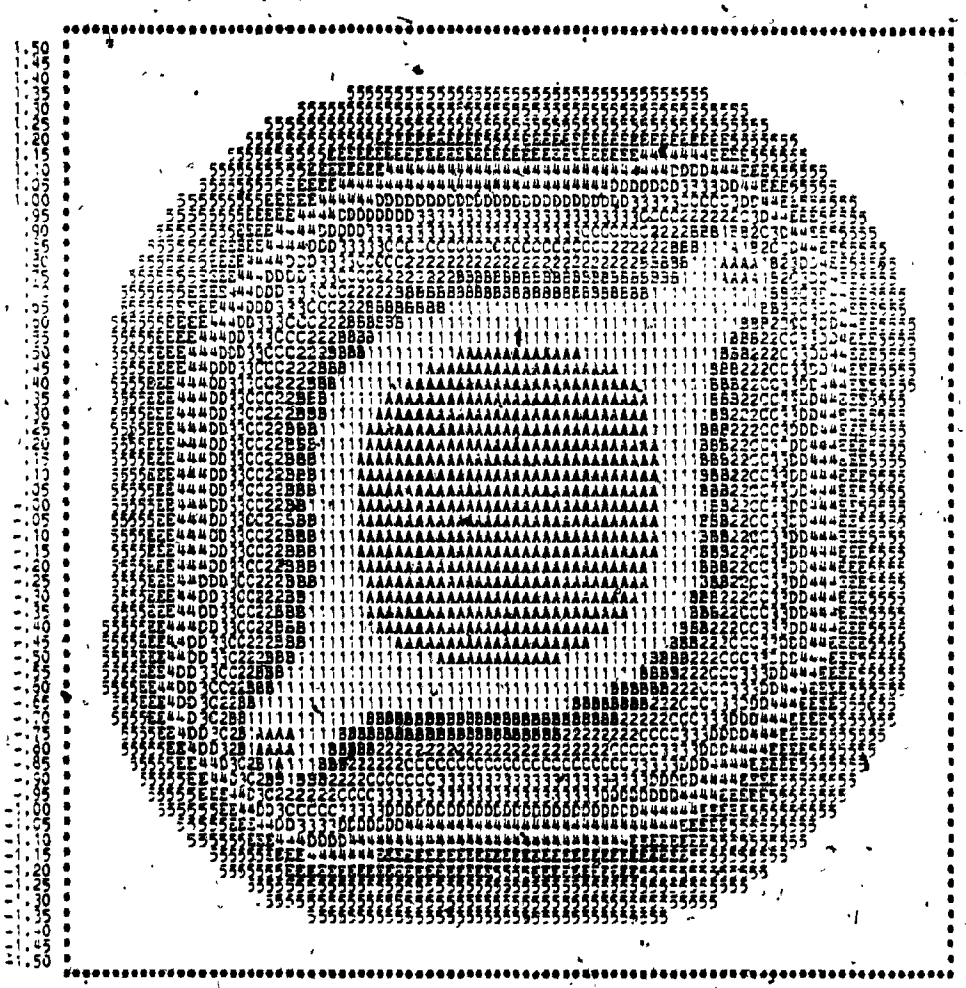

FIG. 5.11 THE MAGNITUDE RESPONSE OF THE 2-D DIGITAL FILTER DERIVED FROM THE ANALOG NETWORK OF FIG. 5.2

COMPONENTS

INDUCTORS	.5176	1.9319	1.4142	.5176	1.9319	1.4142
CAPACITORS	1.4142	1.9319	.5176	1.4142	1.9319	.5176

RESISTORS RS= 1.0000 RL= 1.0000

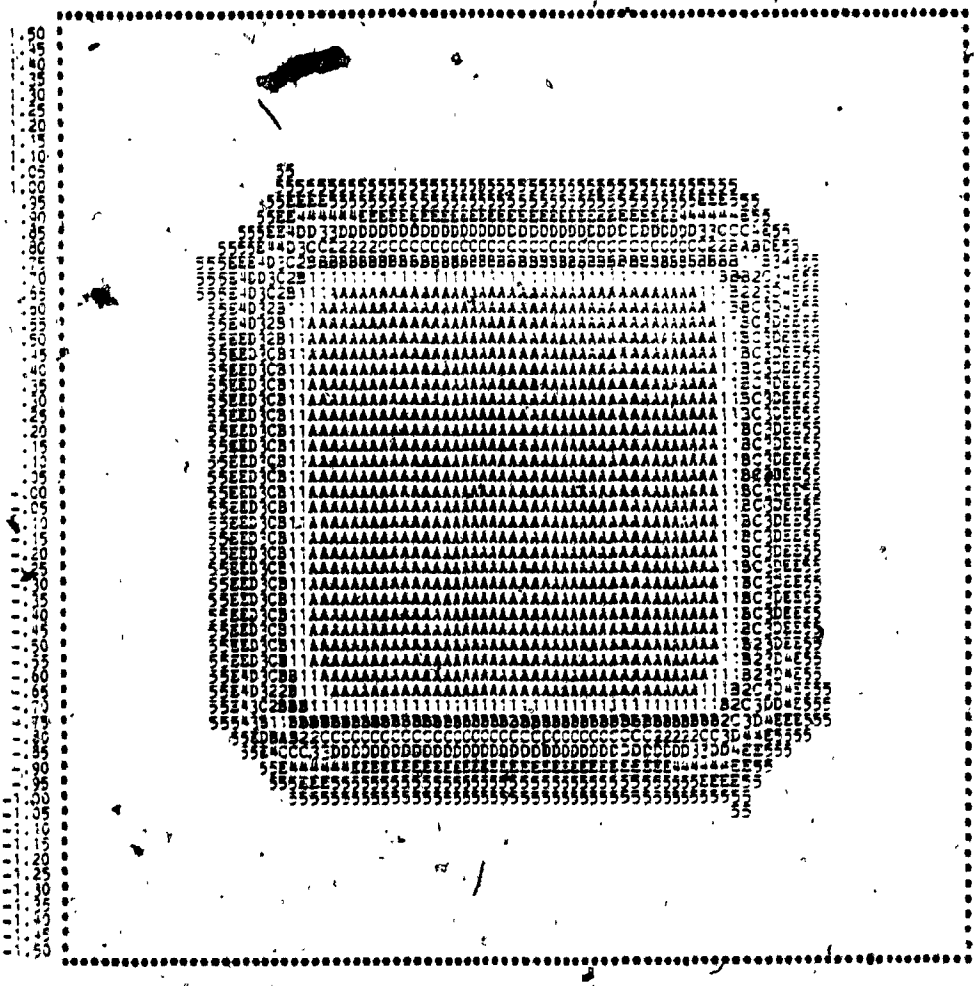

FIG. 5.12 THE MAGNITUDE RESPONSE OF THE 2-D DIGITAL FILTER DERIVED FROM THE ANALOG NETWORK OF FIG. 5.3

COMPONENTS

INDUCTORS	0.0000	.7619	.7619	3.4813	4.5375	3.4813
CAPACITORS	3.4813	4.5375	3.4813	.7619	.7619	0.0000

RESISTORS RS= 1.0000 RL= 1.0000

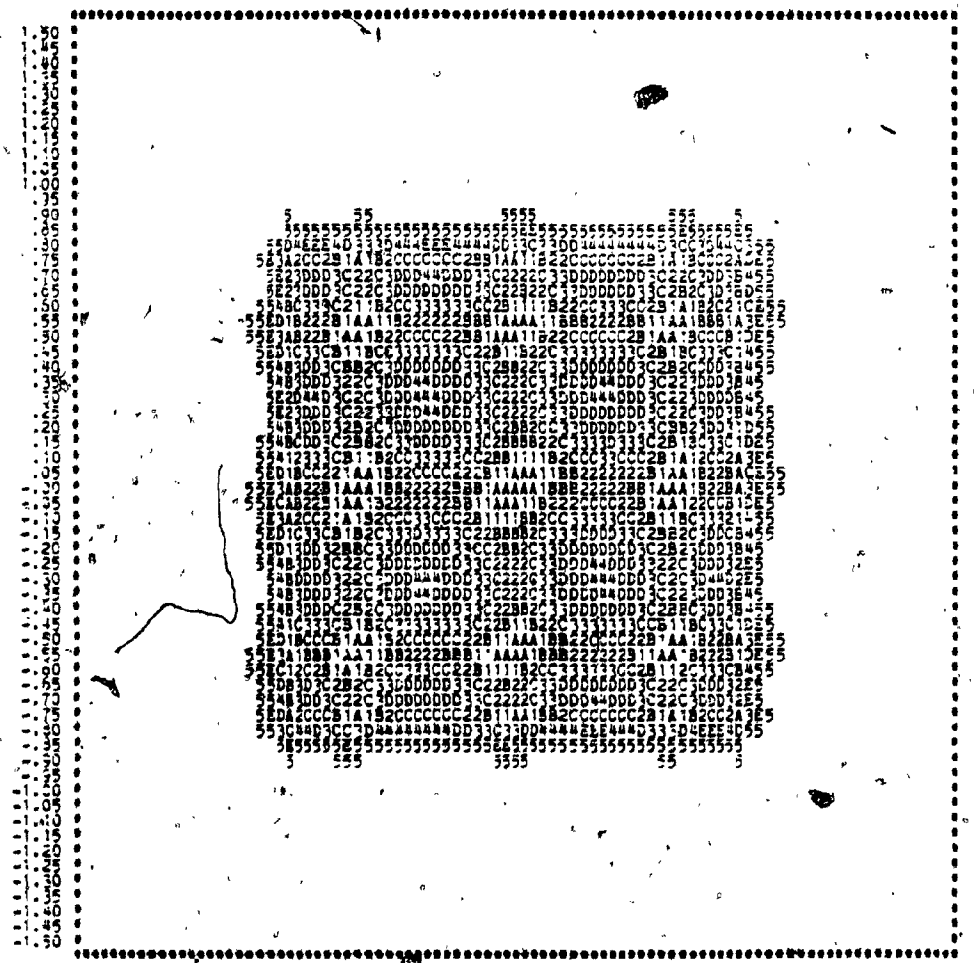

FIG. 5.13 THE MAGNITUDE RESPONSE OF THE 2-D DIGITAL FILTER DERIVED FROM THE ANALOG NETWORK OF FIG. 5.7

COMPONENTS

INDUCTORS	0.0000	.3896	.9782	2.2533	.6485	.1312
CAPACITORS	.1312	.6485	2.2533	.9782	.3896	0.0000

RESISTORS RS= 1.0000 RL= 1.0000

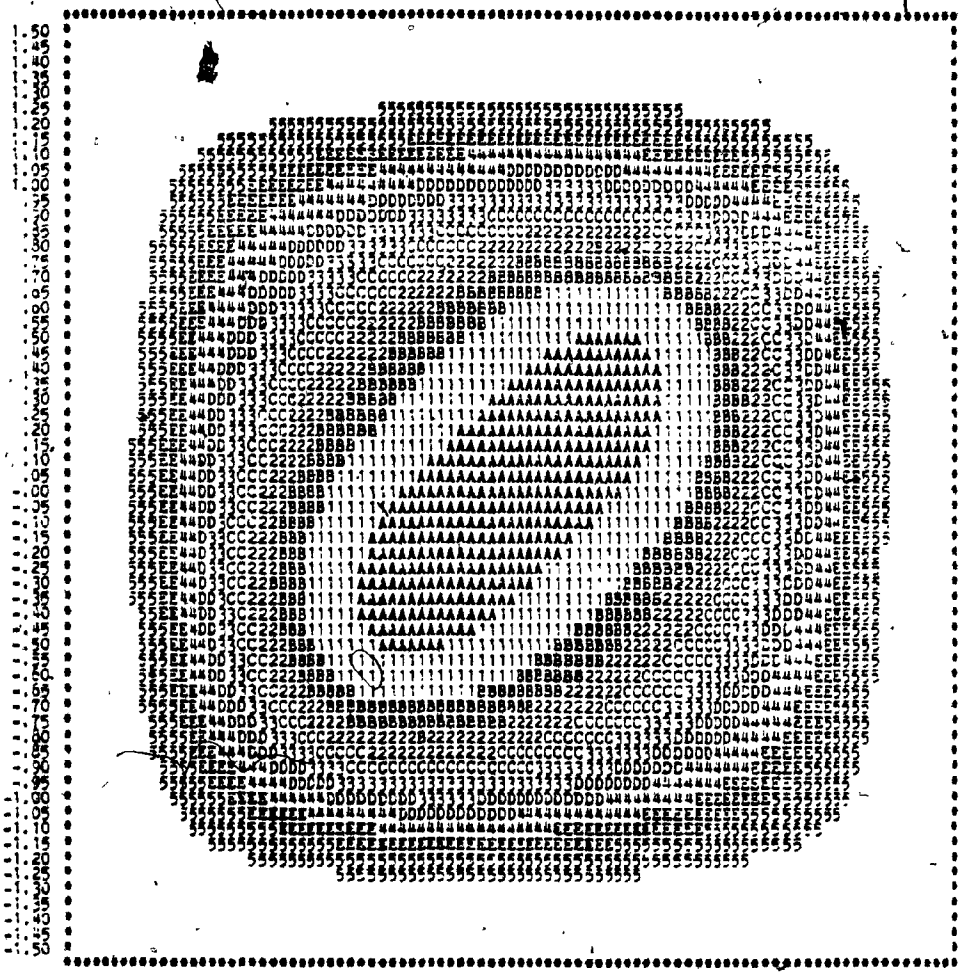

FIG. 5.14 THE MAGNITUDE RESPONSE OF THE 2-D DIGITAL FILTER DERIVED FROM THE ANALOG NETWORK OF FIG. 5.8

to obtain good phase linearity for 2-D digital transfer functions derived from doubly-terminated two-variable cascade separable ladder networks.

We have seen that the problem of unity magnitude occuring along a diagonal in the ω_1-ω_2 plane is due to the cancellation of the reactances of the p_1 and p_2 reactive elements along $\omega_1 = -\omega_2$. It has been shown in Sections 5.3 and 5.4 that such cases also give rise to the non-essential singularity of second kind. Hence by avoiding these cases, we avoid both the problems.

5.6 Approximation of type 2

The lowpass two-variable doubly-terminated cascade separable ladder network transfer function can be written as

$$T(p_1,p_2) = \frac{K}{Q_1P_2+P_1Q_2} = \frac{K/Q_1Q_2}{Z_{11a}+Z_{11b}} \qquad (5.6.1)$$

where $Z_{11a} = P_1/Q_1$ and $Z_{11b} = P_2/Q_2$ are driving point impedances of lowpass ladder networks as defined earlier with all their transmission zeros at $p_1 = \infty$ and $p_2 = \infty$ respectively. If Z_{11a} and Z_{11b} are identical functions in p_1 and p_2, then the inverted p_1 network and the p_2 network have identical elements. In such a case, as we have seen before, we get an allpass response along the diagonal $\omega_1 = -\omega_2$, because the reactance of each element of the inverted p_1 network cancels with the reactance of the corresponding element of the p_2 network, at these frequenies.

To overcome this problem, Z_{11a} and Z_{11b} are assumed as reciprocal functions in p_1 and p_2 respectively. The p_2 network is obtained as the dual of the inverted p_1 network. If for example, $Z_{11a} = P_1/Q_1$ is realized as a resistively terminated lossless ladder network starting with a shunt capacitor, then $Z_{11b} = Q_2/P_2$ is realized as a resistively terminated dual lossless ladder network, starting with a series inductor. The two-variable transfer function thus realized is

$$T(p_1,p_2) = \frac{K/Q_1P_2}{(P_1/Q_1)+(Q_2/P_2)} \qquad (5.6.2)$$

If we consider the magnitude response at low frequencies in the pass band, both Z_{11a} and Z_{11b} are approximately constant and at high frequencies, Z_{11a} tends to become zero whereas Z_{11b} tends to become infinity. Thus $T(p_1,p_2)$ approximates to K/Q_1Q_2 in the stopband.

A better approximation to a variable separable function both in the passband as well as in the stopband is achieved by introducing a scaling factor for Z_{11a} and Z_{11b}. If the impedances Z_{11a} and Z_{11b} are scaled by factors k_1 and k_2 respectively, then we have

$$T(p_1,p_2) = \frac{K/(Q_1P_2)}{k_1(P_1/Q_1)+k_2(Q_2/P_2)} \qquad (5.6.3)$$

and with $k_1 << 1$ and $k_2 = 1/k_1$, we see that $T(P_1,p_2)$ approximates to $K/(k_2Q_1Q_2)$ both in the passband as well as

in the stopband. The symmetry improves as the ratio k_2/k_1 is increased. Alternatively if $k_2 << 1$ and $k_1 = 1/k_2$, then $T(p_1,p_2)$ approximates to a variable separable transfer function $K/(k_1P_1P_2)$. This technique can be used for obtaining a two-variable function from known single-variable approximations such as the Butterworth, Chebyshev or Gaussian approximations.

The inverted p_1 network is obtained by realizing the given function as a singly-terminated ladder network and then impedance scaling it by a factor k_1. The p_2 network is then obtained as the dual of the above. Fig. 5.15 shows the magnitude response of a two-variable network in which the Butterworth approximation is used to realize the singly-terminated ladder network. A good circular symmetry is obtained when a Gaussian approximation is used as shown in Fig. 5.16. In both the above cases, a scale factor of $k_1 = 1/k_2 = 0.1$ has been used. Variation of the scale factors can vary the magnitude response to a very large extent as demonstrated in Fig. 5.17 for the type 2 Gaussian approximation with a scale factor $k_1 = k_2 = 1$. The response for a type 2 approximation with Chebyshev 4th order p_1 and p_2 sections, is given in Fig. 5.18 for a scale factor of $k_1 = 1/k_2 = 0.1$. The responses for $k_1 = k_2 = 1$ for all filters are accentuated along the diagonal $\omega_1 = \omega_2$, as seen from Fig. 5.17 for the type 2 approximation using Gaussian 4th order filter and also from Fig. 5.19 for the type 2 Butterworth 4th order approximation. The responses in such

COMPONENTS

INDUCTORS	.0383	.1577	0.0000	15.3070	10.8240	0.0000
CAPACITORS	10.8240	15.3070	0.0000	.1577	.0383	0.0000

RESISTORS RS= .1000 RL=10.0000

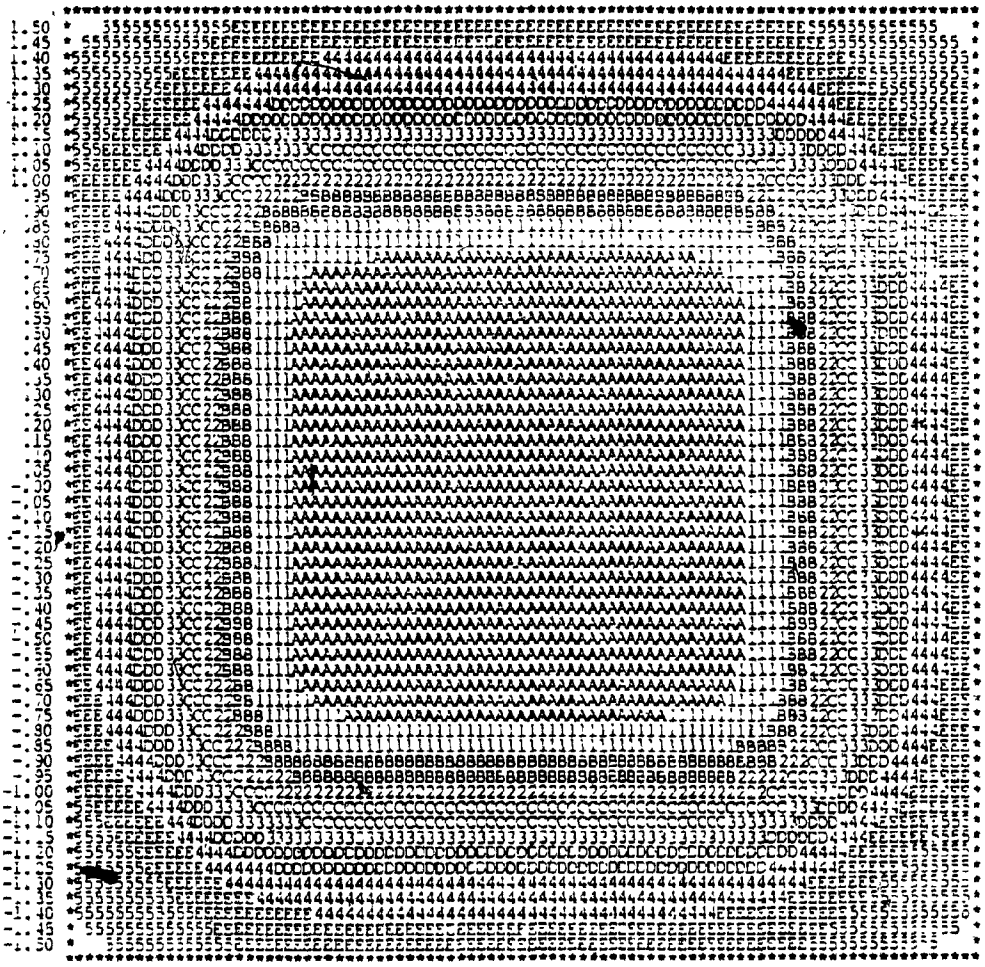

FIG. 5.15 TYPE 2 APPROXIMATION : MAGNITUDE RESPONSE OF A NETWORK WITH FOURTH-ORDER BUTTERWORTH LADDERS ($k_1 = 0.1$, $k_2 = 10$)

COMPONENTS

INDUCTORS	0.0000	.0161	.0826	14.7708	4.9904	0.0000
CAPACITORS	0.0000	4.9904	14.7708	.0826	.0161	0.0000

RESISTORS RS= .0983 RL=10.1744

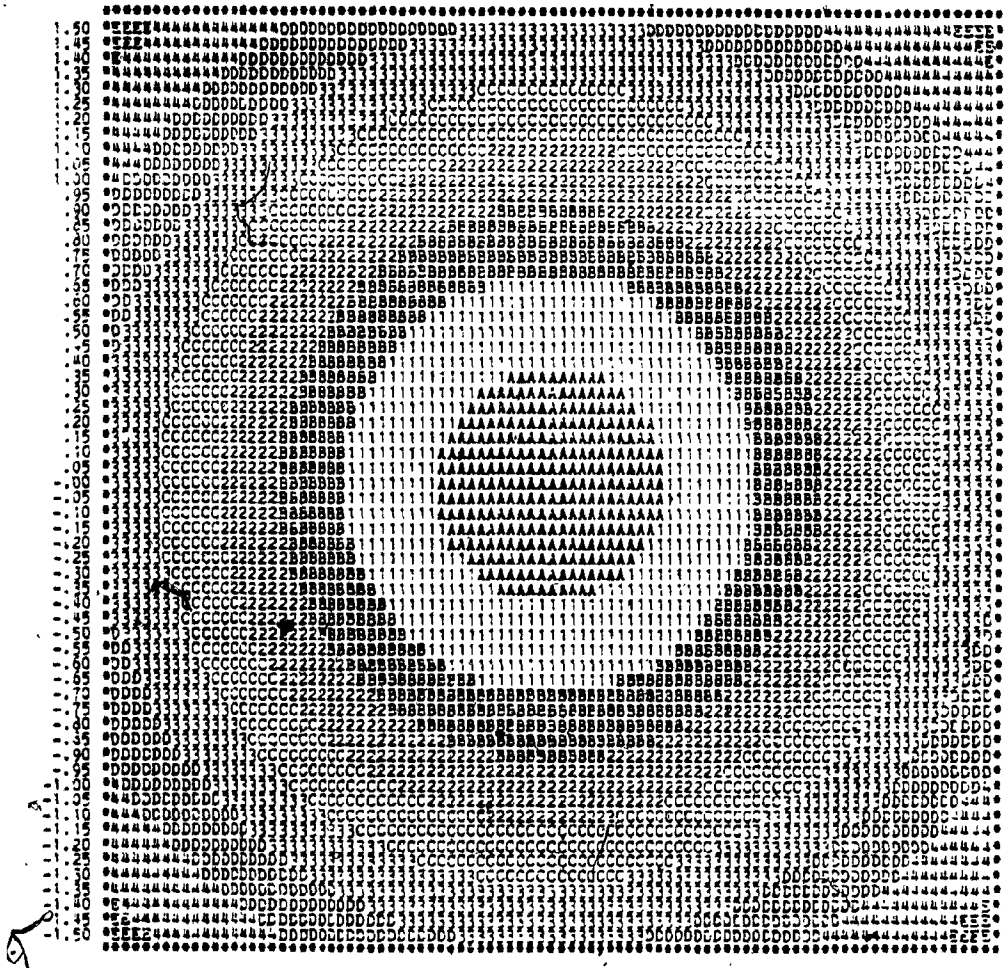

FIG. 5.16 TYPE 2 APPROXIMATION : MAGNITUDE RESPONSE OF A NETWORK WITH FOURTH-ORDER GAUSSIAN LADDER SECTIONS (k_1 = 0.1, k_2 = 10)

COMPONENTS						
INDUCTORS	.1614	.8262	0.0000	1.4771	.4990	0.0000
CAPACITORS	.4990	1.4771	0.0000	.8262	.1614	0.0000

RESISTORS RS= .9829 RL= 1.0174

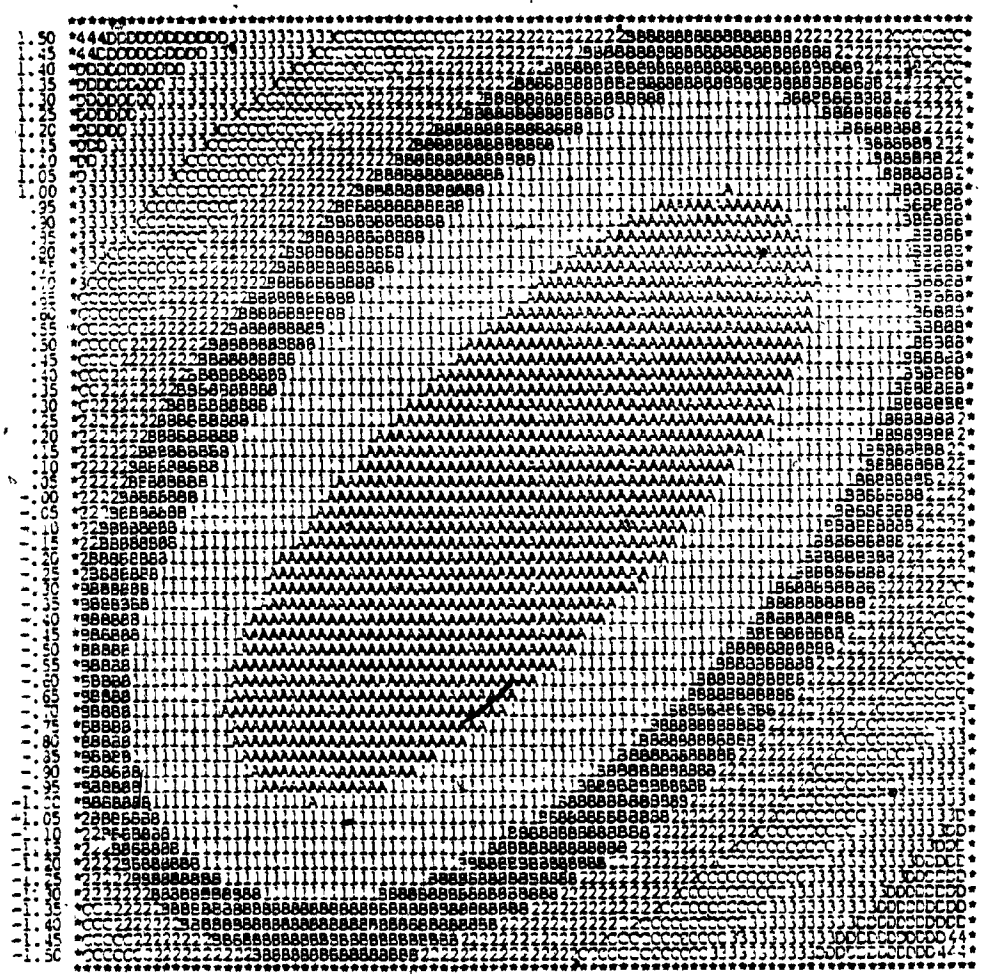

FIG. 5.17 TYPE 2 APPROXIMATION : MAGNITUDE RESPONSE OF A NETWORK WITH FOURTH-ORDER GAUSSIAN FILTER SECTIONS ($k_1 = k_2 = 1$)

COMPONENTS

INDUCTORS	.1720	.2527	0.0000	10.5780	12.2920	0.0000
CAPACITORS	12.2920	10.5780	0.0000	.2527	.1720	0.0000

RESISTORS RS= .1000 RL=10.0000

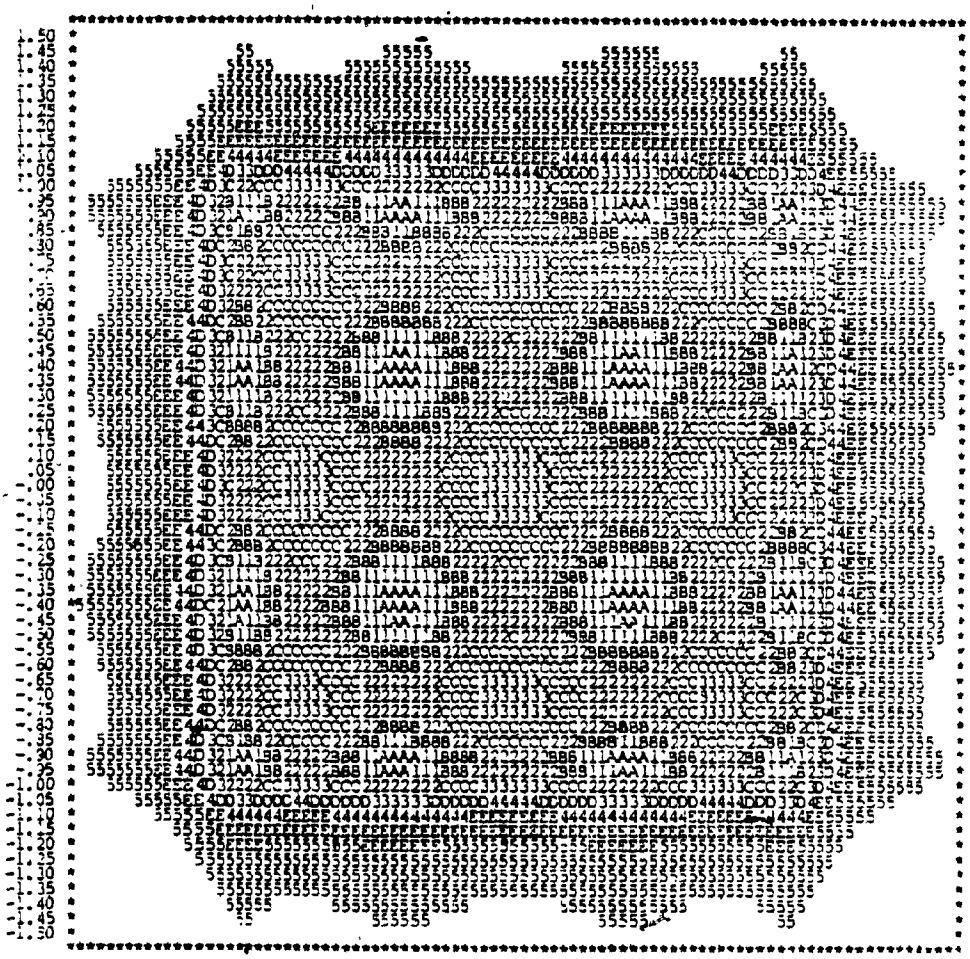

FIG. 5.18 TYPE 2 APPROXIMATION : MAGNITUDE RESPONSE OF A NETWORK WITH FOURTH-ORDER CHEBYSHEV FILTER SECTIONS ($k_1 = 0.1, k_2 = 10$)

COMPONENTS

INDUCTORS	.3827	1.5772	0.0000	1.5307	1.0824	0.0000
CAPACITORS	1.0824	1.5307	0.0000	1.5772	.3827	0.0000

RESISTORS RS= 1.0000 RL= 1.0000

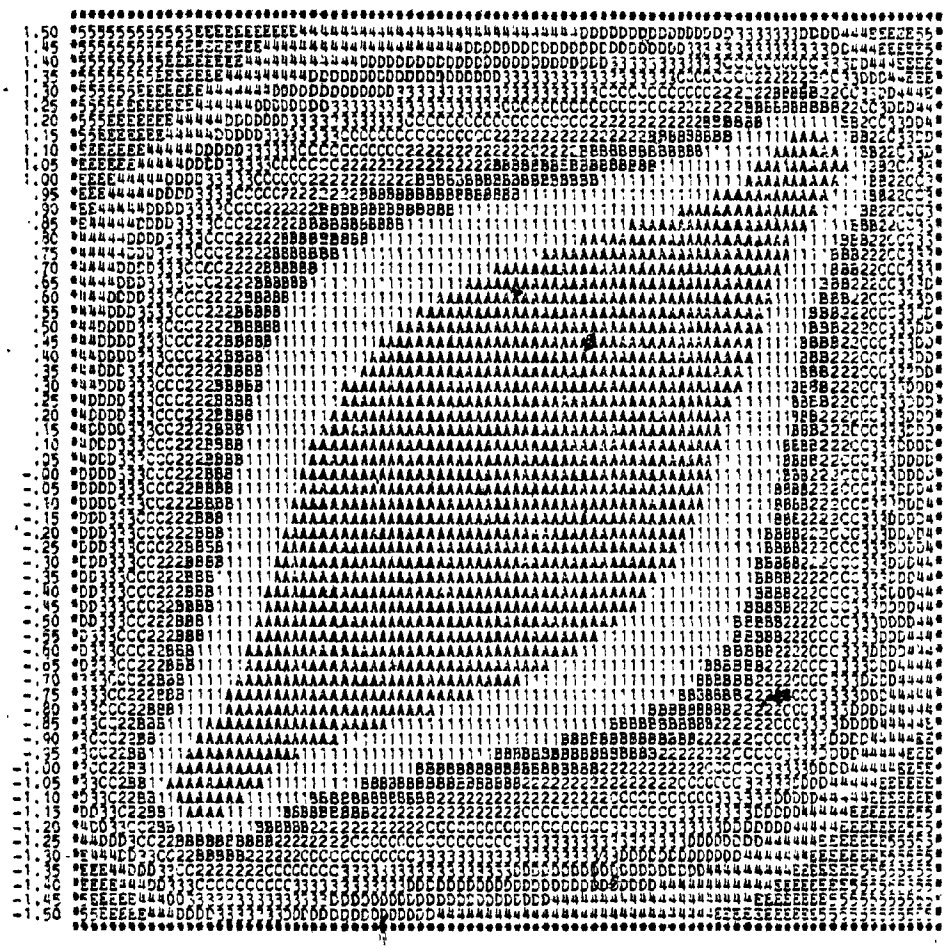

FIG. 5.19 TYPE 2 APPROXIMATION : MAGNITUDE RESPONSE OF A NETWORK WITH FOURTH-ORDER BUTTERWORTH SECTIONS ($k_1 = k_2 = 1$)

cases resemble those of rotated filters. The response for a linear phase approximation is shown in Fig. 5.20.

5.7 2-D Digital transfer functions derived from type 2 approximations

As discussed in section 5.5 for Type 1 approximations, we can transform also the Type 2 approximations of section 5.6 into 2-D digital functions using the double bilinear transformation. As before, the magnitude properties of the original analog function (such as the MFM or the ERM characteristic) are carried over to the digital domain. However circular symmetry in magnitude response is preserved only for low frequencies. Prewarping can be done in both the variables to obtain the required magnitude response in the digital domain. The 2-D digital filter magnitude response corresponding to the Butterworth, Gaussian and Chebyshev type response of Figs. 5.15, 5.16 and 5.18 are shown in Figs. 5.21-5.23 respectively.

Linear phase approximation is again not possible because of the warping effects of the double bilinear transformation. An improved phase linearity can be obtained using the optimization technique described in Chapter 6 for the 1-D digital filter and then extending the approximation to 2-D.

As discussed in Sections 5.3 and 5.4 the problem of all-pass diagonal can be avoided by noting that the elements of the p_2 network and those of the inverted p_1 network are not constant multiples of each other. The second kind

COMPONENTS

INDUCTORS	.1000	.4627	0.0000	.7101	.2899	0.0000
CAPACITORS	.2899	.7101	0.0000	.4627	.1000	0.0000

RESISTORS. RS= 1.0000 RL= 1.0000

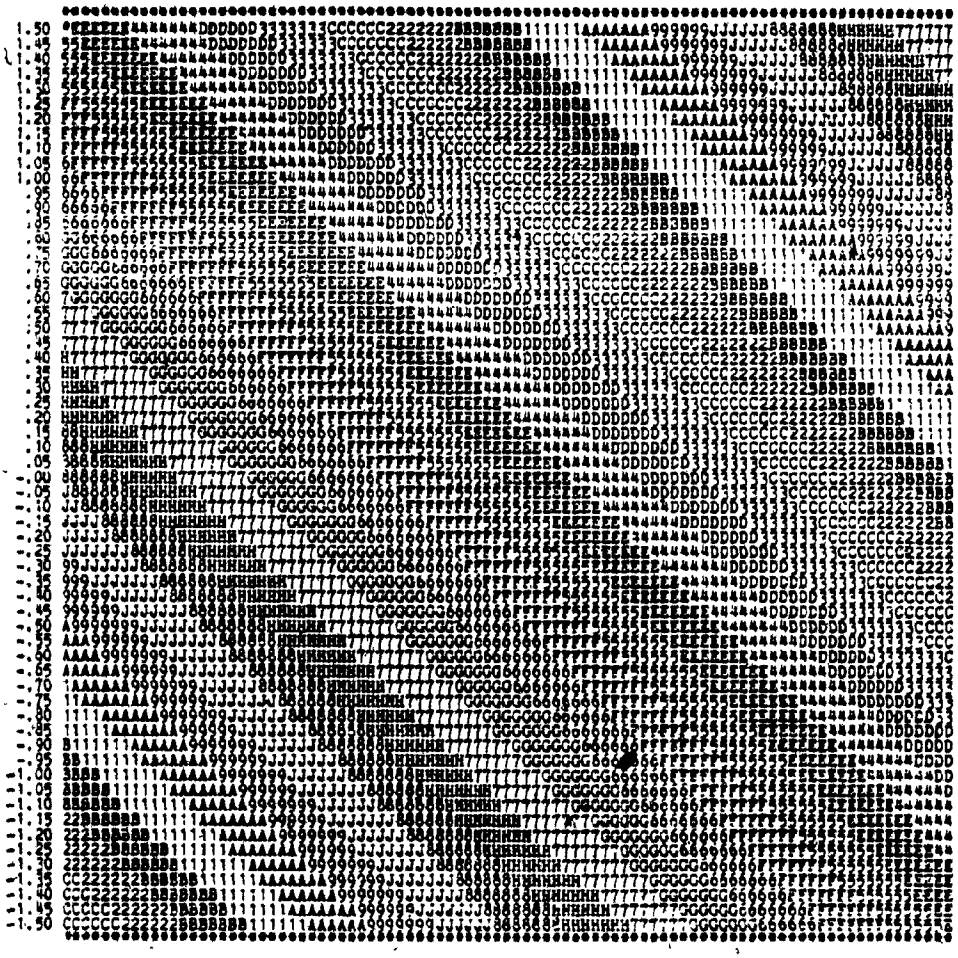

FIG. 5.20 TYPE 2 APPROXIMATION : PHASE RESPONSE OF A NETWORK WITH FOURTH-ORDER MAXIMALLY FLAT TIME DELAY SECTIONS ($k_1 = k_2 = 1$)

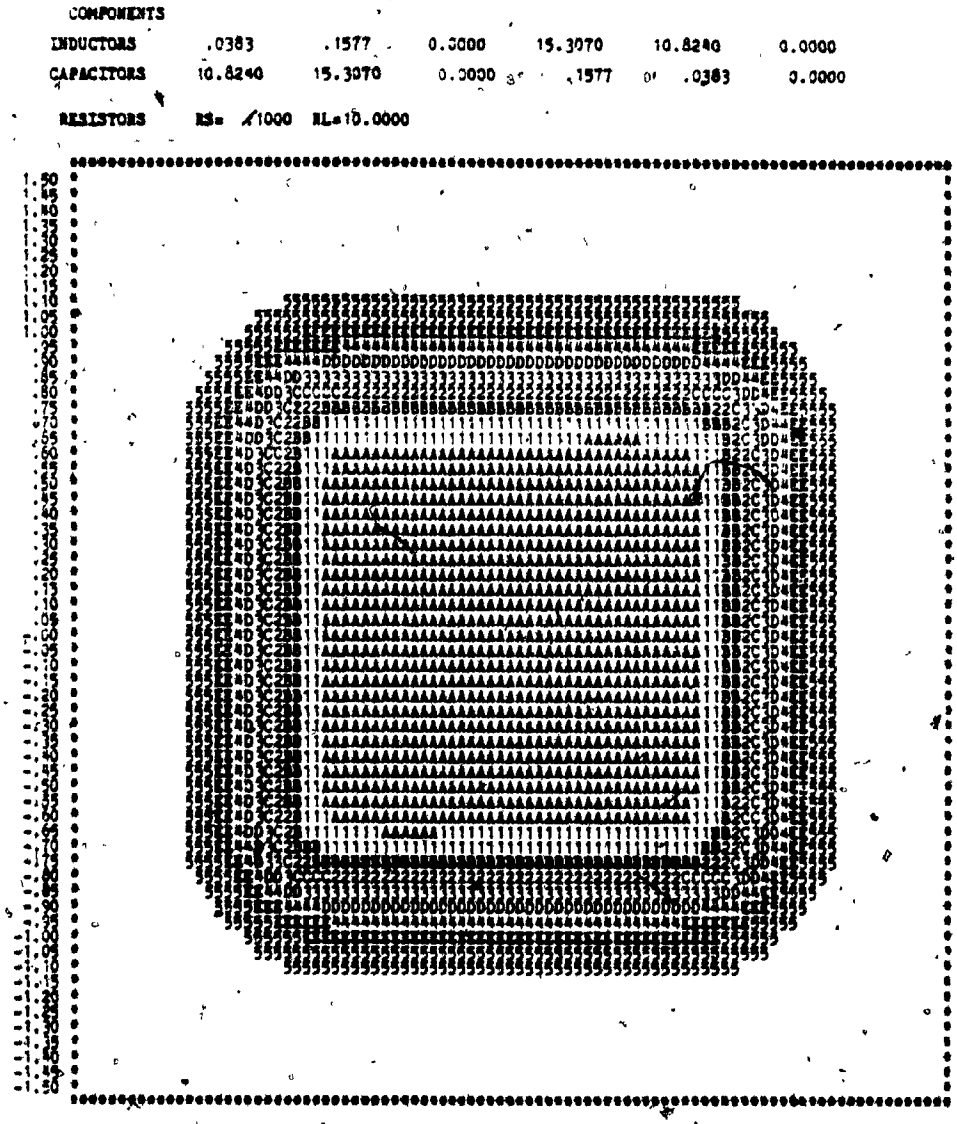

FIG. 5.21 THE 2-D DIGITAL FILTER MAGNITUDE RESPONSE CORRESPONDING TO THAT OF FIG. 5.15

COMPONENTS						
INDUCTORS	0.0000	.0151	.0825	18.7708	4.9904	0.0000
CAPACITORS	0.0000	4.9904	18.7708	.0826	.0161	0.0000

RESISTORS RS= .0983 RL=10.1744

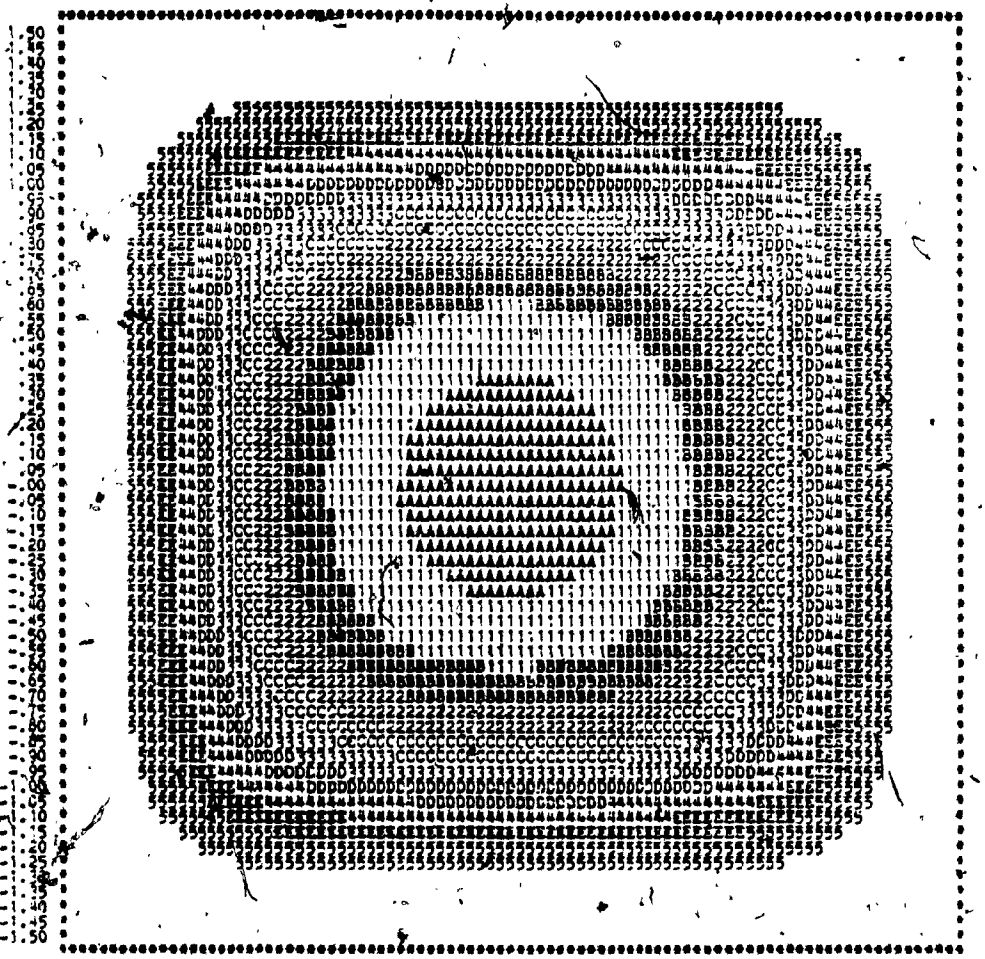

FIG. 5.22 THE 2-D DIGITAL FILTER MAGNITUDE RESPONSE CORRESPONDING TO THAT OF FIG. 5.16

COMPONENTS

INDUCTORS	.1720	.2527	0.0000	10.5780	12.2920	0.0000
CAPACITORS	12.2920	10.5780	0.0000	.2527	.1720	0.0000

RESISTORS RS= .1000 RL=10.0000

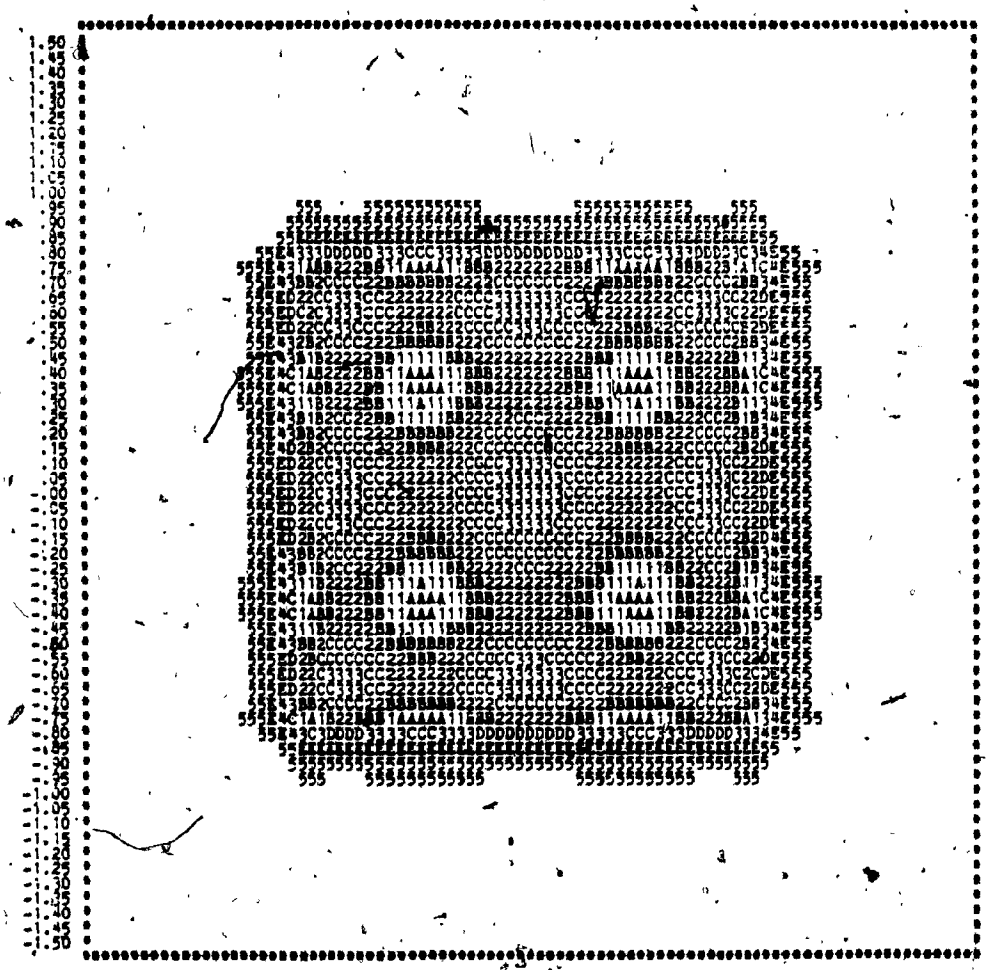

FIG. 5.23 THE 2-D DIGITAL FILTER MAGNITUDE RESPONSE CORRESPONDING TO THAT OF FIG. 5.18

singularity is avoided by choosing starting elements of different types for the p_2 and inverted p_1 networks.

5.8 Frequency transformations

So far only lowpass two-variable transfer functions have been discussed. These can be transformed into highpass, bandpass or bandstop filters in both the variables, by using reactance transformations. These transformations preserve the quadrantal symmetric property of the prototype filter.

If a lowpass to highpass transformation given by $p_i \rightarrow 1/p_i$, $i=1,2$ is applied to the lowpass transfer function of (3.3.1.10), then the resulting highpass transfer function is of the form

$$T_{HP}(p_1,p_2) = \frac{Kp_1^n p_2^n}{D_1(p_1,p_2)} = \frac{Kp_1^n p_2^n}{[M'_{11}(p_1)+N'_{21}(p_1)][M'_{12}(p_1)+N_{12}(p_1)] + [M'_{21}(p_1)+N'_{11}(p_1)][M'_{22}(p_2)+N'_{22}(p_2)]} \qquad (5.8.1)$$

where, n is the order of the functin in p_1 and p_2. The M' and N' polynomials can be derived directly from the corresponding M and N polynomials as shown below.

Let us consider a two-variable transfer function $T(p_1,p_2)$ given by $T(p_1,p_2) = K/D(p_1,p_2)$, where the denominator can be written as

$$D(p_1,p_2) = [p_1^n p_1^{n-1} \ldots 1][A] \begin{bmatrix} p_2^n \\ p_2^{n-1} \\ \vdots \\ 1 \end{bmatrix} \qquad (5.8.2)$$

and [A], the coefficient matrix is of the form

$$\begin{bmatrix} A_{11} & A_{12} & \cdots & A_{1,n+1} \\ A_{21} & A_{22} & \cdots & A_{2,n+1} \\ \vdots & \vdots & & \vdots \\ A_{n+1,1} & A_{n+1,2} & & A_{n+1,n+1} \end{bmatrix}$$

By applying the transformation $p_i \to 1/p_i$, $(i=1,2)$ to (5.8.2) we get

$$D(p_1,p_2)\Big|_{\substack{p_i \to \frac{1}{p_i} \\ i=1,2}} = [\frac{1}{p_1^n} \frac{1}{p_1^{n-1}} \ldots 1][A] \begin{bmatrix} 1/p_2^n \\ 1/p_2^{n-1} \\ \vdots \\ 1 \end{bmatrix}$$

$$= (p_1^n p_2^n)^{-1} [1 \; p_1 \ldots p_1^n][A] \begin{bmatrix} 1 \\ p_2 \\ \vdots \\ p_2^n \end{bmatrix}$$

$$= (p_1^n p_2^n)^{-1} [p_1^n p_1^{n-1} \ldots 1] \begin{bmatrix} 0 & & 1 \\ & \ddots & \\ 1 & & 0 \end{bmatrix} [A] \begin{bmatrix} 0 & & 1 \\ & \ddots & \\ 1 & & 0 \end{bmatrix} \begin{bmatrix} p_2^n \\ p_2^{n-1} \\ \vdots \\ 1 \end{bmatrix}$$

$$= (p_1^n p_2^n)^{-1} [p_1^n p_1^{n-1} \ldots 1] \begin{bmatrix} A_{n+1,n+1} & A_{n+1,n} \cdots A_{n+1,1} \\ A_{n,n+1} & A_{n,n} \cdots A_{n,1} \\ - & - & - \\ A_{1,n+1} & A_{1,n} \cdots A_{11} \end{bmatrix} \begin{bmatrix} p_2^n \\ p_2^{n-1} \\ \vdots \\ 1 \end{bmatrix}$$

$$= (p_1^n p_2^n)^{-1} D_1(p_1, p_2) \qquad (5.8.3).$$

Since the transformation is obtained by just a change of variables from p_1 to $1/p_1$, the symmetry properties are still preserved in the resulting transfer function.

If the normalized transformation $p_i \to p_i + 1/p_i$, $(i=1,2)$ is applied to the lowpass function of (3.3.1.10), the resulting bandpass function is of the form

$$T_{BP}(p_1, p_2) = K/D(p_1, p_2) \Big|_{\substack{p_i \to p_i + \frac{1}{p_i} \\ i=1,2}} = K p_1^n p_2^n / D_2(p_1, p_2)$$

$$= \frac{K p_1^n p_2^n}{[M''_{11}(p_1)+N''_{21}(p_1)][M''_{12}(p_2)+N''_{12}(p_2)] + [M''_{21}(p_1)+N''_{11}(p_1)][M''_{22}(p_2)+N''_{22}(p_2)]} \qquad (5.8.4)$$

where n is the order of the function in the p_1 and p_2 variables. The M'' and N'' polynomials can be obtained directly from the M and N polynomials by the following manipulations. For the nth order case considered earlier,

$$D(p_1,p_2)]_{\substack{p_i \to p_i + \frac{1}{p_i} \\ i=1,2}} = [(p_1+\frac{1}{p_1})^n (p_1+\frac{1}{p_1})^{n-1} \ldots 1][A][(p_2+\frac{1}{p_2})^n (p_2+\frac{1}{p_2})^{n-1} \ldots 1]^T$$

$$= (p_1^n p_2^n)^{-1} [p_1^{2n} p_1^{2n-1} \ldots 1][Q][A][Q^T] \begin{bmatrix} p_2^{2n} \\ p_2^{2n-1} \\ \vdots \\ 1 \end{bmatrix}$$

$$= (p_1^n p_2^n)^{-1} \; D_2(p_1,p_2) \qquad (5.8.5)$$

where [Q] is of the form

$$\begin{bmatrix} {}^{n}c_{n} & 0 & & & & \\ 0 & {}^{n-1}c_{n-1} & & & & \\ {}^{n}c_{n-1} & 0 & 1 & & & \\ 0 & {}^{n-1}c_{n-2} & 0 & 1 & & \\ \vdots & \vdots & \ddots & 2 & 0 & 1 \\ {}^{n}c_{1} & 0 & 0 & 1 & & \\ 0 & {}^{n-1}c_{0} & 1 & & & \\ {}^{n}c_{0} & & & & & \end{bmatrix} \qquad (5.8.6)^{*}$$

and ${}^{j}c_{i}$ represents the number of ways of selecting i objects from j distinct objects, for j,i=0 to n. The premultiplication and postmultiplication of the matrix[[A] by the triangular type of matrix [Q] and its transpose as above, results in an inners-symmetric matrix [79]. As an example, for a second order case, the coefficient matrix for $D_2(p_1,p_2)$ is given by

---

* The dotted lines are used to denote the structure of the matrix elements [79].

$$\begin{bmatrix} A_{11} & A_{12} & 2A_{11}+A_{13} & A_{12} & A_{11} \\ A_{21} & A_{22} & 2A_{21}+A_{23} & A_{22} & A_{21} \\ 2A_{11}+A_{31} & 2A_{12}+A_{32} & \begin{matrix} 4A_{11}+2A_{31} \\ +2A_{13}+A_{33} \end{matrix} & 2A_{12}+A_{32} & 2A_{11}+A_{31} \\ A_{21} & A_{22} & 2A_{21}+A_{23} & A_{22} & A_{21} \\ A_{11} & A_{12} & 2A_{11}+A_{13} & A_{12} & A_{11} \end{bmatrix} \qquad (5.8.7)$$

which is inners-symmetric.

Similarly, the normalized bandstop transformation $p_i \to 1/(p_i+1/p_i)$, i=1,2 gives rise to a function

$$T_{BS}(p_1,p_2) = K(p_1^2+1)^{-n}(p_2^2+1)^{-n}/D_3(p_1,p_2) \qquad (5.8.8)$$

where the coefficient matrix for $D_3(p_1,p_2)$ is given by $[Q][A][Q]^T$ and $[Q]$ is of the form

$$
\begin{bmatrix}
 & & & & & & {}^{n}C_{n} \\
 & & & & & {}^{n-1}C_{n-1} & 0 \\
 & & & & 1 & 0 & {}^{n}C_{n-1} \\
 & & & 1 & 0 & {}^{n-1}C_{n-2} & 0 \\
 & & 1 & 0 & 2 & \cdots \; \vdots & \vdots \\
 & & & 1 & 0 & & \\
 & & & & 1 & 0 & {}^{n}C_{1} \\
 & & & & & {}^{n-1}C_{0} & 0 \\
 & & & & & & {}^{n}C_{0}
\end{bmatrix}
\qquad (5.8.9)
$$

Here again $[Q][A][Q]^T$ is an inners-symmetric matrix.

It is to be noted that if [A] is symmetric, then the coefficient matrices for $D_2(p_1,p_2)$ and $D_3(p_1,p_2)$ are also symmetric and possess rotational symmetry about the diagonals. If $D(p_1,p_2)$ is variable separable, then $D_2(p_1,p_2)$ and $D_3(p_1,p_2)$ are also variable separable.

All the above transfer functions can be transformed into 2-D digital filters having a HP, BP or BS type of response by using the double bilinear transformation.

5.9 Summary and Conclusions

In this Chapter, the properties of doubly-terminated cascade separable ladder networks observed in Chapter 3, have been used to obtain useful approximations. It is shown that the transfer function of this network is not variable separable and hence exact quadrantal symmetry cannot be obtained using this network. However, a good approximation towards quadrantal symmetry is achieved by using two different methods. The approximations concerning the magnitude response alone can be transformed into the digital domain using the double bilinear transformation, since phase linearity is not preserved by this transformation.

Imposing the constraints of MFM response at the origin of the (ω_1,ω_2) plane, on the network function, it is shown that the p_1 and p_2 ladders are constrained to possess the Butterworth filter elements. Extension of the Type 1 approximations to Chebyshev and Gaussian responses along the ω_1 and ω_2 axes is seen to produce near quadrantal symmetry and a good behaviour in the passband as well as in the stopband. Similar extension of the maximally flat time delay response produces a maximally flat time delay in both the ω_1 & ω_2 directions for the two-variable filter.

The transfer functions obtained by using the Type 2 approximation are almost variable separable and the degree to which they approximate a variable separable function is controlled by scale factors k_1 and k_2 in (5.6.3). With $k_1 = k_2 = 1$, the response resembles that of a rotated

filter, with accentuation along the diagonal $\omega_1 = \omega_2$.

In some of the above approximations for a lowpass two-variable function, it is seen that the response produced by a network containing p_1 and p_2 lowpass sections, produces an allpass response along the diagonal $\omega_1 = -\omega_2$. In certain cases, it is also observed that the digital filter obtained by the double bilinear transformatin possesses a non-essential singularity of the second kind at the point $z_1 = z_2' = -1$. These cases are avoided by suitable choice of the p_1 and p_2 networks.

Although we have considered only extensions of single-variable lowpass filters of the all-poletype, it is easily seen that other types such as the elliptic filter can also be extended to two-variables, by using the above techniques. Reactance transformations are observed to preserve the quadrantal symmetry properties of the prototype filter. By using standard reactance transformations, filters of any type with any desired cut off frequencies can be designed. In designing 2-D digital filters, the necessary prewarping has to be carried out in order to obtain the desired critical frequencies. Since the transfer functions generated by the approximations are realizable as doubly-terminated cascade separable two-variable networks, the corresponding digital transfer functions can be implemented as wave digital filters.

CHAPTER 6

A SINGLE-VARIABLE APPROXIMATION AND ITS EXTENSION TO TWO-VARIABLES

6.1 Introduction

From the discussions in the previous chapter, it is clear the the two-variable extensions of a single-variable approximation obtained by using the Type 1 and Type 2 methods generally preserve the magnitude and phase properties of the single-variable functions, such as the maximally flat or equiripple magnitude property or phase linearity, in a particular sense. In the Type 1 method, the approximation is done by choosing the required response along the ω_1 and ω_2 axes whereas in the Type 2 method, a technique is used by which the transfer function becomes almost variable separable. The 2-D filters used in image processing require a good magnitude as well as phase response. The double bilinear transformation does not preserve the phase linearity of the filters obtained using the Type 1 and Type 2 methods. This requires an approximation to be carried out in the digital domain for phase linearity. In this Chapter we discuss a technique which involves the approximation of a 1-D digital filter with a good phase linearity and then its extension to 2-D using the Type 1 or Type 2 method.

A method for generation of single-variable analog transfer functions with a specified ripple in the passband and with

5) The roots of the polynomial

$$M^2(p)-N^2(p) = p^8+1.24p^6+0.3912p^4+0.0256p^2+0.550404$$

are found to be $\pm$ 0.276955 $\pm$j1.016472

and $\pm$0.708848 $\pm$ j0.407375.

Rejecting the right half plane roots, the polynomial $M(p)+N(p)$ is obtained. The required transfer function is given by

$$T_v(p) = \frac{A}{M(p)+N(p)}$$

$$= \frac{0.732781}{p^4+1.971606p^3+2.563615p^2+1.943725p+0.741892}$$

Fig. 6.1 gives a sketch of the magnitude squared response i.e., $|T_v(j\omega)|^2$ as a function of ω.

With the above procedure, we can design a filter which has maxima and minima in its magnitude response in the pass-band, at specified critical frequencies. The stopband response is monotonic in behaviour. Since the decomposition is unique, the transfer function obtained is also unique for a given set of critical frequencies and a specified ripple.

The reverse process of finding the critical frequencies for any given transfer function is quite simple. If the denominator polynomial of the all-pole transfer function is given as $M(p) + N(p)$, then

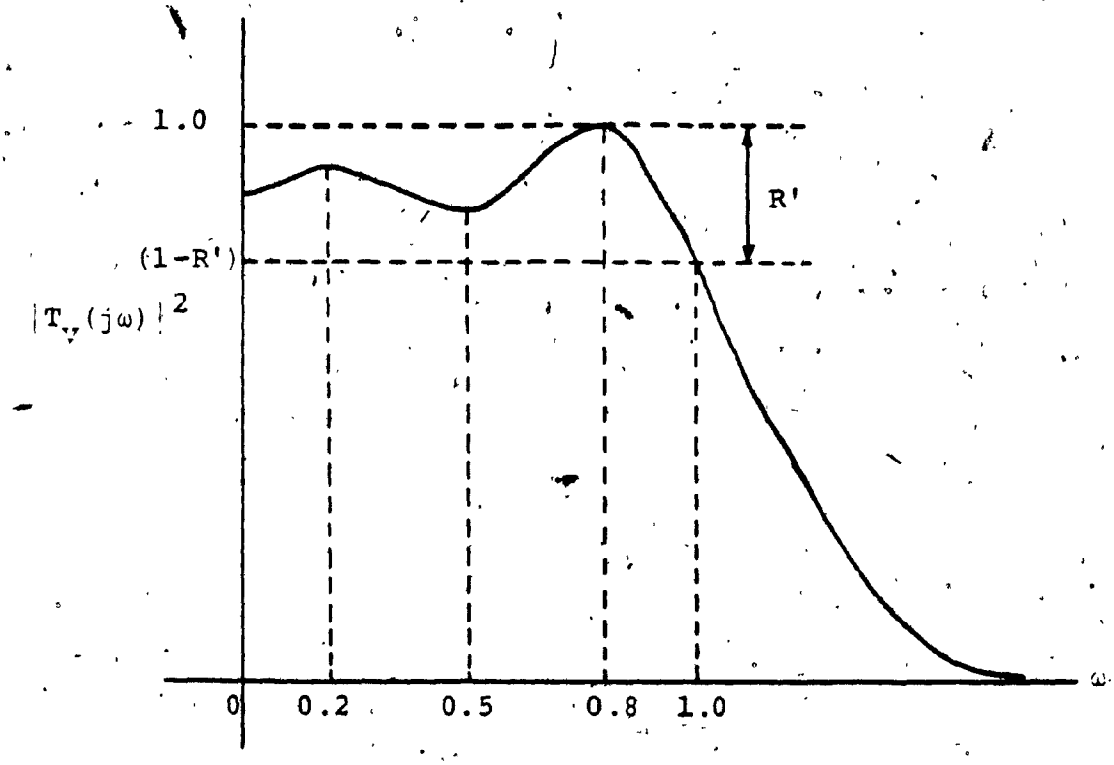

FIG. 6.1 SKETCH OF THE MAGNITUDE SQUARED RESPONSE OF THE FILTER IN EXAMPLE 6.1

$$M(p)M'(p) - N(p)N'(p) = Cp \prod_{i=1}^{n-1} (p^2+a_i^2) \qquad (6.2.9)$$

where C is a constant and a_i, i=1,2,...,n-1 are the n-1 critical frequencies apart from the critical frequency at $\omega=0$, n being the order of the given function. In (6.2.4) the coefficients of $G(p^2)$ are made up purely by the critical frequencies. For example, if $M(p)+N(p)$ is of 4th order

$$\frac{1}{2}[M^2(p)-N^2(p)] = \frac{p^8}{8} + \frac{p^6}{6}(a_1^2+a_2^2+a_3^2) + \frac{p^4}{4}(a_1^2a_2^2+a_2^2a_3^2+a_3^2a_1^2) + \frac{p^2}{2}(a_1^2a_2^2a_3^2) + K \qquad (6.2.10)$$

From (6.2.10) and (6.2.2) it can be seen that if $a_1=a_2=a_3=0$, the resulting transfer function is maximally flat at the origin. If the coefficients A and K are chosen such that $|T_v(j\omega)|^2$ is unity at $\omega=0$ and -3 dB at $\omega=1$, then we have the Butterworth function. If the critical frequencies correspond to those of a Chebyshev function, then we get an equiripple response in the passband. Here again A and K can be chosen suitably in order to get the desired ripple. We have considered only cases in which the cricital frequencies are real quantities. They can also be complex.

6.3 Optimization for linear phase

As it is possible to generate different transfer functions by varying the critical frequencies in the passband with the procedure described in Section 6.2, we can use the critical frequencies as variables in an optimization procedure,

to find out whether the linearity of the phase function can be optimized in the passband. The criteria for the optimization can be chosen, in different ways. Based on this, we compute a suitable error function which can be minimized, by using standard numerical methods for unconstrained optimization. In this section we discuss the different criteria for optimization and selection of the proper error function to meet these requirements.

If it is desired to optimize for a linear phase response in the passband with the phase function having a definite slope S in the passband, then the error function is computed as the sum of the squares of the errors of the phase function with respect to the line of slope S, at m points in the passband. The optimization thus minimizes the least square error for the phase function in the passband, if m is sufficiently large. If the passband is divided into 50 equal intervals, we have 51 points including the origin, at which the error is to be computed. Since the phase function is always zero at the origin, this point is excluded from the computation and we have m=50. The passband is assumed to be from 0 to 1 rad/sec. The error function to be minimized is given by

$$F = \sum_{\omega=0,0.02,\ldots,1} \{\angle T_v(j\omega) - S\omega\}^2 = \sum_{i=1}^{m} \{\angle T_v(j\omega) - S\omega_i\}^2 \qquad (6.3.1)$$

where $\omega_i = 1,\ldots,m$ are the frequencies at which the error is computed. The flowchart for the optimization algorithm is

shown in Fig. 6.2, where the inputs to be specified are the order of the filter n, starting values of the critical frequencies $a_1,\ldots,a_{n-1}$, the passband ripple R, the desired slope S and the passband edge ω_p. The algorithm gives the optimized critical frequencies as its output. The results of this optimization for a 4th order and a 5th order filter are given in Table 6.1. The S values 2.9394 and 3.632 in the table correspond to the least square error slopes of the 4th and 5th order Butterworth filters respectively. The results show that there is a wide variation of the error function F for different values of S.

If the objective is to obtain a linear phase response in the least squares sense in the passband without regard to any definite slope, then we adopt a slightly different procedure. The slope S1 of the straight line which is a least squares fit to the phase response, is first found as follows. The error

$$F = \sum_{i=1}^{m} \{ S_1\omega_i - \angle T_v(j\omega_i)\}^2$$

is minimized in the least squares sense when $\partial F/\partial S_1 = 0$.

i.e., $$\frac{\partial}{\partial S_1} \{ \sum_{i=1}^{m} \{S_1\omega_i - \angle T_v(j\omega_i)\}^2 \}$$

$$= \sum_{i=1}^{m} \frac{\partial}{\partial S_1} [S_1\omega_i - \angle T_v(j\omega_i)]^2 = \sum_{i=1}^{m} 2[S_1\omega_i - \angle T_v(j\omega_i)]\omega_i = 0 \qquad (6.3.2)$$

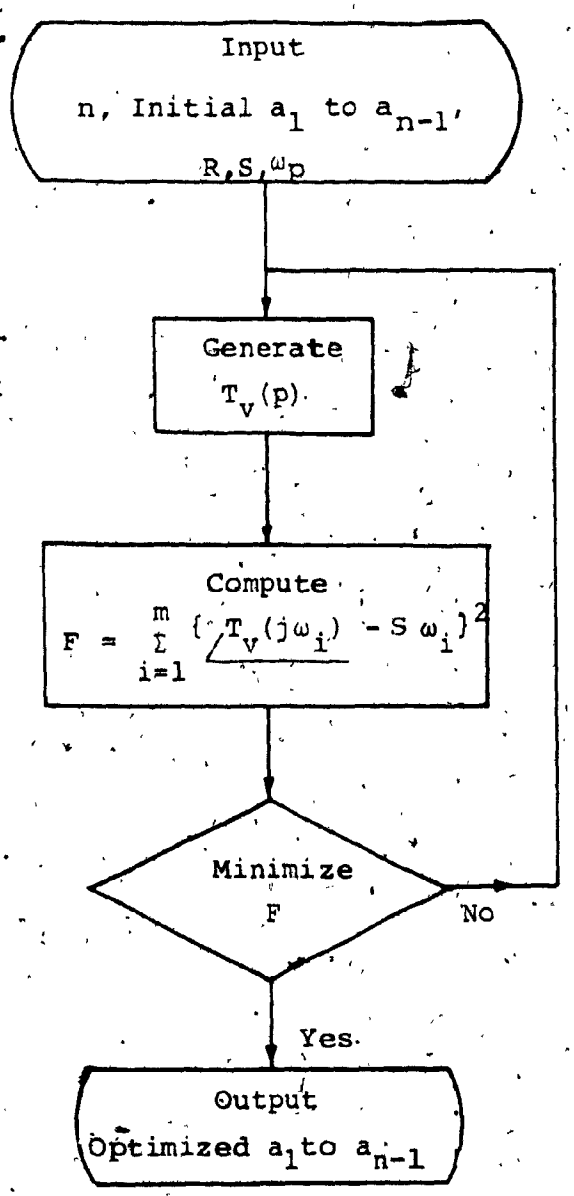

FIG. 6.2 ALGORITHM TO MINIMIZE THE ERROR FUNCTION FOR A DEFINITE PHASE SLOPE S IN THE PASSBAND

TABLE 6.1

RESULTS OF OPTIMIZATION (FOR SPECIFIED S)

Order n	Specified Slope S	Ripple in dB	Optimized Parameters a_1 to a_{n-1}	Normalized Error F
4	1.0	1	1,1,1	1086.7
	2.0	1	0.9859, 0.9944,1	8.94
	2.9394	1	0.2385, 0.7723,1	48.8
	3.0	1	0.2661, 0.7581,1	6.42
	π	1	0.2939, 0.7431, 0.9729	12.8
	4.0	1	0.3827, 0.7071, 0.9239	336.5
	2.9394	3	0.1744, 1,1	2.38
5	1.25π	1	0,1680, 0.2968, 0.8064,1	19.1
	3.632	1	0,0,0.8651,1	10.6
	3.632	3	0.7677, 0.7857, 0.8746, 0.8928	14.2

gives

$$S_1 = \sum_{i=1}^{m} \angle T_v(j\omega_i) \} \omega_i / \sum_{i=1}^{m} \omega_i^2 \qquad (6.3.3)$$

The least squares error of the phase functin w.r.t. this line of slope S_1 is computed and used as the objective function for the minimization and as before the critical frequencies a_1 to a_{n-1} are used as the variables. The flowchart for the algorithm is given in Fig. 6.3. The algorithm gives the optimized values of a_1 to a_{n-1} and the slope S_1 of the best fit straight line for the phase response, in the least squares sense. The results of the optimization for different cases are given in Table 6.2.

As seen from the table, there can be more than one optimum point, since the function converges to a local minimum. The different optimal points for a particular case have been obtained by using different starting points.

6.4 Improving the stopband response

In the above methods, the rolloff of the magnitude characteristic in the stopband and the 3 dB bandwidth were not considered. The rolloff in all cases except those in which the critical frequencies are all near to 1, is better than in the Butterworth case; however, the 3 dB frequency in many cases is pushed well into the stopband. This virtually extends the 3 dB bandwidth, though the ripple in the assumed passband (ω=0 to 1 rad/sec) is still maintained. It is possible that in such cases the designed filter does not

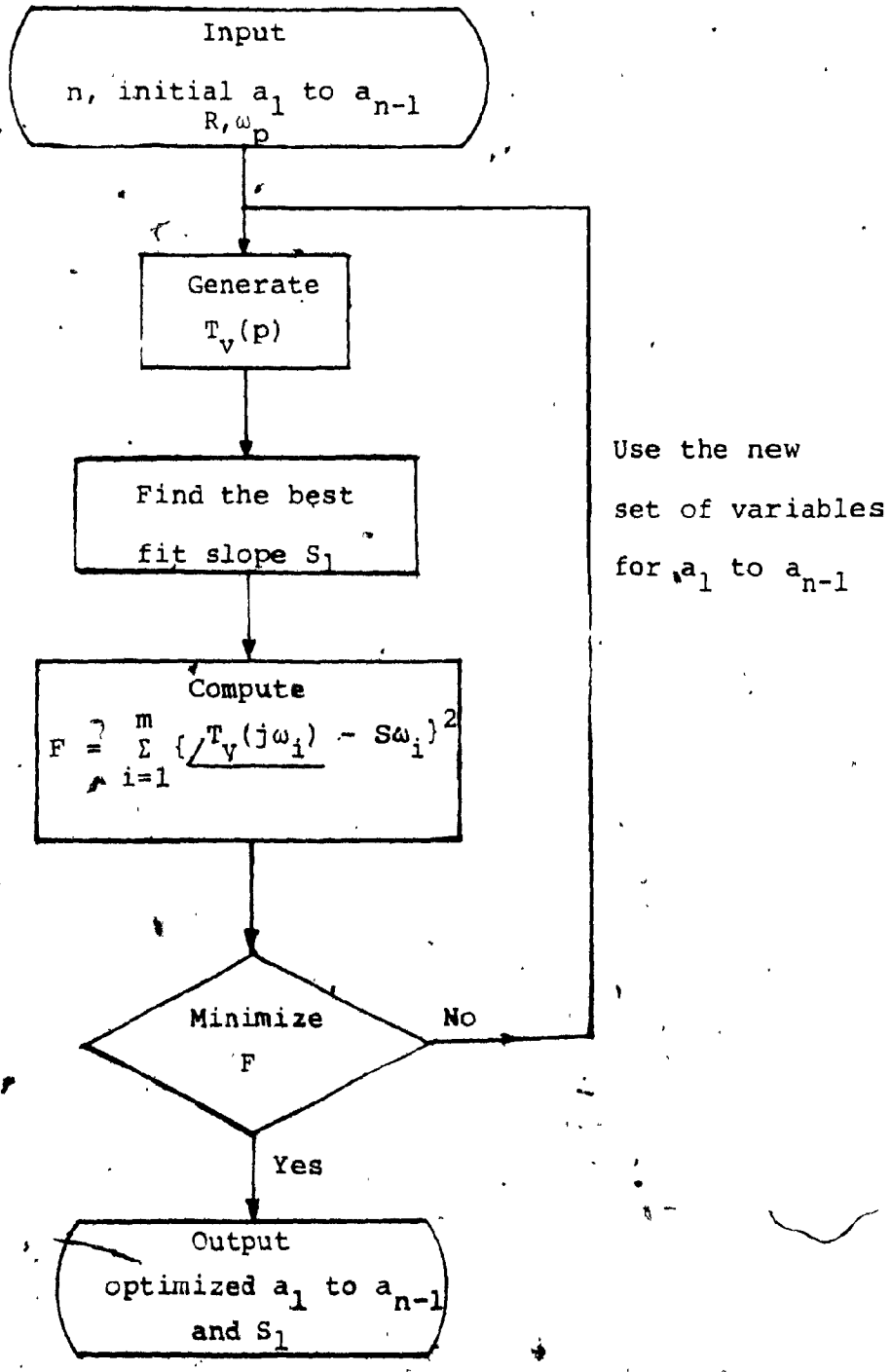

FIG. 6.3 ALGORITHM FOR LEAST SQUARES ERROR IN THE PASSBAND FOR AN ARBITRARY PHASE SLOPE

TABLE 6.2.

RESULTS OF OPTIMIZATION (FOR ARBITRARY S)

Order n	Slope S	Ripple in dB	Optimized Parameters	Normalized Error F
4	2.4492	1	0,1,1	0.64
	3.1613	3	0.2066, 0.9372, 0.9372	2.14
5	3.1657	1	0,0,0,1	18.12
	3.3231	1	0,0,1,1	6.18
	3.8242	3	0,0,1,1	2.74
6	4.1673	1	0,0,0,1,1	17.98
	3.7264	1	0,1,1,1,1	2.32

meet the stopband attenuation specifications.

To avoid this problem, the objective function is modified in such a way as to include the error in the stopband response at the stopband edge. If $|T_v(j\omega)|_{\omega=\omega_s} > SBM$ where ω_s and SBM are the stopband edge frequency and the stopband magnitude specifications, then a factor

$$C\{|T_v(j\omega)|_{\omega=\omega_s} - SBM\}$$

where C is a constant, is added to the least squares phase error to get the error function F. The constant C can be chosen in accordance with the weightage given to the stopband specifications. The procedure is illustrated in the flowchart of Fig. 6.4. The results of optimization are given in Table 6.3. The error in each of the above cases is much lower than that of a Butterworth filter of corresponding order. The least square error slopes and the error values for the Butterworth filter are given in Table 6.4. The values are found as before, by minimizing the square of the error at 50 points in the stopband. Compared to the Butterworth filter of the same order, the optimized filter has a better phase linearity in the passband, a steeper passband to stopband transition in magnitude and a better rolloff in the stopband.

An alternative method to improve the stopband response is to introduce zeros in the stopband. A method of introducing stopband zeros without affecting the linearity of the

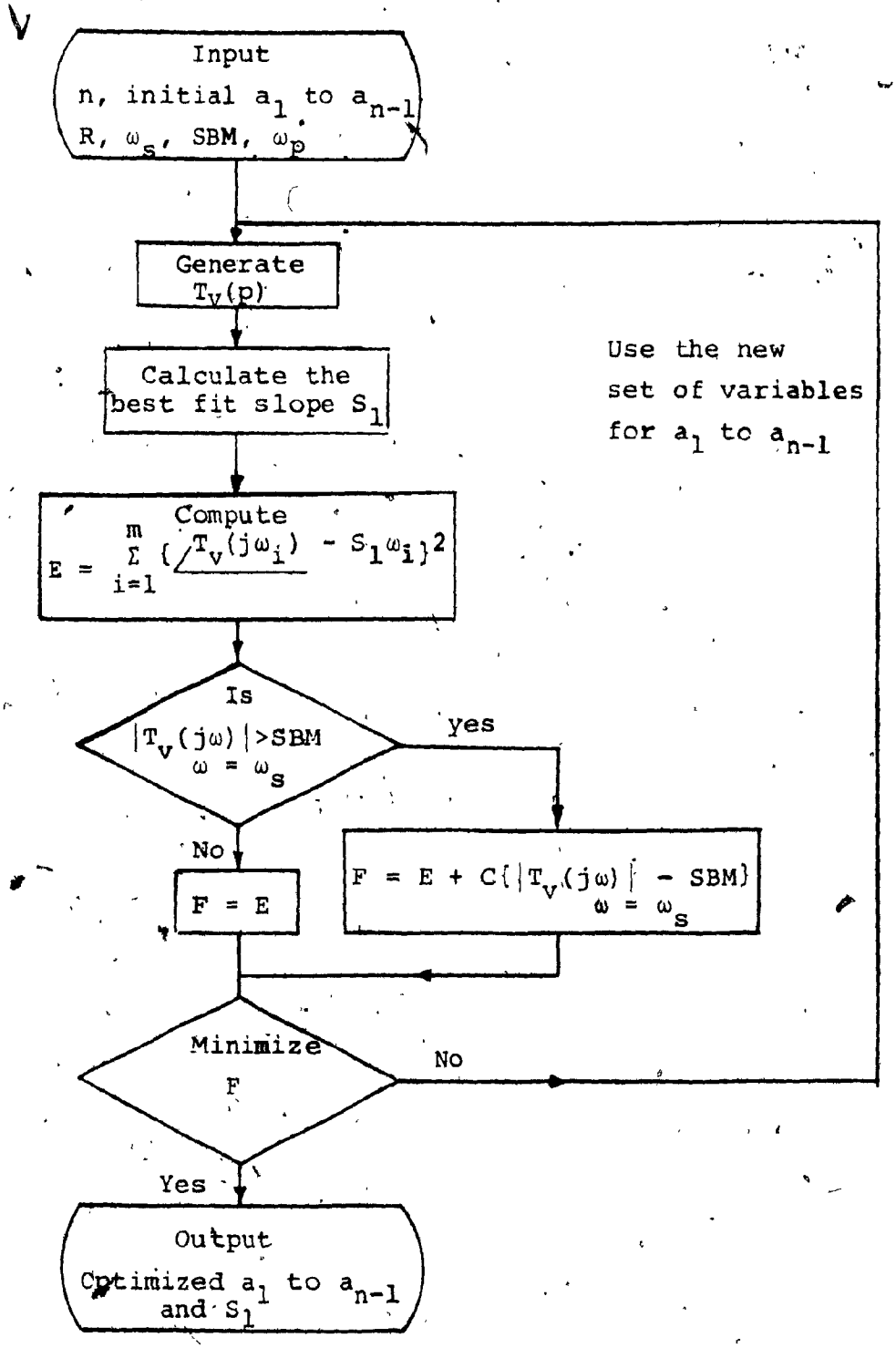

FIG. 6.4 ALGORITHM TAKING INTO ACCOUNT THE STOPBAND SPECIFICATIONS

TABLE 6.3

RESULTS OF OPTIMIZATION TAKING INTO ACCOUNT THE STOPBAND SPECIFICATIONS

Stopband edge ω_s = 1.2 rad/sec

Passband edge ω_p = 1 rad/sec

SBM = Magnitude of the Butterworth filter at ω_s

Order n	Ripple in dB	Optimized Parameters	Slope S_1	Phase Error E & Total error F (normalized)
4	1	0.3140, 0.7429, 0.9292	3.2466	21.3
	3	0.1792, 0.8953, 0.8965	3.2794	2.62
5	1	0.4429, 0.6117, 0.7671, 0.9999	4.0188	30.44
	3	0.001, 0.0013, 0.8820, 1	4.0943	3.94
6	1	0.02, 0.0705, 0.0747, 0.8262,	4.7052	36.18
	3	0,0.0001, 0.0006, 0.9437, 1	4.8595	18.36

TABLE 6.4

LEAST SQUARE ERROR OF THE PHASE RESPONSE
w.r.t. THE BEST FIT STRAIGHT LINE FOR THE BUTTERWORTH FILTER

Order n	Slope of the best fit line	Least Square error. (normalized)
4	2.9394	27
5	3.6320	47.38
6	4.3262	71.52

phase characteristic is described in [83]. By introducing zeros in the stopband, we can see that the numerator of the transfer function which is of the form $\prod_{j=1}^{k}(p^2+\omega_j^2)$ is a purely even quantity for the passband frequencies where $|\omega| \leq \omega_j$ and hence does not affect the phase. The procedure for choosing the ω_j lies in specifying a Chebyshev stopband [84], [85].

If we use a transformation

$$w = \sqrt{1 + \frac{p^2}{\omega_s^2}} \qquad \mathrm{Re}(w) \geq 0 \qquad (6.4.1)$$

then the stopband region $\omega_s \leq \omega \leq \infty$ is mapped onto the entire imaginary axis in the complex w-plane. For a given optimized filter denominator polynomial $e(p)$ which has its roots at p_i, we can find the transformed roots

$$w_i = \sqrt{1 + \frac{p_i^2}{\omega_s^2}} \qquad \mathrm{Re}(w_i) \geq 0 \qquad (6.4.2)$$

By constructing

$$E(w^2) + wF(w^2) = \prod_{i=1}^{n}(w+w_i) \qquad (6.4.3)$$

we get the transformed polynomial in the w-plane, which is a Hurwitz polynomial in w, since $\mathrm{Re}(w_i) \geq 0$. For $w = jv$, wF/E is a reactance function in w and $-(vF/E)^2$ varies between $+0$ and $+\infty$, remaining always positive.

If we choose a transfer function T such that

$$|T|^2 = \frac{E^2}{10^{\alpha_s/10}(E^2-w^2F^2)} = \frac{1}{10^{\alpha_s/10}[1 - (\frac{wF}{E})^2]} \tag{6.4.4}$$

then the attenuation is given by

$$\alpha'(w) = 10\log_{10}(\frac{1}{|T|^2}) = \alpha_s + 10\log_{10}[1 - (\frac{wF}{E})^2] \tag{6.4.5}$$

which varies between α_s and $+\infty$. In order to guarantee that $\alpha=0$ at $\omega=0$ (which is equivalent to the condition $\alpha'(w) = 0$ at $w=1$), we must have

$$10^{\alpha_s/10}[1 - (\frac{wF}{E})^2]\Big|_{w=1} = 1 \tag{6.4.6}$$

Also if n is odd, $\alpha\to\infty$ for $\omega\to\infty$, since $\omega\to\infty$ corresponds to $w\to\infty$ and the polynomial $E^2 - w^2F^2$ is of higher order than E^2. For even n, the $\alpha\to\infty$ for $\omega\to\infty$ condition can be achieved by using an iterative procedure [84]. The minimum stopband loss α_s can be computed from (6.4.6). By retransforming into the p domain using (6.4.1), we obtain the required transfer function as

$$T_v(p) = \frac{E(w^2)\Big|_{w^2 = 1 + \frac{p^2}{\omega_s^2}}}{10^{\alpha_s/20}\left[\frac{E(w^2)\Big|_{w=0}}{|e(j\omega_s)|}\right]e(p)} \tag{6.4.7}$$

where the factor $\frac{E(w^2)\Big|_{w=0}}{|e(j\omega_s)|}$

is needed to make sure that $|T_y(j\omega_s)| = 10^{-\alpha_s/20}$.

The Chebyshev stopband improves the selectivity of the filter; however, the passband magnitude characteristics of the optimized filter are also affected to a certain extent.

6.5 Extension of the method for lowpass digital transfer functions

Just as in the case of an analog transfer function, it is possible to generate a digital transfer function, once the frequencies of maxima and minima and the passband ripple are specified. The procedure is to find out the prewarped critical frequencies and obtain the corresponding analog transfer function, for the required ripple in the passband. By applying the bilinear transformation to this analog function, the resulting digital transfer function has its maxima and minima at the specified frequencies and has the same ripple value.

The method of optimization can also be extended to the approximation of digital filters, by a slight modification of the procedure adopted for the analog filter approximation. Here the warping of the frequency scale due to the bilinear transformation is taken into account by doing the necessary prewarping on the analog prototype filter. Since the frequency in the analog domain, ω and the digital filter frequency Ω are related by

$$\omega = \frac{2}{T} \tan \frac{\Omega T}{2} \qquad (6.5.1)$$

for any given frequency domain specifications for the digital filter, the corresponding analog frequencies can be obtained. The optimization is carried out for this analog filter with a minor difference. The least square error in the phase response is computed for the digital transfer function instead of the analog function. Then the bilinear transformation is used to obtain the optimized digital filter. The flowchart for the optimization is shown in Fig. 6.5 and the results for certain cases are indicated in Table 6.5.

As in the case of the analog filter, it is also possible to introduce stopband zeros for the digital filter transfer function, to obtain a Chebyshev type of attenuation in the stopband [78],[86]. If the digital filter transfer function is transformed by the inverse bilinear transformation, we get an all-pole analog transfer function. By using the techniques described in the previous section, zeros can be introduced to obtain a Chebyshev type of response in the stopband. This process does not alter the phase function in the passband. Now if the new analog transfer function with the stopband zeros is transformed back into a digital transfer function, we obtain a filter having a Chebyshev type of stopband response with its phase response inthe passband identical to that of the optimized filter. In this method, the step involving the comparison of magnitude at the stopband edge with SBM

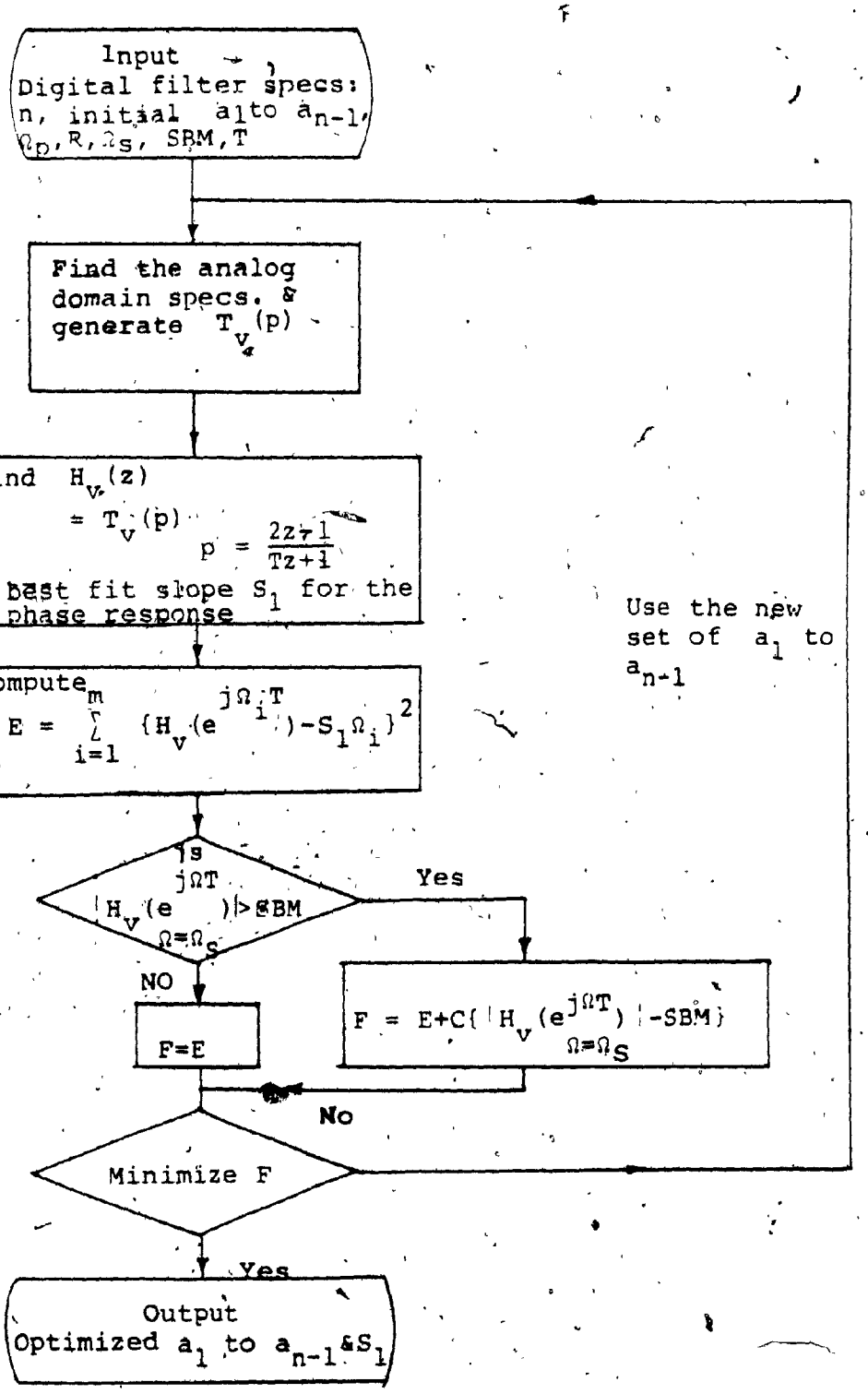

FIG. 6.5 OPTIMIZATION ALGORITHM FOR PHASE LINIEARITY IN A LOWPASS DIGITAL FILTER.

TABLE 6.5

RESULTS OF OPTIMIZATION FOR A DIGITAL FILTER

Stopband edge ω_s = 1.08 rad/sec

Passband edge ω_p = 1 rad/sec

SBM = Magnitude of the Butterworth digital filter at ω_s.

Sampling period = T = 2

Order n	Ripple in dB	Optimized Parameters	Slope S_1	Phase Error E & Total error F (normalized)
4	1	0.5171, 0.6700, 0.9371	2.5073	251.04
	3	0.0512, 0.089, 0.1311	2.3893	204.8
5	1	0.2898, 0.5466, 0.7073, 0.9383	3.1036	359.32
	3	0.8065, 0.8250, 0.8616, 0.9825	3.2919	182.12
6	1	0.0566, 0.1438, 0.2691, 0.9310 0.9832	3.8472	454.26
	3	0.0004, 0.0029, 0.1320, 0.3439, 0.9999	3.4238	376.82

in Fig. 6.5 is ignored. Later the stopband zeros are introduced by following the above procedure.

Just as in the case of the analog transfer function, if the critical frequencies are assumed to be equal to zero and the passband ripple is equal to 3 dB, then the resulting digital filter produces a Butterworth response. If the critical frequencies correspond to those of the Chebyshev filter, then the filter has an equiripple magnitude characteristic. A better phase approximation may be possible if the critical frequencies are chosen to be complex values instead of real numbers. It is to be noted that all the techniques which have been employed earlier for the approximation of analog transfer functions are equally applicable to digital transfer functions also.

6.6 Generation of two-variable approximations

Techniques used in Type 1 and Type 2 approximations discussed in Chapter 5 can be applied to single-variable optimized filters, to obtain two-variable filters with good magnitude and phase properties. Since the optimized single-variable transfer functions are all-pole functions, they can be realized as doubly-terminated networks. The synthesized filters realizing the 5th and 6th order optimized transfer functions are given in Figs. 6.6a and 6.6b. The magnitude and phase characteristics of the two-variable filter with optimized 6th order p_1 and p_2 sections obtained by using the Type 1 method are shown in

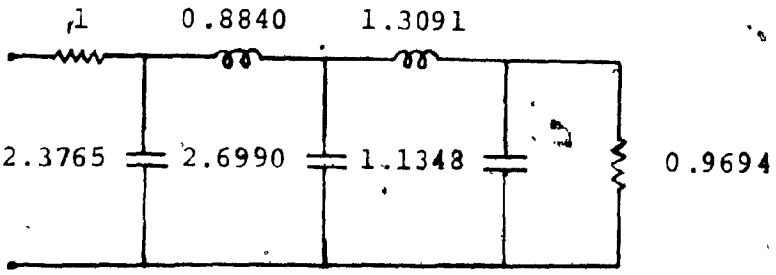

5th Order optimized filter:

Ripple = 1dB, ω_p = 1 rad/sec, ω_s = 1.2 rad/sec,

Critical frequencies: 0.4429, 0.6117, 0.7671, 0.9999

(a)

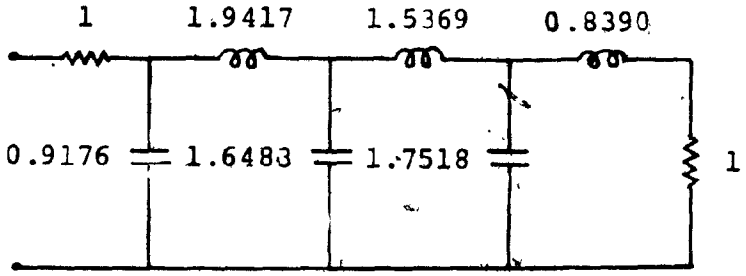

6th Order optimized filter:

Ripple = 1dB, ω_p = 1 rad/sec, ω_s = 1.2 rad/sec,

Critical frequencies: 0.02, 0.0705, 0.0747, 0.8262, 1.0

(b)

FIG. 6.6 REALIZATIONS FOR THE 5th AND 6th ORDER OPTIMIZED TRANSFER FUNCTIONS

Figs. 6.7a and 6.7b. Such extensions can be made using any single-variable transfer function which has the desired magnitude and phase characteristics.

So far we have discussed only the case of normalized lowpass filters. It is known that the reactance transformations do not preserve the phase linearity of the prototype lowpass filter. Hence in designing such filters the following method can be used.

1. The specifications of the lowpass prototype are found which on transformation gives the required LP,HP,BP or BS response.

2. The lowpass prototype filter is designed using the analytical procedure described earlier from an arbitrary set of critical frequencies.

3. By using a suitable reactance transformation, the required filter is obtained. The phase response of this filter is computed and the least square error of this response w.r.t. a linear response in the passband is found.

4. This error is minimized using an optimization routine in which the critical frequencies are chosen as the variables. This method is applicable to the case of digital filters also. The only difference here is to find the prewarped frequencies, design the required filter using the magnitude specifications and optimize for the phase linearity of this filter.

After finding the optimized single-variable filter, the

COMPONENTS

INDUCTORS	.8390	1.5369	1.9417	.8396	1.5369	1.9417
CAPACITORS	1.7518	1.6483	.9176	1.7518	1.6483	.9176

RESISTORS RS= 1.0000 RL= 1.0000

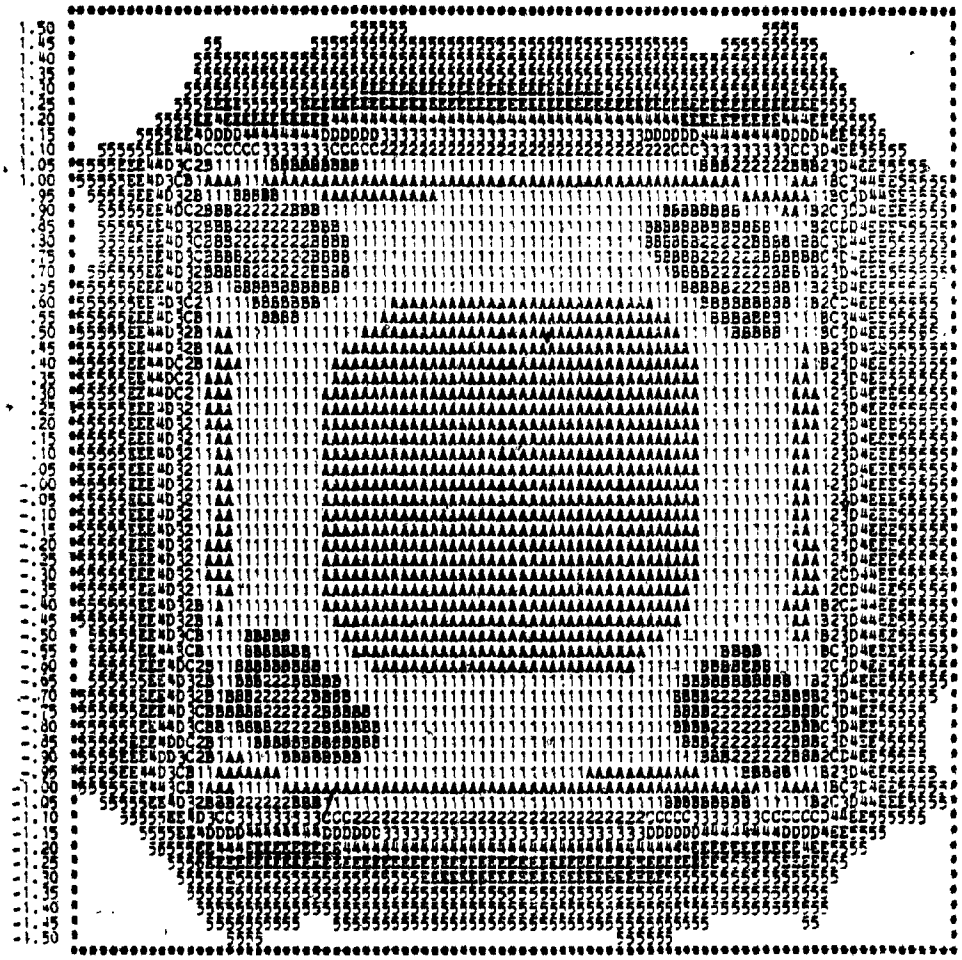

FIG. 6.7(a) TYPE 1 APPROXIMATION : MAGNITUDE RESPONSE WITH SIXTH-ORDER OPTIMIZED p_1 AND p_2 SECTIONS

COMPONENTS

INDUCTORS	.8390	1.5369	1.9417	.8390	1.5369	1.9417
CAPACITORS	1.7518	1.6483	.9176	1.7518	1.6483	.9176

RESISTORS RS= 1.0000 RL= 1.0000

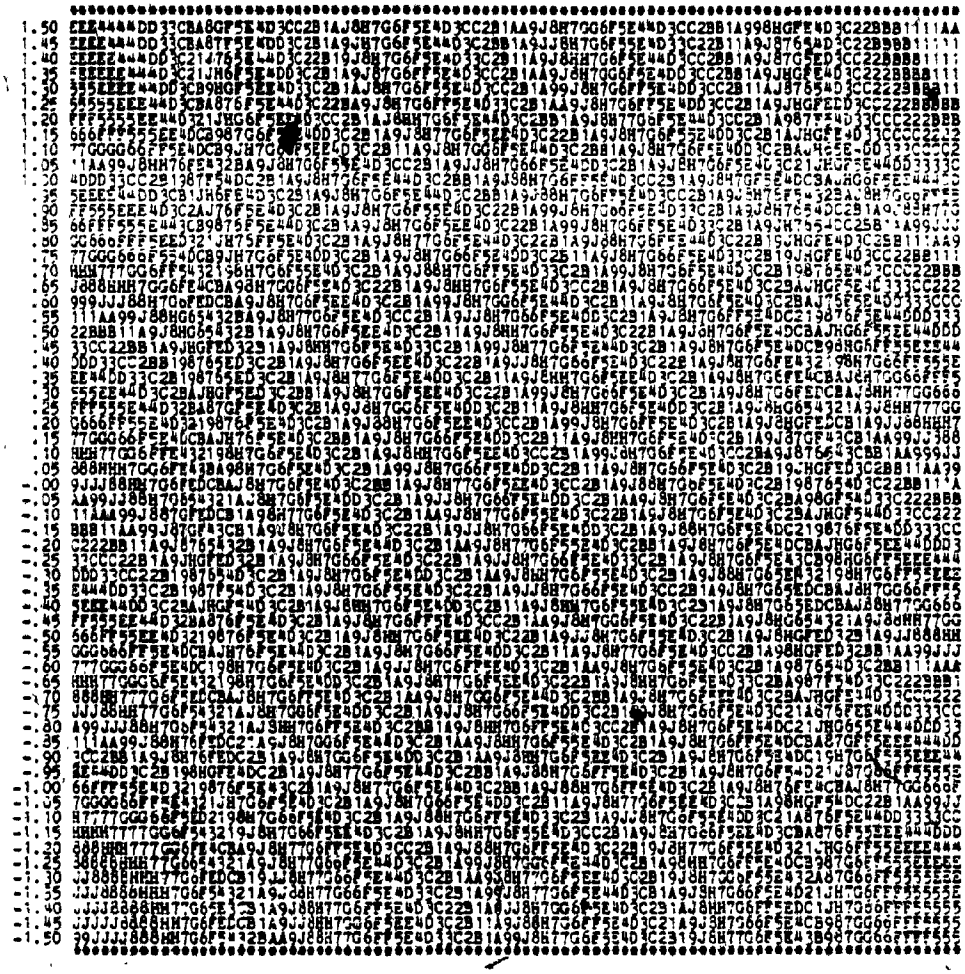

FIG. 6.7(b) TYPE 1 APPROXIMATION ; PHASE RESPONSE WITH SIXTH-ORDER OPTIMIZED p_1 AND p_2 SECTIONS

corresponding two-variable analog or the digital filter is obtained using the Type 1 and Type 2 approximations.

6.7 Summary and Conclusions

In the conventional method of single-variable filter approximation, we define

$$\left|\frac{1}{T_v(p)}\right|^2 = 1 + |K(p)|^2, \quad p = j\omega \qquad (6.7.1)$$

where $K(p)$ is called the characteristic function [84]. The attenuation in dB is defined as

$$\alpha(\omega) = 10\log_{10}\left(\frac{P_{max}}{P_2}\right) = 10\log_{10}[1 + |K(j\omega)|^2] \qquad (6.7.2)$$

where P_{max} is the maximum power available from the source and P_2 is the power absorbed by the load. In order to have a low attenuation in the passband and a high attenuation in the stopband, all the zeros of $K(p)$ are located on the $j\omega$ axis in the stopbands. This gives rise to maxima and minima in the passband and in the stopband. All the maxima in the passband have a value of unity for a normalized filter. In the technique developed in this chapter, the passband has maxima and minima as before; but the maxima values are not fixed at unity. This gives us a unique method for generation of a transfer function which has its passband maxima and minima at specified critical frequencies and has a definite passband ripple.

Since the maxima and minima can be located anywhere within the passband, we have the freedom of using them as variable paremeters in an optimization procedure where the passband phase error is minimized. Better results may be obtained by choosing these critical frequencies as complex instead of real values. It is to be noted that in conventional filters such as Butterworth, Chebyshev or elliptic filters these critical frequencies are real values, whereas in the maximally flat time delay filter, these frequencies are complex.

The optimization techniques are also shown to be useful for digital filter approximation. The stopband response is improved either by incorporating the stopband requirements in the optimization procedure or by introducing stopband zeros without affecting the phase response. The extension of the above filters to two-variables by using the two approximation techniques of Chapter 5 show that the magnitude as well as the phase properties of these filters are carried over to the two-variable filter. The techniques are also shown to be applicable for HP, BP or BS filters with suitable modifications.

CHAPTER 7

2-D WAVE DIGITAL FILTER REALIZATION AND QUANTIZATION EFFECTS

7.1 Introduction

This far we have considered 2-D transfer functions which are derived from a doubly-terminated cascade separable ladder network. It is possible to implement these transfer functions as wave digital filters in two dimensions. In 1-D filter realizations, it is known that the wave digital filter has better sensitivity properties compared to other realizations since the wave approach preserves these properties of the analog network.

In this chapter we extend the methods of realization for the different types of wave digital filters described in the Appendix to two dimensions. In the case of the realization due to Swamy and Thyagarajan for which an extension to 2-D has already been made [33], certain alternate realizations in this approach can be obtained from alternate, equivalent analog network structures.

With the objective of implementing the filters in fixed point form with truncation by rounding, a scaling method is proposed and the product quantization and coefficient quantization effects are studied. The proposed scaling method is an extension of a technique available for 1-D wave digital filters. The product and coefficient quantization effects

are analyzed for both the 2-D direct canonic filter and the wave digital filter and their performance is compared. The techniques used for the above error analysis are again extensions of methods which are being used for this type of analysis in the case of 1-D digital filters.

7.2 Realization of 2-D wave digital filters:

One-port approach

The design of 1-D wave digital filters using the one-port approach due to Fettweis is discussed in the Appendix. Here we discuss the extension of this method to 2-D wave digital filters.

The wave digital realization of one-port impedances and voltage sources is obtained in the same way as before for each element of the two-variable network. Depending on the variable associated with a particular analog element (p_1 or p_2) the corresponding variable in the digital domain (z_1 or z_2) is associated with the wave digital realization of the element. The steps to be followed in obtaining the 2-D wave digital filter from the two-variable analog network are essentially the same as in the 1-D case, involving

(a) identification of the series and parallel interconnections

(b) assigning the port resistances

(c) calculation of the multiplier values for each

adaptor and

(d) replacement of the analog elements in each variable by their corresponding digital realizations.

The steps are illustrated for the doubly-terminated two-variable cascade separable network given in Fig. 7.1.

Example 7.1

Let the element values of the network be $R_1=R_2=1\Omega$, $L_1=\sqrt{2}H$, $C_1=\sqrt{2}F$, $L_2=\sqrt{2}H$, $C_2=\sqrt{2}F$. The sampling frequencies in both the variables are assumed as 5 rad/sec.

$$T_1 = T_2 = 2\Pi/5 \text{ sec} = 1.256627061$$

Adaptor 1: Type S1

$$R_{11} = R_1 = 1$$

$$R_{31} = 2L_1/T_1 = 2.25079079$$

$$R_{21} = R_{11} + R_{31} = 3.2507979.$$

$$\alpha_{11} = R_{11}/R_{21} = 0.3076174582$$

Adaptor 2: Type P1

$$G_{12} = 1/R_{21} = 0.3076174582$$

$$G_{32} = 2C_1/T_1 = 2.2509079$$

$$G_{22} = G_{12}+G_{32} = 2.558408249$$

$$\beta_{12} = G_{12}/G_{22} = 0.1202378308$$

Adaptor 3: Type S1

$$R_{13} = 1/G_{22} = 0.3908680331$$

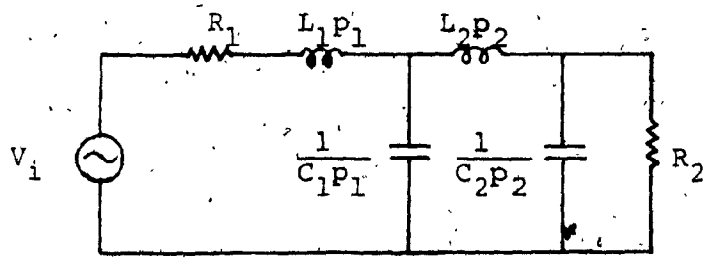

(a) Analog filter

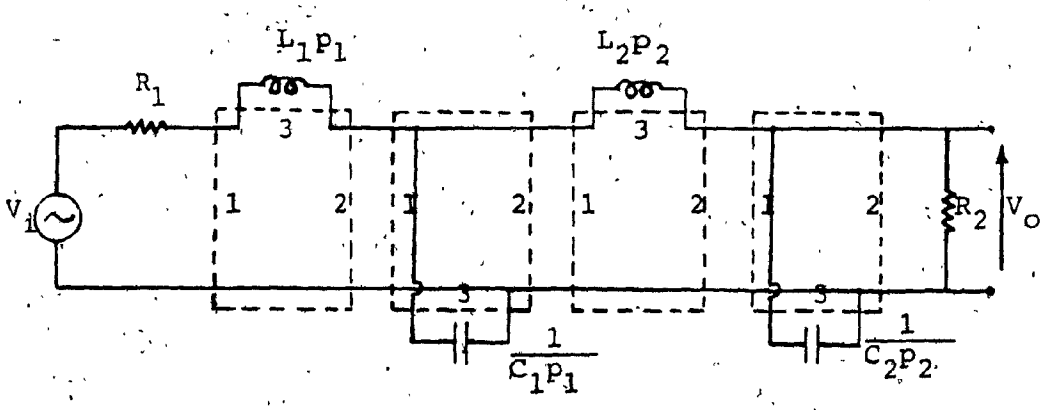

(b) Identification of wire interconnections

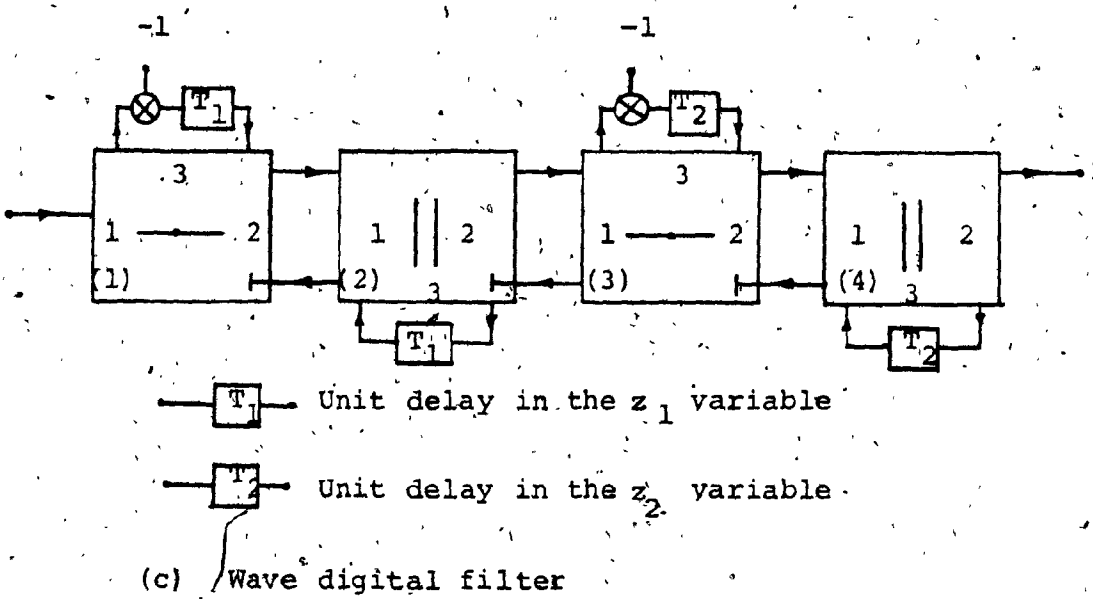

(c) Wave digital filter

FIG.7.1 REALIZATION OF A WAVE DIGITAL FILTER FROM A GIVEN ANALOG NETWORK - ONE-PORT APPROACH

$R_{33} = 2L_2/T_2 = 2.25079079$

$R_{23} = R_{13} + R_{33} = 2.641658823$

$\alpha_{13} = R_{13}/R_{23} = 0.14[illegible]631017$

Adaptor 4: Type P2

$G_{14} = 1/R_{23} = 0.3785500198$

$G_{34} = 2C_2/T_2 = 2.25079079$

$G_{24} = 1/R_2 = 1.$

$\beta_{14} = 2G_{14}/(G_{14}+G_{24}+G_{34}) = 0.2086053857$

$\beta_{24} = 2G_{24}/(G_{14}+G_{24}+G_{34}) = 0.5510642578$

7.3 Realization of 2-D wave digital filters:

Two-port approach

It is possible to obtain many realizations with the two-port approach using linear transformations. Extensions of these methods to the case of 2-D wave digital filters is straightforward. The 2-D extensions for the IVR and MTA methods due to Constantinides and the scattering matrix formulation due to Swamy and Thyagarajan are discussed here.

7.3.1 IVR and MTA methods

The methods to be adopted for the 2-D case are essentially the same as that for the 1-D filter, except that two variables z_1 and z_2 have to be assigned in the digital domain for the digital sections derived from the elements

in the variables p_1 and p_2 respectively. The methods for the 1-D case are described in detail in the Appendix. Here we illustrate the procedure for applying it to the 2-D case with the following example.

Example 7.2

We consider the analog network given in Fig. 7.1 and transform it into a wave digital filter using (a) the IVR method and (b) the MTA method. The element values of the network are $R_1=R_2=1\Omega$, $L_1=\sqrt{2}H$, $C_1=\sqrt{2}F$, $L_2=\sqrt{2}H$, $C_2=\sqrt{2}F$. Sampling frequencies in both variables = 5 rad/sec.

(a) IVR method

$$T_1 = T_2 = 2\pi/5 = 1.256637061$$

Shunt C_2: $R_2=1$ $G_{24}=1/R_2=1$

$$G_{14} = G_{24}+2C_2/T_2 = 3.25079079$$

$$\alpha_{22} = 2C_2/T_2G_{14} = 0.6923825418$$

Series L_2: $R_{23} = 1/G_{14} = 0.3076174582$

$$R_{13} = R_{23} + 2L_2/T_2 = 2.558408249$$

$$\alpha_{12} = \frac{R_{23}-(2L_2/T_2)}{R_{23}+(2L_2/T_2)} = -0.7595243383$$

Shunt C_1: $G_{22} = \frac{1}{R_{13}} = 0.3908680331$

$$G_{12} = G_{22} + (2C_1/T_1) = 2.641658823$$

$$\alpha_{21} = 2C_1/T_1G_{12} = 0.852036893$$

Series L_1: $R_{21} = 1/G_{12} = 0.3785500198$

$$R_{11} = R_{21} + (2L_1/T_1) = 2.62934081$$

$$\alpha_{11} = \frac{R_{21} - (2L_1/T_1)}{R_{21} + (2L_1/T_1)} = -0.7120570918$$

Source: $R_s = 1\Omega$

$$\alpha_v = R_s/(R_{11}+R_s) = 0.2755321289$$

(b) MTA method

$$T_1 = T_2 = 2\Pi/5 = 1.256637061$$

Shunt C_2: $R_2 = 1\Omega$ $G_{24} = 1/R_2 = 1$

$$G_{14} = G_{24} + (2C_2/T_2) = 3.25079079$$

$$\alpha_{22} = \frac{(2C_2/T_2) - G_{24}}{(2C_2/T_2) + G_{24}} = 0.3847650836$$

Series L_2:

$$R_{23} = 1/G_{14} = 0.3076174582$$

$$R_{13} = R_{23} + (2L_2/T_2) = 2.558408249$$

$$\alpha_{12} = R_{23}/R_{13} = 0.1202378308$$

Shunt C_1:

$$G_{22} = 1/R_{13} = 0.3908680331$$

$$G_{12} = G_{22} + (2C_1/T_1) = 2.641658823$$

$$\alpha_{21} = \frac{(2C_1/T_1) - G_{22}}{(2C_1/T_1) + G_{22}} = 0.7040737966$$

Series L_1: $R_{21} = 1/G_{12} = 0.3785500198$

$R_{11} = R_{21} + (2L_1/T_1) = 2.62934081$

$\alpha_{11} = R_{21}/R_{11} = 0.1439714541$

Source : $R_s=1$ $\alpha_v = -R_{11}/(R_{11}+R_s) = -0.7244678711$

$\Delta_0 = V_0/(R_{11}+R_s) = V_0/3.62934081$

The realizations are shown in Fig. 7.2.

7.3.2 Swamy and Thyagarajan Method

An extension of this method to 2-D wave digital filters has been carried out by Swamy, Thagarajan and Ramachandran [33]. It can be shown that the alternate realizations I(b), I(c) and I(d) discussed in [33] and [87] are related to the analog dual and transpose networks. In fact if we start with an analog network N and if N_D, N^T and N_D^T are the dual, transpose and the dual of the transpose of the network N respectively, then the following similarities are observed.

Type I(b) realization of N ≡ Type I(a) realization of N_D

Type I(c) realization of N ≡ Type I(a) realization of N^T

Type I(d) realization of N ≡ Type I(a) realization of N_D^T.

Example 7.3

We find the wave digital filter corresponding to the

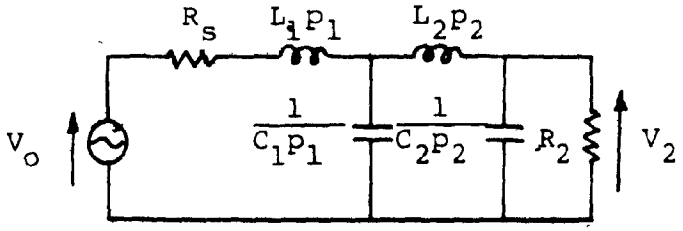

(a) Analog filter.

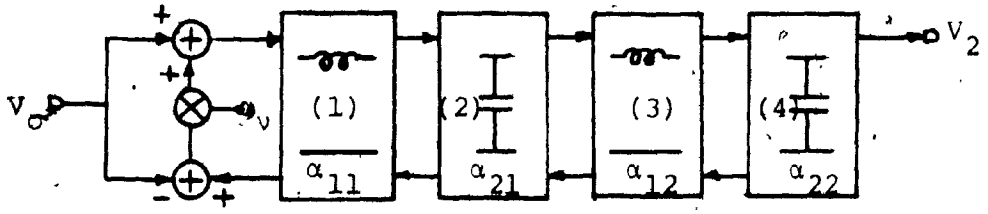

(b) Realization by the IVR method

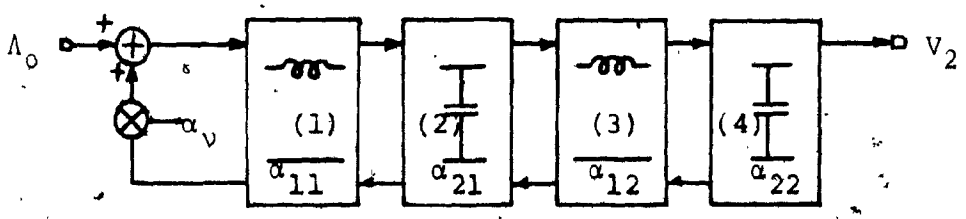

(c) Realization by the MTA method

FIG. 7.2 WAVE DIGITAL FILTER REALIZATIONS USING THE TWO-PORT REPRESENTATION

analog network of example 7.1. $R_s = R_L = 1\Omega$, $L_1 = L_2 = \sqrt{2}$, $C_1 = C_2 = \sqrt{2}$, $\Omega_{s1} = \Omega_{s2} = 5$ rad/sec, $T_1 = T_2 = 2\pi/5 = 1.256637061$ sec.

Type 1 method

N_a(shunt C_2): $R_2 = R_L = 1$, $\phi = 0$

$G_2 = 1$

$G_a = G_2 + (2C_2/T_2) = 3.25079079$

$\alpha_a = G_2/G_a = 0.3076174582$

N_b(series L_2): $R_b = R_a + (2L_2/T_2) = 2.558408249$

$\alpha_b = R_a/R_b = 0.1202378308$

N_c(Shunt C_1): $G_c = G_b + (2C_1/T_1) = 2.641658823$

$\alpha_c = G_b/G_c = 0.1479631017$

N_d(Series L_1): $R_d = R_c + (2L_1/T_1) = 2.62934081$

$\alpha_d = R_c/R_d = 0.1439714541$

$\theta = (R_d - R_s)/(R_d + R_s) = 0.4489357422$

The type I realizations are shown in Fig. 7.3.

Type II method

N_D(series L_1): $R_s = 1\Omega$, $\theta = 0$

$R_D = R_s + (2L_1/T_1) = 3.25079079$

$\alpha_D = R_s/R_D = 0.3076174582$

N_C(Shunt C_1): $G_C = G_D + (2C_1/T_1) = 2.558408249$

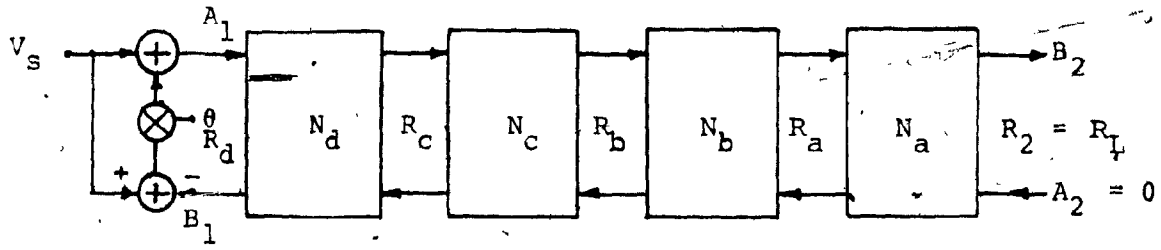

Realization I(a): $\dfrac{B_2}{V_s} = 2H(z_1, z_2)$

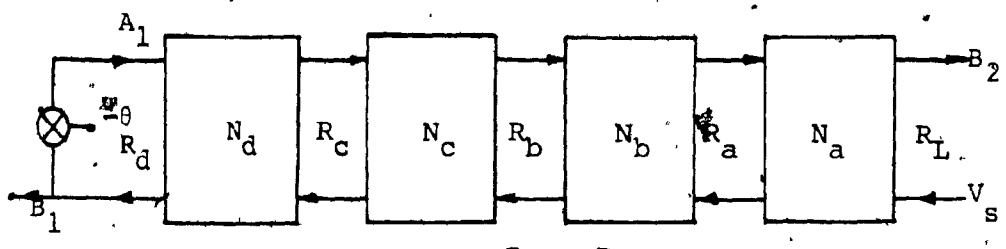

Realization I(b): $\dfrac{B_1}{V_s} = \dfrac{R_d}{R_L} \dfrac{2}{1+\theta} H(z_1, z_2)$

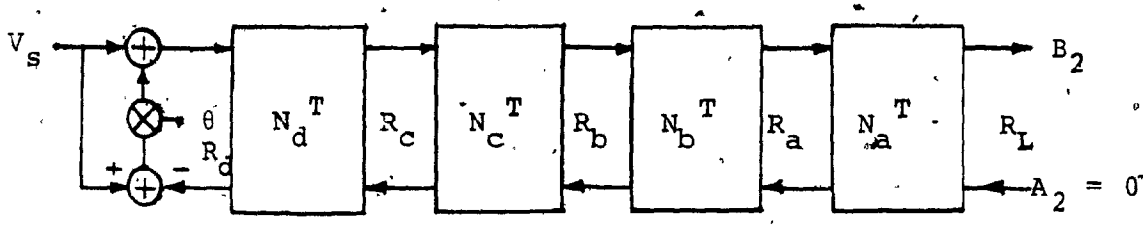

Realization I(c): $\dfrac{B_2}{V_s} = \dfrac{R_d}{R_L} 2H(z_1, z_2)$

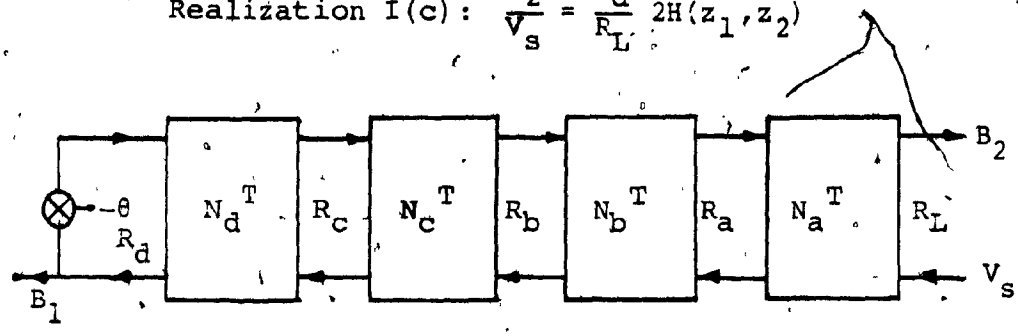

Realization I(d): $\dfrac{B_1}{V_s} = \dfrac{2}{1+\theta} H(z_1, z_2)$

$$\theta = \frac{R_d - R_s}{R_d + R_s}, \quad \phi = 0$$

FIG. 7.3 TYPE I REALIZATIONS FOR EXAMPLE 7.3

$$\alpha_C = G_D/G_C = 0.1202378308$$

N_B(Series L_2): $R_B = R_C + (2L_2/T_2) = 2.641658823$

$$\alpha_B = R_C/R_B = 0.1479631017$$

N_A(Series C_2): $G_A = G_B + (2C_2/T_2) = 2.62934081$

$$\alpha_A = G_B/G_A = 0.1439714541$$

$$\phi = (R_L - R_A)/(R_L + R_A) = 0.4489357422$$

The type II realizations are given in Fig. 7.4.

7.4 Scaling

In fixed point arithmetic implementation of a 2-D digital filter, the signal level has to be scaled at different nodes of the filter in order to avoid overflows and at the same time utilize the full dynamic range of the filter registers thus maintaining a high signal to noise ratio. The scaling procedure based on Jackson's technique [88], [89] has been extended to wave digital filters [90], [91].

According to the above procedure, the upper bound on the signal level at any node of a digital filter is given by

$$|v_i(n_1,n_2)| \leq \|H_i(e^{j\omega_1},e^{j\omega_2})\|_p \, \|X(e^{j\omega_1},e^{j\omega_2})\|_q \qquad (7.4.1)$$

with

$$\frac{1}{p} + \frac{1}{q} = 1, \quad p,q \geq 1 \qquad (7.4.2)$$

where $v_i(n_1,n_2)$ is the digital sequence at the ith branch node, $H_i(e^{j\omega_1},e^{j\omega_2})$ is the transfer function from the

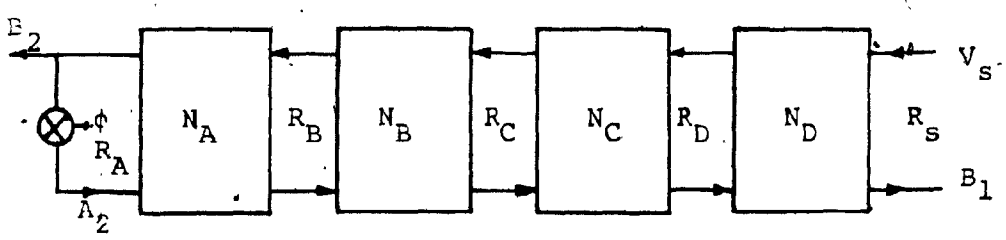

Realization II(a): $\frac{B_2}{V_s} \quad \frac{2}{1+\phi} H(z_1, z_2)$

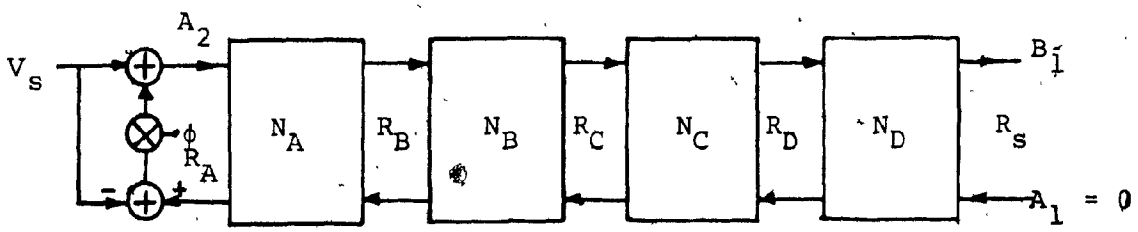

Realization II(b): $\frac{B_1}{V_s} = \frac{R_s}{R_L} 2H(z_1, z_2)$

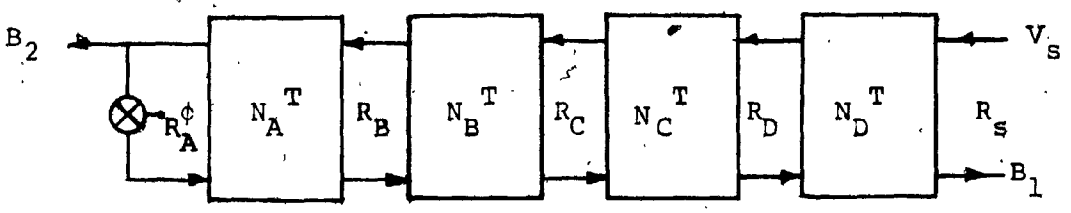

Realization II(c): $\frac{B_2}{V_s} = \frac{R_s}{R_A} \frac{2}{1+\phi} H(z_1, z_2)$

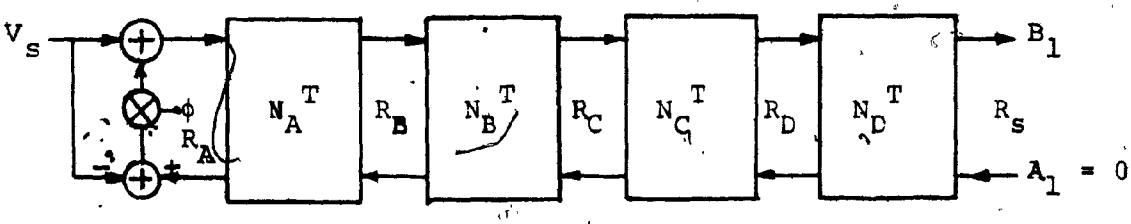

Realization II(d): $\frac{B_1}{V_s} = \frac{R_A}{R_L} 2H(z_1, z_2)$

$$\phi = \frac{R_L - R_A}{R_L + R_A} \quad , \theta = 0$$

FIG. 7.4 TYPE II REALIZATIONS FOR EXAMPLE 7.3

input to the ith branch node, $X(e^{j\omega_1},e^{j\omega_2})$, the Fourier transform of the input data and $\|A(e^{j\omega_1},e^{j\omega_2})\|_p$ denotes the L_p norm of $A(e^{j\omega_1},e^{j\omega_2})$. To avoid any overflow, we must ensure that $|v_i(n_1,n_2)| \leq 1$. The L_∞ norm of $H(e^{j\omega_1},e^{j\omega_2})$ is easy to compute since it amounts to finding the maximum value of $|H_i(e^{j\omega_1},e^{j\omega_2})|$ in the interval $-\omega_{s1} \leq \omega_1 \leq \omega_{s1}$, $-\omega_{s2} \leq \omega_2 \leq \omega_{s2}$, where ω_{s1} and ω_{s2} are the sampling frequencies along the ω_1 and ω_2 directions. Thus with $p = \infty$, $q = 1$, we require that

$$\|H_i(e^{j\omega_1},e^{j\omega_2})\|_\infty \leq 1 \qquad (7.4.3)$$

if $\|X(e^{j\omega_1},e^{j\omega_2})\|_1 \leq 1$ so that $|v_i(n_1,n_2)| \leq 1$

The nodes 'i' at which it is required to find the transfer function are taken to be the inputs of the multipliers and the output of the filter section. A scaling multiplier S is used at the input of the filter section such that the amplitudes of the multiplier inputs are bounded by a value of 1, if the input $|x(n_1,n_2)| \leq 1$. In the case of intermediate sections of the wave digital filter, both the incident and reflected waves at the input port of the section have to be scaled by the factors S and 1/S respectively. This is equivalent to introducing ideal transformers of ratio S: 1 between every series and shunt element in the analog structure [90-92]. It is sufficient to consider the multiplier inputs to find the scaling factor S. The adder outputs need not be considered for this

purpose because a machine- representable sum is always evaluated correctly in the 1's or 2's complement arithmetic, even if overflow does occur in one of the partial sums [36].

Considering the filter given in Fig. 7.5a, the procedure adopted for scaling is as follows [90].

(a) Find max $(\|H_{i1}\|_\infty)$ in the first section of the wave digital filter where H_{i1} denotes the transfer functions from the filter input to the inputs of the multipliers in the first section and to the output of the first section. Scale the input by the factor

$$S_0 = 1/\max\ (\|H_{i1}\|_\infty) \qquad (7.4.4)$$

(b) With the scale factor S_0 introduced at the input of the filter, find max $(\|H_{i2}\|_\infty)$ for the second section. Scale the incident and reflected waves at the input port of the second section by

$$S_1 = 1/\max\ (\|H_{i2}\|_\infty) \qquad (7.4.5)$$

and $1/S_1$ respectively.

Repeat the above for all the sections.

The scaled filter is shown in Fig. 7.5b. For convenience, the scaling constants can be chosen to be powers of 2 satisfying the overflow constraints, so that the scaling operation is accomplished by data shifts. Let the digital chain matrices for the networks N_a, N_b, N_c and N_d be

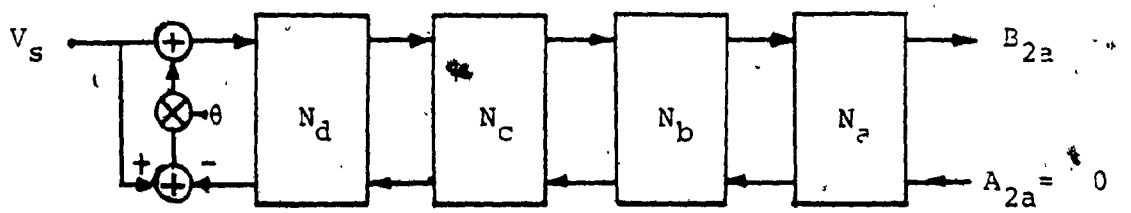

(a) Given wave digital filter

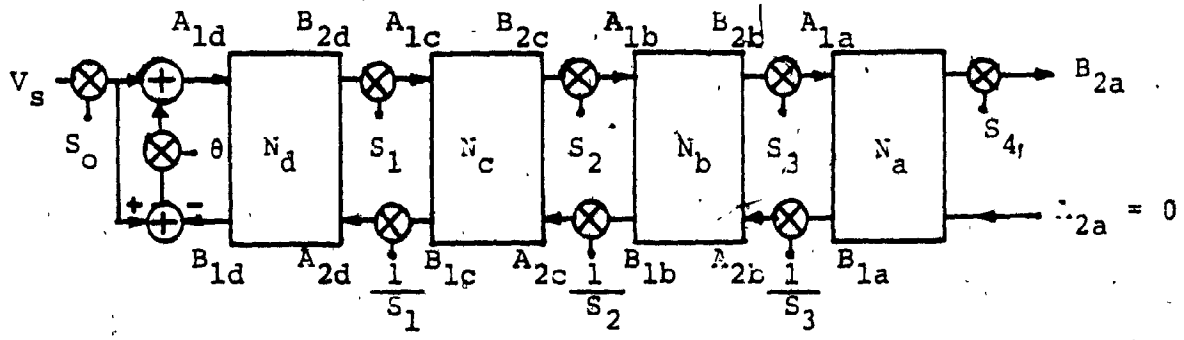

(b) Scaled wave digital filter

FIG.7.5 SCALING PROCEDURE FOR WAVE DIGITAL FILTERS

represented by

$$[F_i] = \begin{bmatrix} \mu_i & \lambda_i \\ \nu_i & k_i \end{bmatrix} \quad , \quad i=a,b,c,d \text{ respectively.}$$

The input V_s and the output B_{2a} of the filter are related by

$$\begin{bmatrix} V_s \\ 0 \end{bmatrix} = \frac{1}{S_0 S_1 S_2 S_3 S_4} [F_T] \begin{bmatrix} B_{2a} \\ A_{2a} \end{bmatrix} \qquad (7.4.6)$$

where $[F_T] = [F_s][F_d][F_c][F_b][F_a]$,

$$[F_s] = \begin{bmatrix} \frac{1}{1+\theta} & \frac{\theta}{1+\theta} \\ 0 & 0 \end{bmatrix} \quad \text{and} \quad A_{2a} = 0$$

Using the digital two-port chain matrices, F_a, F_b, F_c and F_d, the signals at the ports can be computed. The signal values at the inputs of the multipliers are obtained from the port signals.

Using the above procedure, the transfer functions H_{il} etc. are calculated. Because of the inherent symmetry in the frequency response of the transfer functions, it is necessary to evaluate the magnitude of the transfer functions only in two adjacent quadrants. For example, the transfer functions can be evaluated for $0 \leq \omega_1 \leq \omega_{s1}$, $-\omega_{s2} \leq \omega_2 \leq \omega_{s2}$.

The following results are obtained for the type Ia realization of example 7.3

Scale factors:

$S_0 = 0.190165$ $\quad 1/S_0 = 5.258591$

$S_1 = 1.78645$ $\quad 1/S_1 = 0.559769$

$S_2 = 0.63834$ $\quad 1/S_2 = 1.566563$

$S_3 = 4.61135$ $\quad 1/S_3 = 0.216856$

$S_4 = 1$

If we choose the scale factors to be powers of 2, then we get $S_0 = 0.125$, $S_1 = 2$, $S_2 = 0.5$, $S_3 = 8$ and $S_4 = 1$. The scale factor S_4 is used to boost the signal value at the output so that it has a maximum value of unity.

In the case of the direct canonic realization of the transfer function $H(z_1,z_2) = N(z_1,z_2)/D(z_1,z_2)$ we have to find only the input scale factor S_0, using the transfer functions $H(z_1,z_2)$ and $H_1(z_1,z_2) = 1/D(z_1,z_2)$.

$$S_0 = 1/\max\ (\|H\|_\infty, \|H_1\|_\infty) \qquad (7.4.9)$$

For the analog network of example 7.1, the transfer function is given by

$$T_v(p_1,p_2) = \frac{0.5}{2p_1^2p_2^2+\sqrt{2}\,p_1^2p_2+\sqrt{2}p_1p_2^2+p_1^2+p_2^2+2p_1p_2+\sqrt{2}p_1+\sqrt{2}p_2+1}$$

whose corresponding digital transfer function is

$$H_v(z_1^{-1},z_2^{-1}) = \frac{K(1+z_1^{-1})^2(1+z_2^{-1})^2}{b_{22}z_1^{-2}z_2^{-2}+b_{21}z_1^{-2}z_2^{-1}+b_{12}z_1^{-1}z_2^{-2}+b_{20}z_1^{-2}} + b_{02}z_2^{-2}+b_{11}z_1^{-1}z_2^{-1}+b_{10}z_1^{-1}+b_{01}z_2^{-1}+1$$

where $K = 0.0125411295$, $b_{22} = 0.2021724204$

$b_{21} = b_{12} = -0.4204764295$ $b_{11} = 0.8795263335$

$b_{20} = b_{02} = 0.3469497923$ $b_{10} = b_{01} = -0.7666646674$.

The scale factors are $S_0 = 0.025082259$ and $S_1 = 1$.

7.5 Product Quantization

The errors due to product quantization can be regarded as noise sources which contribute to the output noise [36]. A finite word length multiplier gives rise to a quantized output

$$Q[c_i x(n_1,n_2) = c_i\, x(n_1,n_2) + e_i(n_1,n_2) \qquad (7.5.1)$$

where $c_i\, x(n_1,n_2)$ is the exact product and $e_i(n_1,n_2)$ is the quantization error. This is represented in Fig. 7.6a. Each multiplier is replaced by this equivalent circuit to obtain the noise model for the filter. If quantization is by rounding, each noise source $e_i(n_1,n_2)$ can be regarded as a random variable of value $-q/2 \le e_i(n_1,n_2) \le q/2$, where q is the quantization step. It has a uniform probability density.

$$p\{e_i(n_1,n_2)\} = \begin{cases} 1/q & \text{for } -q/2 \le e_i(n_1,n_2) \le q/2 \\ 0 & \text{otherwise} \end{cases} \qquad (7.5.2)$$

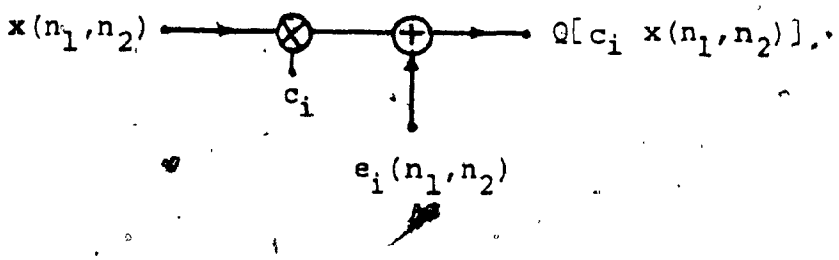

(a) Quantization of a multiplier output

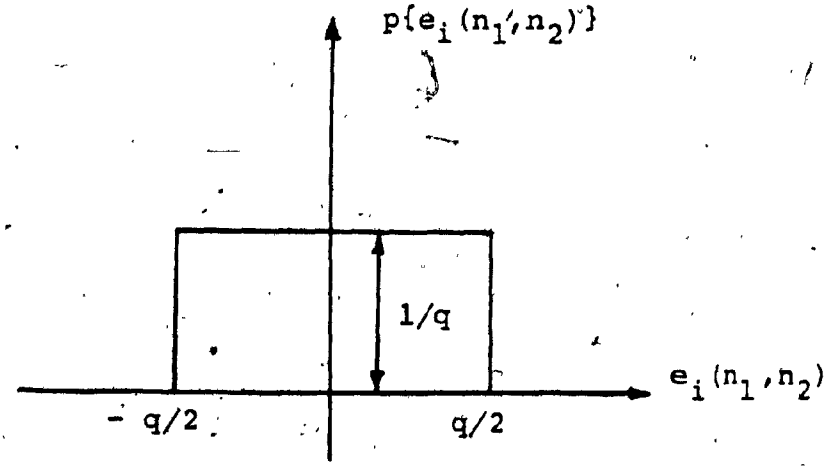

(b) Probability density function of the product quantization noise

FIG. 7.6 PRODUCT QUANTIZATION EFFECTS

as illustrated in Fig. 7.6b. The mean of $e_i(n_1,n_2)$ is

$$E\{e_i(n_1,n_2)\} = \int_{-\infty}^{\infty} e_i(n_1,n_2)p\{e_i(n_1,n_2)\}d\{e_i(n_1,n_2)\} = 0 \qquad (7.5.3)$$

and its variance is

$$\begin{aligned}\sigma_{e_i}^2 &= E\{[e_i(n_1,n_2) - E\{e_i(n_1,n_2)\}]^2\} \\ &= E\{[e_i(n_1,n_2)]^2\} \text{ due to (7.5.3)} \qquad (7.5.4) \\ &= \int_{-q/2}^{q/2} \{e_i(n_1,n_2)\}^2 p\{e_i(n_1,n_2)\}d\{e_i(n_1,n_2)\} = q^2/12\end{aligned}$$

If the signal levels are much larger than q at all the nodes, the following assumptions hold.

(1) $e_i(n_1,n_2)$ and $e_i(n_1+k_1, n_2+k_2)$ are statistically independent for any (n_1,n_2) for $k_1,k_2 \neq 0$.

(2) $e_i(n_1,n_2)$ and $e_j(n_1+k_1, n_2+k_2)$ are statistically independent for any value of (n_1,n_2) or (k_1,k_2) for $i \neq j$.

The autocorrelation function of the random process $e_i(n_1,n_2)$ is written as

$$r_{e_i}(k_1,k_2) = E\{e_i(n_1,n_2)e_i(n_1+k_1,n_2+k_2)\} \qquad (7.5.5)$$

For $k_1=k_2=0$,

$$r_{e_i}(0,0) = E\{[e_i(n_1,n_2)]^2\} = q^2/12 \qquad (7.5.6)$$

For $k_1, k_2 \neq 0$,

$$r_{e_i}(k_1,k_2) = E\{e_i(n_1,n_2)\}E\{e_i(n_1+k_1, n_2+k_2)\} \quad (7.5.7)$$

by assumption (1). Since the mean of each noise source is zero, we get

$$r_{e_i}(k_1,k_2)\Big|_{k_1,k_2\neq 0} = 0 \quad (7.5.8)$$

From (7.5.6) and (7.5.8) we can write

$$r_{e_i}(k_1,k_2) = \frac{q^2}{12}\,\delta(k_1,k_2) \quad (7.5.9)$$

where $\delta(k_1,k_2)$ is the impulse function. The power spectral density (PSD) of $e_i(n_1,n_2)$ is

$$s_{e_i}(\omega_1,\omega_2) = [\mathcal{Z}_2\, r_{e_i}(k_1,k_2)]\Big|_{\substack{z_1=e^{j\omega_1 T_1}\\ z_2=e^{j\omega_2 T_2}}} = q^2/12 \quad (7.5.10)$$

where $\mathcal{Z}_2$ is the 2-D z-transformation. This shows that $e_i(n_1,n_2)$ is a white-noise process.

The autocorrelation of the sum of $e_i(n_1,n_2) + e_j(n_1,n_2)$ is

$$r_{e_i+e_j}(k_1,k_2) = E\{[e_i(n_1,n_2)+e_j(n_1,n_2)][e_i(n_1+k_1,n_2+k_2) + e_j(n_1+k_1,n_2+k_2)]\}$$

$$= E\{e_i(n_1,n_2)e_i(n_1+k_1,n_2+k_2)\}+E\{e_i(n_1,n_2)\}E\{e_j(n_1+k_1, n_2+k_2)\}$$

$$+ E\{e_j(n_1,n_2)\}E\{e_i(n_1+k_1,n_2+k_2)\}+E\{e_j(n_1,n_2)e_j(n_1+k_1, n_2+k_2)\}$$

by assumption (2)

$$= r_{e_i}(k_1,k_2) + r_{e_j}(k_1,k_2) \qquad (7.5.11)$$

The PSD of the sum of two processes is equal to the sum of their respective PSDs, since

$$S_{e_i+e_j}(z_1,z_2) = \mathcal{Z}_2[r_{e_i}(k_1,k_2)+r_{e_j}(k_1,k_2)] = S_{e_i}(z_1,z_2) + S_{e_j}(z_1,z_2) \qquad (7.5.12)$$

gives

$$S_{e_i+e_j}(\omega_1,\omega_2) = S_{e_i}(\omega_1,\omega_2) + S_{e_j}(\omega_1,\omega_2) \qquad (7.5.13)$$

For a 2-D digital filter having a transfer function $H(z_1,z_2)$ if the input and output are $x(n_1,n_2)$ and $y(n_1,n_2)$ respectively, then the 2-D z-transforms of $r_x(k_1,k_2)$ and $r_y(k_1,k_2)$ are related by

$$S_y(z_1,z_2) = H(z_1,z_2)H(z_1^{-1},z_2^{-1})S_x(z_1,z_2) \qquad (7.5.14)$$

or

$$S_y(e^{j\omega_1T_1},e^{j\omega_2T_2}) = |H(e^{j\omega_1T_1},e^{j\omega_2T_2})|^2 S_x(e^{j\omega_1T_1},e^{j\omega_2T_2}) \qquad (7.5.15)$$

Because of (7.5.13) the effect due to each noise source can

be added up using superposition, to obtain the output PSD. Thus if there are m noise sources,

$$S_y(z_1,z_2) = \sum_{i=1}^{m} H_i(z_1,z_2)H_i(z_1^{-1},z_2^{-1})S_{e_i}(z_1,z_2) \qquad (7.5.16)$$

where $H_i(z_1,z_2)$ denotes the transfer function from the noise source input node (multiplier output) to the output of the filter. The output noise spectrum is expressed as the relative power spectral density (RPSD) given by

$$\text{RPSD} = 10\log_{10}\{S_0(\omega_1,\omega_2)/S_i(\omega_1,\omega_2)\} \qquad (7.5.17)$$

where $S_0(\omega_1,\omega_2)$ is the output noise PSD and $S_i(\omega_1,\omega_2)$ is the PSD of a single noise source, which is equal to $q^2/12$.

The RPSD plots for the wave digital filter of example 7.3 and for a direct canonic realization which realizes the same transfer function, are shown in Fig. 7.7 and 7.8 respectively. In the case of the direct canonic realization, the plot tends to have the form of the filter response. The RPSD value is also much higher in the passband compared to that of the wave digital filter. The signal word length can be chosen to satisfy the signal-to-noise ratio

---

The notation used in the two figures is as follows. The RPSD values are in db.

A→70 to 80 D→50 to 55 7→35 to 40 4→20 to 25 1→5 to 10

B→60 to 70 9→45 to 50 6→30 to 35 3→15 to 20 0→0 to 5

C→55 to 60 8→40 to 45 5→25 to 30 2→10 to 15

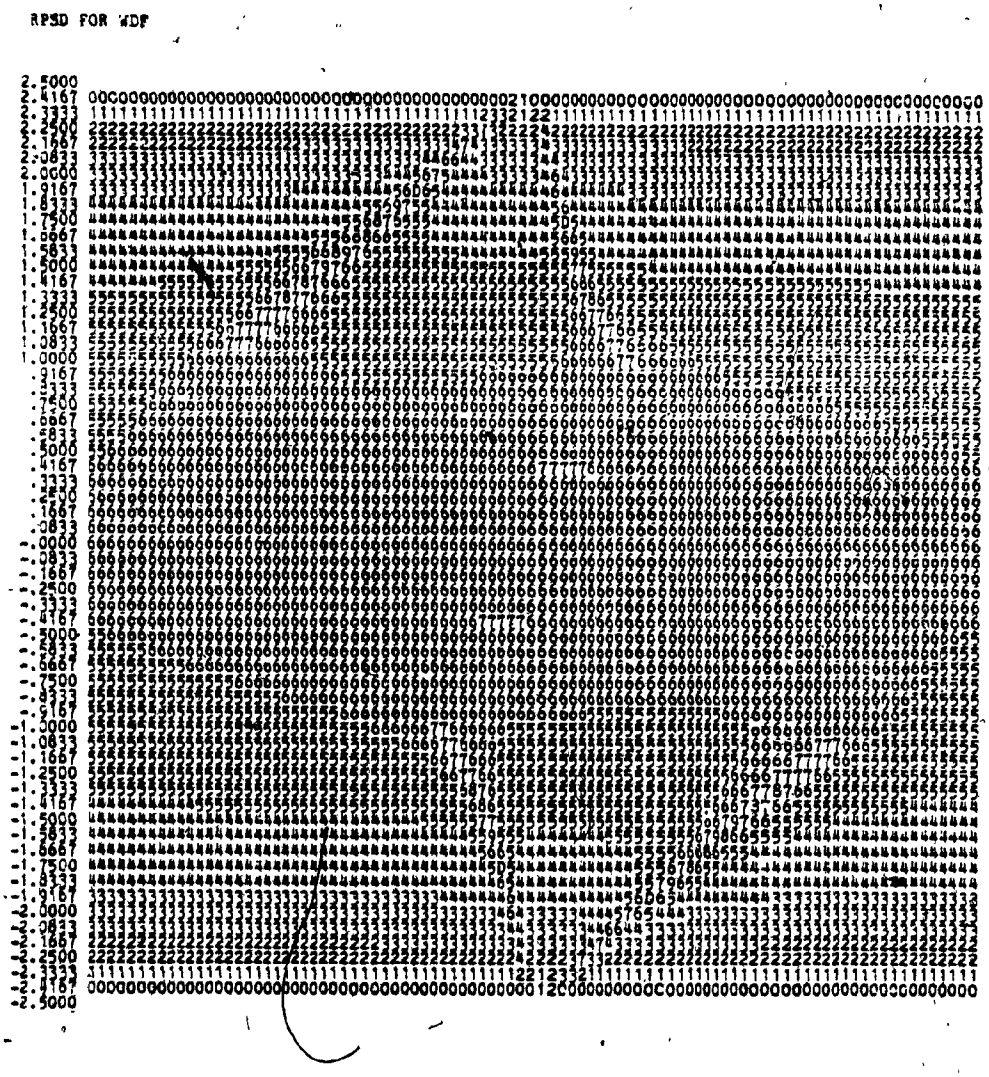

FIG. 7.7 RPSD PLOT FOR THE WAVE DIGITAL FILTER

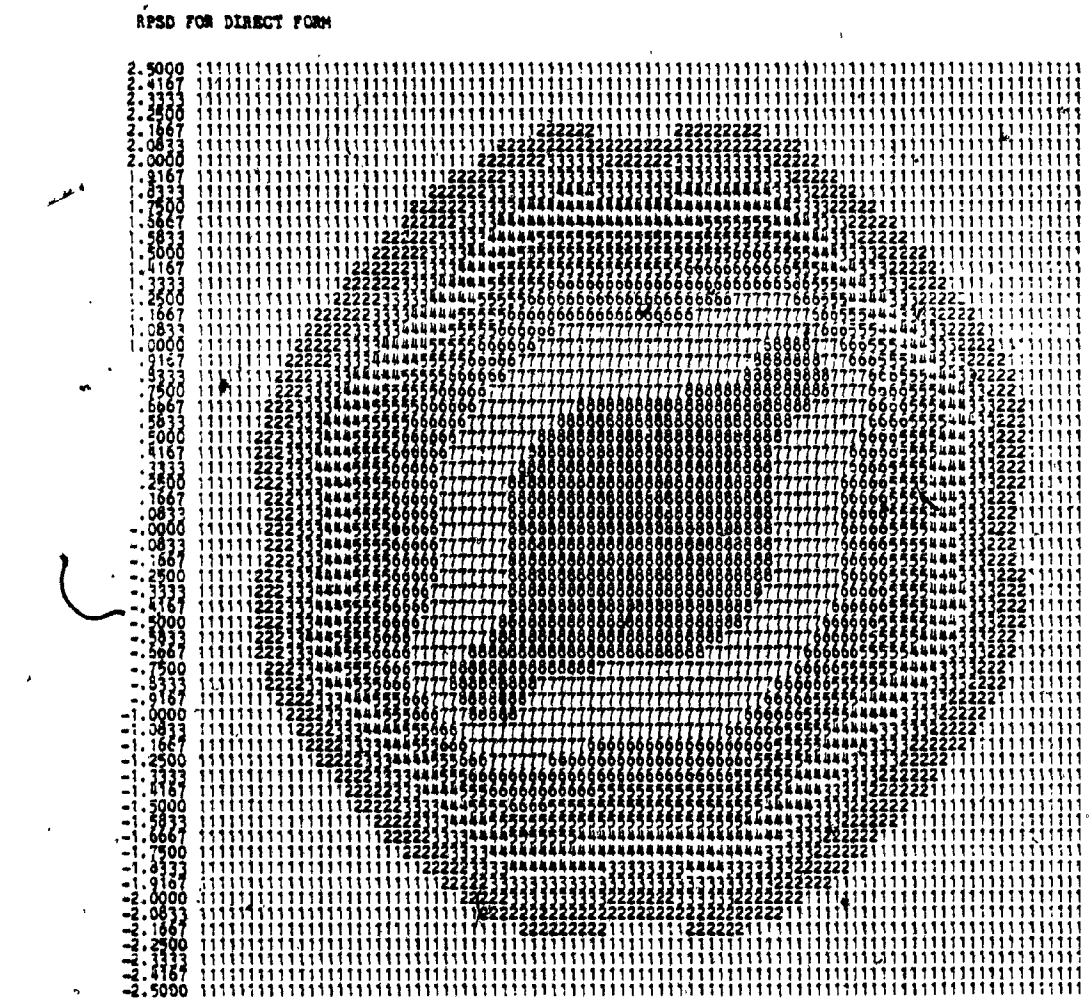

FIG. 7.8 RPSD PLOT FOR THE DIRECT CANONIC REALIZATION

requirements.

7.6 Coefficient Quantization

The coefficient quantization errors result in changes in the zeros and poles of the transfer function, thus altering the frequency response characteristics of the filter. The coefficient wordlength is chosen to satisfy the frequency response specifications [36].

Let $M_q(\omega_1,\omega_2)$ and $M(\omega_1,\omega_2)$ be the magnitude responses with and without quantization. Then quantization introduces an error

$$\Delta M = M(\omega_1,\omega_2) - M_q(\omega_1,\omega_2) \qquad (7.6.1)$$

If the maximum permissible error in the magnitude response is $\Delta M_{max}(\omega_1,\omega_2)$, the optimum wordlength can exactly be found by computing $|\Delta M|$ as a function of frequency for successively increasing values of wordlength until

$$|\Delta M| \leq \Delta M_{max}(\omega_1,\omega_2) \qquad (7.6.2)$$

An easier approach is based on a statistical method proposed by Avenhaus [93] and modified later by Crochiere [94]. In a fixed-point implementation with quantization carried out by rounding, the error in coefficient c_i $(i=1,2,\ldots,m)$ denoted by Δc_i, is a random variable varying between $-q/2$ to $+q/2$ where q is the quantization step. If Δc_i is assumed to have a uniform probability density,

$$p(\Delta c_i) = \begin{cases} 1/q \text{ for } -q/2 \leq \Delta c_i \leq q/2 \\ 0 \text{ otherwise} \end{cases} \qquad (7.6.3)$$

then from (7.5.3) and (7.5.4)

$$E\{\Delta c_i\} = 0 \qquad (7.6.4)$$

and

$$\sigma^2_{\Delta c_i} = q^2/12 \qquad (7.6.5)$$

The variation ΔM is also a random variable given by

$$\Delta M = \sum_{i=1}^{m} \Delta c_i \, S^M_{c_i} \qquad (7.6.6)$$

where $S^M_{c_i} = \partial M(\omega_1,\omega_2)/\partial c_i$ is the sensitivity of $M(\omega_1,\omega_2)$ with respect to variations in c_i. Hence

$$E\{\Delta M\} = \sum_{i=1}^{m} S^M_{c_i} \, E\{\Delta c_i\} = 0 \qquad (7.6.7)$$

If Δc_i and $\Delta c_j (i \neq j)$ are statistically independent, then it can be shown that

$$\sigma^2_{\Delta M} = \sum_{i=1}^{m} \sigma^2_{\Delta c_i} (S^M_{c_i})^2 = q^2 s^2_T/12 \qquad (7.6.8)$$

where $S^2_T = \sum_{i=1}^{m} (S^M_{c_i})^2$

We do not discuss the case where Δc_i and Δc_j $(i \neq j)$ are not statistically independent. For such a case procedures

indicated in [95], have to be adopted. For lage m, ΔM is approximately Gaussian with a zero mean and hence

$$p(\Delta M) = \frac{1}{\sigma_{\Delta M}\sqrt{2\pi}} e^{-\Delta M^2/2\sigma^2_{\Delta M}}, \quad -\infty \leq \Delta M \leq \infty \qquad (7.6.9)$$

ΔM will be in some range $-\Delta M_1 \leq \Delta M \leq \Delta M_1$ with a probability

$$y = \frac{2}{\sigma_{\Delta M}\sqrt{2\pi}} \int_0^{\Delta M_1} e^{-\Delta M^2/2\sigma^2_{\Delta M}} d(\Delta M) \qquad (7.6.10)$$

By using the variable transformations

$$\Delta M = x\sigma_{\Delta M}, \quad \Delta M_1 = x_1 \sigma_{\Delta M} \qquad (7.6.11)$$

equation (7.6.10) becomes

$$y = \frac{2}{\sqrt{2\pi}} \int_0^{x_1} e^{-x^2/2} dx \qquad (7.6.12)$$

For an acceptable confidence factor y, the corresponding x_1 can be obtained. Since ΔM_1 is a statistical bound on ΔM, if we choose the coefficient word length such that

$$\Delta M_1 \leq \Delta M_{max}(\omega_1, \omega_2) \qquad (7.6.13)$$

the desired specifications would be satisfied within a confidence factor y. The resulting wordlength is referred to as the statistical wordlength. From (7.6.8), (7.6.11) and (7.6.13), the statistical bound on q is obtained as

$$q \leq \frac{\sqrt{12}\ \Delta M_{max}\ (\omega_1, \omega_2)}{x_1 S_T} \qquad (7.6.14)$$

To accomodate the quantized value of the largest coefficient in the register, if

$$Q[\max c_i] = \sum_{i=-K}^{J} b_i\, 2^i \qquad (7.6.15)$$

where b_J and $b_{-K} \neq 0$, the register wordlength must be

$$L = 1 + J + K \qquad (7.6.16)$$

Since $q = 2^{-K}$, the statistical bound on the wordlength is given by

$$L \geq 1 + J + \log_2 \frac{x_1 S_T}{\sqrt{12}\ \Delta M_{max}(\omega_1, \omega_2)} \qquad (7.6.17)$$

By assuming $x_1 = 2$, we have a confidence factor of 0.95 which gives a reasonable agreement between the statistical and exact wordlengths [37], [95].

The sensitivities $S_{c_i}^M$ can be computed by using the transpose or adjoint approach. For the digital network in Fig. 7.10 if $H(z_1, z_2)$ is the transfer function between the input and output, then the sensitivity of $H(z_1, z_2)$ w.r.t. variation in c_i is given by

$$S_{c_i}^H (z_1, z_2) = \frac{\partial H(z_1, z_2)}{\partial c_i} = H_{13}(z_1, z_2) H_{42}(z_1, z_2) \qquad (7.6.18)$$

where $H_{13}(z_1,z_2)$ is the transfer function between nodes 1 and 3 and $H_{42}(z_1,z_2)$ is the transfer function between nodes 2 and 4 as shown in Fig. 7.9.

$$S_{c_i}^{H}(e^{j\omega_1 T_1},e^{j\omega_2 T_2}) = \partial H(e^{j\omega_1 T_1},e^{j\omega_2 T_2})/\partial c_i$$

$$= Re[S_{c_i}^{H}(e^{j\omega_1 T_1},e^{j\omega_2 T_2})]+jIm[S_{c_i}^{H}(e^{j\omega_1 T_1},e^{j\omega_2 T_2})] \tag{7.6.19}$$

If

$$H(e^{j\omega_1 T_1},e^{j\omega_2 T_2}) = M(\omega_1,\omega_2)e^{j\theta(\omega_1,\omega_2)} \tag{7.6.20}$$

we have

$$\frac{\partial H(e^{j\omega_1 T_1},e^{j\omega_2 T_2})}{\partial c_i} = e^{j\theta(\omega_1,\omega_2)}\frac{\partial M(\omega_1,\omega_2)}{\partial c_i}$$

$$+jM(\omega_1,\omega_2)\,e^{j\theta(\omega_1,\omega_2)}\frac{\partial\theta(\omega_1,\omega_2)}{\partial c_i} \tag{7.6.21}$$

From (7.6.19) and (7.6.21), we find that

$$Re[S_{c_i}^{H}(e^{j\omega_1 T_1},e^{j\omega_2 T_2})] = \cos[\theta(\omega_1,\omega_2)]\frac{\partial M(\omega_1,\omega_2)}{\partial c_i}$$

$$-\sin[\theta(\omega_1,\omega_2)]M(\omega_1,\omega_2)\frac{\partial\theta(\omega_1,\omega_2)}{\partial c_i} \tag{7.6.22}$$

$$Im[S_{c_i}^{H}(e^{j\omega_1 T_1},e^{j\omega_2 T_2})] = \sin[\theta(\omega_1,\omega_2)]\frac{\partial M(\omega_1,\omega_2)}{\partial c_i}$$

$$+M(\omega_1,\omega_2)\cos[\theta(\omega_1,\omega_2)]\frac{\partial\theta(\omega_1,\omega_2)}{\partial c_i} \tag{7.6.23}$$

and hence

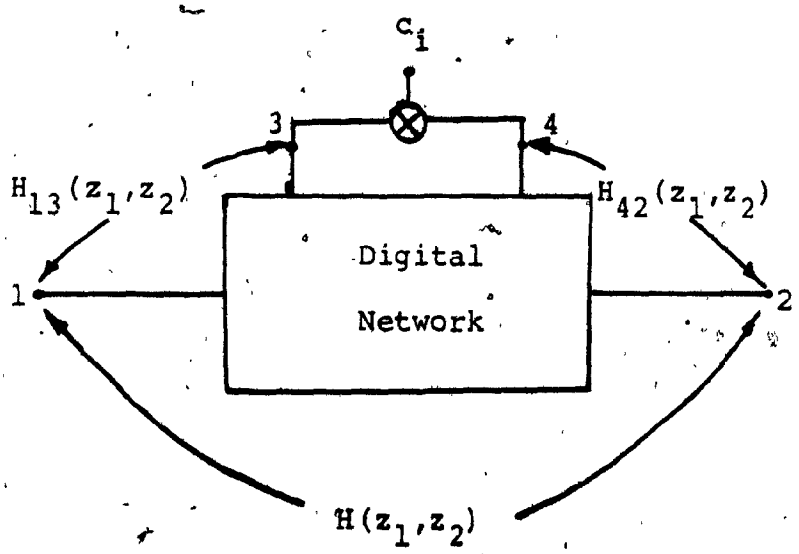

$$S^{H}_{c_i}(z_1,z_2) = \frac{\partial H(z_1,z_2)}{\partial c_i} = H_{13}(z_1,z_2)\ H_{42}(z_1,z_2)$$

FIG. 7.9 DIGITAL NETWORK FOR COMPUTATION OF SENSITIVITIES

$$S_{c_i}^{M} = \partial M(\omega_1,\omega_2)/\partial c_i$$

$$= \cos[\theta(\omega_1,\omega_2)]\mathrm{Re}[S_{c_i}^{H}(e^{j\omega_1 T_1}, e^{j\omega_2 T_2})]$$

$$+ \sin[\theta(\omega_1,\omega_2)]\mathrm{Im}[S_{c_i}^{H}(e^{j\omega_1 T_1}, e^{j\omega_2 T_2}) \qquad (7.6.24)$$

and

$$S_{c_i}^{\theta} = \partial\theta(\omega_1,\omega_2)/\partial c_i$$

$$=\{\cos[\theta(\omega_1,\omega_2)]\mathrm{Im}[S_{c_i}^{H}(e^{j\omega_1 T_1}, e^{j\omega_2 T_2})]$$

$$- \sin[\theta(\omega_1,\omega_2)]\mathrm{Re}[S_{c_i}^{H}(e^{j\omega_1 T_1}, e^{j\omega_2 T_2})]\}/M(\omega_1,\omega_2)$$

(7.6.25)

$S_{c_i}^{M}$ and $S_{c_i}^{\theta}$ are the sensitivities of the magnitude and phase responses w.r.t. variations in c_i.

In doing the analysis for coefficient wordlength for the digital filter in example 7.3, a direct method is first used, followed by the statistical method. In the direct method, the wordlength is assumed to take values in the range of 4 to 20 bits. The frequency response is computed for the quantized filter and the value of $|\Delta M|$ is computed over the passband as given by (7.6.1). The maximum value of $|\Delta M|$, the average value of $|\Delta M|$ and its standard deviation in the passband are computed for different wordlengths. The results for the direct canonic and the wave digital filter realizations are plotted in Figs. 7.10-7.12.

The statistical wordlength is computed as a function of frequency for the direct canonic and the wave digital filter realizations. In equation (7.6.17), x_1 is assumed

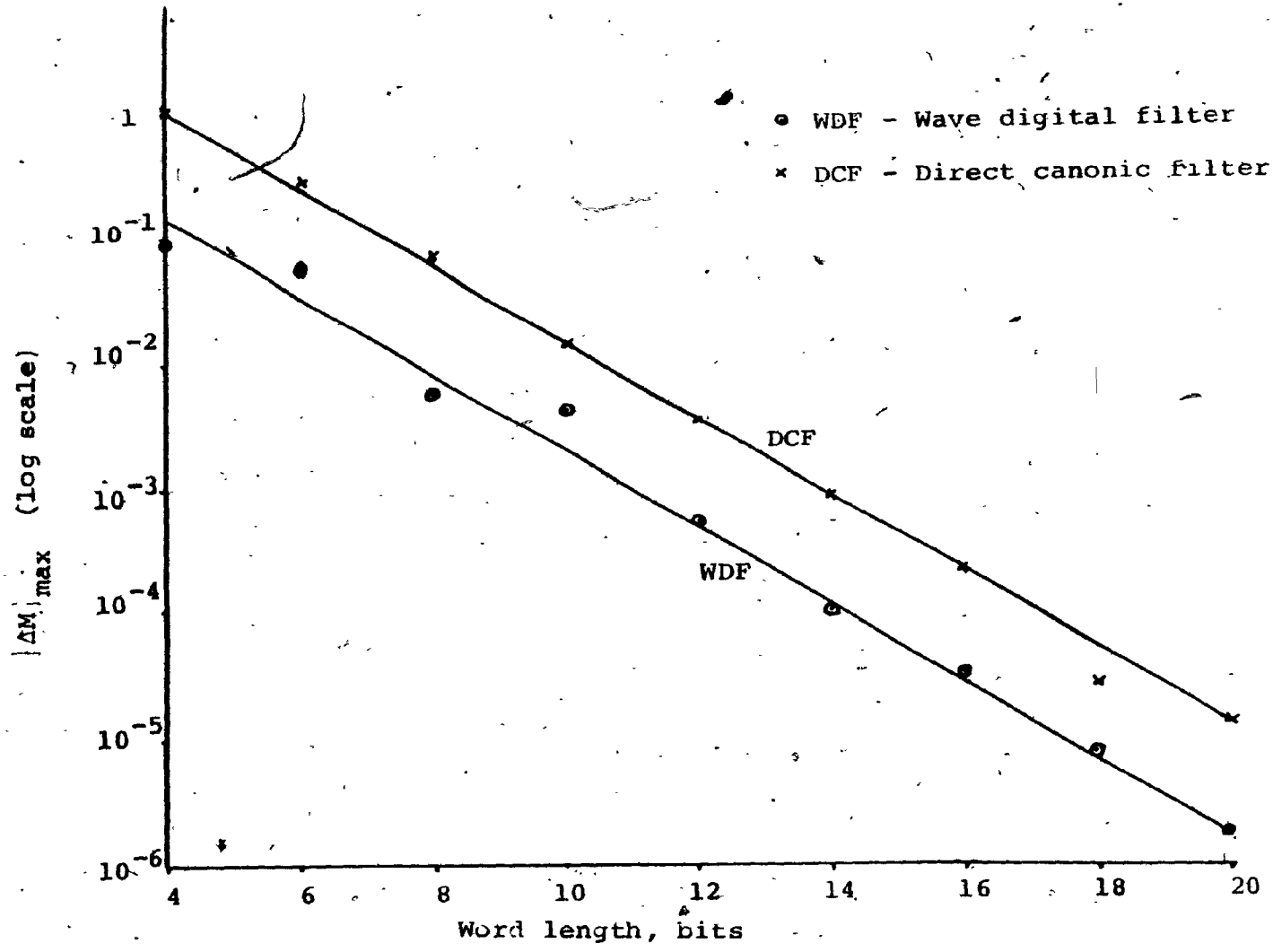

FIG. 7.10 PLOT OF $|\Delta M|_{max}$ VS. WORD LENGTH

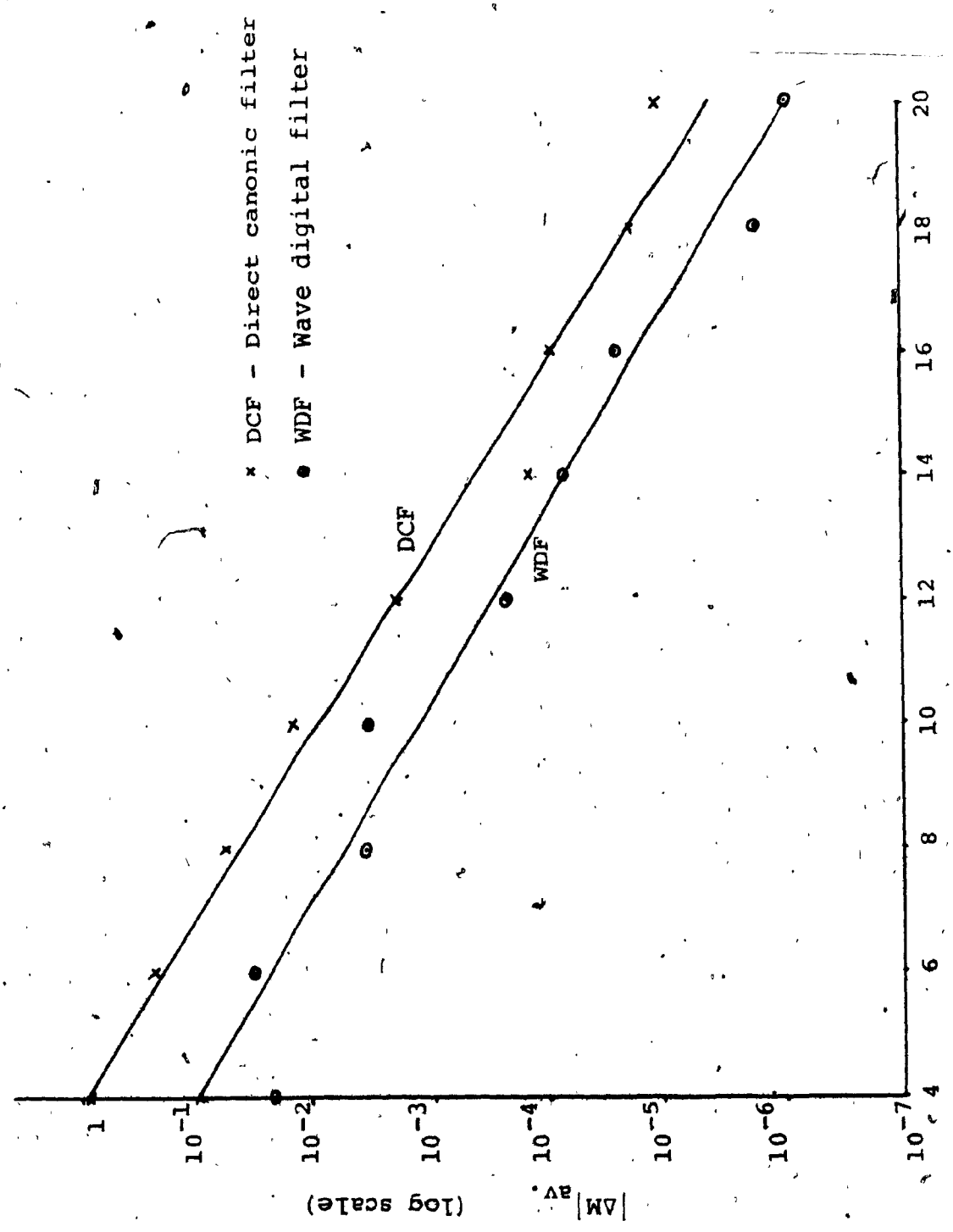

FIG. 7.11 PLOT OF $|\Delta M|_{av.}$ VS WORDLENGTH

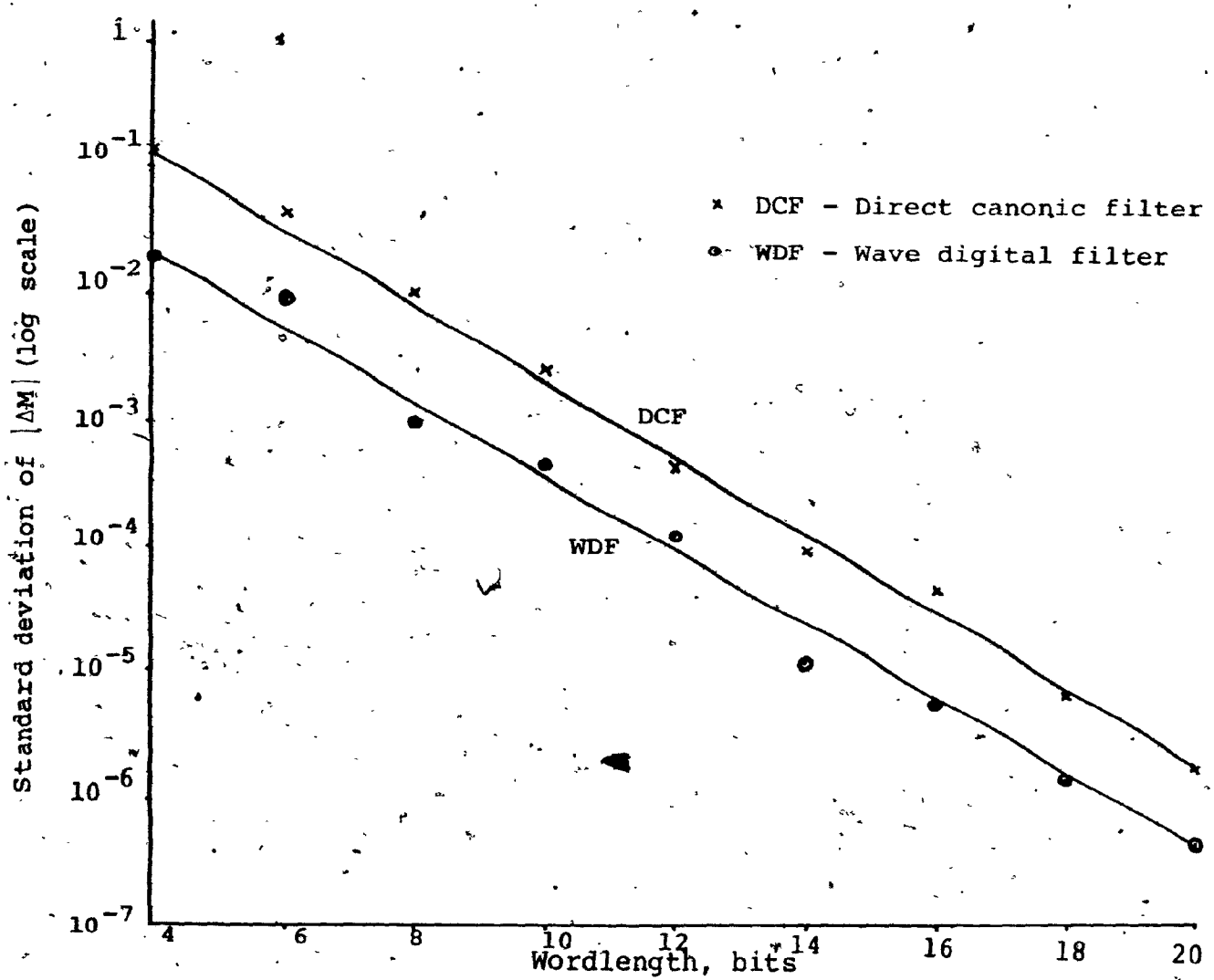

FIG. 7.12 PLOT OF THE STANDARD DEVIATION OF |ΔM| VS. WORDLENGTH

as 2 and $\Delta M_{max}(\omega_1,\omega_2)$ is assumed as 0.02. The results are plotted in Figs. 7.13 and 7.14.* The plots show that the wave digital filter has better coefficient sensitivity properties as compared to the direct canonic form as far as the magnitude response is concerned. A similar study can also be carried out for the phase response sensitivity $S^{\theta}_{c_i}$ to obtain a suitable wordlength. It is seen that there is a good agreement between the results obtained by the direct method and the statistical method.

7.7 Summary and Conclusions

We have studied alternate methods for the realization of the 2-D transfer functions obtained earlier. Since the transfer functions are not decomposable into parallel or cascade second order sections, we study only the direct canonic realization and the wave digital filter realization. Different forms of the wave digital filter realization are possible by the use of linear transformations.

With the object of implementing these filters using fixed point arithmetic with quantization by rounding, a suitable scaling technique is used to avoid overflows and at the same time to use the entire dynamic range of the registers. The method used for scaling is an extension

* The numbers in the two figures directly represent the required wordlength in bits with A and B denoting 10 and 11 bits respectively.

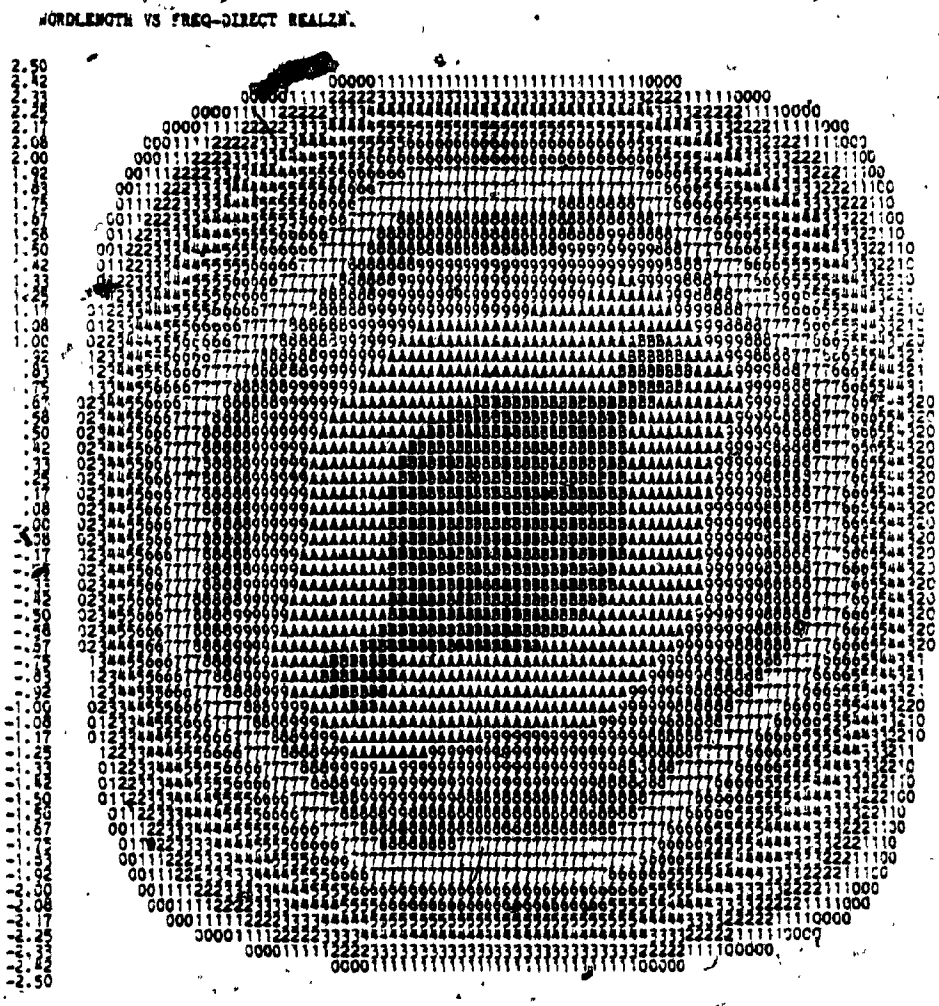

FIG. 7.13 WORDLENGTH $L(\omega_1,\omega_2)$ VS. FREQUENCY PLOT FOR THE DIRECT CANONIC FORM

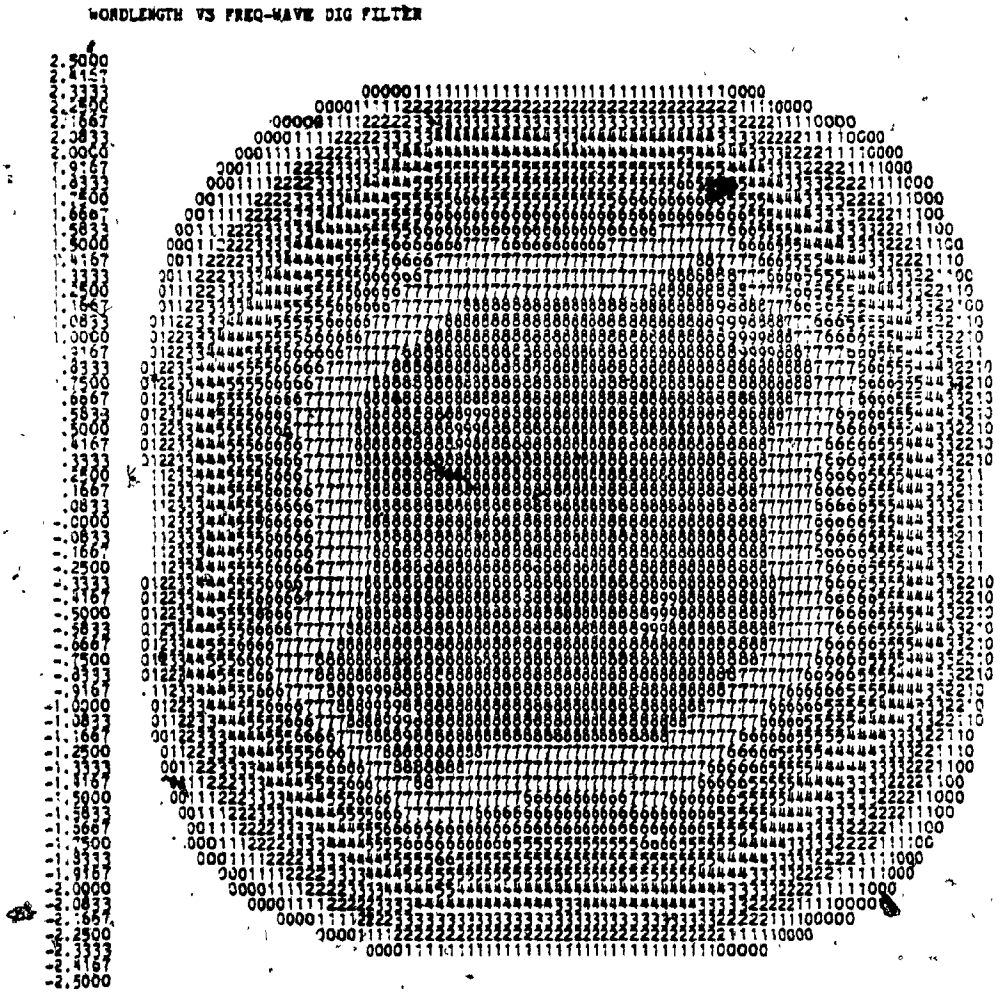

FIG. 7.14 WORDLENGTH $L(\omega_1,\omega_2)$ VS. FREQUENCY PLOT FOR THE WAVE DIGITAL FILTER

of a method available for 1-D filters.

The standard techniques available for the study of product quantization and coefficient quantization errors in the case of 1-D digital filters are extended to the case of 2-D filters. Product quantization errors are studied by introducing noise sources at the multiplier outputs and finding the RPSD at the filter output. This gives a picture of the output noise spectrum due to product quantization. The RPSD plots for the direct canonic and the wave digital filter realizations show very clearly that the S/N ratio is much better for the wave digital filter.

In studying the effects of coefficient quantization, a direct method and a statistical method are used to find the maximum deviation in the magnitude response due to coefficient quantization. The results obtained by both the methods are seen to be in good agreement in finding the necessary coefficient wordlength. It is seen that the wave digital filter needs a much smaller wordlength compared to the direct canonic filter.

CHAPTER 8.

SUMMARY AND CONCLUSIONS

8.1 Conclusion

In this thesis an attempt has been made to study a class of 2-D functions which are realizable as multivariable ladder networks in the analog domain and as wave digital filters in the digital domain. Because of the problems in the stability testing of 2-D digital filters and the non-availability of a method of factorization leading to cascade or parallel realizations, it is seen that the wave digital realization is a very useful alternative in the design of stable 2-D transfer functions.

In Chapter 2, a new multivariable array A is formulated which comprises of homogeneous polynomials. Using this array, conditions for the ladder realization of an MPRF are obtained. The realization obtained here is different from existing ones since the elements in each arm of the ladder can be in any variable and elements in some of the variables can be missing. Thus the synthesis described here is for a more general class of functions compared to the existing ladder realizations. It is shown that multivariable reactance transformations can be used to obtain other forms of the ladder network. The synthesis of an all-pole multivariable tranfer function in the above form is possible only when the denominator MHP satisfies the conditions of the multivariable array B, which lead to the

continued fraction expansion of a multivariable reactance function. For the cascade separable two-variable ladder network which is a particular case of the above, conditions for the synthesis of different combinations of the p_1 and p_2 networks are derived such as the LP,HP,BP and BS ladders. This helps in the identification and synthesis of a class of functions which are realizable as above and also in the generation of such functions.

The properties of a doubly-terminated multivariable ladder network are studied in Chapter 3 and the difficulty in obtaining a general synthesis procedure for such a network is explained. In the absence of such a general procedure, it is of use to find methods for generation of such functions. Two such methods are described for the doubly-terminated cascade separable network transfer function. These methods are useful for the approximation of two-variable transfer functions.

In Chapter 4, polynomials are formulated in the digital domain which correspond to the even and odd polynomials in the analog and these are used for finding the conditions for cascade separability of 2-D digital transfer functions. When these conditions are satisfied, the corresponding two-variable analog transfer function is realizable as a cascade separable network. This helps in studying the properties of this class of functions directly in the digital domain. This is also helpful in the direct generation of digital

transfer functions of the type whose analog counterpart is realizable as a doubly-terminated cascade separable network. It is shown that these transfer functions may give rise to non-essential singularities of the second kind which can be easily identified.

No direct analytical method is available at present for the approximation of two-variable cascade separable network transfer functions. It is shown in Chapter 5 that a good approximation for quadrantal symmetry in the magnitude response is possible even though the transfer function of the doubly-terminated cascade separable network is not variable separable. Two types of two-variable approximations are described, which lead to extensions of 1-D methods used for MFM, ERM and maximally flat time delay responses. In the Type 1 approximation, the response along the ω_1 and ω_2 axes is approximated. In the Type 2 case, a technique for making the two-variable transfer function nearly variable separable is employed. The double bilinear transformation is used for transforming the above two-variable functions into the digital domain, with suitable prewarping. However, since the double bilinear transformation distorts the phase response of the analog function, it cannot be directly used for the maximally flat time delay approximation.

A new method is developed in Chapter 6 for the approximation of single variable analog and digital transfer functions having non-equiripple magnitude response in the passband with a specified ripple value and a monotonic variation

in the stopband. The maxima and minima of the magnitude response in the passband occur at specified critical frequencies. Using these critical frequencies as optimization parameters, a numerical method for minimizing the least square phase error in the passband is described for both the analog as well as the digital lowpass transfer functions. The above method is easily extended to HP, BP or BS transfer functions with suitable modifications.

Alternate methods for the wave digital filter realization are described in Chapter 7. The methods described here are extensions of those available in 1-D. Since it is usual to implement digital filters using the fixed point arithmetic for finite wordlength, the effect of quantization by rounding is studied for the case of the product quantization and the coefficient quantization errors. The methods developed here are direct extensions of efficient methods available in 1-D for such an analysis. In the study of product quantization effects, the RPSD plots for the direct canonic and the wave digital filters show a much better S/N ratio all over the passband for the wave digital filter as compared to the direct canonic realization. Similarly in the case of coefficient quantization studies, the wave digital filter is shown to require a much smaller wordlength compared to the direct canonic form. These analysis techniques can be employed for any type of 2-D filter realizations and hence are very useful. Since we are interested in a fixed point implementation where the signal overflows have to be

avoided at different nodes and at the same time the dynamic range of the registers have to be efficiently utilized, a good scaling technique is to be used in the implementation. The method described here is an extension of a method available for scaling 1-D wave digital filters.

In the absence of a factorization procedure for multivariable polynomials the wave digital filter realization appears to be a good alternative to conventional cascade or parallel realizations and using the approximations developed here, realizations are possible which have good sensitivity and noise properties. The methods described here are simple extensions from 1-D to 2-D and and from analog to digital and hence the well known single-variable techniques in the analog can be easily extended to the design of stable causal 2-D digital filters.

8.2 Scope for futher work

Because of the advantages of the wave digital filter realization pointed out earlier, it is useful to study the properties of two-variable networks involving different types of structures such as the lattice, parallel and cascade combinations etc. This can lead to synthesis of additional classes of 2-D transfer functions.

In the area of approximation, different methods can be tried, for example, by choosing the frequency response along different axes instead of the ω_1 and ω_2 axes used

here. It would be useful to find out analytical approximations for other classes of transfer functions realizable with different network structures. Since consideration of the phase response is important, an allpass approximation for phase equalization would be useful. In place of the double bilinear transformation, methods such as the invariant impulse response method can be used to overcome the problem of phase distortion.

The alternate realizations discussed in Chapter 7 can be analyzed for their performance regarding quantization effects. Problems such as limit cycle and overflow oscillations should be studied for 2-D filters in order to establish bounds for such oscillations.

In this thesis only 1IR 2-D filters are considered. It is worthwhile to compare these results with the maximally flat 2-D nonrecursive filters obtained in [97].

APPENDIX

WAVE DIGITAL FILTER REALIZATIONS IN SINGLE VARIABLE

A.1 Wave digital filters: One-port representation

In the Fettweis representation, a one-port impedance is described by its reflection coefficient as

$$B = A \frac{Z(s)-R}{Z(s)+R} \qquad \text{(A.1.1)}$$

where R is an arbitrary resistance assigned to the port and $A = V+IR$ and $B=V-IR$ are the incident and reflected waves as indicated in Fig. A.1a [96]. By treating each of the impedances of the ladder network as an one-port, we can transform each impedance into a digital one-port as shown in Fig. A.1b [36]. The digital one-ports are interconnected using series and parallel "adaptors" as shown in Figs. A.2 and A.3.

A.2 Wave digital filter: two-port representation

The ladder elements can also be represented as two-ports as shown in Fig. A.4, characterized by the equations

$$\begin{bmatrix} A_i \\ B_i \end{bmatrix} = \begin{bmatrix} 1 & R_i \\ 1 & -R_i \end{bmatrix} \begin{bmatrix} V_i \\ I_i \end{bmatrix} \text{ for } i=1,2 \qquad \text{(A.2.1)}$$

In addition, for the two-port,

$$\begin{bmatrix} V_1 \\ I_1 \end{bmatrix} = \begin{bmatrix} A & B \\ C & D \end{bmatrix} \begin{bmatrix} V_2 \\ -I_2 \end{bmatrix} \qquad \text{(A.2.2)}$$

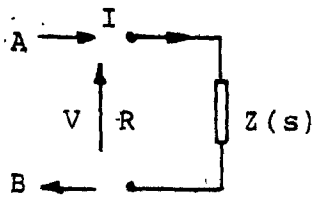

$$A = V + IR$$

$$B = V - IR$$

(a) One-port representation of an impedance

Element	R	Realization	Representation
R	R	A	A
C	$\frac{T}{2C}$	A, T, B	A, C, B
L	$\frac{2L}{T}$	A, -1, T, B	A, L, B
V_i R	R	V_i B	V_i B
V_i C	$\frac{T}{2C}$	V_i, -1, T, A, B	V_i, C, A, B
V_i L	$\frac{2L}{T}$	V_i, -1, T, A, B	V_i, L, A, B

(b) Wave digital realization

FIG. A-1 WAVE DIGITAL REALIZATION OF ONE-PORT IMPEDANCES AND VOLTAGE SOURCES

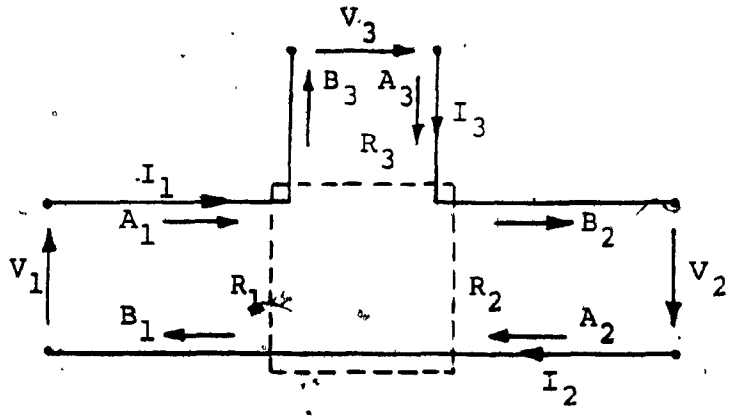

(a) Series Interconnection

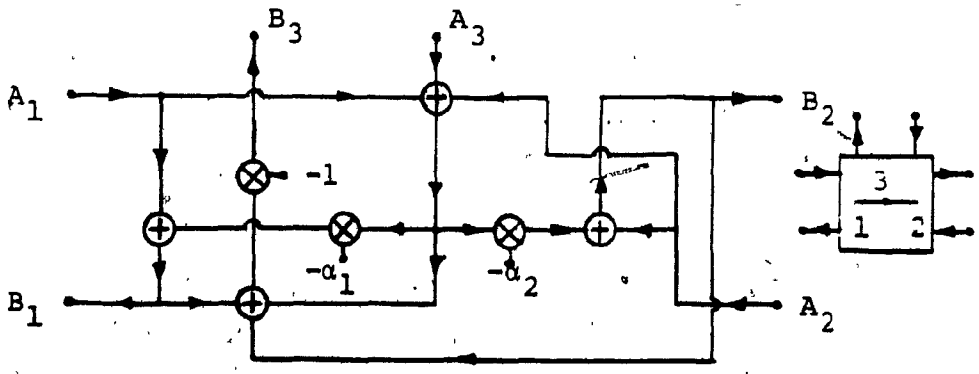

(b) S2 adaptor

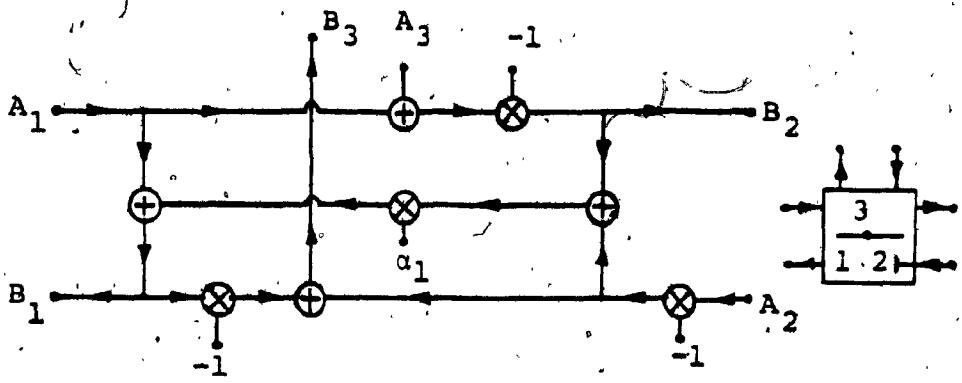

(c) S1 adaptor (with $R_2 = R_1 + R_3$)

FIG. A-2 SERIES ADAPTOR REALIZATION

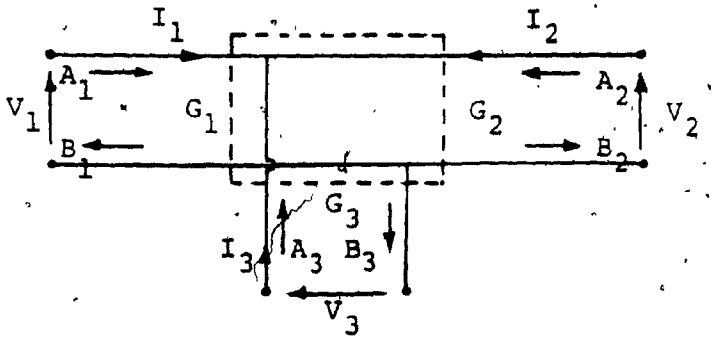

(a) Parallel Interconnection

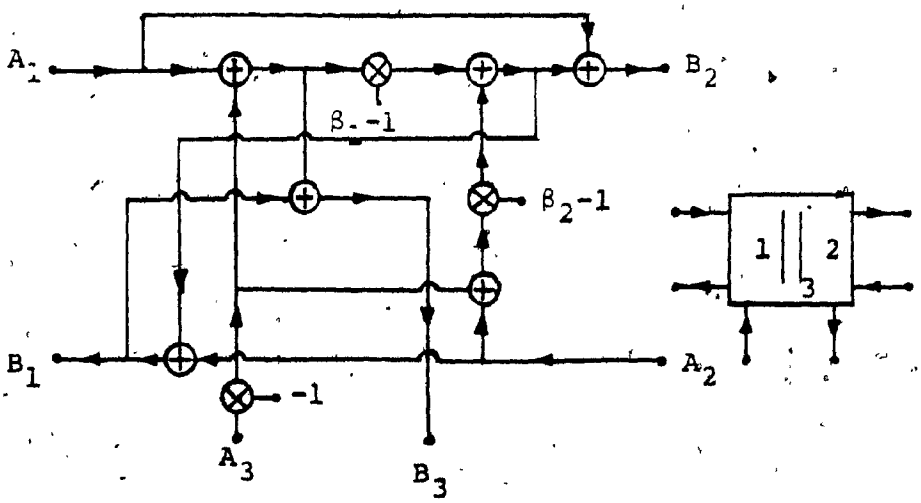

(b) R2 adaptor

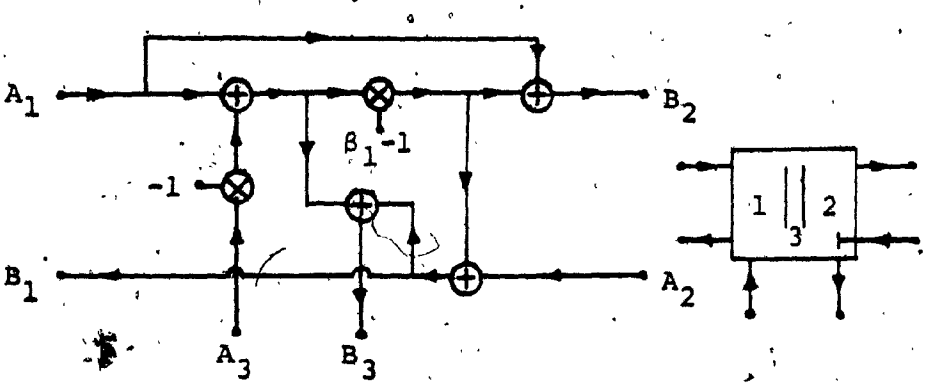

(c) P1 adaptor (with $G_2 = G_1 + G_3$)

FIG. A-3 PARALLEL ADAPTOR REALIZATION

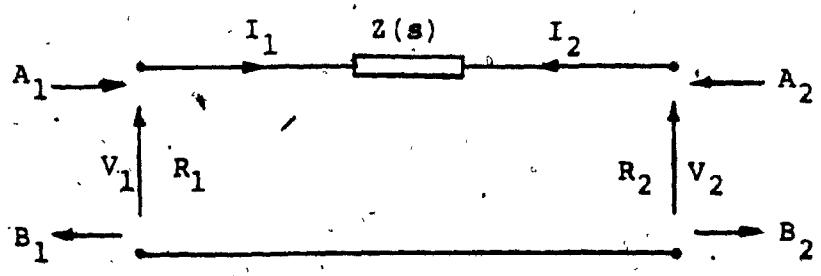

(a) Series element representation

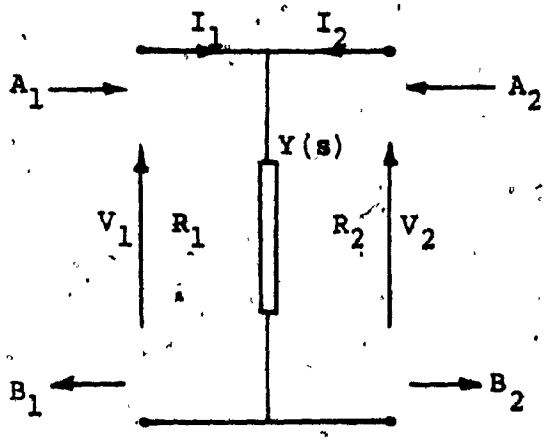

(b) Shunt element representation

FIG. A-4 TWO-PORT REPRESENTATION OF LADDER ELEMENTS

Using the two-port scattering matrix form based on voltage waves

$$\begin{bmatrix} B_1 \\ B_2 \end{bmatrix} = \begin{bmatrix} S_{11} & S_{12} \\ S_{21} & S_{22} \end{bmatrix} \begin{bmatrix} A_1 \\ A_2 \end{bmatrix} \qquad (A.2.3)$$

where the scattering parameters S_{11}, S_{12}, S_{21} and S_{22} can be obtained for any series impedance $Z(s)$ or shunt admittance $y(s)$. If the two-ports are interconnected, then at the interconnection, the reflected wave at one-port must equal the incident wave at the other port. Certain extra conditions have to be satisfied to avoid delay-free loops [96].

Through linear transformation of variables, the above two-port approach can be used for generalizations which give rise to many choices for the realization [96]. Defining a new set of variables for the two-port as

$$\begin{bmatrix} X_1 \\ Y_1 \end{bmatrix} = P \begin{bmatrix} V_1 \\ I_1 \end{bmatrix} \quad \text{and} \quad \begin{bmatrix} X_2 \\ Y_2 \end{bmatrix} = Q \begin{bmatrix} V_2 \\ I_2 \end{bmatrix} \qquad (A.2.4)$$

we have

$$\begin{bmatrix} X_1 \\ Y_1 \end{bmatrix} = PTQ^{-1} \begin{bmatrix} X_2 \\ Y_2 \end{bmatrix} \qquad (A.2.5)$$

where

$$T = \begin{bmatrix} A & B \\ C & D \end{bmatrix}.$$

A.2.1 Invariant voltage ratio [IVR] method:

In this method, we have

$$P = \begin{bmatrix} 1 & 0 \\ 1 & -R_1 \end{bmatrix} \quad \text{and} \quad Q = \begin{bmatrix} 1 & R_2 \\ 1 & 0 \end{bmatrix} \qquad \text{(A.2.1.1)}$$

This gives $X_1=V_1$ and $Y_2=V_2$. With X_i as the stimuli and Y_i as the responses, the transfer function obtained is the same as the voltage transfer ratio of the original analog network. The responses Y_i are expressed in terms of the stimuli X_i as

$$\begin{bmatrix} Y_1 \\ Y_2 \end{bmatrix} = \begin{bmatrix} \sigma_{11} & \sigma_{12} \\ \sigma_{21} & \sigma_{22} \end{bmatrix} \cdot \begin{bmatrix} X_1 \\ X_2 \end{bmatrix} \qquad \text{(A.2.1.2)}$$

The two-port wave digital realization for series and shunt arm inductances are shown in Fig. A.5. To derive the structures for the other elements of the ladder, the Constantinides frequency transformations as given in Table A.1 are used.

The digital equivalents of the two-port source and load elements are obtained as follows. For a source V_0 with a series resistance R_s,

$$V_0 = [1 \; R_s] \begin{bmatrix} V \\ I \end{bmatrix} \qquad \text{(A.2.1.3)}$$

and since

$$\begin{bmatrix} X \\ Y \end{bmatrix} = \begin{bmatrix} 1 & 0 \\ 1 & -R \end{bmatrix} \begin{bmatrix} V \\ I \end{bmatrix} \qquad \text{(A.2.1.4)}$$

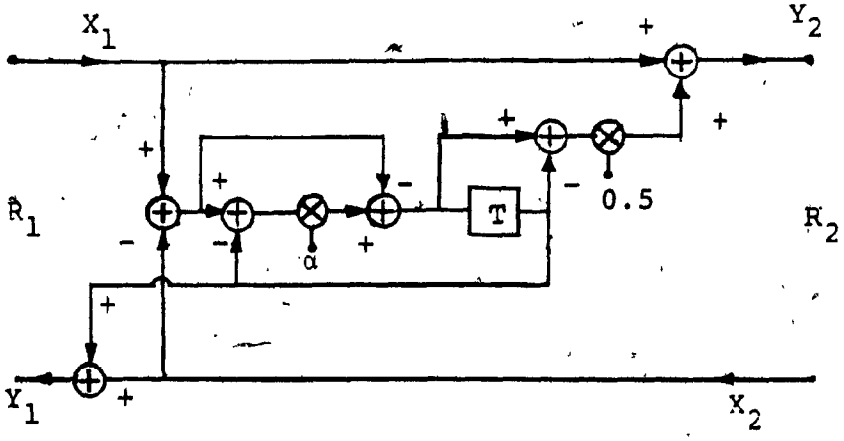

(a) Equivalent of series arm inductance

$$\alpha = \frac{R_2 - L}{R_2 + L}, \quad R_1 = R_2 + L$$

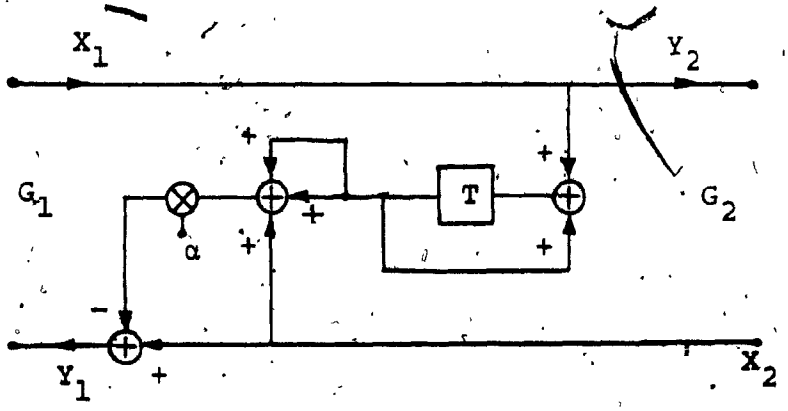

(b) Equivalent of shunt arm inductance

$$\alpha = \frac{1}{G_1 L}, \quad G_1 = G_2 + \frac{1}{L}$$

FIG. A-5 WAVE DIGITAL STRUCTURE FOR SERIES AND SHUNT ARM INDUCTANCES BY THE IVR METHOD

TABLE A-1 DIGITAL FREQUENCY TRANSFORMATIONS

ELEMENT	L (GIVEN) $\longrightarrow z^{-1}$	
	REPLACE L BY	REPLACE z^{-1} BY
C	$\frac{1}{C}$	$-z^{-1}$
L_s in series with C_s	$L_s + \frac{1}{C_s}$	$-z^{-1}\left(\frac{z^{-1}+\beta}{1+\beta z^{-1}}\right)$ where $\beta = \frac{(1-L_sC_s)}{(1+L_sC_s)}$
L_p in parallel with C_p	$\frac{1}{C_p + \frac{1}{L_p}}$	$z^{-1}\left(\frac{z^{-1}+\beta}{1+\beta z^{-1}}\right)$ where $\beta = \frac{(1-L_pC_p)}{(1+L_pC_p)}$

we get

$$X = \alpha y + (1-\alpha)\, V_0 \qquad \text{(A.2.1.5)}$$

where $\alpha = R_s/(R+R_s)$

For the resistive load we have

$$V = R_L I \qquad \text{(A.2.1.6)}$$

and this gives

$$Y = \beta X \qquad \text{(A.2.1.7)}$$

where $\beta = (R_L-R)/R_L$

The structures are shown in Fig. A.7.

A.2.2 Modified transfer admittance (MTA) method

Here the transformations used are

$$P = \begin{bmatrix} 0 & 1 \\ G_1 & -1 \end{bmatrix} \quad \text{and} \quad Q = \begin{bmatrix} G_2 & 1 \\ 0 & -1 \end{bmatrix} \qquad \text{(A.2.2.1)}$$

The realizations are shown in Fig. A.6.

Since for the MTA case, for the source V_0 and series resistance R_s,

$$\begin{bmatrix} X \\ Y \end{bmatrix} = \begin{bmatrix} 0 & 1 \\ G & -1 \end{bmatrix} \begin{bmatrix} V \\ I \end{bmatrix} \qquad \text{(A.2.2.2)}$$

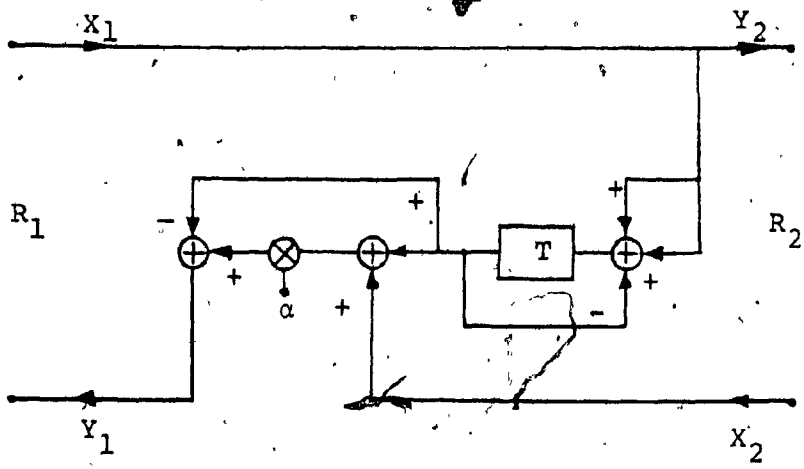

(a) Equivalent of series arm inductance

$$\alpha = \frac{R_2}{R_1}, \quad R_1 = R_2 + L$$

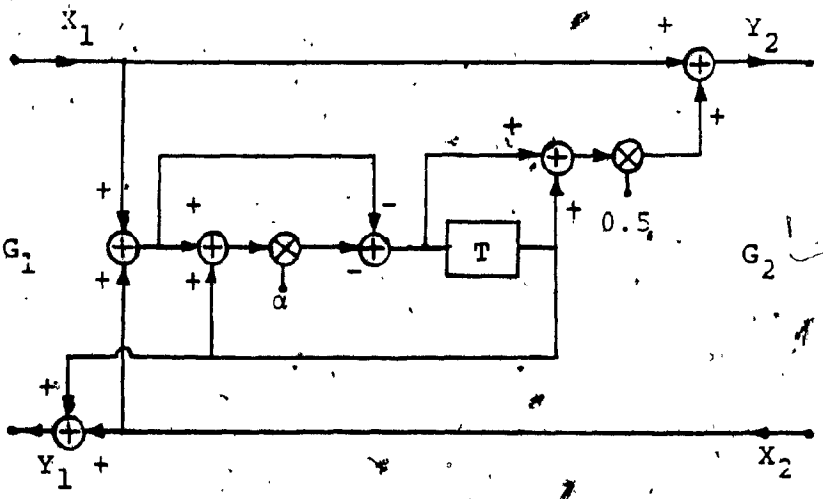

(b) Equivalent of shunt arm inductance

$$\alpha = \frac{1 - LG_2}{1 + LG_2}, \quad (G_1 - G_2)L = 1$$

FIG. A-6 WAVE DIGITAL STRUCTURE FOR SERIES AND SHUNT ARM INDUCTANCES BY THE MTA METHOD

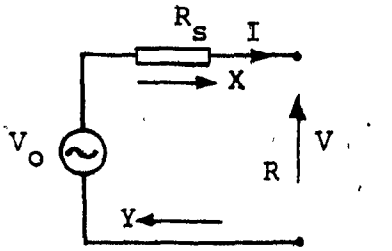

(a) Resistive voltage source

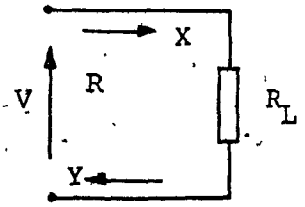

(d) Resistive load

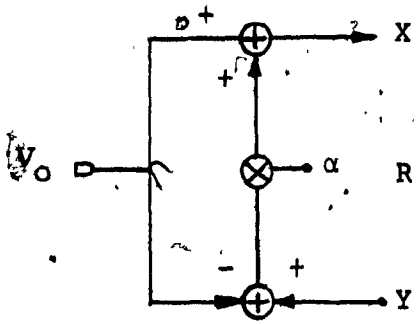

(b) IVR formulation

$$\alpha = \frac{R_s}{R + R_s}$$

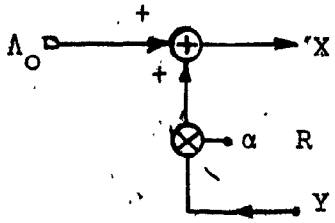

(c) MTA formulation

$$\alpha = \frac{R}{R + R_s}$$

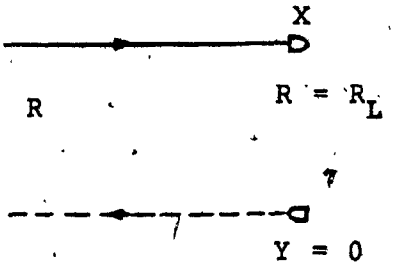

(e) Digital equivalent in the IVR and MTA cases for $R = R_L$

FIG. A-7 DIGITAL EQUIVALENT STRUCTURES FOR THE RESISTIVE SOURCE AND LOAD USING THE IVR AND MTA FORMULATIONS

we have

$$X = \alpha Y + \Lambda_0 \qquad \text{(A.2.2.3)}$$

where $\alpha = \frac{-R}{R+R_s}$ and $\Lambda_0 = \frac{V_0}{R+R_s}$

For the load, the equation is identical to (A.2.1.7). The structures for the resistive source and load are shown in Fig. A.7.

A.2.3 Swamy-Thyagarajan Method [87]

Here the realization is based on the two-port scattering matrix formulation discussed earlier. The two-port representation is illustrated in Fig. A.8. For the source and load terminations,

$$V_1 = V_s - I_1 R_s$$

$$V_2 = -I_2 R_L \qquad \text{(A.2.3.1)}$$

Hence

$$A_1 = V_s(1+\theta) - B_1\theta \qquad \text{(A.2.3.2)}$$

where $\theta = (R_1-R_s)/(R_1+R_s)$ for the source and

$$A_2 = \phi B_2 \qquad \text{(A.2.3.3)}$$

where $\phi = (R_L-R_2)/(R_L+R_2)$ for the load.

The realization for a series L using the scattering parameters is shown in Fig. A.9a. The realization for shunt C

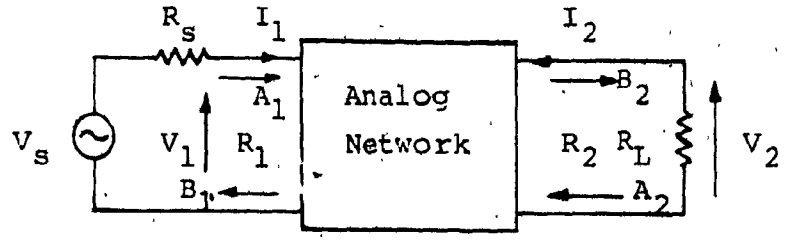

(a) Analog two-port network representation

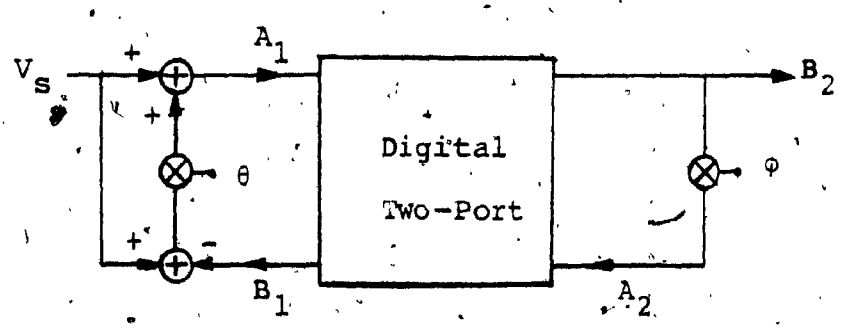

$$\frac{B_2}{V_s} = \frac{2H(z_1, z_2)}{1 + \phi}$$

(b) Wave digital filter

FIG. A-8 WAVE DIGITAL FILTER REALIZATION (TYPE Ia) DUE TO SWAMY AND THYAGARAJAN

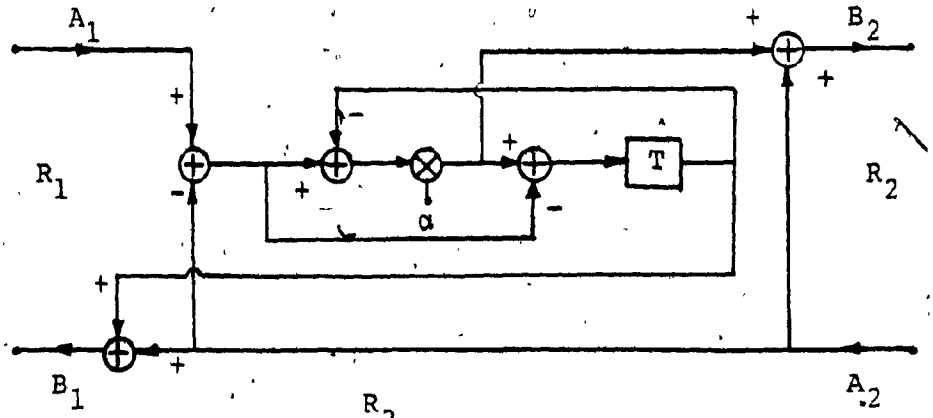

$$\alpha = \frac{R_2}{R_1}, \quad R_1 = R_2 + L$$

(a) Equivalent of series L

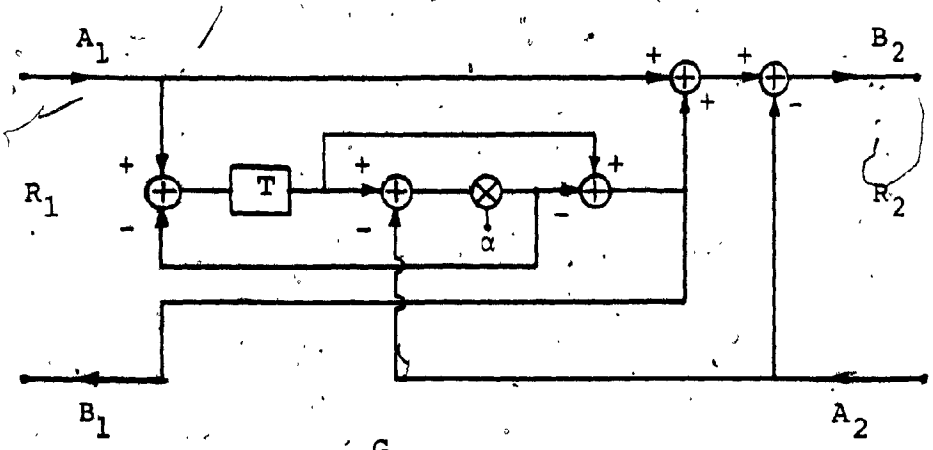

$$\alpha = \frac{G_2}{G_1}, \quad G_1 = G_2 + C$$

(b) Equivalent of shunt C

FIG. A-9. REALIZATIONS FOR SERIES L AND SHUNT C

(Fig. A.9b) is obtained using the transpose (adjoint) network. If the chain matrix [F] of a digital two-port is defined as

$$\begin{bmatrix} A_1 \\ B_1 \end{bmatrix} = [F] \begin{bmatrix} B_2 \\ A_2 \end{bmatrix} \qquad \text{(A.2.3.4)}$$

where $[F] = \begin{bmatrix} \mu & \lambda \\ \nu & k \end{bmatrix} = \begin{bmatrix} \frac{1}{S_{21}} & -\frac{S_{22}}{S_{21}} \\ \frac{S_{11}}{S_{21}} & \frac{S_{12}S_{21} - S_{11}S_{22}}{S_{21}} \end{bmatrix}$

then the chain matrix for the transposed network with the signs of A_2 and B_1 changed, is given by

$$F' = \frac{1}{|F|} \begin{bmatrix} \mu & -\lambda \\ -\nu & k \end{bmatrix} \qquad \text{(A.2.3.5)}$$

where $|F| = \frac{S_{12}}{S_{21}} = \frac{R_1}{R_2}$.

The above realizatization is referred to as the Type Ia realization.

An alternative realizatization is obtained by reversing the ports of the digital two-port network. The chain matrix for this network is given by

$$[F_r] = \frac{R_2}{R_1} \begin{bmatrix} \mu & -\nu \\ -\lambda & k \end{bmatrix}$$

The realizations are obtained by reversing the ports and interchanging R_1 and R_2 and are called as Type IIa realizations. Three more alternate realizations are possible by using alternative constraints and by transposition, for each of the above types and these are named (b), (c) and (d) in [87].

48. P.M. Ebert, J.E. Mazo and M.G. Taylor, "Overflow oscillations in digital filters", Bell System Technical J., Vol. 48, No. 9, pp. 2999-3020, 1969.

49. M. Ni and J.K. Aggarwal, "Two-dimensional digital filtering and its error analysis", IEEE Trans. on Computers, Vol, C-23, No. 9, Sept. 1974.

50. G.A. Maria and M.M. Fahmy, "Bounds for the amplitude of quantization in forced 1st order two-dimensional digital filters", Circuit Theory and Applications, Vol. 6, pp. 221-223, 1977.

51. S.H. Mneney, A.N. Venetsanopoulos and J.M. Costa, "The effects of quantization errors on rotated filters", Proc. 22nd Midwest Symp. on Circuits and Systems, pp. 650-657, June 1979.

52. S.H. Mneney and A.N. Venetsanopoulos, "Finite register length effects in two-dimensional digital filters", Proc. 22nd Midewst Symp. on Circuits and Systems, pp. 669-676, June 1979.

53. H.J. Orchard, "Inductorless filters", Electronics Letters, Vol. 2, pp. 224-225, June 1966.

54. N.K. Bose, "New techniques and results in multidimensional problems", J. Franklin Inst., Vol. 301, Nos. 1 & 2, pp. 83-101, Jan./Feb. 1976.

55. V. Ramachandran and A.S. Rao, "A multivariable array and its application to ladder networks", IEEE Trans. Circuit Theory, Vol. CT-20, No. 5, pp. 511-518, Sept. 1973.

56. M.O. Ahmad, C.H. Reddy, V. Ramachandran and M.N.S. Swamy, "Ladder realizations of multivariable positive real functions", J. of the Franklin Inst., Vol. 307, No. 2, pp. 71-81, Feb. 1979.

57. Y. Kamp, Realization of multivariable functions by cascade of lossless two-ports separated by non-commensurate stubs", Philips Res. Rep., Vol. 26, No. 6, pp. 443-452, Dec. 1971.

58. M.O. Ahmad, C.H. Reddy, V. Ramachandran and M.N.S. Swamy, "A class of multivariable positive real functions realizable by resistively-terminated lossless ladder networkds", IEEE Trans. Circuits and Systems, Vol. CAS-26, No. 8, pp. 659-662, Aug. 1971.

59. V. Ramachandran and A.S. Rao, "The real part of a multivariable positive real function and some applications", IEEE Trans. Circuits and Systems, Vol. CAS-21. No. 5, pp. 598-605, Sept. 1974.

60. M.O. Ahmad, C.H. Reddy, V. Ramachandran and M.N.S. Swamy, "Ladder realization of a class of two-dimensional voltage transfer functions with application to wave digital filters", Archiv fur Electronik and Ubertragungstechnik (Electronics and Communication), Band 33, Heft 2,

pp. 81-85, 1979.

61. A. Bhumiratana and S.K. Mitra, "Darlington-type of realization of two-variable driving-point functions", Int. J. Electronics, Vol. 39, No. 5, pp. 545-550, 1975.

62. C.H. Reddy, V. Ramachandran and M.N.S. Swamy, Darlington-type of realization for a class of multivariable positive real functions", 9th Asilomar Conf. on Circuits, Systems and Computers, 1975.

63. M.O. Ahmad, C.H. Reddy, V. Ramachandran and M.N.S. Swamy, "Cascade synthesis of a class of multivariable positive real functions", IEEE Trans. Circuits and Systems, Vol. CAS-25, No. 10, pp. 871-878, Oct. 1978.

64. L. Weinberg, Network Analysis and Synthesis, McGraw Hill Book Co., Inc., New York, 1962.

65. Van Valkenberg, Modern Network Synthesis, John Wiley & Sons, Inc., 1960.

66. M.N.S. Swamy, C. Bhushan and B.B. Bhattacharyya, "Generalized duals generalized inverses and their applications", The Radio and Electronics Engr., J. of the IERE, Vol. 44, No. 2, pp. 95-99, Feb. 1974.

67. B. Raman, V. Ramachandran and M.N.S. Swamy, "Realization of cascade separable two-dimensional digital transfer functions", Proc. 22nd Midwest Symp. on Circuits and Systems, pp. 663-668, June 1979.

68. D.A. Vaughan Pope and L.T. Bruton, "Transfer function synthesis using generalized doubly terminated two-pair networks", IEEE Trans. Circuits and Systems, Vol. CAS-24, No. 2, pp. 79-88, Feb. 1977.

69. A.G. Constantinides, "Spectral transformations for digital filters", Proc. IEE, Vol. 117, pp. 1585-1590, Aug. 1970.

70. M.N.S. Swamy and K.S. Thyagarajan, "Frequency transformations for digital filters", Proc. IEEE, Vol. 65, pp. 165-166, Jan. 1977.

71. N.K. Bose, "Problems and progress in multidimensional system theory", Proc. IEEE, pp. 824-840, June 1977.

72. C.H. Reddy, P. Karivaratharajan, M.N.S. Swamy and V. Ramachandran, "Generation of two-dimensional digital functions without non-essential singularities of the second kind", IEEE Trans. on Acoustics, Speech and Signal Processing, Vol. ASSP-28, No. 2, pp. 216-223, April 1980.

73. H.C. Reddy, P.K. Rajan and M.N.S. Swamy, "Design of two-dimensional digital filters using analog reference filters without second kind singularities", Int. Conf. on Acoustics, Speech and Signal Processing, pp. 692-695, Mar. 1981.

74. S. Chakrabarti and S.K. Mitra, "Theory and applications of spectral transformations in two-dimensional filtering", Tech. Rep. No. 141, Univ. of California, Davis,

June 1977.

75. P. Karivaratharajan and M.N.S. Swamy, "Quadrantal Symmetry associated with two-dimensional digital transfer functions", IEEE Trans. Circuits and Systems, Vol. CAS-25, pp. 340-343, June 1978.

76. D.S. Humphreys, The Analysis Design and Synthesis of Electrical Filters, Prentice Hall, Englewood Cliffs, 1970.

77. Dan E. Dudgeon, "The existence of cepstra for two-dimensional rational polynomials", IEEE Trans. on ASSP, Correspondence, pp. 242-243, April 1975.

78. K. Thyagarajan, "Two-dimensional IIR digital filters with maximally flat group delay and Chebyshev stopband attenuation", Proc. 22nd Midwest Symp. on Circuits and Systems, pp. 677-681, June 1979.

79. E.I. Jury, Inners and Stability of Dynamic Systems, John Wiley, New York, 1974.

80. J.D. Rhodes, Theory of Electrical Filters, John Wiley & Sons, 1976.

81. Chandra M. Kudsia, A Generalized Approach to the Design and Optimization of Symmetrical Microwave Filters for Communication Systems, D.Engg. Thesis, Concordia University, Nov. 1978.

82. R.E. Thomas, "Polynomial decomposition in active network synthesis", IRE Trans. Circuit Theory, pp. 270-274,

Sept. 1961.

83. G.C. Temes and S.K. Mitra, Eds., Modern Filter Theory and Design, John Wiley & Sons Inc., 1973.

84. R. Unbehauen, "Lowpass filters with predetermined phase or delay and Chebyshev stopband attenuation", IEEE Trans. Circuit Theory, Col. CT-15, No. 4, pp. 337-341, Dec. 1968.

85. G.C. Temes, M. Gyi, "Design of filters with arbitrary passband and Chebyshev stopband attenuation", IEEE Internat. Conv. Rec., Vol. 15, pt. 5, pp. 2-12, 1967.

86. P. Thajchayapong and P. Lomtong, "A maximally flat group delay recursive digital filter with stopband attenuation, Proc. IEEE, Vol. 66, pp. 255-257, Feb. 1978.

87. K.S. Thyagarajan, One and Two-Dimensional Wave Digital Filters with Low Coefficient Sensitivities, D.Engg. Thesis, Concordia University, May 1977.

88. L.B. Jackson, "On the interaction of roundoff noise and dynamic range in digital filters", Bell System Tehcnical J., Vol. 49, pp. 159-184, Feb. 1970.

89. J.B. Jackson, "Roundoff-noise analysis for fixed point digital filters realized in cascade or parallel form", IEEE Trans. Audioelectroacoustics, Vol. AU-18, pp. 107-122, June 1970.